# Fast Chemical Reactions in Turbulent Flows: Theory and Practice

Rustam Ya Deberdeev,
Alexander Al Berlin,
German S. Dyakonov,
Vadim P. Zakharov
and
Yuri B. Monakov

SMITHERS RAPRA

# Fast Chemical Reactions in Turbulent Flows: Theory and Practice

Rustam Ya Deberdeev, Alexander Al Berlin, German S. Dyakonov,
Vadim P. Zakharov and Yuri B. Monakov


**A Smithers Group Company**

Shawbury, Shrewsbury, Shropshire, SY4 4NR, United Kingdom
Telephone: +44 (0)1939 250383 Fax: +44 (0)1939 251118
http://www.polymer-books.com

First Published in 2013 by

**Smithers Rapra Technology Ltd**

Shawbury, Shrewsbury, Shropshire, SY4 4NR, UK



A catalogue record for this book is available from the British Library.



ISBN: 978-1-90903-026-8 (hardback)
978-1-90903-027-5 (softback)
978-1-90903-028-2 (ebook)

Typeset by Integra Software Services Pvt. Ltd.

## Dedication

This book is dedicated to the blessed memory of my teacher, friend and colleague, Professor Karl S. Minsker.

# Contents

Preface ..... ix

1 Fundamentals of Fast Liquid-phase Chemical Processes ..... 1

1.1 Operation Problems of Fast Liquid-phase Processes ..... 1
1.2 Calculation and Simulation of Fast Chemical Processes ..... 4
1.3 Fundamentals of Fast Chemical Processes in Turbulent Flows ..... 12
1.3.1 Various Macroscopic Modes ..... 12
1.3.2 Relationship between a Reaction Zone Size and Kinetic and Hydrodynamic Parameters ..... 15
1.3.3 The Influence of Linear Flow Rate on Molecular Characteristics of Forming Polymers ..... 18
References ..... 21

2 Heat and Mass Exchange Intensification in Fast Liquid-phase Processes ..... 25

2.1 Turbulent Mixing of a Single-phase Reaction Mixture ..... 26
2.1.1 Mathematical Modelling ..... 26
2.1.2 The Influence of the Method of Reactant Addition ..... 31
2.1.3 The Influence of Device Geometry ..... 34
2.1.4 Automodel Mode of Reaction Mixture Flow ..... 38
2.2 Turbulent Mixing of a Two-phase Reaction Mixture ..... 49
2.2.1 Mathematical Modelling ..... 50
2.2.2 Turbulent Flows 'Liquid-liquid' ..... 59
2.2.3 Turbulent Flows 'Liquid-gas' ..... 64
2.2.4 Separation of a Two-phase Reaction Mixture in Tubular Devices ..... 67

2.3 Thermal Modes of Fast Chemical Reactions ..... 70
2.3.1 Adiabatic Mode ..... 70
2.3.2 Internal Heat Removal ..... 72
2.3.3 External Heat Removal ..... 74
2.4 Hydrodynamic Structure of Reaction Mixture Flow during Intensification of Heat Exchange Processes ..... 92
2.4.1 Single-phase Reaction Systems ..... 95
2.4.2 Two-phase Reaction Systems ..... 97
2.4.3 Convective Heat Exchange ..... 102
References ..... 105

3 Fast Processes in Polymer Synthesis and Principles of Tailoring their Molecular Characteristics ..... 115

3.1 Polymerisation Processes ..... 115
3.1.1 Isobutylene Polymerisation ..... 115
3.1.2 Pentadiene-1,3 Polymerisation ..... 124
3.2 Polymer-analogous Transformations ..... 134
3.3 Reaction Mixture Formation *via* the Copolymerisation of Olefins and Dienes ..... 137
3.3.1 Synthesis of Ethylene and Propylene Copolymers ..... 138
3.3.2 Synthesis of Stereoregular Polydienes ..... 144
3.3.2.1 Modification of Microheterogeneous Ziegler–Natta Catalysts in the Turbulent Mode ..... 147
3.3.2.2 Dienes Polymerisation Kinetics with Catalyst Formation in Turbulent Flows ..... 151
3.3.2.3 The Influence of Preliminary Reaction Mixture Formation in the Turbulent Mode on Molecular Characteristics of Polydienes ..... 155
3.3.2.4 Polycentrism of Catalytic Systems in Polymerisation Processes ..... 166
References ..... 200

4 Synthesis of Low Molecular Weight Compounds through Fast Reactions in Turbulent Flows ..... 207

4.1 Formation of Mixing and Reaction Front Macrostructures ..... 207
4.2 Fast Chemical Reactions in a Single-phase Reaction Mixture (Neutralisation of Acid and Alkali Media) ..... 216

4.3 Fast Chemical Reactions in 'Liquid-liquid' Systems (Sulfation of Olefins) ..... 220
4.4 Fast Chemical Reactions in 'Liquid-gas' Systems (Liquid-phase Oxidation) ..... 226
4.5 Fast Chemical Reactions in 'Liquid-solid' Systems (Condensation Method of Suspension Synthesis) ..... 231
4.5.1 Synthesis of Barium Sulfate ..... 231
4.5.2 Synthesis of an Antiagglomerator for Synthetic Rubbers Based on Calcium Stearate ..... 236
References ..... 242

5 Novel Approaches to the Instrumentation of Fast Technological Processes ..... 245

5.1 Plug Flow Reactors ..... 245
5.2 Perfect Mixing Reactors ..... 246
5.3 Plug Flow Tubular Turbulent Reactors ..... 248
5.4 Continuous Energy- and Resource-saving Technologies Based on Tubular Turbulent Reactors ..... 250
5.4.1 Oligoisobutylenes and Polyisobutylenes ..... 252
5.4.2 Halobutyl Rubber ..... 254
5.4.3 Ethylene Propylene Rubber ..... 260
5.4.4 Isoprene Rubber ..... 265
5.4.5 Liquid Oligopiperylene Rubber ..... 270
5.4.6 Polymer-polyol ..... 270
5.4.7 Detergents based on Alkylsulfates ..... 273
5.4.8 Ethyl Chloride ..... 275
5.4.9 Gas-liquid Processes with a Large Volume of the Gas Phase ..... 277
5.4.10 Unleaded Gasoline ..... 278
References ..... 282

6 Conclusion ..... 287

Glossary ..... 291
Abbreviations ..... 297
Index ..... 299

# Preface

The intensification of chemical processes, reduction of metal consumption, their energy and resource efficiency, as well as the development of science-based, cost-effective, and compact technologies play a very important role in the modern priority research areas of chemistry and chemical technology. It is usually difficult and time-consuming to study processes and related equipment, designed to solve the aforementioned factors. That is why modelling is a very important tool for the study of processes and equipment, using conditions which can be further scaled to all similar industrial applications.

There are various processes in chemistry and chemical technology resulting in the drastic transformations of chemical reactants, a change of their molecular structure, composition, and aggregate state. The majority of physico-chemical processes are usually accompanied by physical transformations such as the stirring of liquids, their mixing, heating, cooling, dispersing, and so on. Production technology for the variety of chemical products is usually based on universal physical processes and typical chemical transformations, which have a similar behaviour and are carried out in similar types of equipment. Chemical engineering equipment is classified by two antipodal models of reactive devices: perfect mixing and plug flow reactors. Industrial continuous reactors are intermediate devices with characteristic features of both plug flow and perfect mixing modes. The duration of particles passing through such devices exhibits a more uniform distribution than in a plug flow reactor however, it is never as uniform as in perfect mixing reactors [1].

Kinetic and hydrodynamic analyses, and methods for the calculation of the parameters of industrial reactors are sufficiently developed today [2–6]. Computer simulation is also popular because if we know the kinetic and hydrodynamic parameters of processes and the principles of reactor behaviour, it is not a problem to calculate process characteristics and final product performance. This principle is an adequate tool for the description of low and medium rate chemical transformations with uniform concentration fields and isothermic conditions which are easy to achieve. In this case, it is easy to calculate and control all the characteristics of a chemical process under real conditions.

Fast processes with high reaction rates demonstrate different behaviour. The characteristic time of a respective chemical reaction is about 0.001–0.1 s, far less

than the time required to homogenise a reactive blend on the macro- and microlevel [7–16]. In this case, the chemical process exhibits a diffusion area mechanism and is limited by the rate of reactant supply to the reaction zone. It stipulates a specific approach to the selection of equipment for any specific technology. Another substantial complication is the necessity to remove the high exothermic heat from a reaction zone; such processes in modern production technologies are usually implemented by standard bulk mixing reactors and are hard to control. This difficulty arises from the fact that they are far from isothermic and the reactants stay in a reaction zone for an unreasonably long time, the total yield of final product is substantially reduced, the content of by-products is increased, and heat removal is hampered. Polymerisation processes are accompanied by undesirable changes in the molecular structure of polymers and result in a loss of performance of polymer products. The uncontrolled temperature mode of reaction and instantaneous total reaction heat release in a small local area may lead to unpredictable consequences, such as strong hydraulic and pneumatic impacts, emissions, thermal explosions, and so on.

That is why, for fast liquid-phase processes where the volume is within 2–30 $m^3$, an intensive mixing and a well-developed heat removal system cannot be considered a successful or an optimal solution for the aforementioned problems when using continuous industrial reactors. Reactor dimensions substantially exceed the volume of a reaction zone and therefore, the duration of reactant flow through a reactor is several times longer than the duration of the chemical process needed for the required degree of conversion of the initial feedstock. It favours side reactions and reduces the selectivity in relation to the desired main process.

Continuous plug flow reactors are also unsuitable for these purposes because it is usually impossible to obtain an isothermic mode in such reactors, even for reactions with a relatively low rate of reaction. Plug flow reactors usually operate in adiabatic or intermediate modes, which are far from isothermic even with an external heat removal modification. In can be stated that almost all industrial reactors employed for fast processes are not optimally designed and are therefore ineffective. The quality of products is also far from optimal and the processes are generally not perfect from an engineering, economical, or social point of view (decrease of final product yield and quality, increase of nonrecyclable wastes, excessively high consumption of raw materials and low energy efficiency).

Implementation of fast chemical processes under real industrial conditions requires consideration of the fact that the true mechanism contains complications because of diffusion, and mass and heat transfer. The rate of fast chemical processes is limited by the supply of reactants to the reaction zone, which is mixing the reactants. This in turn, determines the dependence of the reaction parameters and synthesised product quality on the sample mass, reaction zone turbulence, and many other ‘nonchemical’

factors. The specifics of fast chemical processes require a macrokinetic approach to the problem of their implementation.

Characteristic examples of industrial fast chemical reactions are: the electrophilic polymerisation of isobutylene [7], its copolymerisation with isoprene [10], chlorination of olefins [17] and butyl rubber [18], ethylene hydrochlorination [17], sulfation of olefins [19], neutralisation of acidic and basic media [20], isobutene alkylation (production of benzines) [21–23], and so on. These examples of fast liquid-phase reactions and a variety of such processes assume a formal approach for their calculation and modelling, based on material and heat balance in the industrial implementation of respective products. It is *a priori* acknowledged that is not difficult to achieve an isothermic mode for fast chemical exothermic processes if you are aware of the process behaviour and can control it.

First publications, dedicated to the study of the macrokinetic behaviour of fast chemical processes [7, 11, 24–26] have demonstrated that at an extremely high reaction rate, many new problems arise in addition to traditional ones, such as guaranteed heat removal, intensification, and control. For example, isobutylene polymerisation for the synthesis of narrow molecular weight distribution (MWD) polymers, including the most probable one ($M_w/M_n = 2$), with the ability to control molecular characteristics of the forming polymer products and so on, requires an isothermic reaction mode. It is usually achieved by the intensive removal of exothermic heat, accompanied by the perfect mixing of a reaction mixture to form a sufficiently uniform temperature field within a reaction zone. However, high reaction exothermicity and low heat conductivity of a hydrocarbon mixture at an intensive stage of macrochain propagation often results in the local overheating of a reaction mixture in a reaction zone, along with the nonuniform space-time distribution of temperature, monomer conversion, concentration of active centres and a monomer in real conditions.

Methodological and experimental approaches, along with original results provided below for the model of the fast chemical reaction of liquid-phase electrophilic (cationic) isobutylene polymerisation are general and applicable to other fast liquid-phase processes. They turned out to be fruitful for the description of various chemical processes as well as nonpolymerisation reactions, especially of those with mass exchange (extraction, mixing, dispersion, and so on) as an important factor [27–32].

The necessity to implement new conditions for carrying out heat and mass exchange processes directly in the reaction zone of fast chemical reactions, resulted in unprecedented designs of tubular reactors with the hydrodynamic flow mode of a reaction mixture as a key parameter [33–35]. These devices are characterised by high specific productivity and make it possible to achieve a quasi-plug flow mode in a reaction zone, providing heat and mass exchange processes with duration comparable to that of a chemical reaction.

In accordance with aforementioned statements, the first chapter of this monograph is dedicated to the fundamentals of fast chemical processes, mainly based on the model reaction of the fast polymerisation of isobutylene. The information provided is useful for professionals in different branches of the industry, engaged in the design of new production technologies and the modernisation of existing ones, characterised by the occurrence of fast chemical reactions, as well as by heat and mass exchange processes.

The second chapter describes new fundamentals of heat and mass exchange processes, in particular, the mixing and hydrodynamics of multicomponent and layered liquid-phase systems, the intensification of convective heat exchange, and the hydrodynamic structure of the reactant flow. The turbulence level is known to exert a determining influence on the behaviour of these processes. Obtained knowledge formed the basis for the designing of small scale and highly efficient jet-type tubular turbulent devices of the following four modifications: cylindrical, shell-and-tube, zonal, and diffuser-confusor.

The third and fourth chapters state new principles of fast chemical processes in the control and quality of products, during the synthesis of polymers and low molecular weight products respectively, through an intentional change of the reactive mode hydrodynamic flow. The increase of turbulence in the mixing zone of the reactants has been shown to be the key method to achieve optimal processes and high-quality products.

The fifth chapter is dedicated to new solutions in the industrial implementation of technological processes for fast reactions. The key solution here is the utilisation of highly efficient and compact tubular plug flow reactors with a highly turbulent operation mode. These processes are highly productive, eco-friendly, and have high material, labour and energy efficiency. There are examples of new technologies, based on tubular turbulent devices in different industrial processes, being implemented in fast chemical and mass exchange processes. This publication mainly provides analysis of the developments of the last decade, based on a survey of research in chemistry and chemical technology of fast processes as far back as 1996 and given in [7].

The authors hope that this monograph will be a helpful advisor for researchers and engineers specialising in the synthesis and theoretical fundamentals of chemical technologies, and will attract more attention to the problems of the implementation of various fast chemical and mass exchange technological processes. This book will also be useful for graduate students pursuing degrees in polymer and process engineering.

Our book is of course not perfect, so any feedback and criticism by the reader is very welcome.

## References

1. A.G. Kasatkin in *Basic Processes and Machinery of Chemical Tehnology*, Khimiya, Moscow, Russia, 1983. [In Russian]

2. H. Kramers and K. Vesterterp in *Chemical Reactors*, Nauka, Moscow, Russia, 1967. [In Russian]

3. K. Denbig in *Theory of Chemical Reactors*, Nauka, Moscow, Russia, 1968. [In Russian]

4. A.A. Berlin and S.A. Volfson, *Vysokomolekulyarnye Soedineniya*, 1994, **36**, 4, 616. [In Russian]

5. S.A. Volfson and N.S. Enikolopyan in *Calculations of Highly Efficient Polymerization Processes*, Khimiya, Moscow, Russia, 1980. [In Russian]

6. A.A. Berlin and S.A.Volfson in *Kinetic Methods in Polymer Synthesis*, Khimya, Moscow, Russia, 1973. [In Russian]

7. A.A. Berlin, K.S. Minsker and K.M. Djumaev in *Novel Unified Energy-and Resource Efficient High Performance Technologies of Increased Ecological Safety Based on Tubular Turbulent Reactors*, Niitjehim, Moscow, Russia, 1996. [In Russian]

8. K.S. Minsker and A.A. Berlin in *Fast Polymerization Processes*, Gordon and Breach Publishers, Amsterdam, Netherlands, 1996.

9. K.S. Minsker, A.A. Berlin, V.P. Zakharov and G.E. Zaikov in *Fast Liquid-Phase Processes in Turbulent Flows*, Brill Academic Publishers, Amsterdam, Netherlands, 2004.

10. J.A. Sangalov and K.S. Minsker in *Isobutylene Polymers and Copolymers: Fundamental Problems and Application Aspects*, Gilem, Ufa, Russia, 2001. [In Russian]

11. A.A. Berlin, K.S. Minsker, J.A. Sangalov, V.G. Oshmyan, A.G. Svinuhov, A.P. Kirillov and N.S. Enikolopyan, *Vysokomolekulyarnye Soedineniya*, 1980, **22**, 3, 566. [In Russian]

12. A.A. Berlin, K.S. Minsker, J.A. Prochuhan, M.M. Karpasas and N.S. Enikolopyan, *Vysokomolekulyarnye Soedineniya*, 1986, **28**, 6, 461. [In Russian]

13. A.A. Berlin, K.S. Minsker and V.P. Zakharov, *Doklady Akademii Nauk*, 1999, **365**, 3, 360. [In Russian]

14. K.S. Minsker, V.P. Zakharov, R.G. Tahavutdinov, G.S. Dyakonov and A.A. Berlin, *Zhurnal Prikladnoy Khimii*, 2001, **74**, 1, 87. [In Russian]

15. K.S. Minsker, V.P. Zakharov and A.A. Berlin, *Russian Polymer News*, 2000, **5**, 3, 18. [In Russian]

16. V.P. Zakharov, K.S. Minsker, I.V. Sadykov and A.A. Berlin, *Himicheskaya Fizika*, 2003, **22**, 3, 34. [In Russian]

17. K.S. Minsker, A.A. Berlin, Y.M. Abdrashitov, J.K. Dmitriev, V.D. Shapovalov, V.P. Malinskaya and N.V. Alekseeva, *Himicheskaya Promyshlennost*, 1999, **76**, 6, 41. [In Russian]

18. K.S. Minsker, S.R. Ivanova, R.Y. Deberdeev and A.A. Berlin, *Russian Polymer News*, 2000, **5**, 4, 30. [In Russian]

19. K.S. Minsker, V.P. Zakharov, A.A. Berlin and R.Y. Deberdeev, *Himicheskaya Tehnologiya*, 2003, **3**, 30. [In Russian]

20. V.P. Zakharov, K.S. Minsker, F.B. Shevlyakov and M.M. Muratov, *Himicheskaya Promyshlennost*, 2003, **80**, 3, 30. [In Russian]

21. R.N. Gimaev, Y.A. Prochukhan, F.H. Kudasheva, M.A. Cadkin and A.D. Badikova, *Khimichaskaya Tekhnologiya Topliv i Masel*, 1998, **5**, 42. [In Russian]

22. R.N. Gimaev, M.A. Cadkin, V.M. Rakitskiy, M.M. Kalimullin, F.H. Kudasheva, S.V. Kolesov, R.R. Rahmanov, A.D. Badikova, G.G. Telyashev and J.M. Maksimenko, *Bashkirskiy Khimicheskiy Zhurnal*, 1998, **5**, 2, 59. [In Russian]

23. S.V. Kolesov, M.A. Cadkin, A.D. Badikova, R.R. Rahmanov, F.H. Kudasheva and R.N. Gimaev, *Khimichaskaya Tekhnologiya Topliv i Masel*, 2002, **4**, 15. [In Russian]

24. K.S. Minsker, A.A. Berlin, A.G. Svinuhov, Y.A. Prochukhan and N.S. Enikolopyan, *Doklady Akademii Nauk SSSR*, 1986, **286**, 5, 1171. [In Russian]

25. A.A. Berlin, K.S. Minsker, Y.A. Prochukhan, M.M. Karpasas and N.S. Enicolopyan, *International Polymer Science and Technology*, 1986, **13**, 11, 95. [In Russian]

26. V.Z. Kompaniec, A.A. Konoplev, A.A. Berlin, Y.A. Prochukhan, K.S. Minsker, M.M. Karpasas and N.S. Enikolopyan, *Doklady Akademii Nauk SSSR*, 1987, **297**, 5, 1129. [In Russian]

27. R.G. Takhavutdinov, G.S. Dyakonov, R.Y. Deberdeev, K.S. Minsker and G.E. Zaikov, *Journal of the Balkan Tribological Association*, 2002, **2**, 1–2, 40.

28. M.G. Krehova, S.K. Minsker, Y.A. Prochukhan and K.S. Minsker, *Teoreticheskie Osnovy Khimicheskoy Tekhnologii*, 1994, **28**, 3, 271. [In Russian]

29. K.S. Minsker, A.A. Berlin, V.P. Zakharov and R.G. Tahavutdinov, *Doklady Akademii Nauk*, 2001, **381**, 1, 78. [In Russian]

30. A.A. Berlin, K.S. Minsker, A.G. Muhametzyanova, R.G. Tahavutdinov, G.S. Dyakonov, G.G. Aleksanyan, B.L. Rytov and A.A. Konoplev in *Transactions of Institute of Chemical Physics, Russian Academy of Sciences*, Moscow, Russia, 2003. [In Russian]

31. A.Y. Fedorov and V.A. Kaminskiy, *Teoreticheskie Osnovy Khimicheskoy Tekhnologii*, 1997, **31**, 2, 177. [In Russian]

32. V.A. Kaminskiy, A.Y. Fedorov and V.A. Frost, *Teoreticheskie Osnovy Khimicheskoy Tekhnologii*, 1994, **28**, 6, 591. [In Russian]

33. A.A. Berlin, K.S. Minsker and V.P. Zakharov, *Himicheskaya Promyshlennost*, 2003, **80**, 3, 36. [In Russian]

34. K.S. Minsker, V.P. Zakharov, A.A. Berlin and G.E. Zaikov, *Konstrukcii iz Kompozicionnyh Materialov*, 2003, **2**, 3. [In Russian]

35. K.S. Minsker, V.P. Zakharov, A.A. Berlin and G.E. Zaikov, *Journal of Applied Polymer Science*, 2004, **94**, 2, 613.

# 1 Fundamentals of Fast Liquid-phase Chemical Processes

## 1.1 Operation Problems of Fast Liquid-phase Processes

Chemistry and chemical technology provide us with examples of extremely rapid liquid-phase processes, meaning equal or higher rates of chemical reactions in relation to the mixing rate of reactants. These particular processes are: the electrophilic polymerisation of isobutylene [1–3], styrene [4], *para*-chlorostyrene [4, 5] and cyclopentadiene [6]; ionic polymerisation of formaldehyde [7]; nonequilibrium polycondensation [8]; isobutylene-isoprene-styrene copolymerisation [3]; chlorobutyl rubber synthesis [9–11]; cationic polymerisation of pentadiene-1,3 (piperylene) [12]; formation of macromolecular growth centres during olefin and diene (co) polymerisation in the presence of Ziegler–Natta catalysts (in particular, for the production of stereoregular isoprene and butadiene rubbers) [13]; as well as for the production of ethylene-propylene elastomers [14]); chlorination, hydrochlorination [15] and sulfation of olefins [16]; alkylation of alkanes and aromatic hydrocarbons by alkenes [17–19]; chlorination of aromatic hydrocarbons [20], and so on [21].

Modern production technologies utilise either capacitive mixing devices (according to the classification of continuous devices in chemical technology) [22–24] of various designs (with a reactor volume ($v_p$) of 0.6–30 $m^3$ and above), which are usually equipped with mechanical mixing devices, or displacement reactors with a length/diameter ratio L/d > 100. Intense mixing in bulky vessels creates high turbulence which results in an equal distribution of temperature and reactant concentrations, as well as in the acceleration of heat supply/withdrawal to/from a reaction zone. The heat exchange surface area may exceed, in this case, 100 $m^2$ for applications with liquid ammonia or ethylene as the cooling agents [21, 25].

The design of plug flow reactors (tubular and tower devices) does not assume mixing in the direction of flow (axial turbulence), therefore the chemical processes within a blend of reactants occurs in laminar flow conditions. A combination of the displacement and plug flow reactors, with consideration of their material and thermal balances, makes it possible to calculate the optimal design of a device for any chemical process.

However, these types of reactors, and their modified versions, are not very effective for rapid liquid-phase chemical processes when the reaction time is much less than

the time required for the mixing of the reactants. In this case, bulk mixing devices will not provide the required heat and mass transfer within the chemical reaction time. Addition of the reactants causes a rapid increase of temperature in the reaction zone (up to 100–600 °C), located several centimetres or even millimetres around the introduction zone. Substantial temperature and concentration gradients emerge and therefore, the assumption of perfect mixing or displacement mode and isothermicity of a process turns out to be meaningless.

The cationic (electrophilic) polymerisation of isobutylene is the most attractive process, in a family of rapid liquid-phase chemical reactions, for theoretical study as it is both theoretically clear and practically important. This process can be considered to be a classical model of a rapid liquid-phase chemical reaction [2, 26].

Oligo- and polyisobutylenes, with a molecular weight (MW) of 112–50000 and above, are industrially produced during the cationic polymerisation of isobutylene in the presence of $AlCl_3$ ($BF_3$, its complexes and so on), in a medium containing hydrocarbons (butanes and so on) and chlorinated hydrocarbons (ethyl chloride, methyl and so on), within the temperature range of -100–80 °C (173–353 K) and employing mixing reactors of 1.5–30 $m^3$ [2]. To enable heat removal and the required process productivity, according to thermal and material balances, reactors are equipped with extended inner and outer heat exchange surfaces (130 $m^2$ and above) using liquid ethylene or ammoniac as a cooling agent, and intense mixing devices provide a linear flow rate of reacting mass of about 1–10 m/s. The reactive volume and productivity of the reactor provide an average reactant contact time of approximately $(1.8–3.6) \times 10^3$ s [21].

The analysis of kinetic parameters has demonstrated that the constants of initiating and chain growth reactions ($k_{in}$, $k_p$) have a minimal value of $10^5$–$10^6$ l/mol·s [26–33], thus determining the characteristic time of a chemical reaction $\tau_{chem} \sim 10^{-1}$–$10^{-3}$ s at real initial values of catalyst and monomer concentrations. Thus, isobutylene polymerises almost fully in the areas of reactant introduction (less than 1–10 cm from the point of catalyst introduction) and the process is limited by the mixing of reactants, i.e., it is a diffusion area process. Heat accumulation in a reacting system, as well as high turbulence (due to agitation) leads, over time, to a temperature oscillation in the reacting zone [27]. The rapid polymerisation reaction, from a topochemical aspect, is a torch-like process with comparable temperature and concentration gradients to a reaction zone coordinate system [27, 34].

Forming a reaction front is similar to the gas-phase combustion process [35, 36]. The major part of a reactor's volume does not participate in the chemical process and acts as ballast, resulting in the reactant taking a longer time to pass through a reacting zone. It favours the formation of by-products in slower reactions. In addition, the reacting zone does not reach the heat exchange walls of a reactor and an external

heat removal approach is inefficient [11, 21, 25, 37]. Therefore, the thermostatic control of rapid polymerisation processes meets considerable obstacles both in the laboratory and industry. A nonisothermic process results in MW and molecular weight distribution (MWD) gradients in a reacting zone during the process [38, 39].

It is important to note that a local polymerisation process has a macroscopic effect on the average MW and MWD dependence on the initial concentration of reactants. The polymer MW, according to the process kinetics chart [27], is fully determined by the chain-to-monomer transfer and therefore, predicts the independence of the MW and MWD on monomer and catalyst concentrations [21]. Catalyst and monomer solutions are usually introduced irregularly into the reactor and do not have enough time for sufficient mixing with the reacting blend due to high polymerisation reaction rates. It favours further destabilisation of the reactor, wider MWD and lower MW of the final product.

Further research [30, 40–44] has demonstrated that known rapid polymerisation effects are scalable to any fast process, including the synthesis of low MW products.

The traditional approach to fast chemical reactions used both for the synthesis of polymers and for the production of low MW products, is based on uncontrollable processes with the quality of products being far from optimal. This fact resulted in the search for the optimisation of fast liquid-phase processes.

A logical conclusion here is to study and perform fast chemical processes, in the form of a jet, in a tubular reactive device with perfect mixing provided by a highly turbulent flow [35, 37]. It is reasonable from several viewpoints. Firstly, jet processes are the best method for the experimental study of fast reactions. Secondly, when these reactions are carried out in classical bulk mixing devices, it is very difficult to provide effective heat and mass exchange in the timescale of a chemical reaction, because of the large volume of the reacting mixture. Thirdly, the turbulence of the moving jets provides maximum intensiveness to chemical processes in a minimal time and volume therefore, satisfying the criterion of the effective use of chemical equipment. Fourthly, studying the stationary jet turbulent mixing reactions is principally easier and more effective compared with single time confined space processes. Finally, fast jet reactions allow varying the characteristic mixing time $\tau_{mix} = R^2/D_{turb}$ (R is the jet radius, corresponding to the radius of the reactor, $D_{turb}$ is the turbulent diffusion coefficient), through changing the flow geometry of reactants and their hydrodynamic mode. This approach provides an opportunity to make the flow mixing time and characteristic reaction time closer.

Optimisation of fast chemical reaction conditions requires the solution of at least three problems [45, 46]: a) the rapid mixing of two and more reactants, especially dense and viscous ones (the ideal prerequisite here is when the mixing time of reactants is

less than or equal to the duration of a chemical process $\tau_{mix} \leq \tau_{chem}$); b) the time taken for the reactants to pass through a reacting zone ($\tau_{pass} = V_r/w$, where w is the volume rate of a reactive mixture $V_r$ is a reactor volume) should not considerably exceed the chemical reaction time because of the presence of lower rate secondary reactions (the ideal case here is: $\tau_{pass} \approx \tau_{chem}$); and c) the effect of considerable heat removal from a small section of the reaction zone, or providing conditions of zero influence of rapid temperature growth, on the chemical reaction sustainability and product quality (such as the molecular characteristics of the product during polymer synthesis processes).

As fast liquid-phase chemical reactions usually occur in the diffusion area, a macrokinetic approach should be used to reveal their aspects and specificity, as it describes reactions with consideration of the heat and mass transfer [47, 48]. This approach to the modelling of fast polymerisation processes, such as the cationic polymerisation of isobutylene [27–30, 38, 39, 49], has revealed aspects of its behaviour. Many problems of fast chemical reactions were solved *via* the creation of sufficiently high turbulence in a reaction zone within small-scale tubular turbulent devices.

## 1.2 Calculation and Simulation of Fast Chemical Processes

Equations of chemical kinetics, heat transfer, diffusion and convection, form the basis for the simulation of fast chemical reactions in a diffusion area and an estimation of process behaviour.

Taking polyisobutylene synthesis as an example, a polymerisation kinetics approach is used which assumes the main macrochain growth limitation to be the chain transfer to the monomer (**Equations 1.1–1.5**):

$$Cat + M \xrightarrow{k_{in}} A_1^* \tag{1.1}$$

$$A_1^* + M \xrightarrow{k_p} A_2^* \tag{1.2}$$

$$A_{n-1}^* + M \xrightarrow{k_p} A_n^* \tag{1.3}$$

$$A_n^* + M \xrightarrow{k_m} A_1^* + P \tag{1.4}$$

$$A_n^* \xrightarrow{k_t} P \tag{1.5}$$

Where: *Cat, M, A*, P* are the catalyst, monomer, growing chain (active centre), and inactive macromolecule respectively; $k_{in}$, $k_m$, and $k_t$ are rate constants of the initiation reactions, chain transfer to monomer, and chain termination respectively.

The initiation rate of isobutylene polymerisation is sufficiently high ($k_{in} >> k_p$) which is why, in process kinetics, the initiation stage is considered to be instant. The concentration of active centres $\Sigma A_n^*$ corresponds to the catalyst concentration in this case.

The number-average degree of polymerisation $P_n$, depends on the monomer concentration (M) in terms of process kinetics:

$$P_n = \frac{k_p}{k_m + \frac{k_t}{[M]}} \tag{1.6}$$

As the main reaction determining the MW and MWD in the isobutylene polymerisation process, over a broad temperature range, is the chain transfer to monomer, then $P_n$ of a polymer, formed in any section of a sufficiently small reaction volume, is determined by temperature only and does not depend on the catalyst or monomer concentration:

$$\rho_n(j) = \frac{1}{P_n}\exp\left(-\frac{j}{P_n}\right),\ P_n = \frac{k_p}{k_m} = f(T) \neq \phi([A^*],[M]) \tag{1.7}$$

Where: $P_n$ is the number-average degree of polymerisation (the polymerisation degree distribution numerical function).

Thus, the change in the MW and MWD of the polymer is due to the effect of temperature on the polymerisation zone.

According to isobutylene polymerisation kinetics, the following differential equations describe the changing concentration of the monomer and active centres, as well as the temperature distribution in a reaction zone [11]:

$$\frac{\partial[M](x,r)}{\partial t} = D_{\text{turb}}\frac{\partial^2[M]}{\partial r^2} + \frac{D_{\text{turb}}}{r}\frac{\partial[M]}{\partial r} + D_{\text{turb}}\frac{\partial^2[M]}{\partial x^2} - V\frac{\partial[M]}{\partial x} - k_p^0[M][A^*]\exp\left(-\frac{E_p}{RT}\right) \tag{1.8}$$

$$\frac{\partial[A^*](x,r)}{\partial t} = D_{\text{turb}}\frac{\partial^2[A^*]}{\partial r^2} + \frac{D_{\text{turb}}}{r}\frac{\partial[A^*]}{\partial r} + D_{\text{turb}}\frac{\partial^2[A^*]}{\partial x^2} - V\frac{\partial[A^*]}{\partial x} - k_t^0[M][A^*]\exp\left(-\frac{E_t}{RT}\right) \tag{1.9}$$

$$\rho C_p\frac{\partial T(x,r)}{\partial t} = \lambda_m\frac{\partial^2 T}{\partial r^2} + \frac{\lambda_m}{r}\frac{\partial T}{\partial r} + \lambda_m\frac{\partial^2 T}{\partial x^2} - V\rho C_p\frac{\partial M}{\partial x} - qk_P^0 MA^*\exp\left(-\frac{E_p}{RT}\right) \tag{1.10}$$

With the following boundary conditions:

If $T(-d_L,r) = T_0$ at $0 < r < R$:

$$[M](-d_L,r) = \begin{cases}[M_0] & at\ \ R > r > r_0\\ 0 & at\ r < r_0\end{cases} \tag{1.11}$$

$$[A^*](-d_L, r) = \begin{cases} 0 & at\ \ R > r > r_0 \\ [A^*] & at\ r < r_0 \end{cases} \tag{1.12}$$

$$\frac{\partial[M](x, r_0)}{\partial r} = \frac{\partial[A^*](x, r_0)}{\partial r} = \frac{\partial T(x, r_0)}{\partial r} = 0 \tag{1.13}$$

If $-d_L < x < 0$:

$$\frac{\partial[M](x, R)}{\partial r} = \frac{\partial[A^*](x, R)}{\partial r} = \frac{\partial[A^*](x, 0)}{\partial r} = \frac{\partial[M](x, 0)}{\partial r} = \frac{\partial T(x, 0)}{\partial r} = 0 \tag{1.14}$$

If $-d_L < x < L$:

$$\frac{\partial T(x, R)}{\partial r} = \alpha\left\{T(x, R) - T_1\right\} \tag{1.15}$$

Where $D_{\text{turb}}$ is the turbulent diffusion coefficient, $\lambda_T$ is the heat conductivity coefficient and $\alpha$ is the heat transfer coefficient: $\alpha$ = Nu/d (Nu is the Nusselt Number, D is the diameter of the reactor), $d_L$ is the return of the active centres to a reaction zone length (this parameter was varied to provide the solution, which is independent of $d_L$), $E_p$, $E_t$ are the activation energies of the chain growth reaction and chain termination reaction respectively.

The contribution of longitudinal monomer diffusion, the presence of active centres and temperature on the formation of temperature and concentration fields in a reaction zone, was considered by introducting the following parameters:

$$D_{\text{turb}} \frac{\partial^2[M]}{\partial x^2};\ D_{\text{turb}} \frac{\partial^2[A^*]}{\partial x^2};\ \lambda_t \frac{\partial^2 T}{\partial x^2} \tag{1.16}$$

The system of differential equations was solved using an implicit difference scheme in a stationary mode under the following conditions:

$$\frac{\partial[M](x, r, t)}{\partial t} = \frac{\partial[A^*](x, r, t)}{\partial t} = \frac{\partial T(x, r, t)}{\partial t} = 0 \tag{1.17}$$

Assumption of a constant flow-parallel turbulent diffusion coefficient $D_{\text{turb}}$ (diffusion model) is generally not correct. However, calculations demonstrate [21] that the more accurate Navier–Stokes model (hydrodynamic model) provides diffusion model-based results with a qualitatively correct description of the basic macrokinetic aspects of fast liquid-phase processes.

In addition to the calculation of monomer concentration fields and volume process rates in a reaction zone [21], the MWD and average MW of synthesised polymer products have been estimated.

The following equations were used to calculate the average distribution function $\rho_w(j)$ of the degree of product polymerisation in the output of an L-length reactor, with distribution function moments $J_0$–$J_3$:

$$\rho_w(j) = \int_{-d_L}^{L}\int_{0}^{R}\frac{j}{P_n^2}\exp\left(-\frac{j}{P_n}\right)k_p[A^*][M]\exp\left(-\frac{E_p}{RT}\right)2\pi r dx dr \tag{1.18}$$

Where:

$$P_n = \frac{k_p}{k_m} = \frac{k_p^0}{k_m^0}\exp\left[-(E_p - E_m)/RT\right] \tag{1.19}$$

$$\begin{aligned} J_0 &= \int_0^{\infty}\frac{\rho_w(j)}{j}dj = \int_0^{R}\int_{-d_L}^{L}k_m^0[A^*][M]\exp\left(-\frac{E_m}{RT}\right)2\pi r dr dx \\ &= \int_0^{R}\int_{-d_L}^{L}\frac{1}{P_n}k_p^0[A^*][M]\exp\left(-\frac{E_p}{RT}\right)2\pi r dr dx \end{aligned} \tag{1.20}$$

$$J_1 = \int_0^{\infty}\rho_w(j)dj = \int_0^{R}\int_{-d_L}^{L}k_p^0[A^*][M]\exp\left(-\frac{E_p}{RT}\right)2\pi r dr dx \tag{1.21}$$

$$J_2 = \int_0^{\infty} j\rho_w(j)dj = \int_0^{R}\int_{-d_L}^{L}2P_n k_p^0[A^*][M]\exp\left(-\frac{E_p}{RT}\right)2\pi r dr dx \tag{1.22}$$

$$\int_0^{R}\int_{-d_L}^{L}\frac{(k_p^0)^2}{k_m^0}[A^*][M]\exp(-(2E_p - E_m)/RT)4\pi r dr dx \tag{1.23}$$

$$J_3 = \int_0^{\infty} j^2\rho_w(j)dj = \int_0^{R}\int_{-d_L}^{L}6P_n^2 k_p^0[A^*][M]\exp\left(-\frac{E_p}{RT}\right)2\pi r dr dx \tag{1.24}$$

$$\int_0^{R}\int_{-d_L}^{L}6\frac{(k_p^0)^3}{(k_m^0)^2}[A^*][M]\exp(-(3E_p - E_m)/RT)2\pi r dr dx \tag{1.25}$$

$$P_n = J_3/J_2 \tag{1.26}$$

$$P_w = J_2/J_1 \tag{1.27}$$

$$P_z = J_3/J_2 \tag{1.28}$$

Where $P_n$, $P_w$, $P_z$ are the number-average, weight-average and z-average rates of product polymerisation within a reactor's output.

$E_p$ and $E_t$ values for fast isobutylene cationic polymerisation processes are sufficiently low [50] therefore, temperature factors $k_p$ and $k_t$ were not considered during the calculations. The rate of diffusion of these processes is also independent of temperature; therefore, the turbulent diffusion coefficient $D_{\text{turb}}$ values can also be calculated.

As the problem of the interrelation of turbulent mixing and chemical transformation is complicated and ambiguous, these processes are simulated together, as shown above in the diffusion model. However, separate analysis of these processes is also interesting in the estimation of their contributions to fast liquid-phase chemical reactions in real conditions.

Simulation of fast isobutylene polymerisation [21] has been carried out on the basis of a mathematical model, which considers the hydrodynamic effects of a reacting mixture during the processes of mixing and chemical transformations.

It is based on the assumption that the average (averaged on the realisation ensemble) characteristics of a multicomponent system flow can be described by continuum mechanic equations and satisfy its laws of conservation.

The following parameters characterise the state of $N$ components of a system and the continuum as a whole at any moment, t, in any reaction zone point: $\rho_N^{(k)}$ is the $k^{th}$ component density:

$$\rho = \sum_{k=1}^{N} \rho_N^{(k)} \tag{1.29}$$

is the mixture volume:

$$\rho V_i = \sum_{k=1}^{N} \rho^{(k)} V_i^{(k)} \tag{1.30}$$

is the momentum of a mixture; T is temperature; and P is pressure.

Then we obtain the following equations for a stationary turbulent flow in terms of dynamic variables (rate-pressure):

$$(\rho V_i)_i = 0 \tag{1.31}$$

and

$$\rho V_j V_{i,j} = \tau_{ij,j} \tag{1.32}$$

Where $(\rho\ V_i)_i$ is the total of a reaction zone differentiation, repeating *i* and *j* induces the mean summation:

$$\tau_{i,j} = -P\sigma_{ij} + \mu(V_{i,j} + V_{j,i}) \tag{1.33}$$

is the tensor of inner tensions, where μ is the dynamic viscosity of a medium. Viscosity is well known to be a function of the temperature and mixture composition. However, such dependence exerts a small influence on the turbulent flow behaviour (self-similar mode, relating to viscosity).

The result of averaging **Equation 1.32**:

$$(\rho V_i)_i = 0 \tag{1.34}$$

$$\overline{\rho}\overline{V}_j\overline{V}_{i,j} = -P_j\delta_{i,j} + \mu(\overline{V}_{i,j} + \overline{V}_{j,i}) - \rho\overline{V}_i^{/}\overline{V}_j^{/} \tag{1.35}$$

Where $\rho\overline{V}_i^{/}\overline{V}_j^{/}$ is the Reynolds pressure.

An assumption is used here and below, that an average value of the pulsation of any parameter is zero, with the liquid medium density remaining unchanged (incompressible flow).

To finalise the system of equations (**Equation 1.35**), the Reynolds pressure should be expressed in terms of averaged flow characteristics or in the form of a defining expression. K-ε, the turbulence model is used in this case.

Where:

$$\mu(\overline{V}_{i,j} + \overline{V}_{j,i}) - \rho\overline{V}_i^{/}\overline{V}_j^{/} = \mu_m(\overline{V}_{j,i} + \overline{V}_{i,j}) \tag{1.36}$$

Where $\mu_{turb}$ is the dynamic factor of turbulent viscosity, which can be expressed in terms of turbulent pulsation energy K and the specific rate of its dissipation, ε. In turn, the corresponding phenomenological defining equations are worked out for these parameters [36, 51].

In the case of an axial-symmetric flow, a good solution is to move from dynamic variables 'rate-pressure' to 'current-vortex' variables, which are determined in the following equations:

$$\rho V_z = \frac{1}{r}\Psi_r \tag{1.37}$$

$$\rho V_r = -\frac{1}{r}\Psi_z \tag{1.38}$$

$$\omega = V_r - V_z \tag{1.39}$$

Where $\Psi$ is the current function and $\omega$ is the vortex tension; solution of the system of **Equations 1.37 – 1.39**, relative to $\Psi$ and $\omega$ will provide us with data of the rate and pressure distributions in a reaction mixture zone.

All the basic equations, characterising axial-symmetric reactive turbulent flow, can be defined in the following form:

$$[\alpha_\phi \phi \Psi_r]_z - [\alpha_\phi \phi \Psi_z]_r - [b_\phi (C_\phi \phi)_z]_z - [b_\phi (C_\phi \phi)_r]_r + d_\phi = 0 \tag{1.40}$$

Where values of the coefficients $\alpha_\phi$, $b_\phi$, $C_\phi$ and the source member $d_\phi$ are provided in [36, 51], $\phi$ = f(Ψ, ω/r, VΘ, r, q, ε, g, h, Yα), Ψ is the current function, ω is the vortex tension, VΘ is the tangential velocity, q is the turbulent energy, ε is the specific dissipation rate of a turbulent energy, g is the root-mean-square of the pulsations of a scalar parameter (temperature, concentration), h is the inhibition enthalpy and Y$\alpha$ is the weight concentration of a component $\alpha$.

The boundary conditions, difference scheme, algorithm, and solution method are provided in [36, 51].

Therefore, a hydrodynamic model makes it possible to calculate real values of the turbulent diffusion coefficient $D_{\text{turb}}$ and consider the influence of the reactants input mode. Within the framework of a diffusion model, the catalyst and monomer input methods can be simulated only via the change of $D_{\text{turb}}$.

**Figure 1.1** demonstrates the diffusion model-based fields of temperature, as well as the monomer and catalyst concentrations during the cationic polymerisation of isobutylene. It is clear that the process and experimental behaviour are close, mainly in the catalyst input areas where it is mixed with the monomer solution. Isobutylene polymerisation is similar to the behaviour of fast chemical processes: the temperature and reaction rate in a reaction zone depend on the initial concentration of reactants, the value $D_{\text{turb}}$ and the factor K, which is the heat transfer through the reactor wall $K_{ht}$. Although the rate of isobutylene polymerisation is maximal within the catalyst input areas, the reaction occurs sufficiently far in the axial direction to result in a change of output characteristics and polymer properties (molecular characteristics) when moving away from catalyst input area.

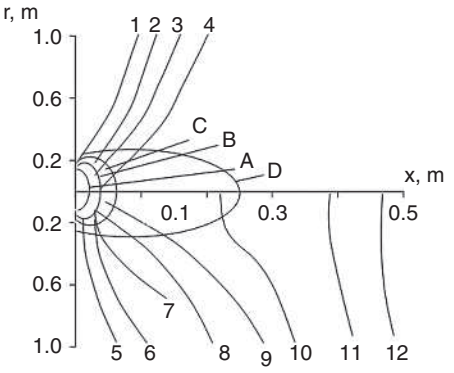


**Figure 1.1** Fields of temperature, monomer, and catalyst concentrations, formed during the isobutylene polymerisation process. T, K: 1 – 310; 2 – 313; 3 – 320; 4 – 330 ($[M]_0$ = 1 mol/l; $[AlCl_3]_0$ = 0.01 mol/l); $[M]_0$, mol/l: *5* – 0.9; 6 – 0.7; 7 – 0.5; 8 – 0.2; 9 – 0.15; 10 – 0.085; 11 – 0.016; 12 – 0.008 ($[AlCl_3]_0$ = 0.01 mol/l; $T_0$ = 20 °C (293 K)); $[AlCl_3]_0 \times 10^4$, mol/l: A – 20; B – 10; D – 1 ($[M]_0$ = 1 mol/l; $T_0$ = 20 °C (293 K)) ($k_p = 10^5$ l/mol·s; $k_t$ = 1 $s^{-1}$; $D_{turb}$ = 1 $m^2$/s; and $K_t$ = 0)

Polymer formation within different points of a reaction zone (therefore, at different temperatures) results in a reduction of the MW and broadening of the MWD, comparing the most probable value:

$$\rho_n(j) = \frac{1}{P_n}\exp\left(-\frac{j}{P_n}\right) \tag{1.41}$$

Such a value is typical for isothermal conditions. Intensification of the external heat removal due to an increase of the heat transfer coefficient $K_t$, when other process parameters are constant, results in some MWD narrowing, indicating a smoothing of the temperature change in a reaction zone. However, the side wall heat transfer may exert an influence only if the reactor's cross section is small and the $D_{turb}$ and $\lambda_T$ values are high. The temperature field in a reaction zone is determined by the process rate and quantity of released heat, and therefore, by the monomer and catalyst concentrations. A consequence is that process parameters do not correspond to the kinetic chart, in particular, the MWD value is distinctly broader and the MW drops upon increasing the monomer concentration (**Figure 1.2**). Similar effects are observed when the catalyst concentration is varied. An increase of polymer output is accompanied by a temperature growth and in this case, temperature gradients appear in a reaction zone and therefore, the average MW drops and the MWD broadens (the increase of $P_w/P_n$) during polymer formation.

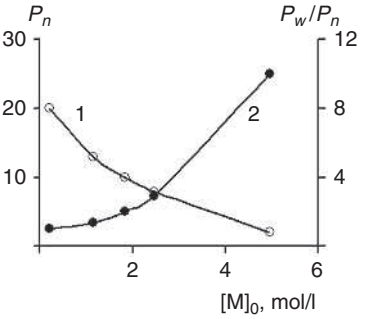


**Figure 1.2** Dependence of the degree of polymerisation $P_n$ (1) and polydispersity index $P_w/P_n$ (2) of polyisobutylene on the initial concentration of a monomer $[M]_0$ ($[AlCl_3]_0 = 3.7 \times 10^{-3}$ mol/l; $k_p = 10^5$ l/mol·s; $k_t = 1$ s$^{-1}$; $D_{turb} = 1$ m$^2$/s; L = 1 m; $K_t = 0$; and $(E_m\text{-}E_p)/R = 5000$ mol × K)

The analysis of fast polymerisation reactions has shown that the effects, revealed during the mathematical simulation (diffusion model), are identical to the experimental effects of the cationic polymerisation of isobutylene (as an example). The important consequence of process nonisothermicity is its adverse effect on polymer quality, while the external thermostating is not effective enough in this case [52].

Production of polymers with a MWD close to typical for isothermal processes sets limitations, resulting in small polymer conversion. It, in turn, sets a limit for a reaction zone volume (device size) and process efficiency. These conclusions are in good agreement with calculated results, while the reaction spread pattern has a local zone ('torch'). 'Torch' size in the isobutylene polymerisation reaction is sufficiently lower than that of the reactor volume; therefore, some unreacted monomer usually skips the reacting zone [1, 2]. The torch mode effect comprising of gradients of temperature, monomer and catalyst concentrations, and monomers skipping along heat-conducting walls of a reactor, results in a lower polyisobutylene output in a single pass and a longer reaction time, and thus lowers the efficiency of the industrial bulk mixing reactors.

Similar results are obtained for the local process in a reaction zone using the mathematical modelling of fast liquid-phase reactions during the synthesis of low molecular weight compounds. Further study of fast chemical processes enables the discovery of new basic concepts for this group of reactions.

## 1.3 Fundamentals of Fast Chemical Processes in Turbulent Flows

### *1.3.1 Various Macroscopic Modes*

The study of fast liquid-phase electrophilic isobutylene polymerisation has revealed the influence of reaction zone geometrical parameters (radius R and length L) on

the output of the final products and the MW characteristics, as well as on the monomer conversion (**Table 1.1**). From the topochemical point of view, there are three macroscopic types of a process: A (plane front), B (intermediate mode) and C (torch) (**Figure 1.3**).

When the radius R is small (type A), the mixing of reactants is effective and active centres $A^*$ are uniformly distributed in a reaction zone (**Figure 1.3b**). The temperature is averaged along the radius of the reaction zone (**Figure 1.3a**). Surfaces of equal concentrations of monomer M, active centres $A^*$, and temperature T are planes, perpendicular to the reactor axis (plane front of a reaction). It guarantees high (up to 100%) (**Table 1.1**) monomer conversion, at sufficient reactor length, and the formation of quasi-plug flow conditions in highly turbulent flows. The consideration of longitudinal mixing (due to turbulence) is the main difference between this mode and the plug flow mode. As a consequence, and this is extremely important for practical applications, the 'smearing' of temperature in a reaction zone, due to longitudinal turbulent diffusion and fluctuations, results in constant temperature conditions in a reaction zone (quasi-isothermic mode). There are no analogues of this macroscopic mode. If the quasi-isothermic mode is achieved, it leads to the easy control of fast chemical reactions.

**Table 1.1 The dependence of monomer conversion rate, MW, and MWD on the isobutylene polymerisation reactor radius ($k_p = 10^5$ l/mol·s, $k_t = 20$ s$^{-1}$, $[M]_0 = 1$ mol/l, $[A^*] = 4.5$ mmol/l, $D_{turb} = 0.025$ m$^2$/s, and V = 1 m/s)**

| Reaction type | R, m | Conversion β, wt% | $P_n^*$ | $P_w/P_n^*$ |
|---|---|---|---|---|
| A | 0.01 | 100 | 13 | 2.0 |
| | 0.03 | 100 | 13 | 2.0 |
| | 0.05 | 100 (97.7) | 12 (30) | 2.1 (3.1) |
| | 0.08 | 99.3 | 10 | 2.1 |
| B | 0.10 | 90.0 (90.0) | 8 (21) | 2.2 (3.7) |
| | 0.25 | 65 | 6 | 2.4 |
| C | 0.50 | 32 (29.7) | 6 (17) | 2.4 (4.0) |

*Values in brackets are experimental results, obtained for isobutylene polymerisation in the presence of $AlCl_3$ in ethyl chloride (-30 °C (243 K)). The differences observed between the calculated and experimental values of $P_n$ and $P_w/P_n$ can be explained by the contribution of the selected $k_p/k_t$ ratios. Thus, these values are in good agreement.

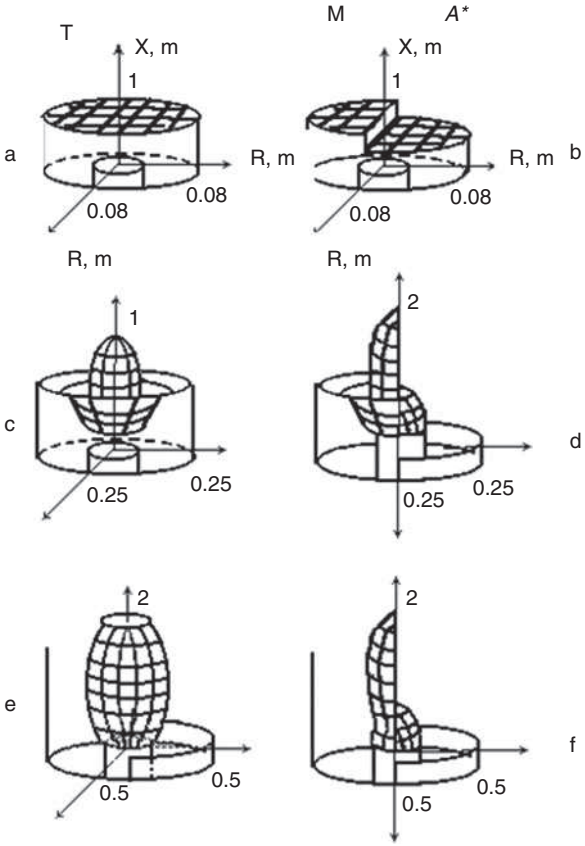


**Figure 1.3** Temperature fields T (a, b, e), concentration of active centres $A^*$ and monomer M (b, d, f), formed during the polymerisation of isobutylene in a flow R = 0.08 (a, b), 0.25 (c, d) and 0.5 m (e, f) ($[M]_0$ = 1 mol/l; $[AlCl_3]_0$ = 4.5 mmol/l; $D_{turb}$ = 0.025 $m^2/s$; $k_p$ = $10^5$ l/mol·s; $k_t$ = 20 $s^{-1}$; $T_0$ = 27 °C (300 K), V = 1 m/s). Macroscopic modes of type: A (a, b); B (c, d); and C (e, f)

Other extreme conditions (local torch mode) are realised at relatively small R values (type C). Active centres $A^*$ become deactivated in this case and do not have enough time for diffusion to the peripheral areas of a reaction zone, which are zones of unreacted monomer skip. As a consequence, the formation of specific and complex configuration fields of monomer concentration M, active centres $A^*$, and temperature are observed (**Figure 1.3e** and **f**). The radial size of a torch zone is determined by the ratio of the two competing processes: mixing of flows (due to turbulent diffusion) and deactivation of active centres. The reaction does not occur at the reactor walls and hence the product yield is always lower than 100% due to unreacted monomer skip (**Table 1.1**).

The third macroscopic mode B, always describes the process with the torch zone formation, but without the monomer skip zones. B mode (**Figure 1.3c** and **d**) (identical to macroscopic mode **C**) exerts a substantial influence on the homogeneity of the forming product (MWD broadens) and the monomer conversion increases compared with mode C (**Table 1.1**). It is necessary to consider that the MWD of a polymer product broadens with distance from the catalyst input point, along the reactor axis, and is an effect of the temperature increase and formation of macromolecules at different temperatures.

### *1.3.2 Relationship between a Reaction Zone Size and Kinetic and Hydrodynamic Parameters*

The critical radius $R_{cr}$, which determines the transition from the torch and intermediate modes of the reactor (macroscopic modes B and C) to the quasi-plug flow mode in turbulent flows (type A), depends on the ratio of monomer diffusion ($D_{\text{turb}}$) to the deactivation of the active centres $A^*$ ($k_t$) [42]:

$$R_{cr} = \sqrt{\frac{D_{\text{turb}}}{k_t}} \tag{1.42}$$

as the conditions required to achieve a quasi-plug flow mode, in turbulent flows, are determined by the following ratio $\tau_{\text{mix}} = R^2/D_{\text{turb}} \leq \tau_{\text{chem}} = 1/k_t$. **Equation 1.42** has the following form for fast reactions involving the synthesis of low MW compounds, as $\tau_{\text{chem}} = 1/k[C]^{n-1}$ [53–55]:

$$R_{cr} = \sqrt{\frac{D_{\text{turb}}}{k[C]^{n-1}}} \tag{1.43}$$

**Equations 1.42** and **1.43** provide the solution for the inverse problem [21]. The forced variation of the reactor geometry and the measurement of monomer conversion dependence on R, enable the estimation of the $D_{\text{turb}}/k_t$ value. It is important, that over a broad range of $k_t$, $D_{\text{turb}}$ and R values, there is a common dependence between the relative yield of polymer products and the ratio:

$$R\sqrt{k_t / D_{\text{turb}}} \tag{1.44}$$

The R variation range (of a reactive mixture V, in conditions of constant linear velocity) includes three hydrodynamic modes of liquid flow: laminar (small R), transient, and turbulent, depending on the numerical values of a characteristic mixing time $\tau_{\text{mix}} = R^2/D_{\text{turb}}$ (**Figure 1.4**).

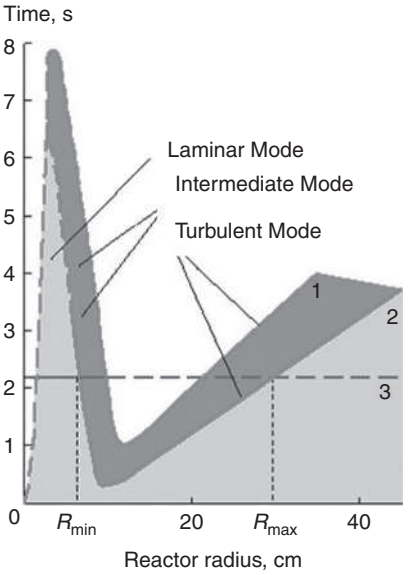


**Figure 1.4** Dependence of the mixing time $\tau_{mix}$ on reactor radius R in laminar, transient, and turbulent modes. V = 2.5 (1) and 5.0 (2) m/s. Dashed line 3 corresponds to the chemical reaction time $\tau_{chem}$

The diffusion coefficient is small in the laminar mode ($D \approx 10^{-9}$ m$^2$/s) and mixing times are high ($\tau_{mix}$ is proportional to $R^2$). Mixing becomes more effective in a transient mode ($D_{turb}$ increases) and $\tau_{mix}$ decreases. $D_{turb}$ values are high in a turbulent mode (>$10^{-3}$ m$^2$/s) and $D_{turb}$ is proportional to R, $\tau_{mix} = R^2/D_{turb} \sim R$. As **Figure 1.4** demonstrates, there are limitations on the minimum and maximum permissive value of the reactor radius for specific velocities of a reactive mixture V. In the $R > R_{max}$ and turbulent modes of reactants, the reaction front transforms from a flow plane into a torch plane, therefore causing an adverse effect on the fast chemical process conditions. At $R < R_{min}$ there is a transition to a transient mode and then to a laminar mode with an adverse effect on the mixing process. The leftmost area of the curve has no practical interest, where $\tau_{mix} < \tau_{chem}$, as efficiency here is negligible.

Therefore, there is a narrow (depending on $\tau_{chem}$ and V, and thus on $D_{turb}$) interval of reactor radius values which provide turbulent flow, with the formation of a plane reaction front, in association with a quasi-isothermal mode in a reaction zone ($R_{min} < R < R_{max}$). In this case, the mixing time of the reactants is lower than the chemical reaction time and the process occurs in a kinetic area. Despite this limitation, the process can be highly productive in reactors with practically feasible radii. For example, at V = 1 m/s and R = 30 mm, the reactor yield is about 20 m$^3$/h, while at V = 1 m/s and R = 150 mm, the yield achieved is 500 m$^3$/h. The increase in linear velocity of the reactive mixture, at a constant reactor radius, results in less time required for the necessary

mixing. Thus, the increase of flow rate V with process efficiency broadens the area of the effective reactor operation ($R_{min}$ decreases and $R_{max}$ increases) (**Figure 1.4**).

Obtaining information about the length of the reaction front L, along the reactor axis, is important for the practical and hardware implementation of a chemical process. As a reaction zone length, along the flow axis, is described by both the flow rate and reaction rate, there is a correlation between the effective time of passing a reactive mixture through a reaction zone ($\tau_{pass} = L/V$), necessary to achieve the required product yield, with the reaction time $\tau_{chem}$. The duration of a chemical reaction, depending on the process conditions, is determined by the smaller of one of two values: $1/k_t$ or $1/k_p[A^*]_0$ (for a fast polymerisation process) [2].

According to the kinetic scheme of polymerisation in a plug flow reactor, the polymer yield β is determined by the following ratio:

$$\beta = 1 - \exp\left\{-\frac{k_p[A^*]_0}{k_t}\left[1 - \exp\left(-k_t\frac{L}{V}\right)\right]\right\} \tag{1.45}$$

Introduction of the parameter $(L/V)_{eff}$, which is the effective passing time determined by a reaction zone length, provides 90% of the theoretical polymer yield at L→∞, giving:

$$\left(\frac{L}{V}\right)_{eff} = -\frac{1}{k_t}\ln\left\{1 + \frac{k_t}{k_p[A^*]_0}\ln\left[0.1 + 0.9\exp\left(-\frac{k_p[A^*]_0}{k_t}\right)\right]\right\} \tag{1.46}$$

The study of **Equation 1.17** will easily prove that the process is described by $k_t/k_p[A^*]$ << 1; inequality at high catalyst concentration and the polymer yield will tend to 100%. In this case:

$$(L/V)_{eff} = 2.3/k_p[A^*]_0 \tag{1.47}$$

The following ratio is achieved at a low catalyst concentration $k_t/k_p[A^*] \geq 1$ and:

$$(L/V)_{eff} = 2.3/k_t \tag{1.48}$$

Calculation of fast polymerisation processes with consideration of the longitudinal diffusion $R < R_{cr}$, demonstrates that the dependence of $(L/V)_{eff}$ -$1/k_p[A^*]_0$ at different $[A^*]_0$ values are close to those calculated by **Equation 1.46** (**Figure 1.5**). This opened the door to the easy and effective experimental estimation of constants $k_p$ and $k_t$ in processes of this type. Studying the dependence of the polyisobutylene yield on a reaction zone length and/or flow rate at various catalyst concentrations enabled the estimation of the constants $k_p$ and $k_t$, if two areas of ratios $1 < k_t/k_p[A^*] < 1$ are used, or at least

one of them is used if two areas are impossible to cover. The obtained value: $k_p = 10^6$ l/mol·s, corresponds to data in the literature [2] and $k_t = 17.5$ s$^{-1}$ at -30 °C (243 K).

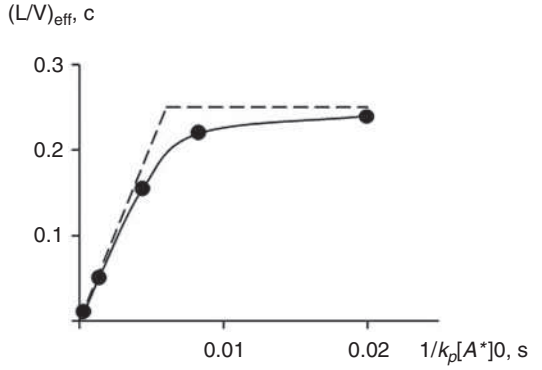


**Figure 1.5** The dependence of $(L/V)_{eff}$ on $1/k_p[A^*]$ for reactors with ideal (dotted line) and quasi-ideal (solid lines with points) displacement (V = 2.5 m/s; L = 0.08 m; $k_p = 10^5$ l/mol·s; $k_t = 10$ s$^{-1}$; and $T_0 = 573$ °C)

Therefore, the kinetic parameters of fast polymerisation processes ($k_p$ and $k_t$) and the linear velocity of reagent flow V determine the geometric size (R, L) and optimal configuration of a reaction zone. New opportunities and methods of process control have been revealed, allowing the control of the monomer conversion rate and MW characteristics of the forming polymer products, in particular, due to the forced change (limitation) of the reaction zone geometry (R, L). The principal conclusion is the necessity to reduce the reactor dimensions to the scale of a reaction zone.

### *1.3.3 The Influence of Linear Flow Rate on Molecular Characteristics of Forming Polymers*

If a polymerisation reaction occurs at $R > R_{cr}$, the reaction front has a torch form and kinetic parameters of a process, as well as the molecular characteristics of the forming polymer, which will not correspond to the theoretical plug flow model calculations. As a reactor's critical radius, which is a key parameter responsible for the transition to quasi-plug flow, is inversely proportional to $D_{turb}$, an increase of $D_{turb}$ leads to the growth of $R_{cr}$ providing an optimal $R < R_{cr}$ ratio. Under real conditions of a fast chemical process, an increase of $D_{turb}$, caused by an increase of V or change of reactor design, will lead to an increase of the conversion (reaction rate) due to the formation of a plane reaction front (excluding skip zones with unreacted monomer). In this case, the 'compression' of a reaction zone can be observed: the reaction mixture flow rate and the process rate (product yield) increase, despite the faster movement of reactants

through a reaction zone (**Figure 1.6**). This phenomenon is a feature of fast chemical reactions only, i.e., diffusion area processes in a mode close to the quasi-plug flow mode. For kinetic area processes, in perfect mixing or plug flow reactors, the dependence of the polymer concentration equilibrium on the reaction mixture flow rate is reverse [56].

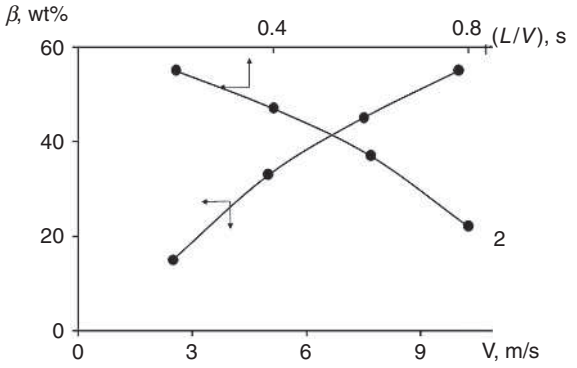


**Figure 1.6** The dependence of polyisobutylene conversion $\beta$ on the reaction mixture flow rate (1) and the passing time of reactants through a reaction zone (2). L = 2 m; $[M]_0$ = 2 mol/l; $[AlCl_3]_0$ = 4.5 mmol/l; R = 0.25 m; and $T_0$ = 27 °C (300 K)

When a fast polymerisation reaction is carried out in a quasi-plug flow mode, the degree of conversion growth with the increase of V (and $D_{turb}$ respectively), increases the polymer quality. This effect is caused by the smoothing of temperature maximums in the reaction zone (**Figure 1.7**), despite an increase of polymer product yield and corresponding heat release in the reaction zone.

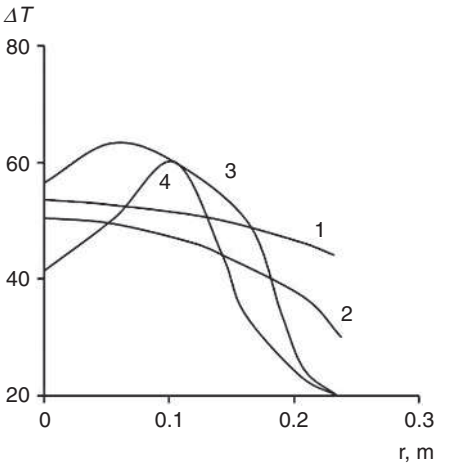


**Figure 1.7** Radial profiles of temperature gradient in a reaction zone $\Delta T$ for $D_{turb}$: 1, 2 – 0.045 $m^2/s$; 3, 4 – 0.01 $m^2/s$ for different monomer-catalyst contact times: 1, 3 – 0.2 s; 2, 4 – 0.1 s

The following equation stipulates a low sensitivity of the MW and MWD to temperature in a reaction zone (being more precise, a low sensitivity to the temperature gradient, which determines the process to be quasi-isothermal):

$$\Delta T < \frac{RT^2}{E_m - E_p} \tag{1.49}$$

Where T is the average temperature in a reactor, $\Delta T$ is the temperature gradient in a reaction zone, $E_m$ and $E_p$ are the activation energies of the chain transfer and chain growth reactions. The temperature gradient $\Delta T$ in a reaction zone is determined by the balance of the heat release process in a reaction zone and its dissipation in a convective transfer process:

$$\frac{\lambda_t \Delta T}{L_{chem}} = \frac{C_p \rho D_m k_t \Delta T}{V} = \rho V q \Delta M \tag{1.50}$$

Where $L_{chem} = V/k_t$ reactive zone length at $k[A^*]_0 \leq k_t$.

The combination of **Equations 1.49** and **1.50** provides us with summarising criteria, determining a quasi-isothermal process mode in turbulent displacement reactors:

$$\frac{k_t \lambda_t R T^2}{\rho V^2 q (E_t - E_p)} \geq 1 \tag{1.51}$$

In general, the quasi-isothermal mode in turbulent plug flow reactors will emerge, if the criteria in **Equations 1.42, 1.43** and **1.51** are met.

Therefore, flow rate variation is the method employed to substantially increase the yield of forming polymer product, increase its MW and quality (narrowing of MWD), i.e., it is an effective control instrument for the polymerisation process and the molecular characteristics of the forming polymers. This method is based on the change of temperature field profiles in the system coordinates of the reacting system reactor. Despite less contact time of a reacting mixture with the thermostating reactor wall ($\tau_{pass} = L/V$), the increase of V results in a substantial increase in the external heat removal efficiency and thus, to MW growth and MWD narrowing of the product yield.

The conclusion, based on the set of obtained results, is that fast liquid-phase polymerisation processes should be considered as a specific class of chemical reactions with individual specificity and methodology of study. The practical implementation of these chemical reactions should involve new variations of original technology, such as small-size tubular reactors, working in turbulent quasi-plug flow mode.

If the diffusion limitations for fast chemical reactions are removed, the key problem of their efficiency will be the intensification of heat and mass exchange efficiency.

## References


1. K.S. Minsker and A.A. Berlin in *Fast Polymerization Processes*, Gordon and Breach Publishers, Amsterdam, Netherlands, 1996.

2. J.A. Sangalov and K.S. Minsker in *Isobutylene Polymers and Copolymers: Fundamental Problems and Application Aspects*, Gilem, Ufa, Russia, 2001. [In Russian]

3. J.P. Kennedy and E. Marechal in *Carbocationic Polymerization*, Wiley, New York, NY, USA, 1982.

4. N. Kanoh, A. Gotoh, T. Higashimura and S. Okamura, *Macromolecular Chemistry*, 1963, **63**, 1, 106.

5. G.R. Brown and D.C. Pepper, *Polymer*, 1965, **6**, 3, 497.

6. M.A. Bonin, W.R. Busler and F.J. Williams, *Journal of American Chemical Society*, 1965, **87**, 6, 199.

7. N.S. Enikolopyan and S.A.Volfson in *Chemistry and Technology of Formaldehyde*, Khimiya, Moscow, Russia, 1968. [In Russian]

8. V.V. Korshak and S.V. Vinogradova in *Nonequilibrium Polycondensation*, Nauka, Moscow, Russia, 1972. [In Russian]

9. K.S. Minsker, A.A. Berlin, R.Y. Deberdeev and S.R. Ivanova, *Khimicheskaya Promyshlennost*, 2000, **11**, 26. [In Russian]

10. A.A. Berlin, K.S. Minsker and R.Y. Deberdeev, *Doklady Akademii Nauk*, 2000, **375**, 2, 218. [In Russian]

11. J.B. Monakov, A.A. Berlin and V.P. Zakharov, *Izvestiya Vuzov. Khimiya I Himicheskaya Tehnologiya*, 2005, **48**, 9, 3. [In Russian]

12. K.S. Minsker, V.P. Zakharov, I.R. Mullagaliev, J.B. Monakov and A.A. Berlin, *Zhurnal Prikladnoy Khimii*, 2000, **73**, 11, 1895. [In Russian]

14. K.S. Minsker, A.A. Berlin, R.H. Rakhimov, P.I. Kutuzov and V.P. Zakharov, *Zhurnal Prikladnoy Khimii*, 1999, **72**, 6, 996. [In Russian]

14. V.M. Busygin, G.S. Dyakonov, K.S. Minsker and A.A. Berlin, *Summa Tehnologiy*, 2000, **3**, 4, 48. [In Russian]

15. K.S. Minsker, A.A. Berlin, Y.M. Abdrashitov, J.K. Dmitriev, V.D. Shapovalov, V.P. Malinskaya and N.V. Alekseeva, *Himicheskaya Promyshlennost*, 1999, **76**, 6, 41. [In Russian]

16. K.S. Minsker, V.P. Zakharov, A.A. Berlin and R.Y. Deberdeev, *Himicheskaya Tehnologiya*, 2003, **3**, 30. [In Russian]

17. R.N. Gimaev, Y.A. Prochukhan, F.H. Kudasheva, M.A. Cadkin and A.D. Badikova, *Khimichaskaya Tekhnologiya Topliv i Masel*, 1998, **5**, 42. [In Russian]

18. R.N. Gimaev, Y.A. Prochukhan, F.H. Kudasheva, M.A. Cadkin, and A.D. Badikova, *Khimichaskaya Tekhnologiya Topliv i Masel*, 1998, **5**, 42. [In Russian]

19. S.V. Kolesov, M.A. Cadkin, A.D. Badikova, R.R. Rahmanov, F.H. Kudasheva and R.N. Gimaev, *Khimichaskaya Tekhnologiya Topliv i Masel*, 2002, **4**, 15. [In Russian]

20. J.R. Islamov, Y.A. Prochukhan and R.N. Gimaev, *Izvestiya Vuzov. Khimiya I Himicheskaya Tehnologiya Tehnologiya*, 1999, **42**, 2, 73. [In Russian]

21. A.A.Berlin, K.S. Minsker and K.M. Djumaev in *Novel Unified Energy and Resource Efficient High Performance Technologies of Increased Ecological Safety Based on Tubular Turbulent Reactors*, Niitjehim, Moscow, Russia, 1996. [In Russian]

22. A.G. Kasatkin in *Basic Processes and Machinery of Chemical Technology*, Khimiya, Moscow, Russia, 1983. [In Russian]

23. K. Denbig in *Theory of Chemical Reactors*, Nauka, Moscow, Russia, 1968. [In Russian]

24. O. Levenshpil in *Engineering Background for Chemical Processes*, Khimiya, Moscow, Russia, 1969. [In Russian]

25. A.A. Berlin and K.S. Minsker, *Nauka Proizvodstvu*, 2002, **53**, 3, 7. [In Russian]

26. K.S. Minsker and J.A. Sangalov in *Isobutylene and its Polymers*, Khimiya, Moscow, Russia, 1986. [In Russian]

27. A.A. Berlin, K.S. Minsker, J.A. Prochuhan, M.M. Karpasas and N.S. Enikolopyan, *Vysokomolekulyarnye Soedineniya*, 1986, **28**, 6, 461. [In Russian]

28. V.Z. Kompaniec, A.A. Konoplev, A.A. Berlin, Y.A. Prochukhan, K.S. Minsker, M.M. Karpasas and N.S. Enikolopyan, *Doklady Akademii Nauk SSSR*, 1987, **297**, 5, 1129. [In Russian]

29. A.Y. Fedorov, G.E. Litvak, L.P. Holpanov and V.A. Maljusov, *Doklady Akademii Nauk SSSR*, 1991, **319**, 2, 422. [In Russian]

30. A.Y. Fedorov, B.L. Rytov, A.A. Berlin and G.G. Aleksanyan, *Doklady Akademii Nauk*, 1995, **342**, 4, 494. [In Russian]

31. A.A. Berlin, K.S. Minsker, Y.A. Prochukhan and N.S. Enikolopyan, *Vysokomolekulyarnye Soedineniya*, 1989, **31**, 9, 1779. [In Russian]

32. A.A. Berlin, K.S. Minsker, Y.A. Prochukhan and N.S. Enicolopyan, *Polymer Plastics Technology*, 1991, **2**, 3, 253.

33. A.A. Berlin, K.S. Minsker, J.A. Sangalov, D.A. Novikov, T.N. Poznyak, Y.A. Prochukhan, A.I. Kirillov and A.G. Svinuhov, *Vysokomolekulyarnye Soedineniya*, 1979, **21B**, 6, 468. [In Russian]

34. A.A. Berlin, K.S. Minsker, Y.A. Prochukhan, M.M. Karpasas and N.S. Enikolopyan, *Doklady Akademii Nauk SSSR*, 1986, **287**, 1, 145. [In Russian]

35. Y.B. Zeldovich in *Chemical Physics and Thermodynamics: Selected Papers*, Nauka, Moscow, Russia, 1984. [In Russian]

36. V.Z. Kompaniec, A.A. Ovsyannikov and A.S. Polak in *Chemical Reactions in Turbulent Gas and Plasma Flows*, Nauka, Moscow, Russia, 1979. [In Russian]

37. K.S. Minsker, A.A. Berlin and V.P. Zakharov, *Vysokomolekulyarnye Soedineniya*, 2002, **44C**, 9, 1606. [In Russian]

38. A.A. Berlin, K.S. Minsker, J.A. Sangalov, V.G. Oshmyan, A.G. Svinuhov, A.P. Kirillov and N.S. Enikolopyan, *Vysokomolekulyarnye Soedineniya*, 1980, **22**, 3, 566. [In Russian]

39. K.S. Minsker, A.A. Berlin, A.G. Svinuhov, Y.A. Prochukhan and N.S. Enikolopyan, *Doklady Akademii Nauk SSSR*, 1986, **286**, 5, 1171. [In Russian]

40. A.A. Berlin and K.S. Minsker, *Doklady Akademii Nauk*, 1997, **355**, 3, 346. [In Russian]

41. A.A. Berlin, K.S. Minsker, K.M. Dyumaev, S.V. Kolesov and S.P.Ganceva, *Himicheskaya Promyshlennost*, 1997, **3**, 54. [In Russian]

42. S.K. Minsker, T.V. Golubeva, A.A. Konoplev, V.Z. Kompaniec, A.A. Berlin, K.S. Minsker and N.S. Enikolopyan, *Doklady Akademii Nauk SSSR*, 1990, **314**, 6, 1450. [In Russian]

43. S.K. Minsker, A.A. Konoplev, K.S. Minsker, Y.A. Prochukhan, V.Z. Kompaniec and A.A. Berlin, *Teoreticheskie Osnovy Khimicheskoy Tekhnologii*, 1992, **26**, 5, 686. [In Russian]

44. K.S. Minsker, K.M. Dyumaev, A.A. Berlin, N.P. Petrova, S.K. Minsker and A.Y. Fedorov, *Bashkirskiy Khimicheskiy Zhurnal*, 1995, **2**, 3–4, 41. [In Russian]

45. A.A. Berlin, K.S. Minsker and V.P. Zakharov, *Doklady Akademii Nauk*, 1999, **365**, 3, 360. [In Russian]

46. K.S. Minsker, V.P. Zakharov and A.A. Berlin, *Teoreticheskie Osnovy Khimicheskoy Tekhnologii*, 2001, **35**, 2, 172. [In Russian]

47. D.A. Frank-Kameneckiy in *Diffusion and Heat Transfer in Chemical Kinetics*, Nauka, Moscow, Russia, 1987. [In Russian]

48. A.A. Berlin, *Sorosovskiy Obrazovatelnyi Zhurnal*, 1998, **3**, 48. [In Russian]

49. A.Y. Fedorov and G.E. Litvak, *Vysokomolekulyarnye Soedineniya*, 1991, **33A**, 10, 2626. [In Russian]

50. D.A. Bajzenberger and D.H. Sebastian in *Engineering Problems of Polymer Synthesis*, Khimiya, Moscow, Russia, 1988. [In Russian]

51. A.D. Gosmen, V.M. Ranchel and D.B. Spolding in *Numerical Methods of Viscous Liquid Flow Study*, Mir, Moscow, Russia, 1972. [In Russian]

52. Y.A. Prochukhan, K.S. Minsker, A.A. Berlin, J.A. Tumanyan and N.S. Enikolopyan, *Doklady Akademii Nauk SSSR*, 1986, **291**, 6, 1425. [In Russian]

53. K.S. Minsker and V.P. Zakharov, *Teoreticheskie Osnovy Khimicheskoy Tekhnologii*, 2000, **34**, 2, 221. [In Russian]

54. K.S. Minsker, V.P. Zakharov, A.A. Berlin and G.E. Zaikov, *Polymer News*, 1999, **24**, 7, 249.

55. K.S. Minsker and V.P. Zakharov, *Bashkirskiy Khimicheskiy Zhurnal*, 1997, **4**, 3, 32. [In Russian]

56. A.A. Berlin, S.A. Volfson and N.S. Enikolopyan in *Polymerization Processes Kinetics*, Khimiya, Moscow, Russia, 1978. [In Russian]

# 2 Heat and Mass Exchange Intensification in Fast Liquid-phase Processes

Agitation in liquid media is the most widespread method to increase the level of turbulence in a reaction zone, and intensify the heat and mass transfer processes in chemical and other industries [1, 2]. Identical conditions of a chemical process must be achieved in order to obtain a product with the same composition and properties in a particular section of a reaction volume. A solution is formed when the intensive mixing of a reactive medium results in the formation of a homogeneous concentration of reactants, where the mixing time does not exceed the duration of the chemical reaction ($\tau_{mix} < \tau_{chem}$). Traditional large volume devices with mechanical agitators cannot usually provide the required uniformity of concentration in a reaction zone of fast chemical reactions, especially when using highly viscous technological blends [3]. In particular, if the efficiency of the agitation of a highly viscous reaction mixture is low (from $10^{-3}$ to $10^{2}$–$10^{3}$ Pa·s), while the macrochain growth rate speed ($k_r > 10^2$ l/mol·s) and the heat released is considerable (60–100 kilojoules/mol), the temperature will rapidly grow in the areas of catalyst and monomer introduction [4].

As a higher production yield and efficiency are preferable, a small-sized device approach becomes attractive as such devices have both high specific production efficiency and are capable of creating sufficient turbulence level in a reaction zone [5, 6]. As demonstrated in publications [7, 8], the turbulence intensiveness reaches 50–70% of its maximal level in cylindrical devices with turbulators (this value reaches 1–3% in conditions of undisturbed flow in smooth channels). Devices with turbulators [9–12] (including ones of convergent-divergent construction [13–15]) do not have internal moving elements and can provide uniform conditions for both chemical reactions and mass exchange physical processes. Use of small-sized tubular devices for processes limited by the mass exchange stage is attractive as they provide an opportunity for controlling these processes by the use of higher turbulence, as the reactants are agitated in a reaction zone. It assumes the development of theoretical methods for studying the flow characteristics in tubular channels to create an optimal basis for carrying out fast chemical processes, as well as intensifying the heat and mass exchange.

## 2.1 Turbulent Mixing of a Single-phase Reaction Mixture

Experimental study of the turbulent flow characteristics in reaction zone coordinates meets considerable and sometimes irresolvable difficulties. In this case, one of the available and effective ways to study this process is by the use of mathematical modelling. This method gives an opportunity of studying a specific process stage, which cannot be measured experimentally, as well as analysing variants, which cannot be experimentally determined in the laboratory.

### *2.1.1 Mathematical Modelling*

The mathematical model, which makes it possible to consider the influence of the hydrodynamic conditions of flow on the processes of mixing and chemical transformations of reacting substances in a liquid phase, assumes that the average flow characteristics of a multicomponent system can be described by the equations of continuum mechanics and will satisfy conservation laws.

The theoretical description of the turbulent mixing of reactants in tubular devices is based on the following model assumptions: the medium is a Newtonian incompressible medium, and the flow is axis-symmetrical and nontwisted; turbulent flow can be described by the standard model [16], with such parameters as specific kinetic energy of turbulence $K$ and the velocity of its dissipation $\varepsilon$; and the coefficient of turbulent diffusion is equal to the kinematic coefficient of turbulent viscosity $D_{\text{turb}} = \nu_T = \mu_T/\rho$.

The numerical solution of the equations of continuum turbulent flow with effective viscosity coefficient $\mu = \mu_T + \mu_m$ ($\mu_m$ – the dynamic coefficient of molecular viscosity) is with a $C$-$\varepsilon$ turbulence model by the finite-element method on a nonequilibrium calculation network [17]. These equations have the following form in cylindrical coordinates [14, 15, 18, 19].

Continuity Equation:

$$\frac{1}{r}\frac{\partial(ru)}{\partial r} + \frac{\partial v}{\partial z} = 0 \tag{2.1}$$

Navier–Stokes Equations (pulse transfer equations):

$$\frac{\rho}{r}\frac{\partial(ruu)}{\partial r} + \rho\frac{\partial(uv)}{\partial z} = -\frac{\partial p}{\partial r} - \left(\frac{1}{r}\frac{\partial(r\tau_{11})}{\partial r} - \frac{\tau_{33}}{r} + \frac{\partial\tau_{21}}{\partial z}\right) \tag{2.2}$$

$$\frac{\rho}{r}\frac{\partial(ruv)}{\partial r} + \rho\frac{\partial(vv)}{\partial z} = -\frac{\partial p}{\partial z} - \left(\frac{1}{r}\frac{\partial(r\tau_{12})}{\partial r} + \frac{\partial\tau_{22}}{\partial z}\right) \tag{2.3}$$

Where tension tensor components are:

$$\tau_{12} = -2\mu \frac{\partial u}{\partial r},\ \tau_{22} = -2\mu \frac{\partial v}{\partial z},\ \tau_{33} = -2\mu \frac{u}{r} \tag{2.4}$$

$$\tau_{12} = \tau_{21} = -\mu\left(\frac{\partial v}{\partial r} + \frac{\partial u}{\partial z}\right) \tag{2.5}$$

Equations of turbulence specific kinetic energy transfer and its dissipation:

$$\frac{\rho}{r}\frac{\partial(ruK)}{\partial r} + \rho\frac{\partial(vK)}{\partial z} = \frac{1}{r}\frac{\partial}{\partial r}\left(\frac{\mu}{\sigma_k}\frac{r\partial K}{\partial r}\right) + \frac{\partial}{\partial r}\left(\frac{\mu}{\sigma_k}\frac{\partial K}{\partial z}\right) + \mu_m G - \rho\varepsilon \tag{2.6}$$

$$\frac{\rho}{r}\frac{\partial(ru\varepsilon)}{\partial r} + \rho\frac{\partial(v\varepsilon)}{\partial z} = \frac{1}{r}\frac{\partial}{\partial r}\left(\frac{\mu}{\sigma_E}\frac{r\partial\varepsilon}{\partial r}\right) + \frac{\partial}{\partial z}\left(\frac{\mu}{\sigma_E}\frac{\partial\varepsilon}{\partial z}\right) \tag{2.7}$$

$$+\mu_m C_1 G\varepsilon / K - C_2\rho\varepsilon^2 / K$$

$$G = \frac{1}{\mu^2}\left(\frac{1}{2}\left(\tau_{11}^2 + \tau_{22}^2 + \tau_{33}^2\right) + \tau_{12}^2\right) \tag{2.8}$$

$$\mu_{\mathrm{T}} = \rho\frac{C_\mu K^2}{\varepsilon} \tag{2.9}$$

Standard parameters of $C$-$\varepsilon$ model of turbulence were used for calculations [91]: $C_1$ = 1.44, $C_2$ = 1.92, $C\mu$ = 0.09, $\sigma_K$ = 1.0, $\sigma_E$ = 1.3.

**Equations 2.1–2.9** are valid for the flow of the main volume of liquid. However, they are inapplicable for the device casing contacting area. In this case, the law of wall should be used: the profile of the flow velocity near the solid wall has a logarithmic distribution:

$$\frac{V_{\tan}}{\sqrt{\tau/\rho}} = \frac{1}{k}\ln\frac{E\delta}{\nu_m}\sqrt{\frac{\tau}{\rho}} \tag{2.10}$$

Where $\delta$ is the distance from the wall. In the process of iteration at the given value of velocity of the coaxial flow of a reacting mixture $V_{\tan}$, the tangential tension $\tau$ value and effective viscosity can be calculated using **Equation 2.10**:

$$\mu = \delta\tau / V_{\tan} \tag{2.11}$$

The kinetic energy of turbulence $C$ can be obtained using the $C$-$\varepsilon$ model of turbulence, while the dissipation of specific kinetic energy of turbulence $\varepsilon$ is calculated in the following way:

$$\varepsilon = \frac{C_\mu^{0.75} K_w^{1.5}}{k\delta} \tag{2.12}$$

**Equations 2.10–2.12** with the following values of constants: $k$ = 0.4, $E$ = 9.0 are standard boundary conditions for all solid surfaces, if flows are in turbulent mode [16].

Reynolds-averaged Navier–Stokes equations with $K$-$\varepsilon$ closure make it possible to estimate the characteristic mixing times of reactants of various scales.

Characteristic time of turbulent mixing [20]:

$$\tau_{\text{turb}} = l^2 / D_{\text{turb}} \tag{2.13}$$

Where $l$ is the linear size of an area, where the creation of a uniform concentration field of reactants is required.

If the turbulent diffusion coefficient $D_{\text{turb}}$ is assumed to be equal to the kinematic coefficient of turbulent viscosity $\nu_T$, which in turn, can be expressed *via* the specific kinetic energy of turbulence $K$ and its dissipation rate $\varepsilon$, then **Equation 2.13** will have the following form:

$$\tau_{\text{turb}} = 11.1\varepsilon\, l^2 / \text{K}^2 \tag{2.14}$$

However, **Equations 2.13** and **2.14** do not consider the molecular diffusion and viscous flow effects, which occur in the turbulent flow of small amounts of substance. That is why, if micromixing processes form the limiting stage, other estimating expressions should be used. The engulfment model is often used in this case [21, 22], with the following equation to estimate the characteristic mixing time:

$$\tau_{\text{micro}} = 17.3(\nu/\varepsilon)^{0.5} \tag{2.15}$$

Where $\nu$ is the kinematic viscosity.

Homogenisation of the medium is, in many cases, limited by the exchange processes between large turbulent vortexes and smaller inner ones, i.e., by mesomixing [23]:

$$\tau_{\text{meso}} = 1 - 2(l^2/\varepsilon)^{1/3} \tag{2.16}$$

Comparison of the aforementioned characteristic mixing times makes it possible to reveal the limiting mechanism of concentration field equalisation during fast chemical processes. It is achieved by the selection of maximum values from those calculated using **Equations 2.13–2.16** and their comparison with the characteristic time of the chemical reaction $\tau_{\text{chem}}$. If the latter value is significantly higher, then the chemical transformation occurs in the kinetic area and diffusion limitations do not exert a negative influence on the composition of the final product. If a mixer for medium

homogenisation is studied without taking the chemical transformation into account, then it is necessary to compare the limiting time of mixing with the average duration of reactants passing through a reaction zone $\tau_{pass}$. To achieve optimal conditions of process realisation, the mixing time should not exceed the duration of a chemical reaction.

To test the suitability of this approach for modelling turbulent mixing in tubular channels, the flow process of a liquid with dynamic viscosity factor $\mu$ = 1 MPa·s and density $\rho$ = 1,000 kg/m$^3$ was determined. The boundary conditions are z-axis symmetry (the longitudinal coordinate) and adhesion of the liquid onto the solid surfaces of a reactor. The reactor output (CD line) and linear flow rate = 5 m/s were set at reactor input (AB line, along with the symmetry axis) (**Figure 2.1**). The length of the input and output openings of a reactor was many times higher than its diameter to eliminate the influence of input and output turbulence parameters on the mixing characteristics of the reactants under study.

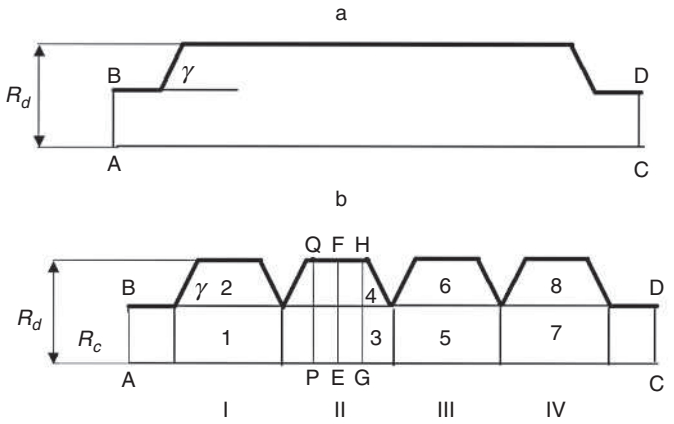


**Figure 2.1** The chart of turbulent tubular units of cylindrical (a) and diffuser-confusor (b) types. $\gamma$- diffuser opening angle; $R_c = d_d/2$ is the wide part radius (of a diffuser); $R_c = d_c/2$ is the narrow part radius (confusor); and 1–8 are device sections; I–IV are diffuser-confusor sections

To confirm adequacy of the calculations, obtained theoretical results have been compared to existing experimental data for a cylindrical reactor (**Figure 2.1**a) (at Reynolds Number (Re) = 2 × 10$^5$) [24]; the obtained results agree with calculations in [25]. In particular, **Table 2.1** demonstrates the circulation zone length values. Such a zone emerges in the peripheral area of a reactor, immediately after the reactants enter the widening channel (conical expansion). It can be seen that the calculated and experimental values are in satisfactory agreement (the error does not exceed 15%).

| Table 2.1 Calculated and experimental length of circulation zone | | | |
|---|---|---|---|
| **Diffusor opening angle γ, degrees** | $L_{circ}/d_d$ | | |
| | **Experiment*** | **Calculation** | |
| | | **Real operation** | **According to [98]**** |
| 30 | 4.1 | 3.4 | 3.5 |
| 90 | 4.6 | 4.7 | 4.7 |
| *Adapted from V.P. Zakharov, A.A. Berlin and G.E. Zaikov, *Bulgarian Chemistry and Industry*, 2005, **76**, 2 [97]<br>**Adapted from J.B. Monakov, A.A. Berlin and V.P. Zakharov, *IzvestiyaVuzov. Himiya I HimicheskayaTehnologiya*, 2005, **48**, 9, 3 [98] | | | |

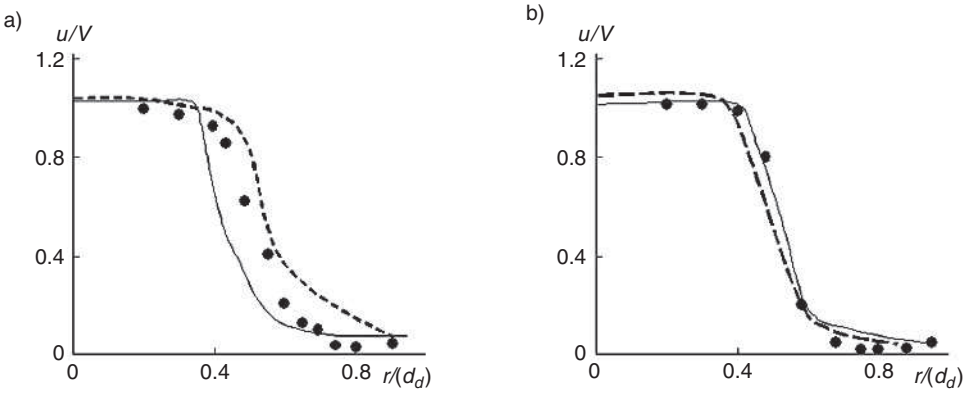


**Figure 2.2** Axial profile of the flow rate in the z = $d_d$ section of cylindrical reactor at $\gamma = 30^o$ (a) and $\gamma = 90^o$ (b): • = experiment [97]; dotted line = calculation [25]; and solid line = calculation (real operation)

The convergence of results can also be seen for the axial flow rate profiles (**Figure 2.2**), as well as for the specific kinetic energy of turbulence (**Figure 2.3**). Obtained results form the basis of the solid calculation-based prediction of reaction mixture turbulent mixing under other conditions. In particular, it can be used for channels of various size and geometry.

Thus, the selected mathematical model enables the calculation of the turbulent mixing characteristics in tubular reactors with different channel geometry. The adequacy of obtained results is confirmed by the correlation of experimental and calculated data with sufficient reliability.

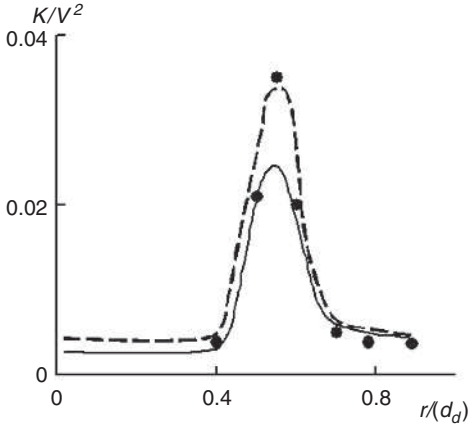


**Figure 2.3** The profile of the specific kinetic energy of turbulence in the z = d section of a cylindrical device at $\gamma = 90^{o}$: • = experiment [97]; dotted line = calculation [25]; and solid line = calculation (real operation)

### *2.1.2 The Influence of the Method of Reactant Addition*

In conditions of diffusion control, the chemical reaction process is determined not only by its rate and heat effect, but by the intensity of heat and mass transfer processes as well. This intensity, in turn, can be strongly dependent on the hydrodynamic conditions, i.e., such factors as the reaction mixture flow rate $V$, the way the feedstock is introduced into a reactor, reactor geometry and size, and so on. Experimental and calculated data [26–28] demonstrate that considerable improvement of mixing and the effective diffusion rate of heat and mass can be achieved, only if circulation zones are present in the reaction area. The formation of circulation zones is achieved by the application of various mechanical devices [29], combined with the intensification of reaction mixture circulation [25, 30]. This fact is confirmed by the analysis of mixing two nonreacting liquid flows in five types of tubular reactors and varying the geometry of feedstock input (**Figure 2.4**) [30, 31].

The results of the modelling of liquid flows, based on Navier–Stokes equations and the $C$-$\varepsilon$ model of turbulence, demonstrate that the turbulent diffusion coefficient $D_{\text{turb}}$ increases ($\tau_{\text{mix}}$ decreases) for reactors with a radial input of reactants (P2- and P3-type mixers), especially for reactors with conical widening at the input of the liquid flows (P4, P5). For P5-type reactors, the time of mixing decreases approximately tenfold compared with the P1-type at given flow parameters (**Figure 2.5**). An increase of $D_{\text{turb}}$ results in a faster equalisation of the reactant concentration profile. Analysis of the construction of the reaction devices confirms that drops of hydraulic pressure

in these mixers, caused by local resistance, have the same decimal order. It is evident to expect, in this case, that intensification of reacting blend mixing will cause a positive effect.

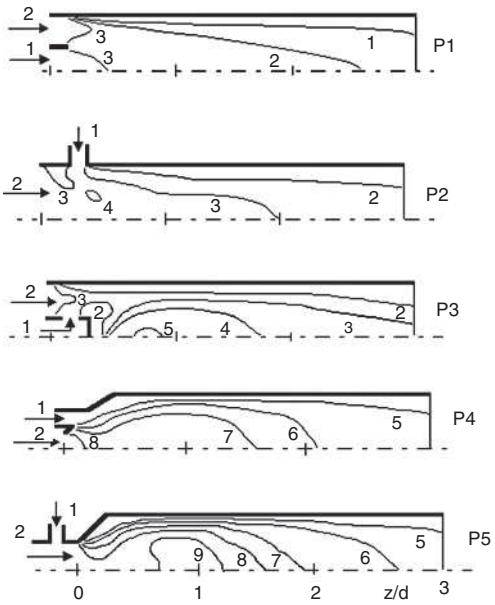


**Figure 2.4** Introduction of reactants and the turbulent diffusion coefficient $D_{turb}$ distribution in the tubular device volume. $V$ = 5 m/s, $R$ = 0.25 m, $D_{turb}$ = 0.01 (1); 0.02 (2); 0.03 (3); 0.04 (4); 0.05 (5); 0.1 (6); 0.15 (7); 0.2 (8); and 0.3 (9) $m^2/s$

A significant factor is the choice of the pulsation characteristics of the input section (the reaction mixture preliminary turbulisation intensity). A change in the initial turbulisation level, expressed by $\sqrt{K/V}$ (C is the specific kinetic energy of turbulence) causes a significant effect on the mixing characteristics in reactors with a coaxial and radial input of reactants (P1-P2), and is insignificant for P4 and P5 reactors with a circulation zone (**Figure 2.5**). For P4- and P5-type reactors, the initial turbulisation exerts a significant influence on the recirculation zone, as the size and intensity are reduced, with the increase of the initial turbulisation causing a decrease of $D_{turb}$ (**Figure 2.5**). Choosing the best hydrodynamic conditions for a process of chemical technology enables an improvement of the transfer processes and therefore, control of the final product quality during fast liquid-phase reactions.

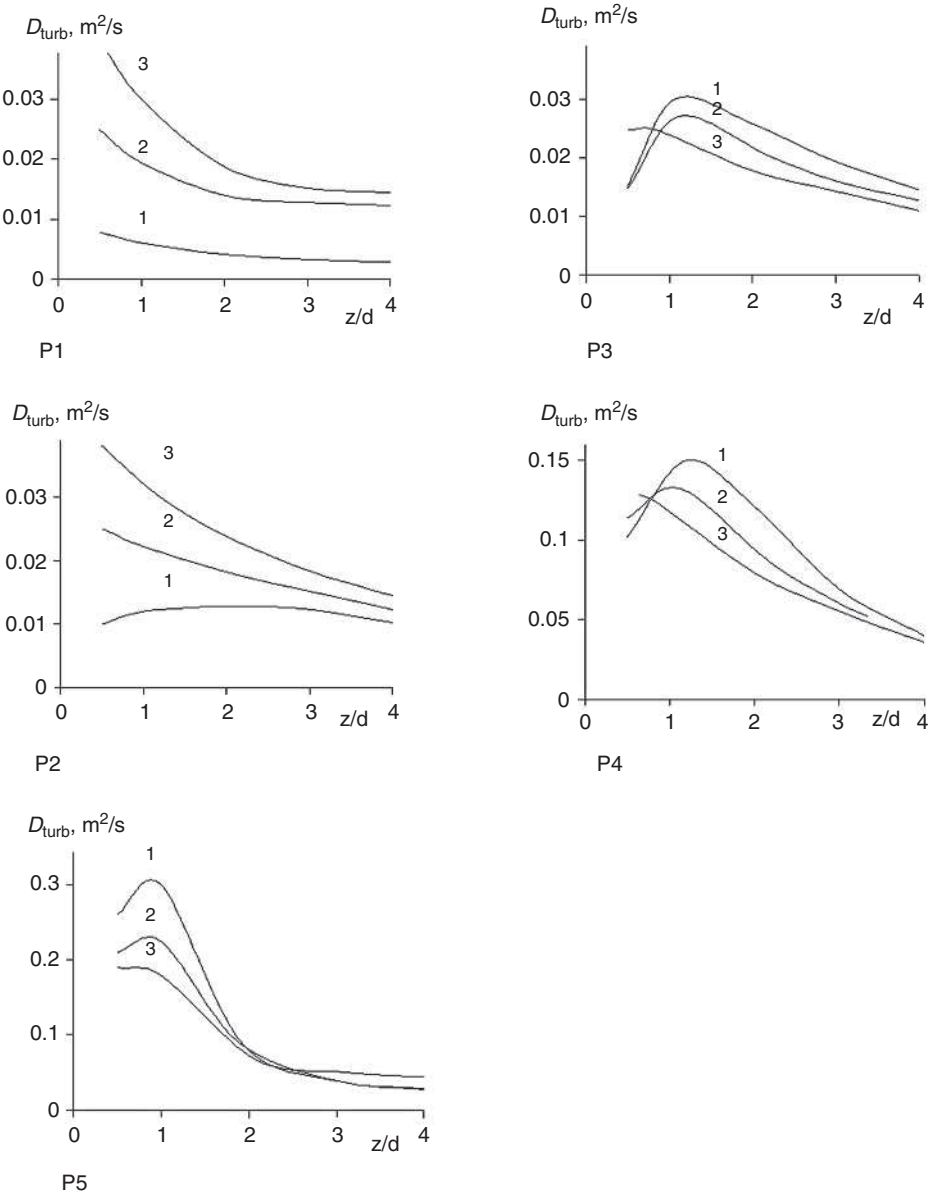


**Figure 2.5** The dependence of the average sectional turbulent diffusion coefficient on the preliminary turbulisation of the flow $\sqrt{K/V}$ = 10 (1), 50 (2), and 100 (3)%

Therefore, the uniform distribution of reaction mixture components can only be obtained with highly turbulent mixing of liquid flows, which is a core requirement for effective fast chemical reactions and mass transfer processes. The effectiveness of the homogenisation of the reaction mixture is substantially affected by the geometry of the reactor's input zone, as well as by the way the flows are introduced. The effectiveness of mixing ($D_{turb}$ increases, $\tau_{mix}$ decreases) grows substantially when one of the reactants is introduced in a radial way. Conic widening at the initial part of the device favours the formation of circulation zones. The value of $\tau_{mix}$ decreases by at least one order of magnitude, compared with the introduction of reactants without conic widening.

Changing the method in which flows are introduced into a tubular device does not solve the problems of the mixing of liquid media which differ in density and especially viscosity [32]. In particular, despite the unlimited solubility of concentrated sulfuric acid ($\rho$ = 1.92 g/sm$^3$, $\mu$ = 27.8 mPa·s) or glycerol ($\rho$ = 1.26 g/sm$^3$, $\mu$ = 1490 mPa·s) in water ($\rho$ = 1 g/sm$^3$, $\mu$ = 1 mPa·s), the phase boundary surface, within bulk mixing devices, demonstrates long-lasting stability even under intensive mechanical mixing. Both sulfuric acid and glycerol form 'puddles' at the bottom of the device and then distribute unevenly in the form of clots, bunches, droplets, and so on. A substantial increase in the effectiveness of mixing two flows, different in density and viscosity, is achieved by an increase and stabilisation of the turbulent coefficient $D_{turb}$ at a certain level along a reaction zone; therefore, the influence of the geometry of the tubular channels on the efficiency of the mixing of the liquid channels, requires consideration.

### *2.1.3 The Influence of Device Geometry*

A substantial increase in the mixing of the reaction mixture, caused by the effect of conical widening in the input section, resulted in the development of device geometry with hydrodynamic resistance in the form of consecutive narrowing and widening along the axis (diffuser-confusor transitions) [33].

Calculations have shown that an increase of the diffuser opening angle $\gamma$ from 5 to 30°, i.e., a change of cylindrical channel (**Figure 2.1a**) to a diffuser-confusor type (**Figure 2.1b**), leads to an almost threefold increase of the turbulent diffusion coefficient. However, the values remain almost unchanged upon further increase of $\gamma$ (**Figure 2.6**). It is interesting to note that the level of turbulent mixing in the peripheral and central areas is constant, thus characteristics of the turbulent mixing of reactants are constant in all volumes over a wide range of diffuser opening angles (**Figure 2.6**); this is first of all determined by the much lower flow rate in the peripheral zone of the tubular turbulent diffuser-confusor device ($R > d_c/2$), than in its central zone ($R < d_c/2$) (**Figure 2.7**).

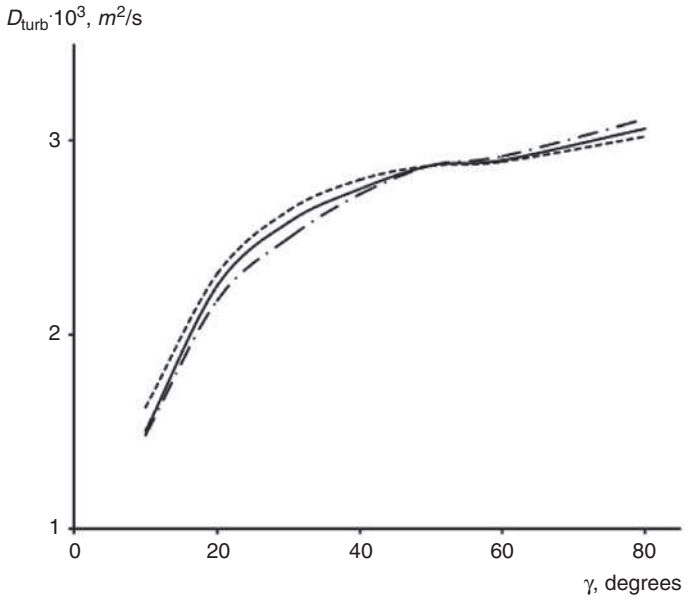


**Figure 2.6** Volume-averaged turbulent diffusion coefficient values in central and peripheral zones

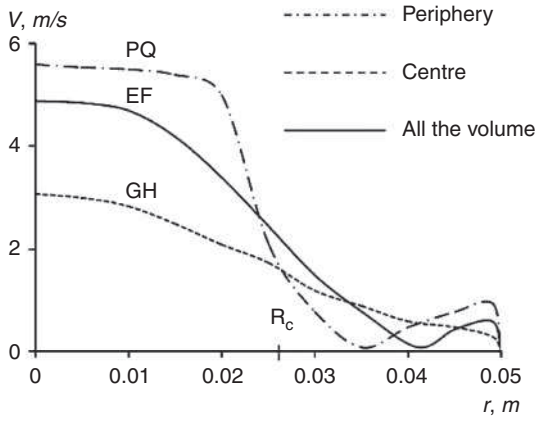


**Figure 2.7** Absolute velocity profiles EF, GH, and PQ at $\gamma = 45^o$ (see **Figure 2.1b**) (Re = $2.5 \times 10^5$, $d_d$ = 0.05 m, and $V$ = 5 m/s, $\rho$ = 1,000 kg/m$^3$)

| **Table 2.2 Averaged values of the turbulent diffusion coefficient $D_{turb} \times 10^3$ m$^2$/s in a tubular device** | | | | | | | | |
|---|---|---|---|---|---|---|---|---|
| **γ** | 5° | 10° | 17° | 30° | 45° | 60° | 75° | 85° |
| **Device zones** | | | | | | | | |
| 1 | 1.03 | 1.34 | 1.55 | 1.60 | 1.58 | 1.54 | 1.48 | 1.42 |
| 2 | 1.17 | 1.54 | 1.90 | 2.22 | 2.38 | 2.47 | 2.49 | 2.49 |
| 3 | 1.12 | 1.76 | 2.36 | 2.78 | 2.86 | 2.88 | 2.97 | 2.92 |
| 4 | 1.01 | 1.50 | 2.05 | 2.60 | 2.79 | 2.88 | 2.98 | 2.98 |
| 5 | 1.09 | 1.75 | 2.49 | 3.16 | 3.47 | 3.67 | 3.97 | 3.94 |
| 6 | 0.94 | 1.43 | 2.04 | 2.74 | 3.09 | 3.31 | 3.55 | 3.58 |
| 7 | 1.09 | 1.75 | 2.43 | 3.08 | 3.38 | 3.60 | 3.81 | 3.90 |
| 8 | 0.99 | 1.43 | 2.03 | 2.65 | 2.96 | 3.20 | 3.40 | 3.48 |
| **Diffuser-confusor sections** | | | | | | | | |
| I | 1.12 | 1.47 | 1.79 | 2.03 | 2.14 | 2.18 | 2.18 | 2.16 |
| II | 1.05 | 1.59 | 2.15 | 2.66 | 2.81 | 2.88 | 2.98 | 2.97 |
| III | 0.99 | 1.54 | 2.18 | 2.87 | 3.21 | 3.42 | 3.68 | 3.69 |
| IV | 1.02 | 1.53 | 2.16 | 2.78 | 3.09 | 3.32 | 3.52 | 3.61 |

Comparison of the turbulent diffusion coefficients $D_{turb}$, in various zones of the tubular reactor (**Table 2.2**), has shown that a sufficiently uniform $D_{turb}$ field is only achieved in the diffuser-confusor device. For real fast liquid-phase chemical processes, a reasonable solution is a diffuser-confusor type reactor with a diffuser opening angle $\gamma$ of 20 – 45°.

In a constant section, the initial input turbulence parameters of the cylindrical reactor exert a significant influence on the degree of turbulisation of a reaction mixture. The $D_{turb}$ value decreases when moving from the input zone, thus decreasing the liquid medium mixing intensity along the longitudinal axis (**Figure 2.8**a). In order to increase the flow turbulisation and therefore, make the mixing of reactants more effective, a diffuser-confusor reactor is a reasonable solution (**Figure 2.1b**). The diffuser-confusor channel allows maintaining high values of turbulisation parameters along the longitudinal axis of the tubular device, which is made of several diffuser-confusor sections (**Figure 2.8b**).

In addition to the diffuser opening angle, $\gamma$, the key parameters allowing the optimisation of turbulent mixing efficiency, in a diffuser-confusor reactor, are the diffuser to confusor diameter ratios $d_d/d_c$ and the length of the diffuser-confusor section $L_c/d_d$.

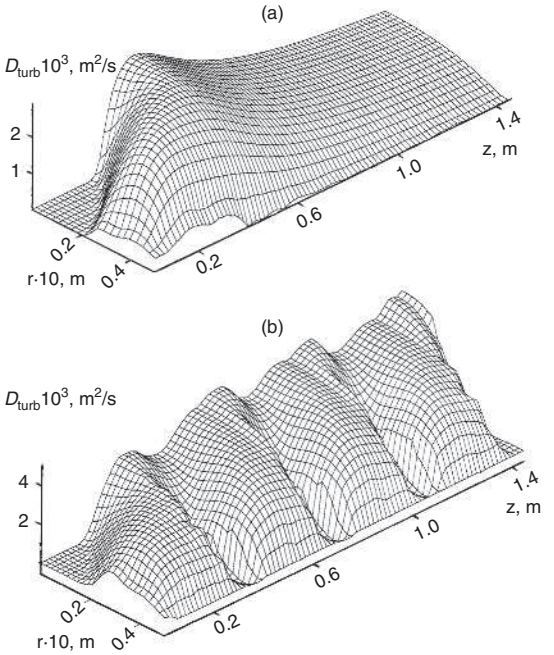


**Figure 2.8** Volume distribution of the turbulent diffusion coefficient $D_{turb}$ along a cylindrical (a) and diffuser-confusor; and (b) types of tubular turbulent device (Re = $2 \times 10^5$, $d_d$ = 0.05 m, and $V$ = 4 m/s, $\rho$ = 1000 kg/m$^3$)

The usual limiting mechanism of the concentration profile alignment of the reactants, in polymer synthesis reactions, is micromixing (molecular level mixing), because of the highly viscous flows. The minimum characteristic micromixing time corresponds to the maximum dissipation of the specific kinetic energy of turbulence $\varepsilon$. It is therefore of primary importance to reveal the correlation between the average value of the dissipation of specific kinetic energy of turbulisation and the ratios of geometrical parameters of the reactor, where the key ratios are $d_d/d_c$ and $L_c/d_d$.

According to calculations [34], an increase of $L_c$ section length, at fixed $\gamma$ and $d_d/d_c$ values, results at first in the growth of specific kinetic energy of turbulence dissipation and then leads to its decrease. Similar effects are observed at other $d_d/d_c$ values. Thus, there is a maximum average specific kinetic energy of turbulence dissipation $\varepsilon$ at certain (optimal) geometric parameters of diffuser-confusor reactors. The problem is lessened for the tubular device by a high degree of mixing, as the ratio of its geometric parameters is independent of the $\gamma$ angle.

The maximum average dissipation of specific kinetic energy of turbulisation $\varepsilon$ has been selected as the optimisation criterion for the geometry of a tubular turbulent

diffuser-confusor device. Optimisation parameters are the diffuser-confusor diameter ratio $d_d/d_c$ and the section length to diffuser diameter ratio $L_s/d_d$. **Figure 2.9** illustrates the dependence of the average dissipation of specific kinetic energy of turbulisation on the ratio of the reactor's geometrical parameters at $\gamma = 45^o$. The maximum (M) indicates the optimal parameters for a diffuser-confusor type reactor and corresponds to a diffuser-confusor diameter ratio of $d_d/d_c$ = 1.6, and section length to diffuser diameter of $L_s/d_d$ = 1.7. The optimal parameters are constant in the $\gamma$range of 30 – 85°.

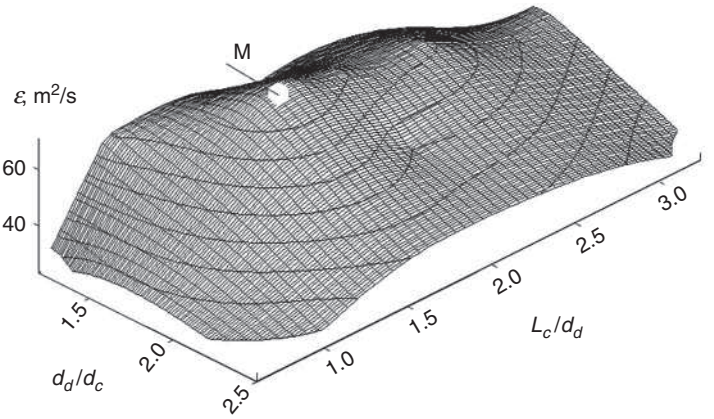


**Figure 2.9** Dependence of the average dissipation of specific kinetic energy of turbulence $\varepsilon$ on the ratio of geometric parameters of a tubular turbulent diffuser-confusor device

Therefore, the tubular turbulent diffuser-confusor device provides uniform conditions and a high level of turbulent mixing, caused solely by the channel geometry, for any chemical and mass exchange process with no additional mixing devices required. Due to its simplicity and high reliability of design, this type of device is extremely promising for fast liquid-phase processes, where maintaining the $\tau_{mix} < \tau_{chem}$ condition is very difficult and production safety requirements are extremely severe. In addition, the diffuser-confusor reactor provides a good deal of versatility to the continuous tubular device when carrying out fast processes in highly viscous reactive systems, with the synthesis of polymers as the most prominent example.

### *2.1.4 Automodel Mode of Reaction Mixture Flow*

A major problem in the solution synthesis of polymers is a one to three orders of magnitude increase of reaction mixture viscosity upon increasing the polymer concentration in a solution. For example, at 295 °C, the dynamic viscosity of *cis*-1,4-isoprene rubber solutions in isopenthane is 90 P for 10%, 170 P for 13%, and 480 P

for 15% solutions, while its value is about 0.004 P for the initial isopenthane-isoprene mixture. High viscosities of polymer solutions do not usually allow intensive mixing of a reaction blend in bulk mixing reactors, as the Re and therefore, turbulent diffusion, fall rapidly. In this case, the most probable mixing mechanism is molecular diffusion. Thus, relatively diluted (up to 10–13 wt%) solutions are used, for example, in the processes of polymerisation, decomposition, polymer stabilisation prior to catalyst removal, and catalyst removal itself. This is a substantial disadvantage of existing production technologies; when the monomer concentration in a reaction mixture decreases, the polymerisation rate and process productivity also drop.

The problem of efficient mass exchange is especially important for fast chemical reactions, where the characteristic time of chain growth reactions is in the range of seconds or fractions of seconds, and the duration of the reaction mixture passage, in bulk mixing reactors, of up to several hours. Input points of reactants demonstrate nonuniform torch-like space-time distributions of temperature, monomer conversion, and concentration of active centres [35]. These conditions prohibit uniform conditions of synthesis in volume mixing reactors, including highly viscous solution processes.

Development and industrial application of highly efficient compact tubular devices turned out to be a successful solution for the majority of problems related to fast chemical processes in highly viscous solutions (isobutylene polymerisation, butyl rubber synthesis, halobutyl rubber synthesis and decomposition of Al, Mg, Ti, V, and so on, catalysts, neutralisation of acidic products, addition of stabilisers before polymer extraction, and so on). The diffuser-confusor design allows a plug flow mode in highly turbulent flows and therefore quasi-isothermic (meaning isothermic in any section of a reactor) conditions [36]. Application of tubular diffuser-confusor type devices solves another very important problem of creating and sustaining a well-developed turbulent mixing all along the device, including processes with highly viscous solutions. In addition, high turbulence in a reaction zone of jet-type tubular diffuser-confusor devices solves a very important problem of the negative influence of highly viscous flows on the technological parameters of industrial processes. The flow of liquids (including highly viscous liquids) is, in these conditions, very irregular and is characterised by a chaotic flow rate pattern at every point of the flow, as well as continuous pulsations, which are based on the cascade-type of interactions at any level of motion, from the highest to the lowest. Homogenisation of a turbulent flow media is mainly influenced by pulsations in the order of characteristic length parameters, which determine the dimensions of the turbulent motion area [37].

It is very interesting and important practically that the viscosity of a liquid does not influence the motion of the major part of a medium in large-scale and highly turbulent flows [37, 38]. The flow pattern is, in this case, automodel in relation to viscosity. Its

influence can only be observed in a narrow area near a wall. All the values describing turbulent mode do not depend on the viscosity of the flows (automodel section in relation to Re) in an automodel mode, when the medium homogenisation is limited by the exchange processes between large turbulent vortexes and smaller internal vortexes [37, 38]. This circumstance narrows the list of factors which determine the properties of turbulent motion in diffuser-confusor tubular devices. There are now only three parameters, characterising the large-scale motions of a reaction mixture, which determine the level of turbulent mixing of liquid flows in conditions which are independent of viscosity: medium density $\rho$, device diameter $d$, and linear flow rate $V$. These values, taken with actual dimensions, can make the only possible equations for average values of turbulence kinetic energy $C_{av}$, its dissipation $\varepsilon_{diss}$, turbulent diffusion coefficient $D_{turb}$, and hydraulic resistance $\Delta p$ [38]:

$$C_{av} \sim V^2;\ \varepsilon_{av} \sim V^3 / d;\ D_{turb} \sim V \times d;\ \Delta p \sim \rho \times V^2 \tag{2.17}$$

This, in particular, is demonstrated by the pressure loss in liquid flows within cylindrical tubular channels, where $\Delta p$ is a function of Re in the laminar mode (Re ≤ 2300) and is independent of channel wall roughness [38]:

$$\Delta p = \frac{32}{\mathrm{Re}} \frac{\rho \times L \times V^2}{d} \tag{2.18}$$

Re = (4–100) × $10^3$ in a turbulent mode. The pressure drop $\Delta p$ in the automodel flow area in relation to Re becomes independent of the hydrodynamic mode of the liquid however, it is still influenced by the roughness of the cylindrical channel walls:

$$\Delta p = \frac{0.387 \times \rho \times L \times V^2}{d(\lg \delta^{-1})^2} \tag{2.19}$$

Where $L$ is the length of the tubular device, $\delta$ is the relative wall roughness, which is the ratio of the average height of asperities on an inner surface of the tubes (absolute roughness) to the tube diameter (the estimate of absolute roughness is 0.06–0.1 mm for new steel tubes, 0.1–0.2 mm for used but not corroded ones, and 0.5–2 mm [38] for contaminated old tubes).

The Re value of the lower automodel area boundary is largely determined by the flow geometry. For example, [38] demonstrates that the automodel area in a sphere-around flow, where the resistance coefficient and therefore, the viscosity is independent of Re, forms at $\mathrm{Re}_{cr} \approx 500$. As higher flow turbulisation is achieved, in comparison with a cylindrical channel in a diffuser-confusor reactor at the same Re values, we can expect automodel mode formation at lower Re values.

The numerical solution of equations for turbulent liquid flows using the $C$-$\varepsilon$ turbulence model (**Equations 2.1–2.12**) confirms this assumption [39, 40]. Formation of an

automodel mode in tubular diffuser-confusor type turbulent reactors starts at $Re_{cr}$ = 800/*f*. The parameter *f*, is the function of the diffuser opening angle $\gamma$, while its values can be obtained using the approximation equation [41]:

$$f = 0.117 + 0.049\gamma - 0.0012\gamma^2 + 1.374 \times 10^{-5}\gamma^3 - 5.9 \times 10^{-8}\gamma^4 \quad (2.20)$$

In particular, diffusion opening angles of intervals 30 – 80° correspond to the formation of an automodel reaction mixture mode at $Re \geq Re_{cr} = 950 \pm 50$; whereas, an automodel mode in a cylindrical reactor forms at $Re > 10^7$, which is four orders of magnitude higher.

Numerical coefficients in **Equation 2.17** have been found for the conditions of automodel mode formation in tubular diffuser-confusor devices.

It has been achieved through the processing of an array of data, obtained as the result of solving the equations describing the turbulent motion of a continuous medium, and using the *K*-$\varepsilon$ turbulence model (**Equations 2.1–2.12**) with the method of finite elements on a nonuniform calculation grid.

The average value of the specific kinetic energy of turbulence:

$$K = f_c f^2 V_c^2 \quad (2.21)$$

The average dissipation rate of the specific kinetic energy of turbulence:

$$\varepsilon = \frac{f_E f^3 V_c^3}{d_c} \quad (2.22)$$

The average value of the turbulent diffusion coefficient:

$$D_m = \frac{0.09 f_c^2 f V_c d_c}{f_E} \quad (2.23)$$

Where $f_c$ and $f_E$ coefficients are determined by the geometric parameters, $d_d/d_c$ and $L_c/d_d$, of a reactor:

$$\begin{aligned} f_c = {} & -0.074 + 0.012 \times \left(\frac{L_c}{d_d}\right) - 8.74 \times 10^{-3} \times \left(\frac{L_c}{d_d}\right)^2 + 8.64 \times 10^{-4} \times \left(\frac{L_c}{d_d}\right)^3 \\ & + 0.078 \times \left(\frac{d_d}{d_c}\right) + 0.021 \times \left(\frac{d_d}{d_c}\right) \times \left(\frac{L_c}{d_d}\right) - 1.31 \times 10^{-3} \times \left(\frac{d_d}{d_c}\right) \times \left(\frac{L_c}{d_d}\right)^2 \\ & - 0.022 \times \left(\frac{d_d}{d_c}\right)^2 - 3.22 \times \left(\frac{d_d}{d_c}\right)^2 \times \left(\frac{L_c}{d_d}\right) \end{aligned} \quad (2.24)$$

$$f_E = -0.138 + 0.226 \times \left(\frac{d_d}{d_c}\right) - 0.116 \times \left(\frac{d_d}{d_c}\right)^2 + 0.019 \times \left(\frac{d_d}{d_c}\right)^3 + 0.03 \times \left(\frac{L_c}{d_d}\right) - 4.95 \times 10^{-3} \times \left(\frac{d_d}{d_c}\right) \times \left(\frac{L_c}{d_d}\right) - 1.93 \times 10^{-3} \times \left(\frac{L_c}{d_d}\right) \times \left(\frac{d_d}{d_c}\right)^2 - 9.62 \times 10^{-3} \times \left(\frac{L_c}{d_d}\right)^2 + 3.22 \times 10^{-3} \times \left(\frac{d_d}{d_c}\right) \times \left(\frac{L_c}{d_d}\right)^2 \quad (2.25)$$

The possibility of viscosity-related automodel mode formation in a diffuser-confusor device, made it possible to develop equations for the estimation of the characteristic mixing time at various volume ranges by placing **Equations 2.21–2.23** in **Equations 2.14–2.16**, with accuracy sufficient for use in engineering calculations.

The characteristic time of turbulent mixing:

$$\tau_{\text{turb}} = \frac{11.1 l^2 f_E}{f_c^2 f V_c d_c} \quad (2.26)$$

The characteristic time of micromixing (mixing by molecular diffusion) can be, in this case, found in the following equation:

$$\tau_{\text{micro}} = 17.3 \sqrt{\frac{\nu dc}{f_E f^3 V_c^3}} \quad (2.27)$$

The characteristic time of mesomixing (the mixing carried out *via* the exchange between large and small (internal) vortexes is calculated in the formula):

$$\tau_{\text{meso}} = \sqrt[3]{\frac{l^2 d_c}{f_E f^3 V_c^3}} \quad (2.28)$$

**Equations 2.26–2.28** are suitable for the calculation of the turbulent mixing characteristics over the range of ratios:

$$d_d / d_c = 1.2 - 2.5 \quad (2.29)$$

$$L_c / d_d = 0.5 - 3.5 \quad (2.30)$$

$$L_c / d_d > (1 - d_d / d_c) ctg\, \gamma \quad (2.31)$$

Comparison of the characteristic mixing times, calculated by **Equations 2.26–2.28**, with the characteristic duration of a chemical reaction $\tau_{\text{chem}}$ or the duration of chemical reactants passing through a reactor $\tau_{\text{pass}}$, makes it possible to calculate the optimal

design of a tubular turbulent device suitable for both fast chemical processes and the homogenisation of flows.

Formation of an optimal hydrodynamic mode, in a diffuser-confusor type reactor, can sometimes help to increase the concentration of polymer products during the synthesis of synthetic rubbers and thermoplastics, as well as for processes with highly viscous solutions, up to the stage of product extraction, including processes with fast chemical reactions. There is an opportunity to upgrade some polymer production processes in solutions and develop a new generation of unified energy- and resource-efficient technologies with high production efficiency and ecological safety, implemented in compact tubular turbulent confusor-diffuser type devices working in a flow mode.

Thus, it is possible to achieve an automodel mode in tubular turbulent diffuser-confusor type devices at relatively low linear flow rates of reactants and therefore, broaden its industrial application to areas of highly viscous media. In addition, it provides us with equations for the calculation of the average values of the turbulent diffusion coefficient $D_{turb}$, specific kinetic energy of turbulence $K$, its dissipation $\varepsilon$, as well as the characteristic mixing times of flows on various scales.

In order to optimise the conditions of fast processes, it is reasonable to reveal a correlation between the geometrical parameters of a tubular turbulent diffuser-confusor device, the dynamics and physical parameters of its liquid flows, and average values of the characteristic turbulent mixing time.

The necessary condition for the absence of diffusion disturbances in fast chemical reactions is their agreement with the equation:

$$\tau_{mix} = \tau_{turb} \leq \tau_{ch} \tag{2.32}$$

Where $\tau_{chem}$ is the duration of a chemical reaction ($\tau_{chem} = 1/k_g$ for a polymerisation process and:

$$\tau_{chem} = 1 / kC^{n-1} \tag{2.33}$$

for fast processes with low molecular weight (MW) reactants). At the same time, the high level of turbulent mixing of the reactants and corresponding optimal conditions for fast chemical processes are determined by the ratio of the characteristic mixing times of flows at macro- and microlevels:

$$\tau_{turb} > \tau_{micro} \tag{2.34}$$

The increase in viscosity of a reaction mixture leads to the gradual transfer of fast chemical and mass exchange processes to the micromixing-limited area, which is not in agreement with the requirement of **Equation 2.34** (**Figure 2.10**). Therefore, the reactants mix inefficiently, mainly by molecular diffusion in highly viscous solutions of polymers in bulk mixing devices, as well as tubular turbulent reactors with a low flow rate of liquid reactants. Upgrade to the diffuser-confusor type of reactor and an increase of the linear flow rate of reactants, leads to the transition to turbulent operation mode, where the mixing time is limited by the effective large-scale turbulent exchange (**Figure 2.10**). **Figure 2.10** also demonstrates that an increase of the reaction mixture flow rate, up to 4 m/s, results in a substantial decrease of the characteristic duration of micro- and macromixing. A further increase of $V$ does not result in a substantial change of the mixing times. Therefore, we can introduce the critical value of flow rate in a tubular channel at $V_{cr} \approx 4$ m/s, which does not need to be increased in real conditions. However, an increase of the reaction mixture flow rate (device efficiency) results in an increase of the kinetic energy of turbulence and therefore, the intensification of heat and mass exchange processes.

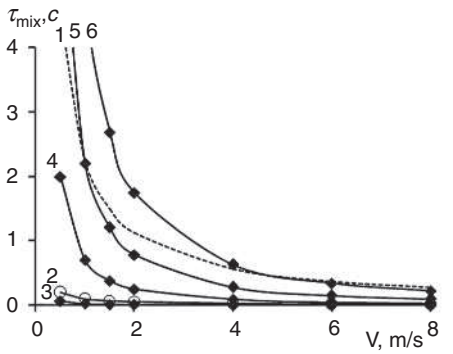


**Figure 2.10** Characteristic times of turbulent mixing $\tau_{turb}$ (1), micromixing $\tau_{micro}$ (3–6) and mesomixing $\tau_{meso}$ (2) dependence on a reaction mixture flow rate $V$. Dynamic viscosity values: 0.001 (3), 1 (4), 10 (5), and 50 (6) Pa·s. $d_c$ = 0.025 m, $\rho$ = 1000 kg/m$^3$

The optimal characteristic times of mixing are also determined by the range of diffuser opening angles $\gamma$ above 30° (**Figure 2.11**). However, for liquid flows with a viscosity of 50 Pa·s, it is impossible to achieve optimal conditions of mass exchange processes at $\tau_{micro} < \tau_{turb}$ and technologically acceptable values of $\gamma$. The solution here is to increase the reaction mixture flow rate $V$ (**Figure 2.10**).

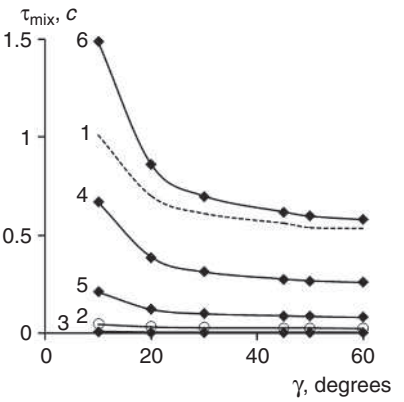


**Figure 2.11** Dependence of the characteristic times of turbulent mixing $\tau_{turb}$ (1), micromixing $\tau_{micro}$ (3–6) and mesomixing $\tau_{mezo}$ (2) in automodel mode on the diffuser opening angle $\gamma$. Dynamic viscosity values: 0.001 (3), 1 (4), 10 (5), and 50 (6) Pa·s. $d_c$ = 0.025 m, $\rho$ = 1000 kg/m$^3$, $V_c$ = 4 m/s

Important characteristics, which determine the opportunity of using tubular turbulent devices for a specific chemical process, in addition to its geometrical parameters, are the characteristic times of turbulent mixing as well as micro- and mesomixing. For example, fast chemical reactions with the process mainly occurring locally at input points are characterised by the substantial role of the characteristic mesomixing time values $\tau_{mezo}$. For emulsifying processes or agglomeration, the average droplet (particle) size of a dispersed phase depends on the mixing of flows at the microlevel, and is determined by the value of the characteristic time of micromixing $\tau_{micro}$. Application of tubular turbulent diffuser-confusor devices in the homogenisation of liquid flows requires similar times of sufficient mixing (determined by the duration of the mixture pass) and the characteristic large-scale turbulent transfer $\tau_{turb}$. In general, optimal mass exchange limited processes in turbulent flows require agreement with the correlation [45]:

$$\tau_{ch} > \tau_{turb} > \tau_{mezo} > \tau_{micro} \tag{2.35}$$

The parameters which determine the characteristic mixing time are the linear flow rate $V$, device diameter $D$, diffuser opening angle $\gamma$, as well as the kinematic viscosity $\nu$ for micromixing processes. Practically, a single and available way of influencing the reaction mixture homogeneity, in a diffuser-confusor reactor, is the variation of its diameter and linear flow rate of reactants.

The mixing of reactants on a microlevel is substantially influenced by the physical characteristics of liquid flows, in particular, by the density and viscosity (**Figure 2.12**). Increasing the viscosity and decreasing the density of the reactants fed into a tubular turbulent device, can result in the situation where the reaction mixture homogenisation will be limited by molecular diffusion, which is common in the case of polymer solutions. The analysis of **Equations 2.26–2.28** makes it possible to propose the criterion for breaking the automodel mode of reaction mixture flow, i.e., reduction in the efficiency of tubular turbulent diffuser-confusor devices with an increase of the medium viscosity [29]:

$$\frac{\mu}{\rho} > \frac{0.412 l^4 f_E^3 f V_c}{f_c^4 d_c^3} \tag{2.36}$$

Tubular device operation can be optimised, in this case, through an increase of the linear rate of flows in accordance with the equation:

$$\tau_{\text{turb}} \sim 1/V \tag{2.37}$$

$$\tau_{\text{mezo}} \sim 1/V \tag{2.38}$$

$$\tau_{\text{micro}} \sim 1/V^{1.5} \tag{2.39}$$

Which also favours process efficiency $w$, because:

$$w \sim V \tag{2.40}$$

An increase of the linear flow rate of a reaction mixture creates optimal values of the characteristic mixing times of liquid flows, turbulent diffusion coefficients, and dissipation of the specific kinetic energy of turbulence. The upper limit of application of tubular turbulent devices (based on dynamic characteristics of their operation) is evidently the input-output pressure drop in accordance with $\Delta p \sim V^2$, while the lower limit will be determined by the values of the turbulent diffusion coefficient:

$$D_{\text{turb}} \leq 10^{-4}\ \text{m}^2/\text{s} \tag{2.41}$$

Decreasing the diameter results in the decrease of the characteristic mixing time, which is the key to optimal conditions for fast processes, however, this favours a decrease of the effective coefficient of the turbulent diffusion $D_{\text{turb}}$. The $D_{\text{turb}}$ values form the lower limit, using geometrical parameters, for the application of tubular turbulent devices under industrial production conditions. Calculations demonstrate, that at $d_c$ < 0.023 m, $V_c$ = 4 m/s, and $\gamma$ = 45° the diffusion coefficient value does not exceed $10^{-4}$ $m^2/s$, which is typical for the transition flow mode in cylindrical channels.

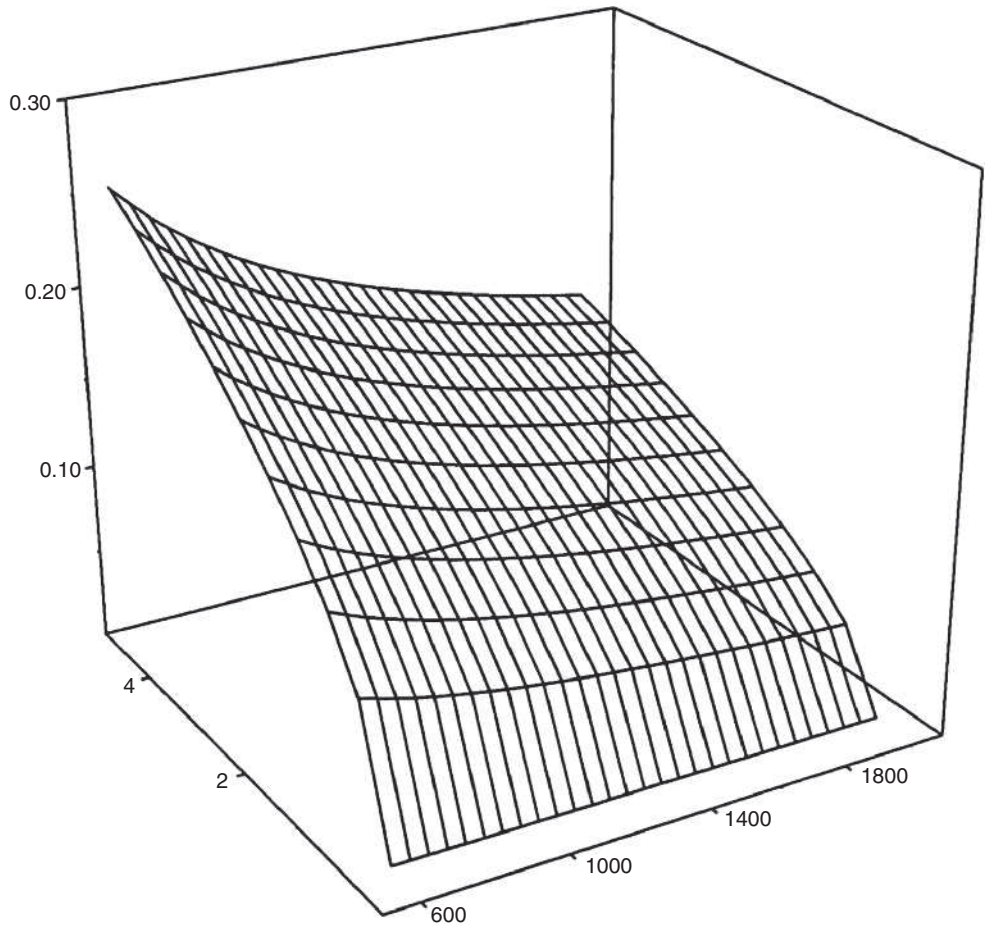


**Figure 2.12** Dependence of the characteristic time of micromixing $\tau_{micro}$ on the density and viscosity of a reaction mixture. $\gamma = 45^{o}$, $d_c = 0.025$ m, $d_d/d_c = 2$, $L_c/d_d = 3$, and $V_c = 4$ m/s

Devices with small diameters are characterised by higher average values of the specific kinetic energy of turbulence dissipation $\varepsilon$. The maximum value of $\varepsilon$ determines the intensity of liquid flows mixing on the microlevel (Kholmogorov scale), enabling the generation of small-scale shearing deformation and resulting in the production of finely dispersed emulsions and suspensions. A decrease of the tubular turbulent diffuser-confusor device diameter and an increase of the reaction mixture linear flow rate correspond, in this case, to an increase of the rotation speed and diameter of the mechanical agitator blades in bulk mixing reactors.

Calculation of the characteristic mixing time and chemical reaction duration, in relation to the mixing and reaction zones lengths, in turbulent reactors reveals the feasibility criterion for fast chemical processes using tubular turbulent devices [29] for polymer synthesis (polymerisation):

$$L \geq L_{\text{chem}} = V_c \tau_{\text{chem}} = \frac{V_c}{k_g} \tag{2.42}$$

For the flow synthesis of low molecular weight products:

$$L \geq L_{\text{chem}} = V_c \tau_{\text{chem}} = \frac{V_c}{k[\text{C}]^{n-1}} \tag{2.43}$$

For the homogenisation of flows:

$$L \geq L_{\text{mix}} = V_c \tau_{\text{turb}} = \frac{11.1 l^2 f_E}{f_c^2 f d_c} \tag{2.44}$$

Taking $l$ = d, **Equation 2.32** transforms into:

$$L \geq \frac{11.1 d_c f_E}{f_c^2 f} \tag{2.45}$$

For a chemical process which is insufficiently fast, application of a tubular polymer device is limited by its relatively long length at low levels of reaction rate constant. For mass exchange physical processes, such as the mixing of flows for the homogenisation of a reaction mixture, the required length of a mixing zone (and therefore the length of a device) depends on the channel geometry only. It provides vast opportunities for the optimisation of almost any process requiring the creation of a uniform field of reactant concentration. Analysis of **Equations 2.30–2.33** confirms the conclusion that optimal fast chemical reactions in quasi-ideal mode, within turbulent flows, require $L_{\text{ch}} \geq L_{\text{mix}}$ [42, 45]:

$$\frac{V_c}{k[\text{C}]^{n-1}} \left( \frac{V_c}{k_g} \right) \geq \frac{11.1 l^2 f_E}{f_c^2 f d_c} \tag{2.46}$$

**Equation 2.34** shows an easy way to calculate the critical values of chemical reaction rates, required for carrying out fast processes without diffusion limitations. **Table 2.3** demonstrates examples of the dependence of the critical rate constant values, of second-order low molecular weight reactions, on the linear flow rate of a reacting mixture $V$, in a tubular turbulent device, as well as on its design. The increase of $V$ and decrease of reactor diameter $d$ lead to optimal conditions of chemical reactions with sufficiently high rate constants. In particular, for technically acceptable d and $V$ values, a chemical reaction process without diffusion resistance is limited by the

rate constant value for low molecular weight compounds, which is in the order of $k \leq 10$ l/mol·s.

**Table 2.3 The dependence of the rate constant critical value of a second-order reaction (l/mol·s) in the kinetic area on the reactant flow rate and tubular turbulent device diameter at C = 1 mol/l**

| **V, m/s** | **$d_c$, m** | | |
|---|---|---|---|
| | 0.01 | 0.02 | 0.03 |
| 0.8 | 0.81 | 0.44 | 0.35 |
| 1 | 1.01 | 0.55 | 0.44 |
| 4 | 4.06 | 2.20 | 1.76 |
| 8 | 8.12 | 4.40 | 3.52 |
| 10 | 10.14 | 5.50 | 4.40 |

For faster liquid-phase reactions with $k >> 10$ l/mol·s in turbulent flows within compact tubular turbulent diffuser-confusor devices, it is necessary to increase the linear flow rate $V$, decrease $d$, and the respective concentrations of input to achieve $\tau_{chem} \geq \tau_{turb}$.

Therefore, by changing the geometry (design) of a tubular turbulent diffuser-confusor device, and consequently the dynamics and physical parameters of reacting flows, we can optimise the values of the turbulent mode characteristics for specific processes, limited by mass exchange. There is a range of diameters of a tubular turbulent diffuser-confusor device, in addition to a linear flow rate, which create conditions for removing the diffusion limitations of fast processes. In accordance with process specifics (kinetic parameters, physical characteristics of liquid flows, and so on), revealed characteristics allow the selection of scientifically grounded optimal conditions for its implementation (reaction zone geometry, dynamic modes, and so on).

Different branches of chemical, petrochemical, and other industries are not only characterised by homogeneous processes. Interface and liquid-liquid, liquid-gas reactions are also a common case. The process rate for the latter reactions is limited by the diffusion of reactants through an interface surface. A primary task, in this case, is to decrease the contribution of diffusion limitation, in particular, through the formation of fine dispersions with a well-developed interface surface.

## 2.2 Turbulent Mixing of a Two-phase Reaction Mixture

Among various devices used for the generation of dispersed systems with a well-developed surface, volume devices are one of the most widespread. They are characterised by the presence of an external turbulisation source (an agitator) and

therefore, by the developed turbulent flow of reactants (the intensity of turbulent mixing is up to 30–50%) [46–48].

There are the following widespread approaches for making emulsions in agitated devices, less dispersed [49, 50]: an increase of the mixing time (the duration of the reactants passing through an intensively agitated reaction zone) and an increase of either the volume of the dispersing zone, or the local dissipation of the specific kinetic energy of turbulisation in the dispersing zone. The most preferable way to reduce the degree of emulsion dispersion in mechanically agitated devices is to increase the local energy dissipation value in the dispersing zone, its maximum being in the area of the agitator blades [46]. In addition, a very important factor influencing the hydrodynamic situation in a reaction zone, is vertical circulation (axial diffusion) [51, 52]. Devices with mechanical agitation, rotor-pulsation devices [53–55], and hydroacoustic devices [56] (based on the formation of an intensive cavitation field in the mixing zone) are also good for the implementation of interface processes. These devices are highly efficient for heterogeneous processes, but they exhibit low energy efficiency and are difficult to produce.

A cornerstone of effective fast chemical reactions is the generation of dispersed systems in a turbulent flow within tubular devices [32, 57, 58–62]. It has been experimentally proven that highly dispersed emulsions form in the range of:

$$L = (20 - 50)d_d \tag{2.47}$$

While the required amount of energy is provided by the flow rate only, which should be about 5–15 m/s [61]. However, [32] demonstrates that the emulsification efficiency can be achieved by an increase (> 30°) of the conical widening at the reactor's input zone. At the same time, the effective dispersing of flows, different in density and viscosity, requires a $D_{\text{turb}}$ value at the reactor's input in the range of 0.065–0.080 $m^2/s$, as well as its stability along the axis of the device [32, 57].

### 2.2.1 Mathematical Modelling

Inhomogeneous or multiphase reaction systems are characterised by the presence of macroscopic (in relation to the molecular level) inhomogeneities. Numerical calculations of the hydrodynamics of such flows are extremely complicated. There are two opposite approaches to their characterisation [63, 64]: the Euler approach, with consideration of the interfacial interaction (interpenetrating continuums model) and the Lagrange approach, of integration by discrete particle trajectories (droplets, bubbles, and so on). The presence of a substantial amount of discrete particles in real systems makes the Lagrange approach inapplicable to study motion in multicomponent systems. Under the Euler approach, a two-phase flow is described

in terms of two interpenetrating continuums, so each of the phases is assumed to be a quasi-continuous phase in conditions of interfacial interaction.

Mathematical modelling of the processes of multiphase system mixing in tubular channels of various shapes, relies on the following assumptions: 1) dispersed phase particles considerably increase the size of the molecular kinetic particles, and 2) dispersed particles are much smaller than the distances of the substantial change of averaged, or macroscopic, parameters of mixtures or phases (despite some zones, which are considered to be rupture surfaces), i.e., the size of inhomogeneities in multiphase flows is much smaller than the size of the diffuser-confusor channels ($L$ and $d_d$). The first assumption allows the use of classical concepts and equations of continuous medium mechanics for the description of processes at the scale of the inhomogeneities themselves (droplets, bubbles, and so on). The second assumption makes it possible to describe the macroscopic processes in a heterophase area by the methods of continuous medium mechanics using averaged or macroscopic parameters.

The description of motions in heterophase systems, by continuous medium mechanics methods based on the Euler approach, correlates with the introduction of the multispeed continuum concept and determination of the interpenetrating motion of the dispersion system components. A multispeed continuum is the sum total of $N$ continuums with each representing its own specific mixture component (phase or component) and fills the same space. For each of the continuums, the density $\rho$ is trivially determined, as well as the motion rate and other parameters. Thus, any point of the area filled by a mixture, is determined by $N$ densities, $N$ rates, and so on. These values can be used for the determination of parameters characterising a whole mixture of components, which are density and the average weight of the mixture flow rate.

Many problems of hydrodynamics, such as the thermal and heat exchange of multiphase flows, cannot be calculated analytically and a single key to their theoretical analysis is their numerical solution. This approach is supported by popular methods of the discretisation of equations on nonorthogonal curvilinear nets, allowing the tracking of the boundary shape of the calculated areas. A computational fluid dynamics system is the standard for studying heat and mass exchange, and hydrodynamics, providing quantitative predictions for the motions of gases, liquids, heat transfer, phase transformations, chemical reactions and so on, based on the classical laws of physics and chemistry.

This study of the turbulent motion in two-phase flows, within a diffuser-confusor reactor, is based on the numerical solution of Reynolds-averaged equations describing the turbulent flow of a continuous medium. A numerical solution has been found for averaged equations of substance (mass, pulse, heat) transfer [63, 65]:

$$\frac{\mathrm{d}(\alpha_i \rho_i \Phi_i)}{\mathrm{d}\tau} + \mathrm{div}(\alpha_i \rho_i \vec{u}_i \Phi_i - \alpha_i \mu_i \mathrm{grad}\Phi_i) = \alpha_i \vec{F}_i \tag{2.48}$$

Where $\alpha_i$, $\rho_i$, $\mu_i$, $\vec{u}_i$ are the volume fraction, density, transfer coefficient (viscosity), and velocity vector of the $i^{th}$ phase respectively (indices: 1 – continuous phase, and 2 – dispersed phase).

The left side of **Equation 2.48** incorporates nonstationary, convection and diffusion members; the right side is the source member. The dependent variable $F_i$ stands for different parameters, in particular, components of rate, weight concentration of reactants, enthalpy or temperature, turbulence kinetic energy or scale. **Equation 2.48** is supplemented by continuity equations expressing the mass conservation law:

$$\frac{\mathrm{d}(\alpha_i \rho_i)}{\mathrm{d}\tau} + \mathrm{div}(\alpha_i \rho_i \vec{u}_i) = 0 \tag{2.49}$$

Differential **Equations 2.35** and **2.36** are easily solved for the nonstationary axial-symmetric nontwisted turbulent flow of a continuous incompressible Newtonian two-phase medium without taking interfacial heat and mass exchange into consideration. Therefore, the source of $\vec{F}_i$ in **Equation 2.35** is the force of interfacial interaction caused by tension. It has been assumed that all the dispersion inclusions (droplets, bubbles, and so on) are spherical.

The intensity of the interfacial interaction is correlated with the slip rate by the interfacial tension coefficient $\sigma$:

$$\vec{F} = \sigma \vec{V}_{slip} \tag{2.50}$$

The slip rate is determined as the difference between the rates of continuous $V_1$ and dispersed $V_2$ phases:

$$\vec{V}_{slip} = \vec{V}_1 - \vec{V}_2 \tag{2.51}$$

The interfacial interaction coefficient depends on the density $\rho_1$, the volume fraction $\alpha_1$ of a continuous medium, and the friction coefficient $C$:

$$f = 0.5CF\rho_1\alpha_1|\vec{V}\,slip|v_r \tag{2.52}$$

Where $F$ is the specific phase contact surface; $v_r$ is the reactor volume. The friction coefficient $C$ depends on the Re:

$$C = \frac{6.3}{\mathrm{Re}^{0.385}} \text{ for } \mathrm{Re} > 100 \tag{2.53}$$

$$C = \frac{16}{\mathrm{Re}} \text{for } \mathrm{Re} < 0.49 \tag{2.54}$$

$$C = \frac{20.68}{\mathrm{Re}^{0.643}} \text{ for } 0.49 < \mathrm{Re} < 100 \tag{2.55}$$

If Re >> 100 and Weber Number (We) > 8, the friction coefficient value is 2.7, while at:

$$\mathrm{Re} >> 100 \ \mathrm{Re} > \frac{2065.1}{\mathrm{We}^{2.6}} \rightarrow \mathrm{C} = \mathrm{We}/3 \tag{2.56}$$

The Re for multiphase flows has been calculated using the following equation:

$$\mathrm{Re} = \frac{\overrightarrow{V}_{slip}\, d_2}{\nu} \tag{2.57}$$

Where $d_2$ is an average diameter of dispersed phase particles; $\nu$ is the kinematic viscosity of a two-phase mixture.

The We is a measure of the inertia of the interfacial forces ratio and characterises the stability of this ratio in corresponding points of such flows:

$$We = \frac{d_2 \rho v^2}{\sigma} \tag{2.58}$$

A characteristic feature of a diffuser-confusor reactor is the formation of circulation areas (**Figure 2.13**). In this case, dispersed phase particles in the near-wall flow area start to move in the opposite direction to the reaction mixture flow due to the pressure gradient.

The numerical study of the behaviour of such flows can be carried out using the following turbulence models [63, 66]: standard (*KEMODL*) [16, 67, 68]; modified (*KECHEN*), and renormalised (*KERNG*) [69–71] *C-ε* models. Despite the two-parameter *C-ε* turbulent model being widely and practically used for the calculations of hydrodynamics and heat exchange in complex turbulent flows, this model has recently been criticised [72, 73].

Calculations have confirmed that the standard *C-ε* model of turbulence gives oversized values, such as the values of kinetic turbulence energy, *C*. Much better results are obtained using the *KECHEN* and *KERNG* models (**Figure 2.14**), especially designed for detached flows with circulation zones.

The primary task of modelling two-phase reaction systems is the estimation of the average diameter of droplets (bubbles and so on) of a dispersed phase and their size distribution in fast interface processes in diffuser-confusor devices. According to Kholmogorov's theory of isotropic turbulence, the specific kinetic energy of turbulence dissipation rates $\varepsilon$ are limiting in this case.

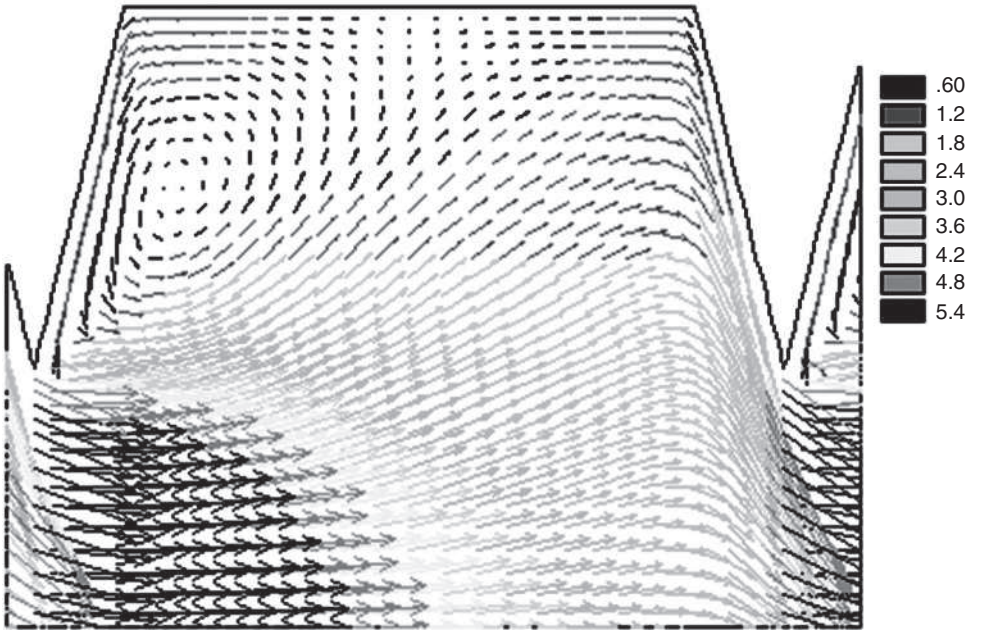


**Figure 2.13** The vector field rates in a diffuser-confusor device ($d_d$ = 0.08 m; $L_c$ = 0.27 m; $V$ = 16 m/s; $\rho_1$ = 6.93 kg/m$^3$; $\rho_2$ = 640 kg/m$^3$; and $\alpha_2$ = 0.2)

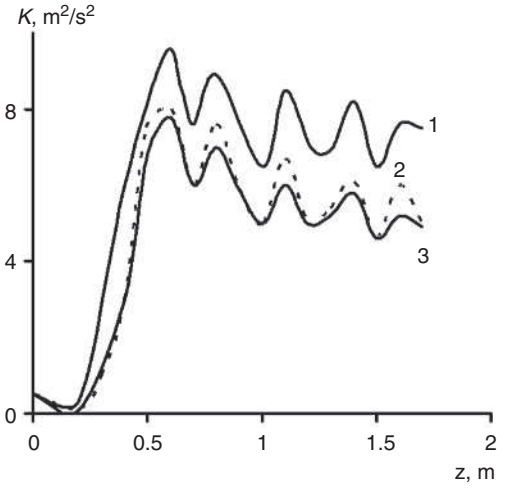


**Figure 2.14** Variation of the specific kinetic energy of turbulence $K$ along the axis of a diffuser-confusor device. Calculations have been carried out using models: *KEMODL* (1), *KECHEN* (2), and *KERNG* (3)

The automodel mode ($Re > 10^3$) for tubular diffuser-confusor devices demonstrates an independence of the average volume characteristics of a turbulent flow on viscosity, and their dependence on the phase density $\rho_1$ and $\rho_2$, volume rate $w_1$ and $w_2$, device diameter $d_c$, and mixture flow rate $V_c$. In accordance with the analysis of dimensions while using statistically significant values, the combination for the average value of the dissipation rate can be composed for the kinetic energy of turbulence of a two-phase flow [63, 65, 66]:

$$\varepsilon_{av} \sim (V_c,\ d_c,\ \rho_1,\ \rho_2,\ w_1,\ w_2) \tag{2.59}$$

The numerical solution of **Equation 2.35** and **Equation 2.36** with corresponding boundary conditions, determined by the mixing zone geometry, physical characteristics, and dispersed system dynamics, resulted in the analytical solution for **Equation 2.59**:

$$\varepsilon_{av} = 0.625\left(\frac{f_E f^3 V_c^3}{d_c}\right) \times \left(1 + \left(\frac{w_2}{w_1 + w_2}\right)^2 \times \left(\frac{\rho_1}{\rho_2}\right)^{-0.3}\right) \tag{2.60}$$

Where f and $f_E$ are obtained from **Equations 2.20** and **2.25** respectively.

The maximum dissipation value of the specific kinetic energy of turbulence $\varepsilon_{max}$ is determined by the following equation:

$$\varepsilon_{max} = 356.6 \times f^3 \times \left(\frac{d_d}{d_c}\right)^{0.79} \tag{2.61}$$

The largest discrepancy between values, calculated using **Equations 2.60** and **2.61** and the corresponding results of numerical calculations, does not exceed 23%, and the average discrepancy is 7%. Thus, proposed equations can be used to estimate the turbulent flow parameters of two-phase reaction systems in tubular turbulent diffuser-confusor devices.

An important factor for the specific interface area is the deformation of droplets (bubbles), which is generally determined by the dynamic influx caused by turbulent pulsations from the dispersion medium, and/or the ratio of phase rates, as a result of their different densities (gravitation component). The minimal size $d_{cr}$ of dispersed phase particles undergoing deformation can be, in this case, calculated using the equation which characterises the stability of the interphase boundary.

A theoretical estimation of the minimal droplet (bubble) size $d_{cr}$, which undergoes deformation in a turbulent flow, can be obtained from the equation characterising the stability of the interphase boundary [47]:

$$\frac{2\sigma}{d_{cr}} = \frac{\rho_1 (v')^2}{2} \tag{2.62}$$

Where σ is the surface tension; $v'$ is the pulsation element scale, which is determined in accordance with the Kholmogorov–Obukhov 'two-thirds' law [74]:

$$v' = (\varepsilon d_2)^{1/3} \tag{2.63}$$

Smaller scale pulsations possess much less energy and cannot deform dispersed phase particles. Larger scale pulsations carry dispersed phase elements away without deforming their surface.

Processing of numerical experimental results led to the equation for the minimal diameter of dispersed phase particles undergoing deformation as a result of the continuous hydraulic impact of the medium [66]:

$$d_{\text{av}} = 0.099 \times \left( \frac{\sigma}{\rho_1} \right)^{0.6} \times \varepsilon^{-0.4} \tag{2.64}$$

The diameter $d_{cr}$ can be taken as the sample diameter $d_2$ of dispersed particles forming in a turbulent flow.

An experimental study of the emulsification process of the hexane (dispersed phase)-water (continuous phase) system in tubular diffuser-confusor reactors has been carried out to check the adequacy of the proposed calculation method [75] (**Figure 2.15**). The frequency curves of the size distribution of the dispersed phase droplets have been obtained by digital photography under intensive transmitted illumination (1/1000 exposures and 400 units of photosensitivity). Calibrating threads of known size were added to the system to eliminate the effect of image distortion caused by the bent shape of the device. The $0.75 \times d_d$ central longitudinal section has been used for the calculations, where the discrepancy between the image-based calculated and real-sized calibrating threads did not exceed 1%. This method also allowed the avoidance of image distortion, due to the refraction effects caused by the glass cone frame of the device, and consideration of the systematic error. Frame-by-frame viewing of the computer image of the moving dispersed systems (24 frames per s) with 10 times zoom and comparison of the dispersed particles linear size (all the particles were spherical) with the linear size of calibrating threads, made it possible to calculate the true size of the droplets (the projection area of a spherical droplet, to be more precise). Droplets were calculated in the following interval (mm): 0–0.4; 0.4–0.6; 0.6–0.8; 0.8–1.0; 1.0–1.5; 1.5–2.0; and above 2.

Experimental data on the efficiency of hexane emulsification in water, using a diffuser-confusor reactor, provide a satisfactory confirmation for the results of calculations based on the developed method (**Figure 2.16**). **Equations 2.43** and **2.47** are correct for densities of both continuous and dispersed phases in the range of 0.689–1111 kg/m$^3$.

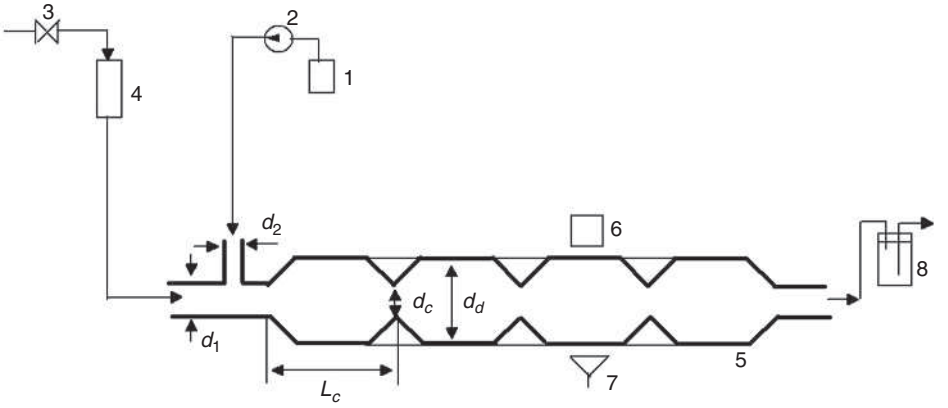


**Figure 2.15** The experimental device for emulsification in a turbulent mode. 1) dispersed phase tank; 2) peristaltic pump; 3) dispersion medium feed line (water); 4) rotameter; 5) tubular turbulent diffuser-confusor (cylindrical) device; 6) digital camera; 7) light source; and 8) sedimentation tank

Thus, the study of two-phase flows in diffuser-confusor devices can provide us with reliable results, based on the interpenetrating continuum model (the Euler approach). The numerical solution of the partial derivatives of the differential equations in the $C$-$\varepsilon$ turbulence model, using the implicit integro-interpolation finite volume method, provides us with the following fields of functions for a diffuser-confusor reactor: axial u and radial v rates for each of the phases; pressure $p$; volume fractions of continuous $\alpha_1$ and dispersed $\alpha_2$ phases; specific kinetic energy of turbulence k and its dissipation $\varepsilon$, as well as some other characteristics.

Description of the dispersing process for a turbulent flow of two-phase systems, in relation to the hydrodynamic mode of operation of tubular diffuser-confusor devices, can be simplified by the introduction of the volume-surface diameter of dispersed phase droplets $d_{32}$ [9, 60, 61, 76, 77]:

$$d_{32} = \frac{\sum m_i d_i^3}{\sum m_i d_i^2} \tag{2.65}$$

Correlating with the specific surface $F$ of spherical particles in a dispersed phase using the following equation:

$$F = \frac{6}{d_{32}} = \frac{6\sum m_i d_i^2}{\sum m_i d_i^3} \tag{2.66}$$

Where $m_i$ is the number of $i^{\text{th}}$ fraction droplets with diameter $d_i$.

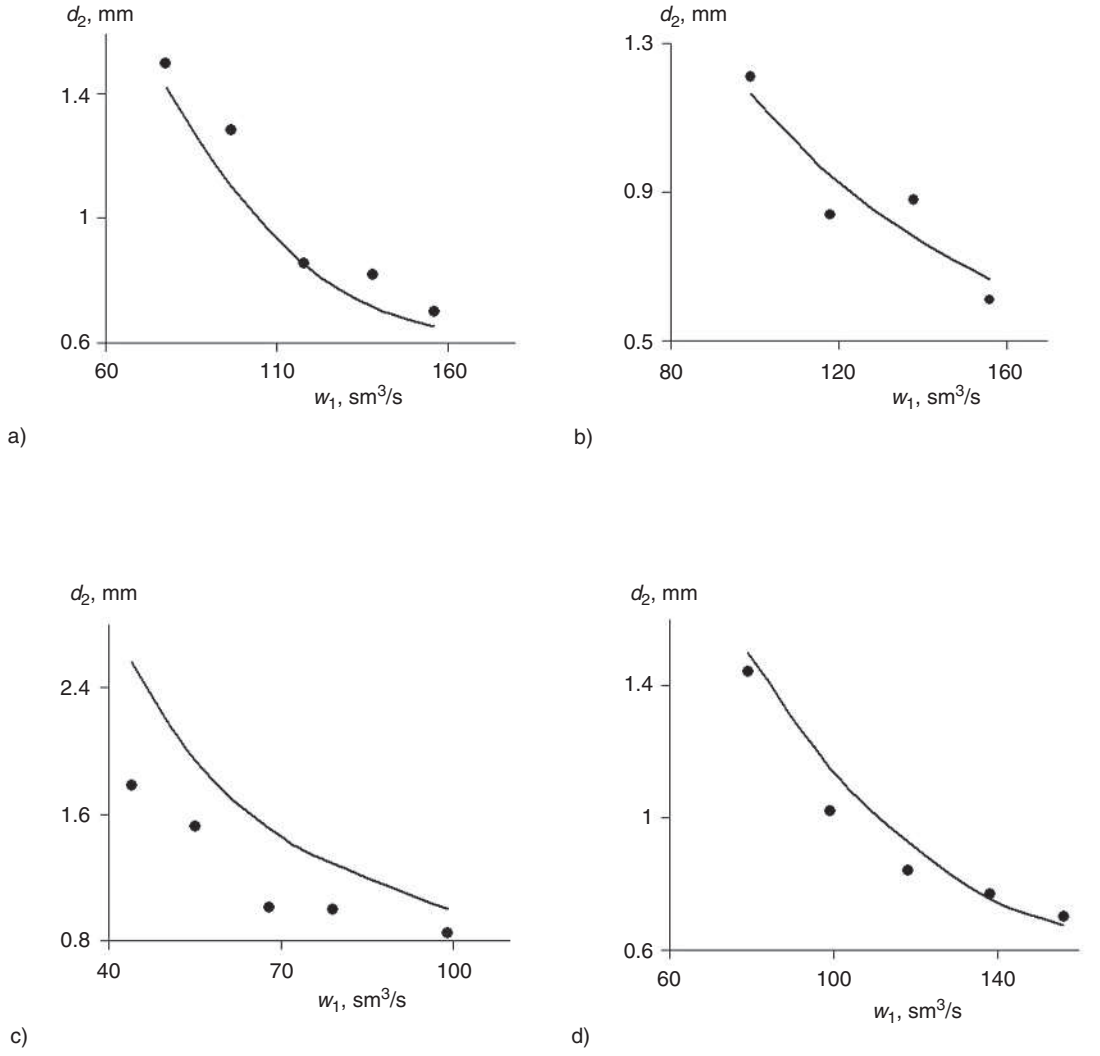


**Figure 2.16** The dependence of volume-averaged droplet diameters $d_2$ on the dispersion medium rate $w_1$. Points are experimental values, the curve is calculated. $d_d/d_c$ = 1.6 (a, d); 2 (b); 3 (c); $L_c/d_d$ = 2 (a–c); 3 (d); $d_d$ = 24 mm, $d_1$ = 10 mm (axial nipple), and $d_2$ = 5 mm (radial nipple)

Another important parameter characterising the quality of dispersed systems is the polydispersity coefficient $k_d$ [78]:

$$K_d = \frac{\sum m_i d_i^3 \times \sum m_i d_i}{\sum m_i d_i^4 \sum m_i} \tag{2.67}$$

$K_d$ = 1 for monodispersed systems and $K_d$ < 1 for polydispersed systems; lower values of $K_d$ lead to a wider size distribution of particles.

### *2.2.2 Turbulent Flows 'Liquid-liquid'*

The study of turbulent mixing in a single-phase reaction mixture has shown that the radial input of reactants and conical widening at the input zone of a reactor can decrease diffusion limitations for fast liquid-phase reactions. At the same time, the size of dispersed phase particles in a two-phase reaction mixture flow is determined by the hydrodynamic influx (shear pressure value) in a dispersion medium, which increases with the growth of the intensity of the turbulent pulsations.

As for the single-phase reaction mixture, the increase of diffuser opening angle $\gamma$ at the input area of a device (conical widening) leads to intensification of the turbulent mixing of a two-phase mixture. It is demonstrated by an increase of the number of emulsion droplets with at least 0.8 mm diameter ($n$, %) when the conical widening angle increases in the range of 0 – 60° (**Figure 2.17**) [18].

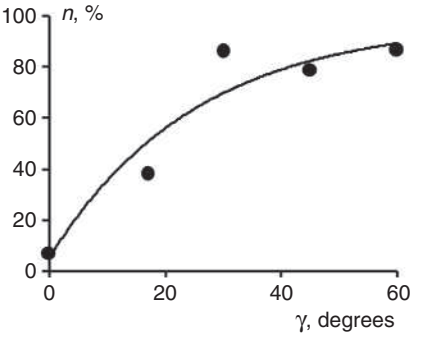


**Figure 2.17** The dependence of the percentage of emulsion droplets with $d$ < 0.8 mm ($n$, %) on the conical widening angle in the input area of a device $\gamma$. $w$ = 85 sm/s, hexane-water

A substantial influence on the specific surface of reacting phases is caused by the ratio of the diameters of the central $d_1$ (dispersion medium) and side $d_2$ (dispersed phase) nipples [79, 80]. **Figure 2.18** demonstrates that the increase of the $d_1/d_2$ ratio at $d_1$ = const, results in a decrease of the volume-surface diameter of the droplets and therefore, to an increase of the phase contact surface. This obviously results in the fact that the final size of the dispersed droplets is determined by their initial diameter, which in turn is influenced by the feeding nipple diameter $d_2$. A substantial influence on the dispersed composition of emulsions in tubular turbulent devices is exerted by

the ratio $d_1/d_2$ at $d_2$ = const, in particular, a decrease of the $d_1/d_2$ ratio (a decrease of $d_1$) results in the formation of systems with a minimal size of droplets under given experimental conditions (**Figure 2.18**). A substantial decrease in the size of the dispersed inclusions is, in this case, determined by a fourfold increase of the linear flow rate of a dispersion medium, in the $d_1$ nipple, at comparable process efficiency. It increases the intensity of the shear deformation of dispersed phase droplets using the radial input method.

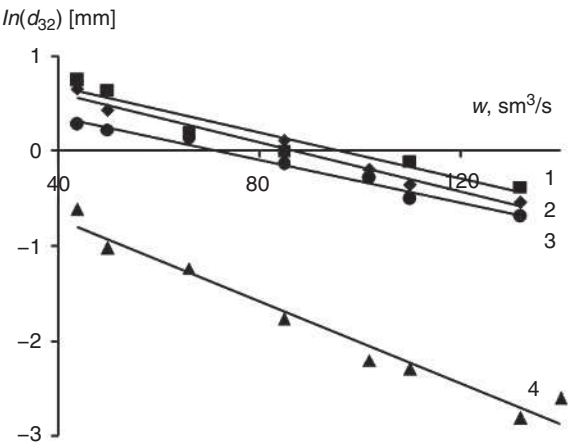


**Figure 2.18** The dependence of $ln(d_{32})$ on w in a diffuser-confusor device. $d_d/d_c$ = 1.6; $L_c/d_d$ = 2; $d_1$ = 5 (4); and 10 (1–3) mm; $d_2$ = 0.8 (3.4), 1 (2), and 3 (1) mm

Formation of finely dispersed systems at points of feedstock input (**Figure 2.19**, curves 3 and 4) does not change the size of the dispersed particles along the reactor axis. The diffuser-confusor channel provides stability of the intensive turbulence while moving away from the reactor input, and maintains the constant value of the phase contact surface by the avoidance of reaction mixture layering and coalescence of droplets. At relatively high values of the $d_2$ diameter, large droplets form at points of reactant input (**Figure 2.19**, curves 1.2) and their size decreases while moving away from the reaction zone. Diffuser-confusor sections also function, in this case, as dispersing devices. In addition, the cylindrical device demonstrates the layering of reactants and a decrease of the chemical reaction rate.

The increase of flow rate w and the number of diffuser-confusor units $N_c$ from 1 to 4 results in a decrease of the volume-surface diameter of dispersed phase droplets and a corresponding increase in the specific interphase surface (**Figure 2.20**); intensifying the whole chemical process in the case of fast chemical reactions [75].

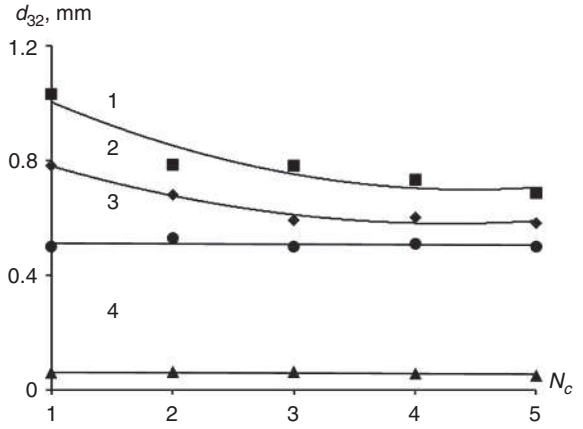


**Figure 2.19** Dependence of the volume-surface diameter of particles $d_{32}$ on the number of diffuser-confusor units $N_c$. See **Figure 2.18** for the legend

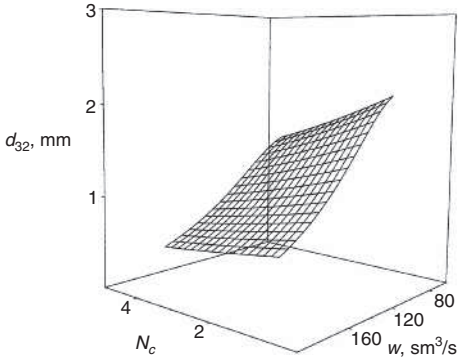


**Figure 2.20** The dependence of $d_{32}$ on the rate w of a two-phase flow and the number $N_c$ of diffuser-confusor units in a tubular device. $d_d$ = 24 mm, $d_d/d_c$ = 1.6, and $L_c/d_d$ = 2

At fixed $d_d$ values, the influence of the reaction mixture flow rate on the specific phase contact surface is independent of the $d_d/d_c$ ratio and $L_c/d_d$ ratio, and follows the general pattern of behaviour (**Figure 2.21**) which can be approximated by the following equation [45]:

$$d_{32} = 4.74\exp(-0.011\times w) \tag{2.68}$$

At the same time, there is a specific range of volume reaction mixture flow rate, which is implemented in a device with the optimal $d_d/d_c$ ratio. This range is limited by the zone of layered two-phase flow as the lower boundary and the energy consumption, due to a pressure difference increase, as the upper boundary. In particular, $d_d/d_c$ = 3 corresponds to the interval of 44 < $w$ < 80 sm$^3$/s and $d_d/d_c$ = 1.6 corresponds to the

interval of 80 < $w$ < 180 sm$^3$/s, further increase of the reaction mixture flow rate ($w$ > 180 sm$^3$/s) requires a further decrease of the $d_d/d_c$ ratio (**Figure 2.21**) down to $d_d/d_c$ = 1, i.e., a cylindrical device is an effective alternative.

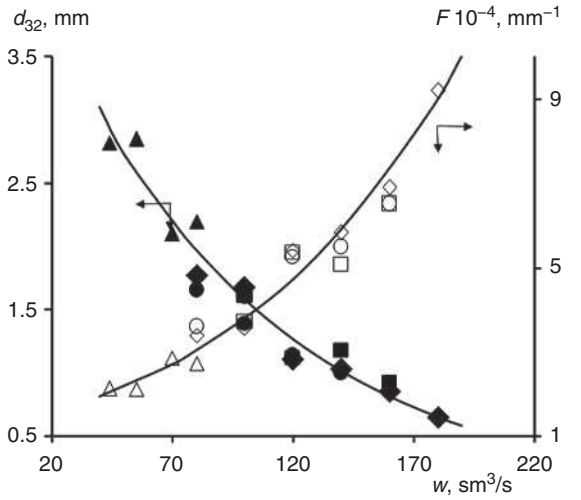


**Figure 2.21** Dependence of the volume-surface diameter of the dispersed phase $d_{32}$ and the specific surface of phase contact $F$ on the geometry of a diffuser-confusor device ($d_d$ = 0.024 m) and reaction mixture flow rate. $d_d/d_c$ = 1.6; $L_c/d_d$ = 2 (◆◇); $d_d/d_c$ = 2; $L_c/d_c$ = 2 (■□); $d_d/d_c$ = 3; $L_c/d_d$ = 2 (▲Δ); $d_d/d_c$ = 1.6; and $L_c/d_d$ = 3 (●○)

The viscosity of the dispersed phase and interfacial tension are the key parameters of the motion of a multiphase liquid system, which influence the interphase boundary and therefore, the diffusion limitations for fast chemical reactions. Their complex effect on the dispersing process makes it possible to consider and, in some cases, control the intensity of the reactants' transition through the interfacial boundary. The model system 'water (continuous phase)-hexane (dispersed phase)' has been studied to analyse the potential of this method, with varied viscosities of the hydrocarbon medium achieved by dissolving industrial samples of SSI-3 grade isoprene rubber, and the varied surface tension achieved by the adsorption of isopropyl alcohol on the interphase boundary. An increase of the dispersed phase viscosity leads to the formation of an emulsion with larger droplets of the hydrocarbon phase (**Figure 2.22**). It results in a decrease of the interfacial surface area and related growth of the diffusion limits for fast chemical reactions. Dispersed phase emulsification at higher values of viscosity does not lead to the formation of spherical droplets, the viscous component forms 'bundles' of various lengths, which orientate coaxially during motion along the device axis. The limit value of the dispersed phase viscosity, which is characterised by the hindered transition of the two-phase flow dispersion, is mainly determined

by the reactor. With a reduced channel profiling depth, which is characterised by the diffuser-to-confusor diameter ratio $d_d/d_c$ = 2; 1.6; 1 (cylindrical device), the limit values of relative viscosity are 40, 30, and 15, respectively.

The negative influence of viscosity on the interphase boundary can be avoided by the addition of surfactants, leading to a decrease of the interfacial tension. The selective distribution of alcohol molecules, near the separating surface level, results in differences in the composition of the nonmixing phases and reduces the work required to form a new surface. In this case, with the continuous phase turbulent pulsation parameters unchanged, reaction mixture dispersion is favoured in a tubular diffuser-confusor device. It should be considered, that interfacial chemical reactions assume the presence of at least three substances in a reaction zone, different in chemical nature, with some able to adsorb onto the interphase boundary. It can influence the size of dispersion inclusions in real conditions.

Variation of the dispersed phase viscosity and interfacial surface energy, which characterise the physical properties of the reacting flows, together with the variation of the tubular turbulent reactor geometry (**Figure 2.22**), the method of reactant input and hydrodynamic mode of operation, constitute various ways of controlling the specific surface area in real processes with a two-phase reaction mixture.

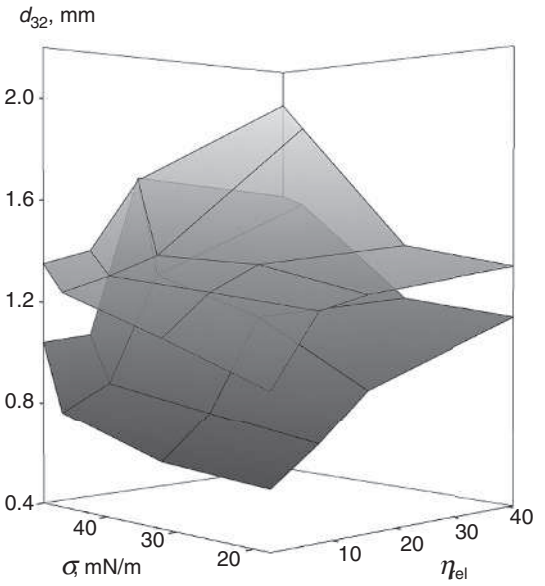


**Figure 2.22** Dependence of the volume-surface diameter $d_{32}$ of dispersed phase particles on its relative viscosity and interfacial tension for a 'liquid-liquid' system motion in a tubular turbulent device. $d_d/d_c$ = 1 (1), 2 (2), $w$ = 125 sm$^3$/s, and $d_d$ = 25 mm

The ratio $L_c/d_d$ exerts almost no influence on the polydispersity of emulsions when creating dispersions with a volume-surface diameter $d_{32}$. An increase of the $d_d/d_c$ value results in an increase of dispersed particle distribution, while uniform emulsions form in the diffuser-confusor channel of a tubular device with $d_d/d_c = 1.6$. In particular, for $L_c/d_d = 2–3$ and $d_d/d_c = 1.6$ $k = 0.72–0.75$, when $d_d/d_c = 2$ and 3, the $k$ value decreases to 0.63 and 0.41 respectively.

### 2.2.3 Turbulent Flows 'Liquid-gas'

Similar to the 'liquid-liquid' system, the volume-surface diameter of dispersed phase particles in a liquid-gas flow is determined by the initial size of the bubbles at the gas input points [81–83]. An increase of the liquid-gas flow rate leads to an increase of the shear deformation influence of the dispersed phase particles and therefore, to a decrease in the diameter of the gas bubbles in the input area of the device. Finally, it leads to the formation of a finely dispersed system in a device with an increase of the liquid-gas flow rate (**Figure 2.23**). Fast chemical reactions in two-phase gas-liquid systems usually occur in a gas-phase excess, so it is reasonable to analyse the influence of the gas content in a flow on the change of phase contact surface.

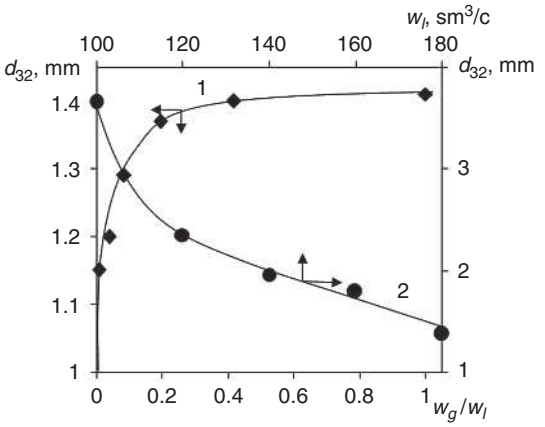


**Figure 2.23** The dependence of $d_{32}$ on the ratio of gas and liquid-phase flow rates $w_g/w_l$ ($w_l$ = 180 sm$^3$/s) (1) and liquid-phase flow rate $w_l$ ($w_g/w_l = 0.1$); and (2) $d_1$ = 10 mm, $d_2$ = 3 mm, and $d_d$ = 24 mm

The increase of $w_g/w_l$ at a constant liquid-gas flow rate leads to an increase of the volume-surface diameter of the dispersed phase particles and thus, reduces the specific phase contact surface area (**Figure 2.23**). A substantial increase of the $d_{32}$ of gas bubbles can be observed with an increase of the gas content in a flow up to

$w_g/w_l$ = 0.2. The bubble mode is formed in this area of the liquid-gas flow. Further increase of the gas content in a flow does not influence the size of the dispersions ($d_{32} \approx 1.4$ mm), which is evidently the effect of the transition to close-packed bubble (foam) mode.

A threefold increase of $d_d/d_c$ for a liquid-gas mixture, i.e., transition from a cylindrical device ($d_d/d_c = 1$) to a diffuser-confusor device ($d_d/d_c = 3$) results in over a fourfold decrease of the $d_{32}$ parameter. However, a ninefold decrease of the $d_2$ of the side input nipple for the gas phase, results in only a 20% decrease of $d_{32}$ (**Figure 2.24**). These effects can be explained by the formation of more intensive turbulent mixing after the transition from a cylindrical-type device to a diffuser-confusor device, with a constant rate of the gas-liquid flow in the mixing zone. This effect is accompanied by an increase of the hydrodynamic impact on the dispersed phase particles, leading to the decrease of their size. The change of the volume-surface diameter of the dispersed phase particles, with a $d_2$ variation, is fully determined by the initial size of the bubbles, which increase with increasing the nipple diameter. Considering that the change of $d_2$ ($d_d/d_c$ = const) does not alter the intensity of turbulent mixing in a continuous medium, there may be a slight increase of the volume mass output coefficient, caused solely by the decrease in size of the dispersed phase particles. At the same time, profiling of device walls in the range of $d_d/d_c$ = 1–3 leads both to intensification of the turbulent mixing (therefore, to an increase of the mass output coefficient in a liquid phase) and to a drop of the $d_{32}$ value, resulting in a phase contact surface growth.

Thus, the ratio of gas and liquid-phase flow rates $w_g/w_l$ in tubular devices, as well as the dispersed system flow rate, exerts a substantial influence on the size of the dispersed inclusions. An increase of the volume-surface diameter of the dispersions, with an increase of the gas content (the growth of the $w_g/w_l$ ratio) can be compensated by the growth of the liquid-gas flow rate. Profiling of tubular turbulent device walls, to form diffuser-confusor transitions, is an effective way of reducing diffuser limitations for fast chemical reactions in the presence of an interphase boundary.

In comparison to 'liquid-liquid' systems, 'liquid-gas' systems are characterised by relatively higher values of the volume-surface diameter of dispersed phase particles (**Figure 2.25**). The effect of substantial differences in densities of flows and surface tension at the interphase boundary is obvious. However, differences between the size of particles in 'liquid-liquid' and 'liquid-gas' flows reduce when we move from a cylindrical device to a diffuser-confusor device (**Figure 2.25**). In particular, when other conditions are equal, the total volume of bubbles is more than 3 times larger than the volume of liquid of a two-phase system in a cylindrical reactor. The diffuser-confusor channel provides the formation of a dispersed system with a comparable size of bubbles and droplets.

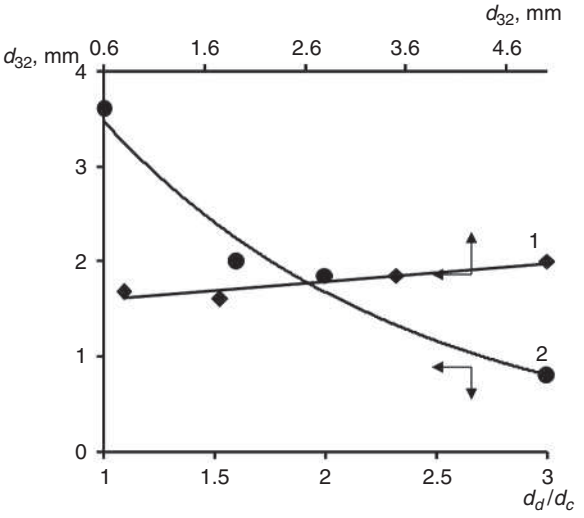


**Figure 2.24** Dependence of the volume-surface diameter $d_{32}$ of dispersed phase particles in a 'liquid-gas' system on the $d_2$ diameter of a gas-phase input nipple ($d_d/d_c$ = 2) (1), and the $d_d/d_c$ ratio ($d_2$ = 3 mm), (2) ($w_l$ = 140 sm$^3$/c, $d_1$ = 10 mm, and $d_d$ = 24 mm)

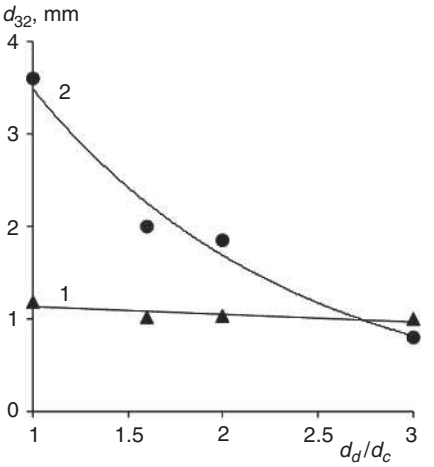


**Figure 2.25** Dependence of the volume-surface diameter $d_{32}$ in 'liquid-liquid' (1) and 'liquid-gas' (2) systems on the $d_d/d_c$ ratio ($d_2$ = 3 mm, $w_l$ = 140 sm$^3$/s, $d_1$ = 10 mm, and $d_d$ = 24 mm)

The upper limit for an increase of the two-phase reaction mixture flow rate and the degree of reactor wall profiling, for the formation of finely dispersed systems, is determined by the fast growth of the input-output pressure drop, leading to an increase

of the energy required to move a reaction mixture. At the same time, substantial differences in densities of the liquid-gas flow components lead to its layering and therefore, to a decrease of the phase contact surface area and growth of diffusion limitations in fast chemical reactions. This is the lower limit of the flow rate and it determines the reasoning of the study of how device geometry influences the layered flow of two-phase reaction systems.

### *2.2.4 Separation of a Two-phase Reaction Mixture in Tubular Devices*

The components of two-phase reaction systems usually differ in density and viscosity, which is the reason for flow layering, especially at high flow rates. This is the lower limit of the output of a tubular turbulent reactor for fast chemical processes, including the interphase boundary.

The part of a mixing zone from the dispersed phase (liquid, gas) introduction to the starting point of layering z was selected as a parameter, characterising the area of a homogeneous reaction flow [45]. In this case, the z parameter characterises the formation area of a homogeneous flow with a uniform size distribution of dispersed phase particles along the cross section of the device. An increase of the device output leads to an increase of the uniform flow area, which is the effect of turbulent diffusion coefficient growth and avoids dispersed phase coalescence *via* the gravitation field (**Figure 2.26**). The homogeneous flow of a two-phase system within diffuser-confusor devices forms at lower volume flow rates than in cylindrical devices. The length of the homogeneous flow section in cylindrical and diffuser-confusor reactors increases with the flow rate of a homogeneous media.

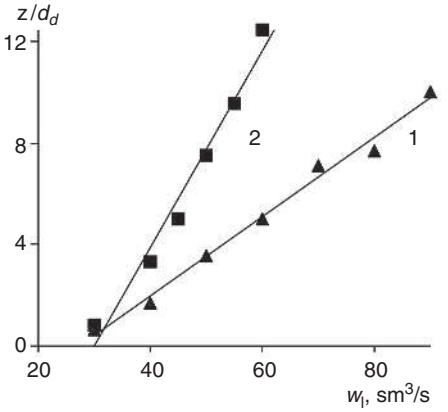


**Figure 2.26** Dependence of the homogeneous 'liquid-liquid' flow area length on the dispersion medium flow rate in a tubular device of diffuser-confusor (1), and cylindrical (2) designs ($d_1$ = 10 mm; $d_2$ = 3 mm; and $d_d$ = 24 mm)

At a constant two-phase flow rate, the length of the homogeneous dispersed system zone increases with an increase of profiled channel depth ($d_d/d_c$ ratio) (**Figure 2.27**). An increase of the $d_2$ diameter of the dispersed phase input nipple results in faster layering of a reaction mixture, which is evidently caused by the growth of the dispersed phase particles and their aggregative instability.

One must note that the uniform distribution of the dispersed phase results in a longer length of the homogeneous flow zone in 'liquid-liquid' systems, than in 'liquid-gas' systems. It is the consequence of less difference in phase densities.

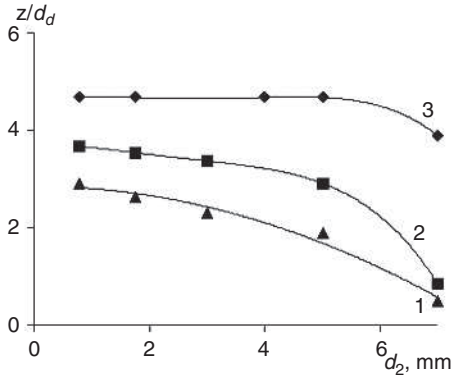


**Figure 2.27** The length of a homogeneous flow zone of a 'liquid-gas' system in a tubular device ($d_d/d_c$ = 1 (1); 1.6 (2); and 2 (3); $w_l$ = 80 mix$^3$/c; $w_g/w_l$ = 0.1; and $d_d$ = 24 mm)

The separation of multiphase reaction system components in tubular turbulent diffuser-confusor devices occurs at high rates of flow. The peripheral area of a tubular turbulent diffuser-confusor device has a pressure gradient, which moves the particles in the opposite direction to the direction of the main flow (circulation zone). A liquid flow rotates in this area and an unusual effect appears: centrifugal forces can lead to phase separation, which is mainly caused by the differences in the density of components participating in the dispersing process. Substantial differences in the densities of continuous $\rho_1$ and dispersed $\rho_2$ phases and following the $\rho_1 < \rho_2$ condition (for example, 'liquid-solid' system) at the device periphery, result in a decrease of the volume fraction of a dispersed phase $\alpha_2$ and the moving of particles to the flow axis by centrifugal forces (**Figure 2.28**). In the case of $\rho_1 > \rho_2$ (for example, a 'liquid-gas' system) the volume fraction of a dispersed phase $\alpha_2$ increases in a circulation zone. If the dispersion medium and dispersed phase densities differ slightly ($\rho_1 \approx \rho_2$), there is no separation or distribution of the dispersed phase uniform volume in a reactor. A homogeneous two-phase flow also forms in the narrow section of a device (confusor). The volume fraction of a dispersed phase $\alpha_2$ has a uniform cross-sectional distribution in this case. Calculations have led to a very important conclusion: the application

of tubular turbulent diffuser-confusor devices requires consideration of the phase separation effect and the phenomenon of nonuniform distribution of dispersed system components, for both chemical reactions and mass exchange physical processes.

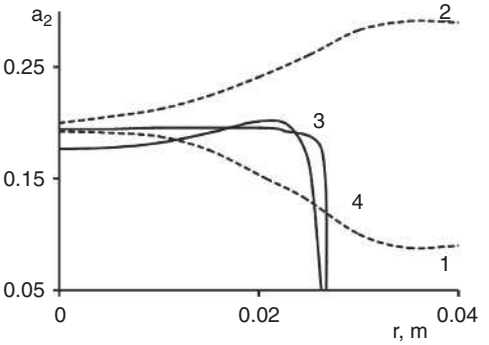


**Figure 2.28** Dependence of the dispersed phase volume fraction distribution $\alpha_2$ on reactor radius in diffuser (1, 2) and confusor (3, 4) areas. Density of the dispersion (continuous) medium $\rho_1$ = 6.93 (1, 3); 1111 (2); 998.2 (4) kg/m$^3$; dispersed phase density $\rho_2$ = 640 (1, 3); 0.689 (2); and 1111 (4) kg/m$^3$ ($d_d$ = 0.04 m, $d_c$ = 0.025 m, $L_c$ = 0.08 m, and $V$ = 16 m/s)

It seems to be very important to avoid phase separation in tubular turbulent diffuser-confusor devices at high two-phase flow rates. To reveal the criterion of the separation effect, it has been assumed that the centrifugal acceleration of a particle in a twisted flow is estimated by the following a = $V^2$/R ratio, where the rotation radius R = ($d_d$-$d_c$)/2. Introducing a modified Archimedes Number $Ar_{\text{mod}}$ and substituting the gravity member g (free fall acceleration) by the centrifugal acceleration [64], we will get the following formula:

$$A_{\text{mod}} = \frac{2d_2^3\rho_1^2V^2(\rho_1-\rho_2)}{\mu_1^2(d_d-d_c)\rho_1} \tag{2.69}$$

Physical analysis proposes the analytical equation estimating the separation, where the numerical coefficient and the power index have been calculated by the processing of numerical calculation results:

$$\frac{\Delta\alpha_2}{\alpha_{2\text{av}}} = \frac{0.06Ar_{\text{mod}}^{1.44}}{\text{Re}^{2.2}} \tag{2.70}$$

Where $\Delta\alpha_2$ is the maximum difference between the volume fractions of the dispersed phase along the device axis and in the periphery; $\alpha_{2\text{av}}$ is the average dispersed phase volume fraction in a reaction flow:

$$\text{Re} = Vd_2\rho_1 / \mu_1 \tag{2.71}$$

The analysis of turbulent motion physics for a reaction mixture in tubular channels of various designs can open the way to a quantitative and scientifically grounded approach for the selection of the optimal geometry, for any fast chemical process, to reduce the diffusion limitation and create uniform conditions for making synthetic products. However, it is necessary to find a solution for another very important problem of theoretical and applied science: the temperature mode control of fast chemical processes with high local heat generation in a reaction zone.

## 2.3 Thermal Modes of Fast Chemical Reactions

A sustainable and required thermal mode in a reaction zone is the necessary prerequisite of any safe and efficient technological process. The increase of temperature in an exothermal reaction zone is determined by thermodynamic and kinetic parameters, concentration of reactants and the method of introduction into the reactor, hydrodynamic mode in a reaction zone, and so on [84, 85]. Problems of controlling the reactor temperature mode are typical for a fast exothermic chemical reaction in a liquid phase, when the duration of a process is in the range of seconds or fractions of a second, while the reaction zone length $L_{react}$ does not usually exceed several centimetres or even fractions of a centimetre. It obviously leads to local heating of the medium, which can result in thermal explosion if the removal of heat is insufficient or absent. For this reason, the application of standard bulk mixing devices, with mechanical agitators and an external heat removal system, to fast chemical processes is technologically not reasonable due to the volume of the temperature gradient ('torch') formation at the reactant input points, which is the area of the nonstationary reaction, resulting in substantial and sometimes unacceptable overheating of a reaction mixture.

Fast chemical processes cannot be controlled using traditional methods, such as the consumption of the reaction heat for adiabatic heating of precooled feedstock or internal heat removal by the boiling of reactants in a reaction mixture [86]. Formation of a quasi-plug flow mode (when a reaction zone reaches the heat-conducting reactor walls) is a logical method for external heat removal.

### *2.3.1 Adiabatic Mode*

Adiabatic temperature growth in a reaction zone $\Delta T_{ad}$ is calculated using the following equation [61]:

$$\Delta T_{ad} = \frac{q \times \Delta P}{C_p \rho} \tag{2.72}$$

Where $q$ is the thermal effect of a reaction, $\Delta P$ is the reaction product yield from the volume unit, $C_p$, $\rho$ are the reaction mixture average heat capacity and density respectively.

**Table 2.4 Fast exothermic processes in a tubular turbulent cylindrical reactor ($T_0$ = 20 °C, $T_{cool}$ = –30 °C, $V$ = 1 m/s)**

| N | Process | $k$, l/mol·s | $q$, kilojoules/kg | $\Delta P$, kg/m$^3$ | $\Delta T_{ad}$, °C | $L_{ch}$, m |
|---|---|---|---|---|---|---|
| 1 | $CH_2=CH_2+HCl \rightarrow CH_2Cl\text{-}CH_3$ | $10^3$ | 552 | 322.5 | 127 | $2 \times 10^{-4}$ |
| 2 | $CH_2=CH_2+Cl_2 \rightarrow CH_2Cl\text{-}CH_2Cl$ | $10^3$ | 1,899 | 495 | 589 | $2 \times 10^{-4}$ |
| 3 | $C_6H_6+Cl_2 \rightarrow C_6H_5Cl+HCl$ | $10^4$ | 1,163 | 627.5 | 490 | $2 \times 10^{-5}$ |
| 4 | $HCl+NaOH \rightarrow H_2O+NaCl$ | $10^8$ | 1,970 | 377.5 | 131 | $2 \times 10^{-10}$ |
| 5 | $\left[CH_2=CH\text{–}CH=CH_2\right]$ (CH$_3$ branch) $\xrightarrow{AlCl_3\,O(C_6H_5)_2}$ $\left[\sim CH_2\text{–}CH=CH\text{–}CH_2\sim\right]$ (CH$_3$ branch) | 6.7 | 1064 | 340.0 | 247 | $5 \times 10^{-2}$ |
| 6 | $H_2SO_4+nH_2O \rightarrow H_2SO_4 \cdot nH_2O$ (n = 3.6) | $10^7 \pm 1$ | 196 | 1465.2 | 84 | $1.1 \times 10^{-8} \pm 1$ |
| 7 | $n\left[CH_2=C(CH_3)\text{–}CH_3\right] \xrightarrow{AlCl_3} n\left[\sim CH_2\text{–}C(CH_3)\text{–}CH_3\sim\right]$ | $10^6$ | 971 | 280.0 | 232 | $5.7 \times 10^{-2}$ |
| 8 | $\sim CH_2\text{-}C(CH_3)=CH\text{-}CH_2\sim + Cl_2 \xrightarrow{-HCl}$ $\sim CH_2\text{-}C(=CH_2)\text{-}CHCl\text{-}CH_2\sim$ | $2 \times 10^2$ | 2706 | 250.0 | 4 | 2 |
| 9 | $RCH=CH_2 + H_2SO_4 \rightarrow R\text{-}CH(CH_3)\text{-}O\text{-}SO_3H$ | 30 | 584 | 350.0 | 200 | 14 |

Depending on the numerical values of the thermal effect q and reaction product yield $\Delta P$ of a chemical process, the increase of temperature $\Delta T_{ad}$ in a reaction zone can be as high as dozens or even hundreds of degrees, where all the heat is released very rapidly (in seconds or fractions of a second) and in a small area:

$$L_{chem} = V \times \tau_{chem} = V / (k[C]^{n-1}) \tag{2.73}$$

For the polymerisation process (**Table 2.4**):

$$L_{chem} = V / k_g \tag{2.74}$$

Fast polymerisation processes, when $R < R_{cr}$, demonstrate an averaging of temperature by intensive longitudinal and cross-sectional mixing in such a way, that the MWD and average MW become similar to isothermal conditions at temperatures corresponding to the adiabatic heat of a mixture. However, adiabatic polymerisation opportunities are usually limited by substantial MW reduction at high temperatures and the occurrence of side processes, such as the destruction and crosslinking of molecules.

The possibility of cooling a feedstock for the process, with the temperature below the boiling point of a reaction mixture, is limited by the boiling point of the cooling agent, such as liquid ethylene ($T_{boil}$ = -90 °C (183 K)). The temperature of a mixture will increase up to the boiling point of a solvent in proportion to the growth of the polymer product yield, see the following equation [88]:

$$\Delta M = \frac{C_p}{q}(T_p - T_0) \tag{2.75}$$

Isobutylene polymerisation has been studied to demonstrate that a temperature of 90 °C (liquid ethylene with $T_{boil}$ = -90 °C (183 K) was used as the cooling agent) allows the polymerisation of about 15 wt% of a liquid, by adiabatic heating of the reaction mixture. There are fewer possibilities for monomer solution cooling when, for example, liquid ammonium is used as a cooling agent ($T_{boil}$ is -30 °C (243 K)), as the reaction mixture heating period will only produce up to 10 wt% of a polymer.

One of the most efficient ways of heat removal from a chemical reaction is the internal heat removal caused by the boiling of the reaction mixture components [84, 89, 90–92].

### *2.3.2 Internal Heat Removal*

A boiling process occurs over a narrow temperature range and $T_{boil}$ is usually a complex function of the reaction mixture composition. For the effective control of the

temperature field, it is necessary to know how the boiling temperature and evaporation heat correlate with the composition of a reaction mixture. In the case of internal heat removal, the reaction mixture temperature can be maintained at a constant level; as for certain processes it is sufficient to utilise the evaporation heat and solvent to maintain the required process temperature, until all the reactants are consumed. The reaction temperature increases up to $T_{\text{boil}}$, then a constant temperature is maintained until the completion of boiling, marked by the transition of the solvent and/or some part of the reactants into a gas phase. When all the boiling liquid becomes steam, the system temperature continues to increase.

The amount of polymer synthesised by the effect of feedstock heating from $T_0$ to $T_{\text{boil}}$ can be estimated by the following equation [88]:

$$q\Delta M = C_p(T_{\text{boil}} - T_0) + \chi_s S_0 + \chi_M(M_0 - \Delta M) \tag{2.76}$$

Thus,

$$\Delta M = \frac{C_p(T_{\text{boil}} - T_0) + \chi_S + (\chi_M - \chi_S)M_0}{\chi_M + q} \tag{2.77}$$

Where $S_0 = (1\text{-}M_0)$, $M_0$ are the initial mass fractions of solvent and monomer in a reaction mixture respectively; $\chi_m$, $\chi_s$ are the heat of evaporation of the monomer and solvent respectively.

When the boiling process occurs at a variable temperature, the following equation:

$$T_{\text{boil}}^{\max} - T_{\text{boil}}^{\min} << \frac{RT_{\text{boil}}^2}{E_M - E_p} \tag{2.78}$$

is the quantitative criterion for constant temperature used for the analysis of polymer molecular weight and molecular weight distribution, where $R$ is the gas constant; $E_p$, $E_M$ are activation energies of the chain propagation and chain transfer to monomer reaction respectively.

A specific equation has been developed for a particular case, i.e., when the rate constants of the chain propagation and active centre elimination reaction do not depend on temperature, the kinetic chart of polymerisation favours fast initiation, the reaction is first-order by monomer and active centre concentration in their elimination reaction [84], then:

$$\sum_{i=1}^{k} \Delta M_i = M_0 \left[ 1 - \exp\left( -\frac{k_p}{k_\Gamma} \sum_{i=1}^{k} A_1^* \right) \right] \tag{2.79}$$

In general, internal heat removal caused by the boiling of components in a reaction mixture is an effective way of thermostating fast liquid-phase chemical reactions. In addition, gas-phase formation in a reaction system intensifies the turbulent mixing of the reactant volume.

### 2.3.3 External Heat Removal

The analysis of the temperature profile in a fast polymerisation reaction flow demonstrates that an increase of reactor radius, under conditions of external heat removal, leads to a substantial change in the temperature of the reaction mode [84, 88, 90, 93–95]. For example, a tubular turbulent reactor of small radius has similar temperatures of central and peripheral flows (the difference can be seen at the initial polymerisation stage only and does not exceed 2 – 5°) (**Figure 2.29**). This parameter reaches its maximum of 50 – 60 °C with an increase of reactor radius, despite low (up to 30 wt%) degrees of monomer conversion. The polymerisation reaction temperature profile is, in this case, distorted and characterised by the area of maximal temperature in the central area of the flow, while the peripheral temperature remains constant. The latter effect means that the reaction zone does not actually reach the reactor walls, i.e., a volume temperature gradient is formed (reaction zone radius $R$ and length $L$ gradient). A reaction in a smaller radius reactor reaches the heat-exchanging walls and the temperature is effectively reduced by external heat removal.

The decrease of temperature gradients in the fast polymerisation processes exerts a substantial influence on the molecular characteristics of the polymers. Heat removal by a heat-conducting wall determines, in many cases, the possibility of the practical implementation of the process. Changing the input method of the reactants into a reaction zone, under conditions of external heat removal, affects the MW characteristics of the products of fast polymerisation processes [30, 31, 95, 96].

The unified mathematical model is presented in [102, 103] for monomer and catalyst input into the flow of the isobutylene polymerisation reaction zone. Two methods of reactant input are proposed: I – central single-point catalyst input *via* a coaxial nipple with the monomer flow being codirectional to the catalyst flow in the near-wall circular area of a reactor; II – circular channel catalyst input along the internal wall (an inverted way in comparison with the method I). Calculations have demonstrated that the method of feedstock input does not affect the MW or MWD of a polymer product in reactors with a small reaction zone radius, under the conditions of no external heat removal. An increase of the external heat removal output leads to differences in the MW and MWD of products, depending on the input method of reactants. The model I method, involving an axial catalyst input demonstrates a $P_n$ increase with a sequential decrease of $P_w/P_n$, reaching the value of 2 at $C_T = 50$. Model II, with the circular near-wall catalyst input, demonstrates a $P_w/P_n$ close to the value of 2 at $C_T = 20$; it is significant that the $P_n$ value for model II always exceeds that of model I, all other things being equal.

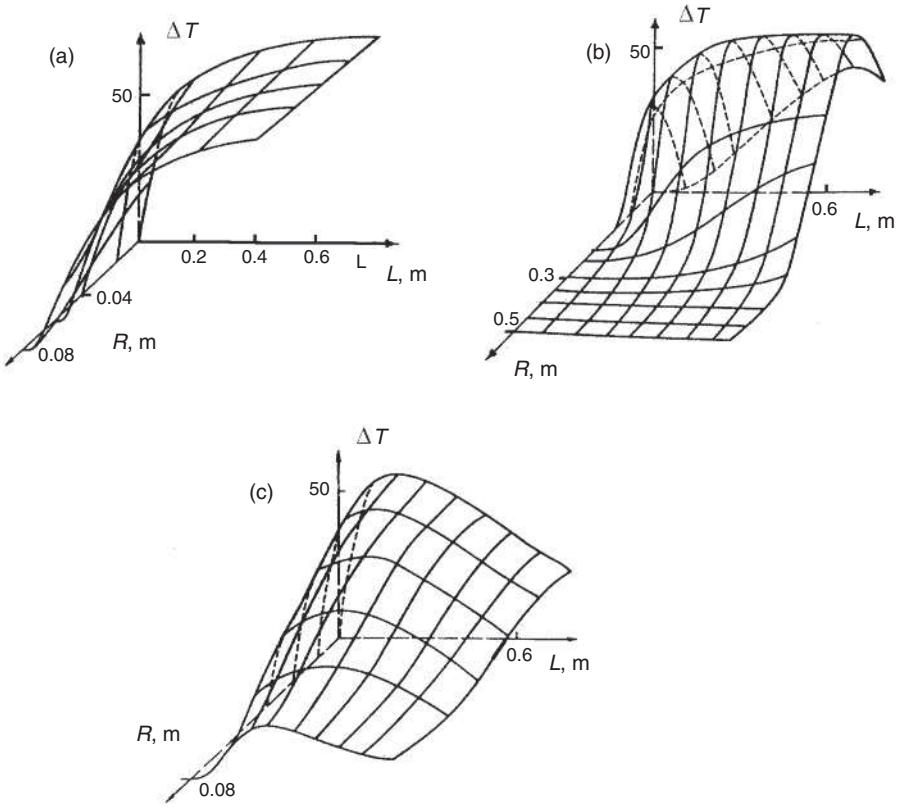


**Figure 2.29** The temperature change of reaction flow in a fast isobutylene polymerisation reaction ($R$ = 0.08 (a), and 0.5 (b) m) in external heat removal conditions ($C_T$ = 50, $R$ = 0.08 m, $C_m$ = 2.5 mol/l, $C_{Al}$ = 4.5 mmol/l, and $T_0$ = 27 °C (300 K))

An increase of the reactor radius during polymer production creates a more perceptible effect on changes of the polymer MW characteristics, the $P_n$ value for method I does not demonstrate significant changes with an increase of the intensity of heat removal through a metallic wall. The polydispersity coefficient stays constant in this case. Catalyst input method II (model II) shows a substantial decrease of $P_w/P_n$, which approaches exponential behaviour and simultaneous growth of $P_n$.

The revealed effect is stipulated by the temperature field patterns in a reaction volume. Using small radii, when the reactor front is planar, the thermostating effect is caused by the decrease of reaction temperature at the initial process stage. It varies along the reaction zone in the same way for both methods of input. When using large radii, the temperature field varies over the entire reactor volume. The near-wall catalyst input method leads to the formation of a maximal temperature zone in the proximity of the thermostated wall, smoothing of the temperature field and facilitating heat

removal. It leads to narrowing of the MWD of the polymer product. In the case of an axial catalyst input into a large radius reactor, the heat removal does not influence the process behaviour, even at higher heat transfer coefficients. This effect is caused by the monomer bypass in the near-wall area, providing heat insulation. Thus, the external heat removal in fast chemical reactions can be efficient only if the reaction reaches the heat removal surface. It can be achieved either by a reduction of the reactor radius to fit the reaction zone or by shifting the reaction front to the peripheral area, for example, by variation of the reactant input method.

A quasi-plug flow mode description, in cylindrical tubular turbulent devices, requires the development of an equation for the calculation of a temperature field in a reaction volume of a fast chemical reaction (assuming 100% at the reactant input points). In this case, a thermal balance equation for the surface element *dF* will be the following [38]:

$$dQ = G_1 C_{\text{pr}}(-dT_p) = G_{\text{cool}} C_{p\text{cool}} dT_{\text{cool}} \tag{2.80}$$

Where $G_r$, $G_{\text{cool}}$, $C_{pr}$, $C_{\text{pcool}}$ are the mass flow rate and heat capacity of a reaction mixture, and a cooling agent respectively.

**Equation 2.80** can be transformed into the following equation:

$$d(T_r - T_{\text{cool}}) = -dQ\left(\frac{1}{G_r C_{pr}} + \frac{1}{G_{p\text{cool}} C_{p\text{cool}}}\right) \tag{2.81}$$

According to the basic heat transfer law:

$$dQ = K_T dF(T_r - T_{\text{cool}}) \tag{2.82}$$

Where $K_T$ is the coefficient of the heat transfer through a wall, therefore **Equation 2.81** can be transformed in the following way:

$$d(T_r - T_{\text{cool}}) = -K_m dF\left(\frac{1}{G_p C_{pr}} + \frac{1}{G_{\text{cool}} C_{p\text{cool}}}\right) \tag{2.83}$$

After separation of the derivatives and integration of the resulting equation from $T_{\text{ad}}$-$T_{x1}$ ($T_{\text{ad}} = T_0 + \Delta T_{\text{ad}}$) to $T_{\text{r}}$-$T_{\text{cool2}}$ ($T_r$ is the required temperature in the reaction zone) and *dF* – from 0 to *F* (at $K_T$ = const):

$$\ln\frac{T_p - T_{\text{cool2}}}{T_{\text{ad}} - T_{\text{cool1}}} = -K_m F\left(\frac{1}{G_r C_{pr}} + \frac{1}{G_{\text{cool}} C_{p\text{cool}}}\right) \tag{2.84}$$

Where $F = 2\pi R L_{\text{cool}}$ and $G = V\pi R^2\rho$.

Calculation of the required cooling zone in a tubular turbulent device using **Equation 2.84** requires the heat transfer coefficient values $K_T$:

$$K_T = \frac{1}{\frac{1}{\alpha_1} + \frac{\delta}{\lambda} + \frac{1}{\alpha_2}} \tag{2.85}$$

Where $\alpha_1$ and $\alpha_2$ are the heat emission coefficients of cooled and heated flow (cooling agent) respectively; $\delta$ is the wall width (0.001 m); and $\lambda$ is the heat conductivity coefficient of the wall (1.389 Joules/m·s·grad for silica glass). Heat emission coefficient values can usually be found in reference books (for water at 50 °C (323 K), $\alpha$ = 1801.44 Joules/m·s·grad).

The value of the heat emission coefficient depends on various factors and is a function of many derivatives. The heat emission coefficient is mainly determined by the following factors: 1) heat carrier-type (gas, steam, droplets of liquid); 2) the type of liquid flow (free or forced flow); 3) wall geometry (length, diameter, and so on); 4) state and properties of a liquid (temperature, pressure, density, heat capacity, heat conductivity, viscosity); 5) motion parameters (flow rate); and 6) wall temperature.

**Figure 2.30** demonstrates the dependence of the cooling zone length on a circular flow rate $w_c$, the values are experimental (curve 1) and calculated (**Equation 2.62**) (curve 2) [45, 97]. The figure demonstrates that for low rates of a circular flow (cooling agent), the experimental and calculated values of $L_{cool}$ do not match. At the same time, the mismatch decreases at high $w_c$ values and the experimental and calculated values of $L_{cool}$ match at the cooling agent flow rate value of about 350 sm/s. As the increase of $w_c$ leads to the growth of $\alpha_2$ (due to the intensification of the circular flow turbulence), the heat transfer coefficient will be determined entirely by the heat emission coefficient $\alpha_1$ of the inner flow.

Therefore, **Equation 2.62** can be transformed considering the following factors: 1) at a high cooling agent flow rate ($G_x \to \infty$), the temperature can be considered to be $T_{cool}$ = const (as tubular turbulent devices are compact, this requirement is followed in most cases); and 2) the heat transfer coefficient can be substituted by the reaction mixture heat emission coefficient for a fast chemical reaction (in accordance with (**Equation 2.63**), the heat conductivity coefficient will be determined by the smallest value of the heat emission coefficients). In this case (**Equation 2.62**) can be transformed using the aforementioned assumptions [97]:

$$\Delta T = T_{ad} - T_r = \left(T_{ad} - T_{cool}\right)\left(1 - e^{-2\alpha L_{cool}/\rho C_p R V}\right) \tag{2.86}$$

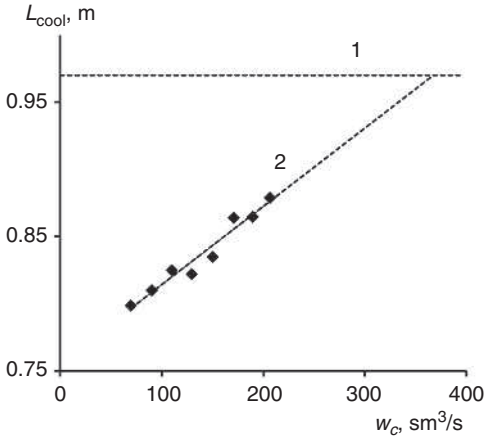


**Figure 2.30** Experimental (1) and calculated (2) cooling zone length values in a cylindrical reactor. $T_{ad}$ = 50 °C, $T_{cool}$ = 4–5 °C, $\alpha_1$ = 1801.44 Joules/(m$^2$·s·K), $\delta$ = 0.001 m, $\lambda$ = 1.389 Joules/(m·s·K), $w_B$ = 47 sm$^3$/s, $R$ = 0.008 m, $C_p$ = 4179.91 Joules/(kg·K), and $\rho$ = 1000 kg/m$^3$

**Figure 2.31** demonstrates the dependence of experimental and calculated, by **Equation 2.86,** temperature drops in a reaction zone on the reaction flow rates. It can be seen that assuming $T_{cool}$ = const, **Equation 2.64** provides a reliable description of experimental data and can be used for the analysis and search for effective control methods for the thermal mode of fast chemical reactions [98–103].

Substitution of the heat conductivity coefficient by the heat emission coefficient in (**Equation 2.86**) facilitates the calculation of the temperature field for a reaction zone, as the heat emission coefficient can be obtained using the similarity theory.

Solving (**Equation 2.64**) to find $L_{cool}$, we can estimate the cooling length, under conditions of external heat removal, required for a sustainable $T_r$ temperature value in a reaction volume:

$$L_{cool} = \frac{\left[\ln\left(1 - \frac{T_{ad} - T_r}{T_{ad} - T_{cool}}\right)\right] C_P \rho R V}{2\alpha} \tag{2.87}$$

$L_{cool}$ grows with an increase of $C_p$, $\rho$, $R$, and $V$ values. The heat emission coefficient $\alpha$ also depends on these parameters. The parameter $\alpha$ (in **Equation 2.65**) can be expressed in terms of the Nusselt Number (turbulent mode):

$$\mathrm{Nu} = 0.023\ (\mathrm{Re})^{0.8}\,(\mathrm{Pr})^{0.3} \tag{2.88}$$

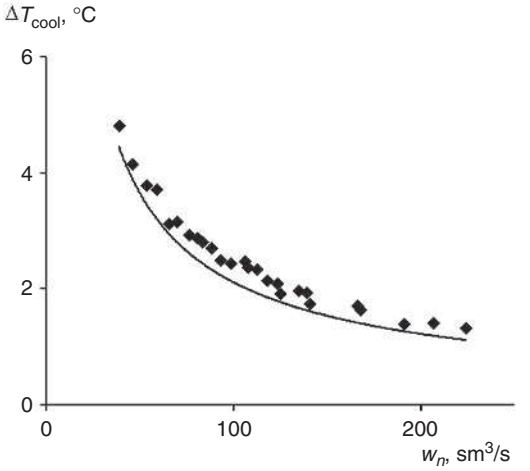


**Figure 2.31** Comparison of the experimental (dots) and calculated (curve) temperature drop $\Delta T_{cool}$ in a cylindrical reactor for various reaction flow rates $w_B$. $w_c$ = 130 sm$^3$/s, $L$ = 1 m, $T_{ad}$ = 50 °C, $T_{cool}$ = 4–5 °C, and $\alpha_2$ = 800 Joules/(m$^2$·s·K), $\alpha_1$ values are taken from a reference book (nomograms)

With the use of the corresponding equations for the Re:

$$\mathrm{Re} = Vd\rho / \mu \tag{2.89}$$

and the Prandtl Number:

$$\mathrm{Pr} = \mu C_p / \lambda \tag{2.90}$$

$$\alpha = \frac{Nu\lambda}{2R} = \frac{0.02\rho^{0.8} C_p^{0.3} \lambda^{0.7} V^{0.8}}{\mu^{0.5} R^{0.2}} \tag{2.91}$$

Transforming **Equation 2.87** with consideration of **Equation 2.91** to get [99, 101]:

$$L_{cool} = \frac{\left| \ln\left(1 - \frac{T_{ad} - T_r}{T_{ad} - T_{cool}}\right) \right| R^{1.2} C_P^{0.7} \mu^{0.5} \rho^{0.2} V}{0.04\lambda^{0.7}} \tag{2.92}$$

Considering that the $C_p$, $\rho$, $\mu$, and $\lambda$ parameters do not depend on temperature in the first approximation, we get:

$$C_p^{0.7} \mu^{0.5} \rho^{0.2} / 0.04\lambda^{0.7} = A = \mathrm{const} \tag{2.93}$$

Therefore:

$$L_{cool} = A\left|\ln\left(1-\frac{T_{ad}-T_r}{T_{ad}-T_{cool}}\right)\right|R^{1.2}V^{0.2} \qquad (2.94)$$

As we can see, the A value is determined solely by the physical parameters of a reaction system and is independent of the kinetic and hydrodynamic parameters of a process. Every chemical process is characterised by the quantitative values of these parameters, which exert a substantial influence on the cooling zone length $L_{cool}$.

**Equation 2.94** determines the possible control methods for fast chemical reaction processes, using a tubular jet device with external heat removal. In particular, changing $T_0$ will lead to cooling of the feedstock; a change of $\Delta P$ will decrease the adiabatic heating of a reaction mixture, due to a decrease of volume product yield; the change of $T_{cool}$ will allow a cooling agent with a lower boiling point temperature; a change of $R$ will increase the reactor radius and still guarantee the formation of the quasi-plug flow mode in turbulent flows; a change of $V$ will increase the reaction mixture flow rate, thus the heat emission coefficient value in a reactor will grow as well as the heat conductivity through a thermal conductive wall, in conditions of a turbulent reaction mixture mode.

A quite easy method of controlling the cooling length $L_{cool}$ is to change the reactor radius $R$ as well as the linear flow rate of reactants $V$, however, this results in a markedly decreased output. In accordance with **Equation 2.94**, an increase of $V$ from 1 to 10 m/s will lead to a 1.6 times increase of $L_{cool}$, while a tenfold change of $R$ will lead to a more than 15 times change of $L_{cool}$.

The dependence of a reaction mixture temperature ($T_r$) in the cooling length ($L_{cool}$) of a tubular device, using the example of the fast reaction of ethylene hydrochlorination at different reactor radius values, is demonstrated in **Figure 2.32**. The decrease of temperature in a device of $R$ = 0.2 m, assuming a 50 °C reaction mixture cooling ($T_{cool}$ = 10 °C (283 K)) can be provided by $L_{cool} \geq 229$ m. A cooling agent with $T_{cool}$ = -30 °C (243 K) will provide about a twofold decrease of $L_{cool}$ ($L_{cool}$ = 110 m), which is still significant. However, a tubular turbulent device with a tenfold less reactor radius $R$ = 0.02 m, will have an $L_{cool}$ length of 14.3 and 7 m respectively, thus it will decrease by more than 15 times and demonstrate a technologically acceptable design. The proposed reactor design provides a quasi-isothermic mode for the reaction, with the obtained final product cooled to the required temperature.

These results give a unique demonstration of the fact that for fast exothermal processes ($k \geq 10^2 \pm^1$ l/mol·s) in jet-type tubular turbulent devices, heat removal can only be possible after the completion of a process (heat removal from the reaction product

but not from the reaction zone). It is practically impossible to achieve a correlation between the reaction zone length and the length of a tubular turbulent reactor, even for a substantially reduced $T_{cool}$ (**Figure 2.33**).

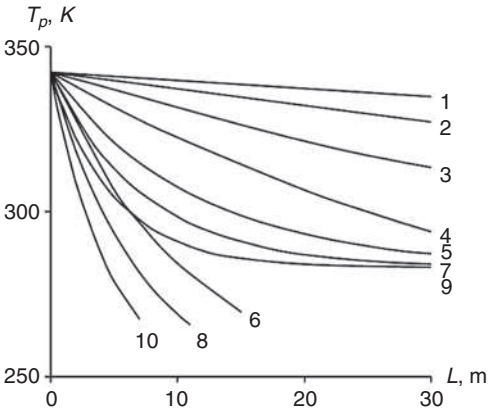


**Figure 2.32** Variation of temperature ($T_p$) along the reactor length ($L$) during ethyl chloride synthesis with external heat removal. $R$ = 0.2 m (1.2); 0.063 m (3.4); 0.02 m (5.6); 0.014 m (7.8); 0.01 m (9.10). $T_{cool}$ = 10 °C (283 K) (1, 3, 5, 7, 9); -30 °C (243 K) (2, 4, 6, 8, 10). ($V$ = 1 m/s, $T_0$ = 0 °C (273 K), and $\Delta P$ = 204 kg/m$^3$, $\Delta T_{ad}$ = 800)

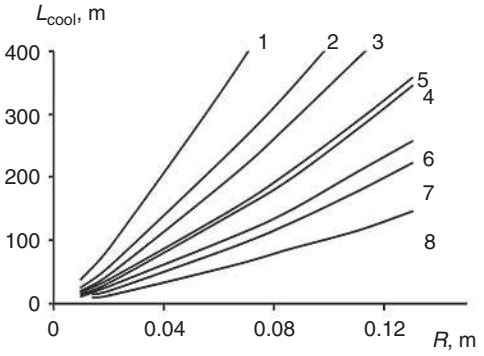


**Figure 2.33** Dependence of the cooling zone length ($L_{cool}$) on reactor radius $R$. Neutralisation process ($\Delta p$ = 204 kg/m$^3$) (1, 2); dichloroethane synthesis ($\Delta P$ = 67 kg/m$^3$) (3, 4); benzene chloride synthesis ($\Delta P$ = 100 kg/m$^3$) (5, 6); and ethyl chloride synthesis ($\Delta P$ = 204 kg/m$^3$) (7, 8). $T_{cool}$ = 10 °C (283 K) (1, 3, 5, 7); and $T_{cool}$ = -30 °C (243 K) (2, 4, 6, 8). ($V$ = 1 m/s, $T_0$ = 0 °C (273 K), and $\Delta T_{ad}$ = 800)

The effective way to control the thermal mode of tubular reactors, during fast turbulent chemical processes, is to decrease the device radius $R$ (**Figure 2.33**). At the same time, a decrease of the cross-sectional area of a reaction flow will inevitably lead to a

decrease of process output, which is unacceptable under industrial conditions. A drastic alternative to increase the parameters responsible for efficient fast chemical processes is the application of shell-and-tube jet turbulent devices, which are technically a collection of $N$ small diameter tubes, washed by a cooling agent (a standard shell-and-tube heat exchanger model) and operating in the quasi-plug flow mode in turbulent flows.

In this case:

$$L_{\text{cool}} = A\left|\ln\left(1-\frac{T_{ad}-T_r}{T_{ad}-T_{\text{cool}}}\right)\right|\frac{R^{1.2}V^{0.2}}{N^{0.6}} \tag{2.95}$$

Partitioning of a uniform flow (single-tube reactor with a large radius) in a jet-type shell-and-tube of $N$ separate flows, allows an $N^{0.6}$ decrease of the cooling zone length $L_{\text{cool}}$, making the process easier and practically more feasible. It is the opportunity to control fast chemical processes in a quasi-plug flow mode, through external heat removal, which offers similar designs of tubular turbulent devices and the heat exchanger equipment used in chemical engineering.

**Table 2.5** demonstrates the dependence of the cooling zone length $L_{\text{cool}}$, which provides 0 °C (273 K) in a reaction zone at a given output and the $T_{\text{cool}}$ values (-35 °C (238 K) and 258 °C (531 K)), on the radius $R$ (the ethylene hydrochlorination process is given as an example) for various numbers of tubes in a shell-and-tube turbulent reactor.

**Table 2.5 The dependence of cooling length zone $L_{\text{cool}}$ ($T_p$ = 0 °C) on the number of tubes $N$ and radius $R_n$ in a shell-and-tube turbulent reactor for the ethylene hydrochlorination process ($\Delta P$ = 322.5 kg/m$^3$, $q$ = 552 kilojoules/kg, $k$ = 10$^3$ l/mol·s, $V$ = 1 m/s, $T_0$ = –10 °C and $\Delta T$ = 100 °C)**

| The number of tubes in a reactor, $N$ | Tube radius $R_n$, m | Cooling zone length $L_{\text{cool}}$, m | |
|---|---|---|---|
| | | $T_{\text{cool}}$ = 238 °C | $T_{\text{cool}}$ = 258 °C |
| 1 | 0.1697 | 90.0 | 138.0 |
| 2 | 0.1200 | 60.0 | 91.0 |
| 10 | 0.0537 | 20.5 | 31.5 |
| 60 | 0.0216 | 7.5 | 12.0 |
| 100 | 0.0170 | 6.0 | 8.8 |
| 150 | 0.0139 | 4.5 | 6.8 |
| 200 | 0.0120 | 3.8 | 5.8 |
| 250 | 0.0107 | 3.3 | 5.0 |
| 300 | 0.0098 | 3.0 | 4.5 |
| 320 | 0.0095 | 2.8 | 4.4 |

Stable 0 °C (273 K) temperature conditions in a reaction zone for $R$ = 0.17 m is almost impossible even at $T_{cool}$ = -35 °C (238 K), as the length of cooling zone will exceed 90 m in this case. However, if a shell-and-tube reactor is used, a sustainable 0 °C (273 K) temperature can be reached starting from $N \geq 60$ even at $T_{cool}$ = -15 °C (258 K) ($L_{cool}$ = 7.5 and 12 m respectively). In addition, it is in principle, possible to carry out a process in conditions close to isothermic ($L$ = 10 m, $N$ = 100).

Therefore, a decrease of reactor radius, and its representation as a collection of tubes, is quite an easy and effective method to control the thermal mode in a reaction volume in fast liquid-phase chemical processes, within tubular turbulent jet-type devices. However, it does not solve the problem of the local overheating of a reaction mixture at input points. The 'zone' model should be used to avoid undesirable overheating of reaction mixtures in fast chemical processes. This model is based on a consecutive joint approach, where several independent reaction zones are linked together. Each input zone is the output of a previous zone, with a reaction mixture cooled down to $T_r$. Each zone is fed by precisely measured portions of reactants (catalysts), which will provide an acceptable temperature growth, determined by the product yield in each zone. The tubular jet-type turbulent device is, in this case, represented by sequential adiabatic plug flow mode mini reactors, operating in turbulent flows with $L_{cool}$ length and separated by a heat removal zone with $L_{cool}$ length.

The water-sulfuric acid interaction process has been selected to demonstrate the operation of a tubular turbulent device in terms of the 'zone' model. This particular process is the dissolution of 90% sulfuric acid by water to a 60% concentration. The process is accompanied by substantial heat generation (**Figure 2.34**).

The intensive water-sulfuric acid interaction ($k = 10^7 \pm 1$ l/mol·s) and substantial thermal effect ($q$ = 196 kilojoules/kg) result in ~84 °C adiabatic increase of temperature in an extremely small local area of the reaction volume ($L_{cool} = 10^{-7} \pm 1$ m). In this case, technologically acceptable conditions (reactor temperature does not exceed 70 °C (343 K)) can be achieved in a two-zone operation model with the partial feed of a 90% acid solution into two zones, separated by the cooling area. This approach provides a technologically acceptable temperature mode for the process. In addition, the partial feeding of acid allows a 20% reduction of the device's radius in the first zone (from 0.01 to 0.008 m). It favours both the required level of flow turbulence and the increase of external heat removal output (additional 15–20% decrease of $L^1_{cool}$). The maximum permissible temperature growth of a reacting system in a tubular device, determines (up to some critical value) the required number of independent reaction zones, under the conditions of partial feeding, i.e., the necessity of 'zone' model utilisation.

The effective control of the thermal field, in a zone of fast liquid-phase reactions, is achieved using the 'zone model', with the reaction zones separated by shell-and-tube refrigerators. The model of this device has been tested using the cationic polymerisation of isobutylene (**Table 2.6**).

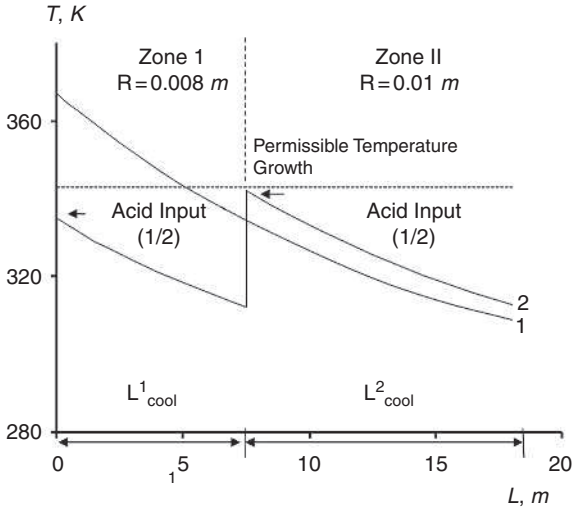


**Figure 2.34** The temperature variation along the axis of the device in conditions of external heat removal during the sulfuric acid-water interaction in the turbulent mode. One-zone (1) and two-zone (2) models are used. ($T_0$ = 10 °C (283 K), and $V$ = 1 m/s)

It should be noted that the external heat removal output in tubular devices is strongly influenced by the hydrodynamic mode of a reaction mixture [102]. The transition from laminar to turbulent mode at a constant process output $w$ (selected value $w = V \times \pi \times R^2 = 10.3$ m$^3$/h), will increase the external heat removal output. It will, in turn, decrease the cooling zone length (**Figure 2.35**). The Reynolds Number will increase from 2300 to $4 \times 10^4$ at a constant process output and therefore, the reactor volume for the process using water will decrease by 1000 times and the reactor volume for ethylene hydrochlorination will decrease by 300 times. The unstable (transition) mode of tubular devices requires a much longer cooling zone, even in comparison with the laminar mode; the aforementioned conclusions require consideration for the implementation of fast chemical processes.

In addition, as the cooling zone length does not usually exceed several centimetres in tubular devices for fast chemical processes (cationic polymerisation of isobutylene, neutralisation of acidic media, and so on), tubular devices with $L/d < 100$ are recommended for such processes. It will provide more than a 1.5 times (up to 1.65 times) increase of external heat removal (heat emission coefficient) output by additional turbulisation from the input and output nipples.

**Table 2.6 The temperature mode and cooling zone parameters for the isobutylene polymerisation process in the tubular reactor ($T_0$ = -20 °C, $C_m$ = 2 mol/l, $k_r$ = $10^6$ l/mol·s, $k_g$ = 17.5 $s^{-1}$ and $V$ = 1 m/s)**

| Parameter | | Tubular turbulent reactor | Zone model | | | |
|---|---|---|---|---|---|---|
| | | | Zone 1 | Zone 2 | Zone 3 | Zone 4 |
| $[AlCl_3] \times 10^5$, mol/l | | 9.3 | 0.69 | 1.15 | 4.62 | 2.84 |
| Conversion, % | | 99.5 | 32.5 | 65 | 97.5 | 99.5 |
| $\Delta T$ | | 92 | 30 | 30 | 30 | 2 |
| $L_{chem}$, m | | 0.057 | 0.057 | 0.057 | 0.057 | 0.057 |
| $L_{cool}$, m (up to $T_p$ = 253 °C) | $T_{cool}$ = 223 °C | 256 | 3.5* (126.6)** | 3.5 (126.6) | 3.5 (126.6) | 0.32 (11.8) |
| | $T_{cool}$ = 243 °C | 424 | 7* (253.2)** | 7 (253.2) | 7 (253.2) | 0.15 (33.3) |
| $L_{total}$, m | $T_{cool}$ = 223 °C | 256 | 11.2* (392)** | | | |
| | $T_{cool}$ = 243 °C | 424 | 21.6* (793)** | | | |

*Shell-and-tube refrigerator (400 $R$ = 0.01 m tubes with cross-section area s = S/N, washed by a cooling agent).
**Single-tube constant diameter refrigerator ($R$ = 0.2 m with cross-section area $S$, washed by a cooling agent).

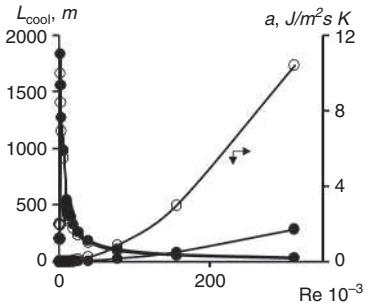


**Figure 2.35** Dependence of the cooling zone length $L_{cool}$ and heat emission coefficient α on the hydrodynamic mode of the tubular device operation using water (O) (heat exchange) and ethyl chloride (•) (heat exchange in the liquid-phase hydrochlorination of ethylene) at constant process output (10.3 $m^3$/h). ($T_{ad}$ = 101 °C; $T_0$ = 5 °C; $T_r$ = 20 °C; and $T_{cool}$ = 10 °C)

Thus, there are several original solutions for the effective control of the thermal mode using external heat removal, in real applications of cylindrical tubular turbulent devices, for fast chemical processes accompanied by high heat release. These solutions are: changing the reactor radius $R$, reactant flow rate $V$, using the 'zone' model for a fast chemical process with the feedstock input partitioned along the reactor axis, and the application of shell-and-tube devices with a collection of tubes of smaller radius. In addition, tubular reactors should be operated in the developed turbulent mode, which allows the creation of a uniform concentration of reactants in a reaction zone (plug flow mode in turbulent flows) and provides an effective control tool for heat removal through an increase of the reaction mixture heat emission coefficient.

External mode heat removal in turbulent flows is determined by the heat transfer, thermal conductivity, and convective heat exchange. There are many different methods for effective heat exchange intensification [104–108]. The most widespread and universal solution for a single-phase flow is turbulisation using local hydrodynamic resistance (turbulisers). As the channels are usually many times longer than the relaxation post turbuliser zone, a notable intensification can be achieved using a sufficiently high number of sustainable turbulisers [109]. Intensification of the near-wall thermal layer is achieved by the widely used method of tubular device knurling (the ratio of the wide diffuser area diameter to the narrow confusor area diameter is $d_d/d_c < 1.1$) [108, 110]. The authors of this publication presume that there is no need to affect the core of a flow, as its turbulisation is a low contribution to heat removal, while it generates substantial hydrodynamic resistance and energy loss. The greatest heat exchange intensification is achieved in the transition area (Re = $(2–5)10^3$) and its value is $\alpha_{prof}/\alpha_{smooth} = 2.83$ ($\alpha_{smooth}$ and $\alpha_{prof}$ are the thermal emission coefficients of a reaction mixture flow in the profiled and smooth channels respectively) at $d_d/d_c \approx 1.08$, and the length of a section $L_c = d_d$. In the area of well-developed turbulent flow, the process is the most efficient at $d_d/d_c \approx 1.06$ and $L_c = (0.25–0.5)d_d$. $\alpha_{prof}/\alpha_{smooth}$ reaches a maximum of 2.3 for liquids and 3–3.1 for gases. In addition, turbulisers in profiled tube devices provide a 3–5 times decrease of crust formation in a heat exchange channel, due to the precipitation of salts [111].

Publications [97, 109, 112–114] analyse the convective heat exchange intensification by deep profiling of a tubular channel of diffuser-confusor design ($d_d/d_c \approx 2$). It has been demonstrated, that the resistance coefficient of a tubular turbulent channel, in a diffuser-confusor device, is approximately 25 times higher than that of a cylindrical device, its value however, is only about 15% of the calculated total of the local resistance. Calculation of the heat emission coefficients, based on criteria models, demonstrates a highly intensive convective heat exchange in tubular turbulent diffuser-confusor devices, in particular, this value is in the order of 3.5–4 in the range of Re = $(1–2)10^4$ [109, 115]. The output of convective heat exchange in tubular turbulent diffuser-confusor devices (and therefore, the intensity of heat removal through

external thermostating of heat-conducting walls) is determined by the formation of local hydrodynamic resistance along the reaction mixture flow. As has been already noted, it leads to an increase of the input-output pressure drop.

A cylindrical device is characterised by similar input and output pressures (**Figure 2.36**); the input-output pressure drop is low in this case, not exceeding 0.03 atmospheres under experimental conditions. Quantitative correlations between pressure in a tubular turbulent device and the reaction mixture flow rate ($R$ is the correlation coefficient) [45, 97]:

$$P_{\text{in}} = 2\times10^{-9} w^{3.47} (\text{input},\ R = 0.98) \tag{2.96}$$

$$P_{\text{out}} = 2\times10^{-10} w^{3.86} (\text{output},\ R = 0.99) \tag{2.97}$$

$$\Delta p = 4\times10^{-6} w^{1.58} (\text{pressure drop}\ \Delta p = p_{\text{in}} - p_{\text{out}},\ R = 0.93) \tag{2.98}$$

A diffuser-confusor reactor demonstrates a substantial increase of pressure at the input and drop at the output (**Figure 2.37**); the pressure drop is high ($\Delta p$ can be approximately up to 1 atm). The correlation between the pressure change in tubular turbulent diffuser-confusor devices and the reaction mixture flow rate can be found in the following equations ($R$ = 0.99) [45, 97]:

$$\Delta p \approx p_{\text{in}} = 1\times10^{-5} w^{2.35} \tag{2.99}$$

$$p_{\text{out}} = 2\times10^{-10} w^{3.86} \tag{2.100}$$

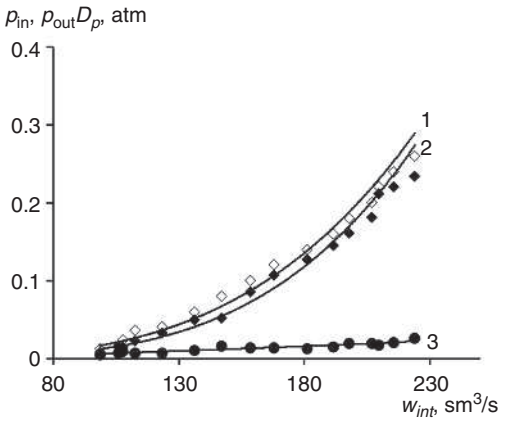


**Figure 2.36** Pressure drop (inner channel) in a cylindrical device. 1 – input ($p_{\text{in}}$); 2 – output ($p_{\text{out}}$); and 3 – pressure drop ($\Delta p$)

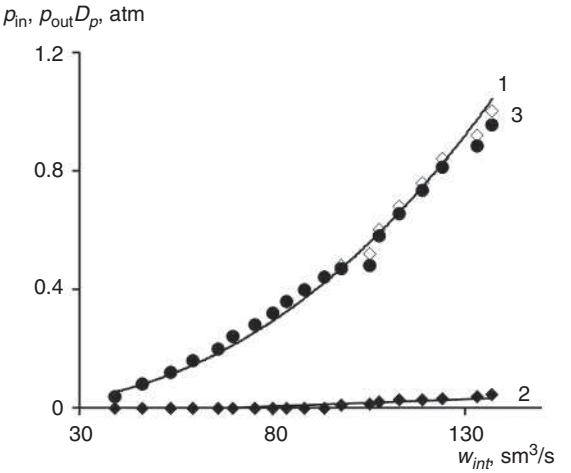


**Figure 2.37** Pressure drop (inner channel) in a diffuser-confusor device. 1 – input ($p_{in}$); 2 – output ($p_{out}$); and 3 – pressure drop ($\Delta p$)

In accordance with **Equation 2.70** and **Equation 2.71**, the input and output pressures of cylindrical and diffuser-confusor devices can be described in terms of a correlation; when efficiencies are similar, the output pressure of both cylindrical and diffuser-confusor tubular turbulent devices are the same.

Thus, a diffuser-confusor reactor has a higher pressure drop than a cylindrical one ($\Delta p$ is up to 25 times higher), which is caused by a higher energy loss from the flow of a reaction mixture through local hydrodynamic resistance. As the mass and heat transfer processes are similar, the increase of hydraulic resistance (turbulisation of flows) should be accompanied by an intensification of the heat transfer through a wall.

The modelling of heat transfer in a fast exothermal chemical process, with external cooling, has been carried out using glass tube turbulent devices with a design similar to double pipe heat exchangers, and the inner channel of a cylindrical ($d_d$ = 16 mm) and diffuser-confusor shaped (diffuser diameter $d_d$ = 16 mm, confusor diameter $d_c$ = 8 mm, unit length $L_c$ = 32 mm) unit with a length of 1 m (**Figure 2.38**). The external channel of these devices has a cylindrical profile, the internal flow travels directly through the cylindrical or diffuser-confusor device, while the circular flow goes through the area between the tubes, formed by the internal and external channels. Water in different flow modes (counter flow) has been used as a heat carrier: a) inner channel liquid heating (the internal flow rate value $w_B$ = 30–150 sm$^3$/s at 5.5 ± 1 °C, the circular flow rate value $w_c$ = const = 130 sm$^3$/s at 60 °C); and b) internal flow cooling ($w_B$ = const = 130 sm$^3$/s at 5.5 ± 1 °C, $w_c$ = 30–210 sm$^3$/s at 60 °C). The standard method has been used to study the hydrodynamic structure of liquid flow in the channels of tubular turbulent devices. The temporal distribution of the indicator flow in the circular and inner channels has been obtained using photometric measuring of the output concentration.

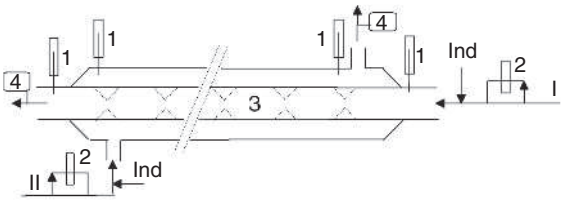


**Figure 2.38** Experimental device chart. 1) thermometer; 2) rotameter; 3) tubular turbulent cylindrical (diffuser-confusor) device with jacket; and 4) spectrophotometer; Ind – indicator input point; I – internal flow; and II – circular flow

An increase of the resistance coefficient for the flow of the reaction mixture, in a diffuser-confusor reactor, favours the output of thermal conductivity through the wall during both heating (**Figure 2.39**) and cooling (**Figure 2.40**). In particular, when the duration of the reactant pass $\tau_{pass}$ in diffuser-confusor and cylindrical devices is similar, the temperature difference $\Delta T_{heat}$ along the device axis is 1.5–1.7 times higher in the former case (**Figure 2.41**). However, to reach the same $\Delta T_{heat}$ value, a liquid flow can pass through the diffuser-confusor channel 1.8 times faster than the cylindrical one. Therefore, $\tau_{pass}$ can be decreased, as well as the probability of the occurrence of side reactions, in fast exothermal processes within tubular turbulent diffuser-confusor devices.

As a thermal flow $Q$, at a comparable input and output temperature difference $\Delta T_{heat}$, is 1.4 times higher in a diffuser channel (**Figure 2.42**), the heated flow rate (in other words, output) can be increased by 1.3–1.4 times. Thus, the specific output of a tubular turbulent diffuser-confusor device is 1.3–1.4 times higher than that of cylindrical device with the same thermal load.

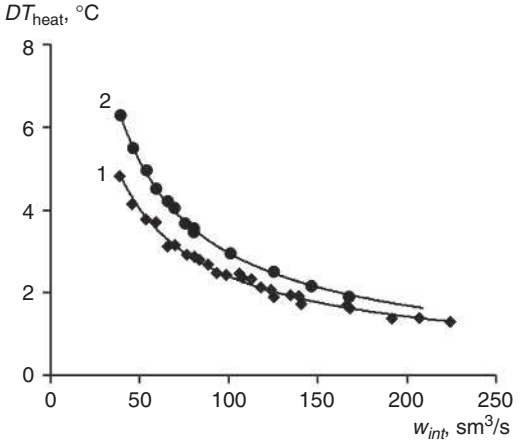


**Figure 2.39** Experimental dependence of the internal flow heating $\Delta T_{heat}$ on the flow rate $w_B$ (4–7 °C) in cylindrical (1) and diffuser-confusor (2) reactors. $w_c$ = 130 sm$^3$/s (50 °C)

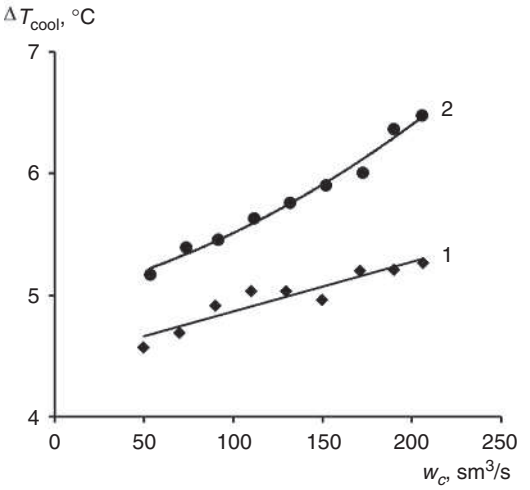


**Figure 2.40** Experimental dependence of the reaction mixture cooling $\Delta T_{cool}$ on the flow rate $w_c$ (50 °C) in cylindrical (1) and diffuser-confusor (2) reactors. $w_B$ = 40 sm$^3$/s (4–7 °C)

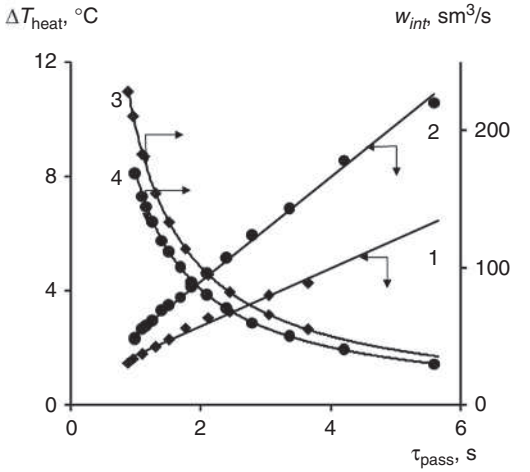


**Figure 2.41** Dependence of the internal flow heating $\Delta T_{heat}$ (1, 2) and its flow rate $w_B$ (4–7 °C) (3, 4) on the duration of the liquid flow pass $\tau_{pass}$ (water) in cylindrical (1) and diffuser-confusor (2) reactors (2.4). $w_c$ = 130 sm$^3$/s (60 °C)

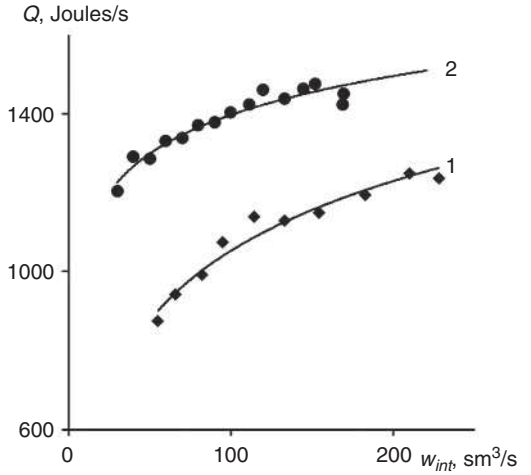


**Figure 2.42** Dependence of a thermal flow $Q$ (heating) on the internal channel flow rate $w_B$ (4–7 °C) in cylindrical (1) and diffuser-confusor (2) reactors. $W_c$ = 130 sm$^3$/s (60 °C)

Heat transfer coefficients $K_T$ have been calculated for studied devices (**Figure 2.43**) using thermal balance equations and considering the equations describing liquid media counter flow (heat exchange surface value $F$ = 0.044 m$^2$ for the diffuser-confusor channel, $F$ = 0.05 m$^2$ for the cylindrical channel). Calculated results demonstrate that the heat transfer coefficient value is 1.4–1.7 times higher in diffuser-confusor channels, than in cylindrical ones. The heat transfer efficiency of a cylindrical device shows a slight decrease in the transition area (Re = (4–10)10$^3$).

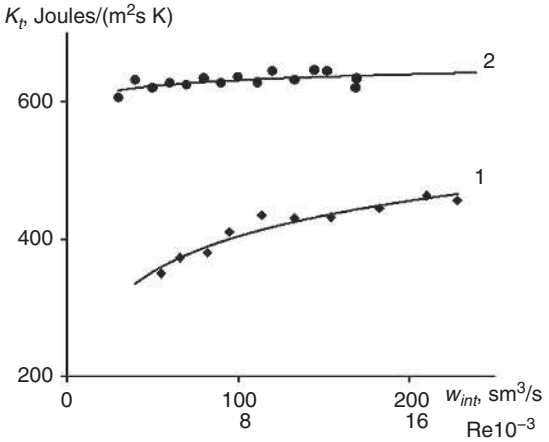


**Figure 2.43** Dependence of the heat transfer coefficient $C_T$ on the reaction mixture flow rate $w_B$ and the Re in cylindrical (1) and diffuser-confusor (2) reactors

An increase of the circular flow rate $w_c$ ($w_B$ = const = 130 sm$^3$/s) in diffuser-confusor devices leads to an increase of the heat transfer coefficient (**Figure 2.44**). The influence of the $w_c$ parameter on the efficiency of convective heat exchange is levelled out in a cylindrical device. As heat transfer coefficients are determined by the smallest of the heat emission coefficients, there is an opportunity of heat exchange intensification in a diffuser-confusor reactor by the increase of the cooling agent flow rate. This opportunity is another tool to control heat transfer processes.

Publication [116] reveals the correlation between the heat emission coefficient and the longitudinal mixing coefficient. Thus, it is interesting to reveal a correlation between the heat and mass transfer processes in tubular turbulent devices, and the hydrodynamic mode of a reaction mixture using the method of pass time distributions; enabling the use of this method for obtaining response curves and heat and mass transfer modelling for fast chemical processes.

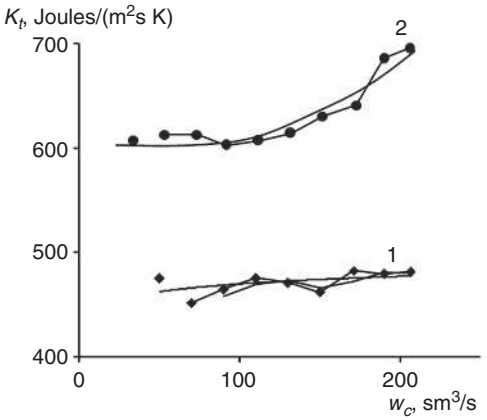


**Figure 2.44** Dependence of the heat transfer coefficient $C_T$ on the cooling agent flow rate $w_c$ in cylindrical (1) and diffuser-confusor (2) reactors

The process of theoretical calculation and reactor design selection, in accordance with process kinetics, is carried out on the basis of idealised mixing and plug flow models, which are determined by the hydrodynamic structure of liquid flows.

## 2.4 Hydrodynamic Structure of Reaction Mixture Flow during Intensification of Heat Exchange Processes

The most complete information regarding the hydrodynamic structure of reactant flows in reactors can be obtained from the instantaneous flow rate values at every point of a device. This parameter is the basis for the formation of temperature and

concentration fields. Therefore, the hydrodynamic structure of the reactant flow in the reaction zone exerts a substantial influence on the rate of chemical technology processes, and its consideration is essential for the calculation of industrial devices, designed for a specific chemical process [4, 38].

Instantaneous flow rate measurements for every point of an industrial device are very difficult and often practically impossible, which is why the hydrodynamic mode of a reaction mixture is determined indirectly by the distribution of liquid particles using the duration of their pass through the reaction zone. A random value (the duration of a particle pass) measurement requires marking of the particles in a way which allows detecting the input and output moments and therefore, drawing the curve of concentration distribution in the flow and at the output. This curve is called the output curve/response curve, responding pulsed input of inert indicator [117, 118].

Such a method is not an easy way to reveal the process mechanisms within a reactor, as the real field of flow rates is unknown and the device is a kind of 'black box'. However, it is quite easy for the analysis of the flow structure, facilitating quantitative processing of obtained data as there is a function of only one derivative, which is time. In addition, pass duration distribution data often provide the basis for the reliable estimation of a real flow structure in a device, i.e., it shines out of the 'black box' [4, 38, 119].

The pass duration time distribution of reactants in a reaction zone is described by the following function [120]:

$$F(\tau) = \frac{C_i(\tau)}{\int_0^\infty C_i(\tau) d\tau} \tag{2.101}$$

Where $C_i$ is the concentration of reactants with the pass duration $\tau_i$.

Experimentally obtained response curves are conveniently represented by the differential curve of pass dimension distribution in dimensionless co-ordinates $C$-$\Theta$, which are calculated using the following equations [76]:

$$C = C_i \upsilon_r / C_0 \tag{2.102}$$

and

$$\Theta = \tau_i / \bar{\tau} \tag{2.103}$$

Where $C_0$ is the concentration of added indicator, $\bar{\tau} = \upsilon_r / w$ is the estimated time of its pass, determined as the ratio of the device volume $\upsilon_r$ to the reaction mixture flow rate $w$.

Cellular and diffusion models are usually used to calculate the efficiency of longitudinal mixing (turbulence) in a reactor and the related degree of deviation of the liquid flow hydrodynamic structure from perfect mixing and plug flow modes [4, 38, 121–123].

According to the cellular model, the structure of curves and response curve shape are described by the differential distribution function:

$$C(\Theta) = \frac{n^n \Theta^{n-1} e^{-n\Theta}}{(n-1)!} \tag{2.104}$$

Where n is the single parameter of the cellular model, equal to the number of cells (devices) in a cascade of perfect mixing reactors. Plug flow mode is achieved at $n \to \infty$ [1]. It is assumed [124] that if the number of cells in a reactor $n \geq 8$, calculation methods for plug flow reactors can be applied to such a device with accuracy sufficient for industrial application.

According to the diffusion model, any deviations in the pass duration distribution of reactants from the plug flow duration are considered to be the effect of longitudinal mixing, independent of the reasons for these deviations. The intensity of such deviations is determined by the turbulence level [4, 119, 125]. According to the diffusion model, the flow pattern is assumed to be plug type, with superposed effects of molecular diffusion, small vortexes, stagnation zones, and radial gradients of the liquid flow rates. A fictitious diffusion coefficient E (longitudinal mixing coefficient) is introduced in this case [120], while the unidirectional diffusion (along the x-axis of a device) is described by the following equation [38]:

$$\frac{dC}{d\tau} = -w\frac{dC}{dx} + E\frac{d^2C}{dx^2} \tag{2.105}$$

The solution of **Equation 2.74** for the pulse mode of indicator input provides us with the formula for the pass duration distribution function [120, 122, 123, 126]:

$$C(\Theta) = \sqrt{\frac{Bo}{4\pi\Theta}} \exp\left(-\frac{Bo}{4}\frac{(\Theta-1)^2}{\Theta}\right) \tag{2.106}$$

Where $Bo = \frac{L^2 w}{v_p E}$ is the Bodenstein Number (or the Pecklet Number for longitudinal mixing $Pe_L$). The numerical value of $Bo$ is an estimation of the flow structure, as it can provide a quantitative deviation value from plug flow ($Bo \to \infty$) or perfect mixing ($Bo \to 0$) modes.

Comparison of experimental pass duration distribution curves, with the curves calculated using **Equations 2.104** and **2.106,** results in obtaining the numerical values Bo and n and therefore, an opportunity for the quantitative estimation of the flow structure deviation in reaction zones with different geometry from an ideal model.

### 2.4.1 Single-phase Reaction Systems

Response curves (**Figure 2.45**) of tubular turbulent devices put them into the category of intermediate-type reactors, as there is a deviation from the plug flow mode caused mostly by the counter flow, with the intensity determined by the longitudinal mixing coefficient E [127]. The pass duration distribution curves, for all the provided designs of tubular turbulent reactors, demonstrate a narrowing with a $\tau_{pass}$ shift to the area of smaller values upon increasing the flow rate of the reactants w.

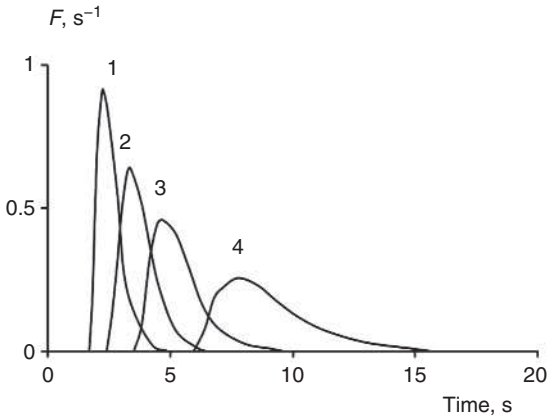


**Figure 2.45** Influence of the liquid flow rates on the indicator pass duration distributions for a cylindrical tubular turbulent device. $d_d$ = 0.03 m; $L$ = 0.7 m; $w$, $sm^3/s$: 130 (1); 91 (2); 62 (3); and 36 (4)

A characteristic feature of tubular turbulent devices, with conical widening at input points (**Figure 2.46**), is the influence of channel geometry on the hydrodynamic mode of their operation. A decrease of the unit length, $L_c/d_d$, ratio to the diffuser diameter, $d_d$, in tubular turbulent diffuser-confusor devices, as well as an increase of the $d_d/d_c$ ratio (profiling depth), makes their operation mode closer to the perfect mixing mode with corresponding low values of the *Bo* number (**Figure 2.47**). The diffuser-confusor section, in this case, acts as static turbulisers which increase the turbulent diffusion coefficient and longitudinal mixing rate [128–130].

Cylindrical turbulent devices with $d_d \geq 0.03$ m are characterised by higher *Bo* values (**Figure 2.47**) than diffuser-confusor ones and therefore, exhibit better similarity of reactant flow pattern to the plug flow mode. As the structure of flows in different cylindrical devices with $d_d \geq 0.03$ m is similar ($Bo \approx 50$), there is no need to use large turbulent reactors for a fast chemical reaction in the quasi-plug flow mode. It does not restrict process efficiency.

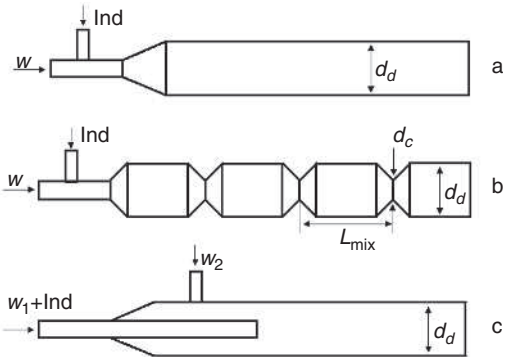


**Figure 2.46** Tubular turbulent devices with cylindrical (a) and diffuser-confusor (b) designs with coaxial (a, b), and radial (c) input of reactants. Ind – indicator input

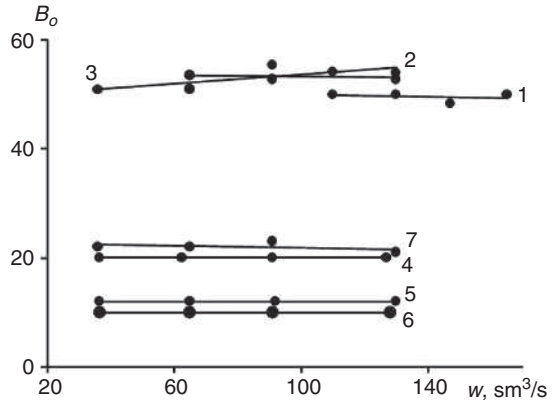


**Figure 2.47** Dependence on the *Bo* on the reaction mixture flow rate w in cylindrical (1–3) and diffuser-confusor (4–7) devices. $d_d$ = 0.024 (4–6), 0.03 (3, 7), 0.04 (2), 0.05 (1) m; $d_c$ = 0.008 (6), 0.015 (4, 5), 0.019 (7) m; $L_c$ = 0.048 (5, 6), 0.06 (7), 0.072 (4) m; and $L$ = 0.64 m

A characteristic feature of any design of a tubular turbulent device, with conical widening at the reactor input, is the fact that the liquid flow rates (device productivity) exert almost no influence on the *Bo* value (**Figure 2.47**) and therefore, on the hydrodynamic mode of operation. This is a result of the increase of longitudinal mixing intensity, because $E \sim w$. Another characteristic feature of devices with a radial input of reactants (**Figure 2.46**), in addition to channel geometry, is the correlation between the ratio of the volume flow rates $w_1$, $w_2$ and a hydrodynamic mode of operation (**Figure 2.48**). At the constant axial flow rate $w_1$, an increase of $w_2$ results in an increase of the *Bo* value, with the operation mode of a device becoming similar to the plug flow mode. At high rates of the central flow $w_1$, the influence of the radial

flow rate $w_2$ on the hydrodynamic structure of the flow is eliminated. Radial input design assumes the possibility of the formation of different modes in the same device, with a differing degree of similarity to the perfect mixing and plug flow modes, which is impossible in existing industrial reactors.

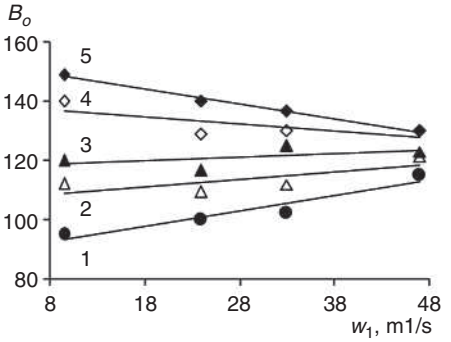


**Figure 2.48** The dependence of the *Bo* on the central flow rate *w*. $w_2$ = 41 (1), 47 (2), 57 (3), 67 (4), 80 (5) $sm^3/s$; $d_d$ = 24 mm; and *L* = 1100 mm

The behaviour of the hydrodynamic mode of single-phase reaction systems in tubular turbulent devices will help to select the optimal conditions for fast liquid-phase homogeneous chemical reactions.

A two-phase mixture flow in the turbulent mode leads to the deformation of the interphase boundary surface, which should change the hydrodynamic mode and conditions of fast chemical reactions.

### *2.4.2 Two-phase Reaction Systems*

The study of the hydrodynamic mode of operation of a tubular turbulent device, in the presence of an interphase boundary, has been carried out for a 'liquid-gas' system [82]. An increase of the gas content in a liquid-gas flow leads to an increase of the longitudinal mixing coefficient *E* (**Figure 2.49**) and therefore, to a decrease of the *Bo*, with the hydrodynamic mode of the reaction mixture becoming closer to the perfect mixing mode. Thus, fast chemical reactions in the presence of an interphase boundary in a 'liquid-gas' system, including reaction mixture boiling, occur in the hydrodynamic mode close to the perfect mixing mode, with a high rate of longitudinal mixing. At the same time, a high rate of longitudinal mixing leads to widening of the pass duration distribution of reactants. This effect is necessary to consider for fast chemical processes occurring in real conditions. The longitudinal mixing coefficient is substantially affected by an increase of the liquid-phase flow rate, when the gas

content in the flow is constant. At the same time, a change of the gas and liquid-phase flow rate ratio $w_g/w_l$ does not influence the efficiency of longitudinal mixing, assuming the total rate of a liquid-gas flow is constant.

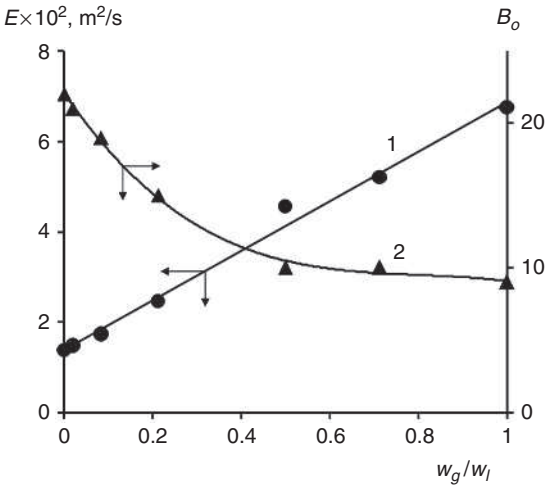


**Figure 2.49** Dependence of the longitudinal mixing coefficient $E$ (1) and $Bo$ (2) on the ratio of gas and liquid-phase flow rates $w_g/w_l$ ($w_l$ = 160 sm$^3$/s, $d_2$ = 1.8 mm, and $d_d/d_c$ = 1.6)

A substantial intensification of longitudinal mixing in a tubular device can be achieved by changing the liquid-gas flow geometry. Transition from a cylindrical device ($d_d/d_c$ = 1) to a diffuser-confusor device ($d_d/d_c$ = 3) results in a threefold increase of the longitudinal mixing coefficient. Changing the gas-phase input nipple diameter does not affect the rate of longitudinal mixing, all other conditions being equal.

Generalisation of the obtained experimental data provides us with a correlation explaining the contribution of various process parameters to the rate of longitudinal mixing of a two-phase flow in a tubular turbulent device (**Figure 2.50**). An increase of the volume-surface diameter of dispersed phase particles up to $d_{32} \approx 2$ mm ($d_{32} = m_i d_i^3/\sum m_i d_i^2$, where $m_i$ is the number of particles with $d_i$) will decrease the longitudinal mixing coefficient. Further enlargement of the dispersed phase particles does not affect the rate of liquid-phase longitudinal mixing. The longitudinal mixing coefficient is mainly determined by the number of dispersed phase particles. The formation of a liquid-gas flow, with a high specific surface area caused by emulsification of the dispersed phase, results in a more intensive longitudinal mixing in the continuous medium, with the operation mode of the device being very close to the perfect mixing mode (**Figure 2.50**). This makes it possible to create uniform concentration fields of 'liquid-gas' system reactants, directly in the reaction zone of fast chemical processes.

For a single-phase chemical reaction, formation of a two-phase flow using the boiling process in a reactor will intensify the mixing of reactants along the axis of the device.

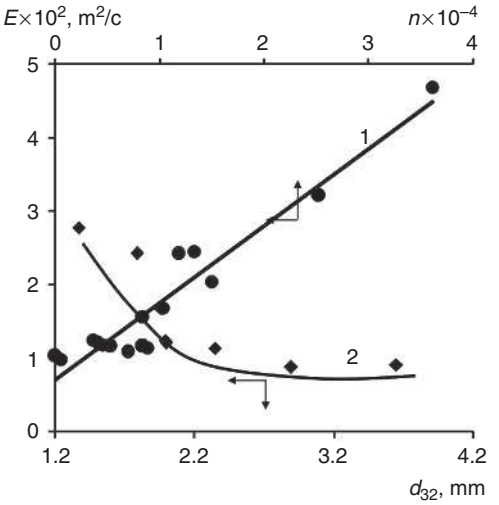


**Figure 2.50** Generalised dependence of the longitudinal mixing coefficient $E$ on the n number (1) and the volume-surface diameter $d_{32}$ (2) of dispersed phase particles in a gas-fluid flow inside a tubular turbulent reactor

An increase of gas content in a flow, i.e., an increase of the $w_g/w_l$ ratio leads to growth of both the size and number of dispersed phase particles and therefore, results in the intensification of longitudinal mixing. High-speed reaction mixture motion, at a fixed gas-fluid composition of a flow, increases the number of dispersed phase particles due to its further emulsification and favours mixing intensification along the axis of the device. This is an obvious reason for reaction zone 'compression' during fast two-phase chemical processes in tubular reactors. A faster pass of the reactants through the reaction zone (as a result of increased device output), results in an increase of the product yield because of the intensified homogenisation of the reaction mixture, with the contribution of the longitudinal mixing component. A change of the gas-phase content, with a constant total rate of liquid-gas flow, leads to an insignificant change in the concentration of the dispersed phase particles and the longitudinal mixing coefficient. The growth of the number of dispersed phase particles, due to the dispersing process, determines the increase of the longitudinal mixing rate upon transition from a cylindrical to a diffuser-confusor device.

The correlation between the longitudinal mixing output and dispersed particle size, in the two-phase reaction flow in tubular turbulent devices, is determined by the mechanical method controlling the phase contact surface. At the same time, there is

another mechanism of decreasing the size of the dispersion inclusions – a decrease of the free energy of the noncompensated intermolecular forces (surface tension) on the interphase boundary. The decrease of surface tension on the interphase boundary in the range of 56–72 mN/m, in the 'water-air' system caused by the addition of a surfactant (butyl alcohol), is accompanied by a 20% decrease of the diameter of the dispersed phase particles (bubbles) (**Figure 2.51**).

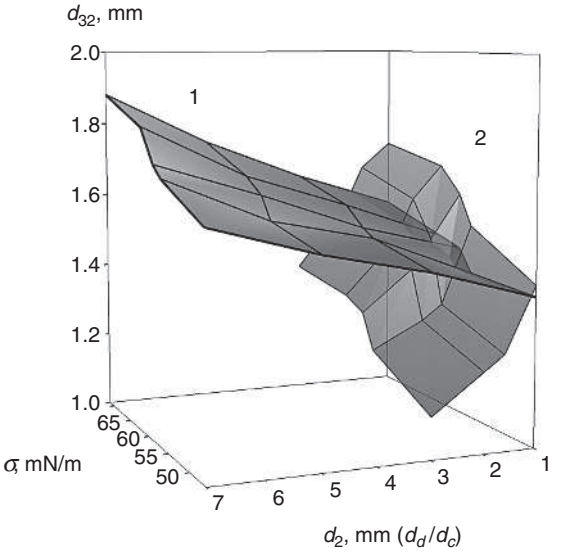


**Figure 2.51** Dependence of the volume-surface diameter $d_{32}$ of bubbles on the diameter of the gas-phase input nipple $d_2$ (1) ($d_d/d_c$ = 1.6), channel profiling depth $d_d/d_c$ (2) ($d_2$ = 5 mm), and surface tension $\sigma$ in a gas-liquid flow. $w_l/w_g$ = 5, and $w_l$ = 100 sm$^3$/s

The analysis of experimental data revealed a correlation between the hydrodynamic mode of a tubular turbulent device and the interphase tension in the flow of the two-phase 'liquid-gas' reaction system (**Figure 2.52**). This correlation confirms that the addition of surfactants is a reasonable solution for a reaction system with an interphase boundary. It leads to a decrease of bubble size and mass exchange intensification in the gas-liquid flow of fast chemical processes. In addition, the liquid-phase longitudinal mixing rate increases and the hydrodynamic mode of a process approaches perfect mixing conditions. Fast chemical processes, in two-phase systems, require consideration of the selective adsorption of feedstock reactants and reaction products on to the interphase boundary, and a change of the hydrodynamic motion structure of the continuous phase. A change in the work required to form the new surface is a typical phenomenon for all types of multiphase systems and depends on

the interphase tension intensity. A similar change of the longitudinal mixing rate, with the change of adsorption, is also typical for 'liquid-liquid' and 'liquid-solid' systems in tubular turbulent devices.

The hydrodynamic mode of a liquid-gas reaction system is influenced by the position of a tubular turbulent diffuser-confusor device in space. In the case of a single-phase reaction system, the device position in space does not influence the rate of longitudinal mixing (**Figure 2.53**). Therefore, industrial turbulent diffuser-confusor devices for fast chemical reactions in a single-phase reaction mixture can be positioned vertically, horizontally, and even in the inclined position.

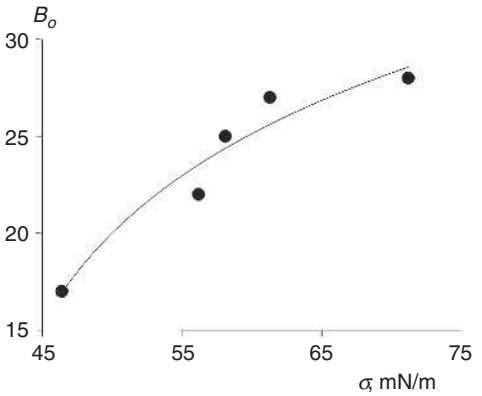


**Figure 2.52** Dependence of the *Bo* on the surface tension coefficient of a liquid-gas flow in a tubular turbulent device ($d_2$ = 3 mm, $w_l/w_g$ = 5, and $d_d/d_c$ = 2)

A liquid-gas flow is characterised by the minimal value of the longitudinal mixing coefficient at an inclination of -40 to 0°. The vertical position of a tubular device (-90°) with a bottom-up direction of a liquid-gas flow, corresponds to the maximum value of the longitudinal mixing coefficient. The size and therefore, the number of dispersed phase particles do not change in this case. It is obvious that the rate of longitudinal mixing of the gas-liquid flow depends on the device position, as gravitation forces are added to the reaction mixture flow, as well as the substantial differences in the density of mixture components. The dependence of the hydrodynamic mode of the gas-liquid mixture on the device position, highlights additional opportunities for tuning conditions of 'liquid-gas' fast chemical reactions. A good solution for fast chemical reactions, in two-phase systems, is a tubular turbulent device in a vertical position with a top-down flow of components, allowing the creation of intensive longitudinal mixing and facilitating the unloading of a reaction mixture when the process is stopped.

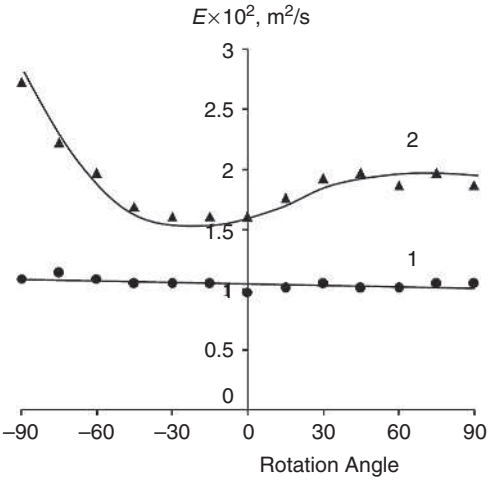


**Figure 2.53** Dependence of the longitudinal mixing coefficient $E$ for single- (1) and two-phase flows (2) on device inclination ($d_2$ = 3 mm, $d_d/d_c$ = 2, $w_l$ = 170 sm$^3$/s, $w_g$ = 40 sm$^3$/s; device position: $\alpha$ = 0 – horizontal, $\alpha$ = 90 – vertical, bottom-up, and $\alpha$ = -90 – vertical, top-down)

Revealed peculiarities of the longitudinal mixing efficiency in gas-liquid flows, inside tubular turbulent diffuser-confusor devices, favour the scientifically grounded selection of the optimal geometry of the zone for reactant mixing, as well as the process mode. Formation of dispersed systems with a well-developed interphase surface and therefore, with intensive longitudinal mixing, help to create uniform concentration and temperature profiles in the local area of a fast chemical reaction and to reduce diffusion limitations. The revealed correlation between the longitudinal mixing rate in a liquid phase, and dispersed phase particle size and concentration in 'liquid-gas' systems, would also be suitable for the description of 'liquid-liquid' and liquid-solid' fast chemical reactions.

### *2.4.3 Convective Heat Exchange*

Experiments [113, 114] have demonstrated (**Figure 2.54**) that the diffuser-confusor reactor has low values of the $Bo$ = 25–45 (high longitudinal mixing coefficient $E$ = (14–40)10$^{-3}$ m$^2$/s) thus, heat exchange is intensive ($C_T$ = 600–650 Joules/(m$^2$s·K)). Due to intensive longitudinal mixing (turbulence), a quasi-isothermic (isothermic in any cross section of a device) mode can form in a diffuser-confusor channel. It will strongly affect the external heat removal efficiency and is a necessary consideration for the implementation of fast chemical processes.

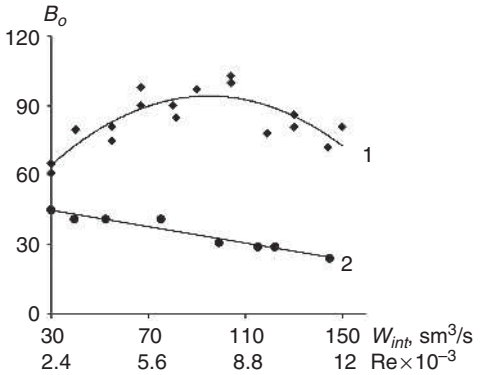


**Figure 2.54** Dependence of the *Bo* on the reaction mixture flow rate $w_B$ and the Re in cylindrical (1) and diffuser-confusor (2) reactors

The cylindrical design of a tubular device is characterised by high *Bo* values, *Bo* = 60–100 (**Figure 2.54**) (low value of the longitudinal mixing coefficient $E$ = (2–10)$10^{-3}$ $m^2/s$) and subsequently, a relatively low heat exchange efficiency ($C_T$ = 350–460 Joules/$m^2$s·K). Therefore, the heat transfer (heat emission) coefficient is a function of the mode of the reaction mixture flow, which is described by the *Bo*. Heat exchange processes within industrial reactors can be modelled by the response curve method. In particular, an increase of the reaction mixture flow rate $w_B$, in a diffuser-confusor channel, leads to a decrease of *Bo* values (**Figure 2.54**) and an increase of the heat transfer coefficient. The dependence of *Bo* on the liquid flow $w_B$ is extreme in a cylindrical channel. The transition area, such as Re = (2.5–8)$10^3$ demonstrates growth of *Bo* with an increase of $w_B$, which approaches a hydrodynamic mode of flow to the plug flow mode and therefore, the heat exchange efficiency in cylindrical channels is low in this range of Re values. According to the results demonstrated in **Figures 2.43** and **2.54**, an increase of the heat transfer coefficient and therefore, the heat exchange intensity in a cylindrical channel, requires a high rate of reactants. This, in turn, requires an increase of the heat exchange surface (reactor dimensions).

Another situation is observed for the hydrodynamic structure of flows (cooling agents) in the circular channels of tubular turbulent devices (**Figure 2.55**). When the flow rate $w_c$ is below ≈ 110 $sm^3/s$, the flows in the circular channels (heat carrier) of a cylindrical and diffuser-confusor device have the same hydrodynamic mode (*Bo* ≈ 80), $w_c$ values in a diffuser-confusor device exceeding 110 $sm^3/s$, lead to a reduction of *Bo* values due to the effect of the longitudinal mixing intensification, and an approach to the perfect mixing mode in a cylindrical channel.

It might be supposed that the heat emission coefficient $\alpha_2$ value of the flow can be increased by the introduction of a cooling agent, with a higher $w_c$ value, into the circular channel of a diffuser-confusor device, especially when $\alpha_2 < \alpha_1$, because $C \approx \alpha_2$. However, the opposite is true, i.e., a tubular turbulent device with a cylindrical channel is not recommended for operation at high heat carrier rates in a circular channel. Indeed, an increase of the heat carrier rate $w_c$ in the circular channel of a diffuser-confusor device ($w_B$ = const = 130 sm$^3$/s) results in the growth of the heat emission coefficient value (**Figure 2.44**), while the influence of $w_c$ on the convective thermal exchange efficiency is eliminated in cylindrical devices.

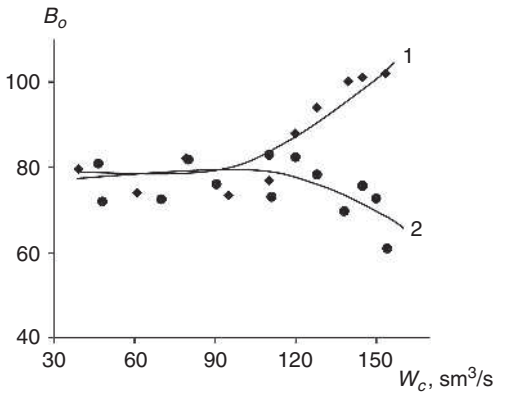


**Figure 2.55** Dependence of the *Bo* on the cooling agent flow rate $w_c$ in cylindrical (1) and diffuser-confusor (2) devices

Thus, the lower efficiency of heat exchange processes in the cylindrical channels of tubular devices, compared with diffuser-confusor devices, is explained by an undesirably close approach of the internal flow and circular flow structures to the plug flow mode. The heat exchange efficiency in a diffuser-confusor device, at $\alpha_2 < \alpha_1$, can be intensified by increasing the cooling agent flow rate $w_c$, which offers another tool for intensification and control of the heat transmission processes.

All the revealed correlations provide solutions for the very important problem of controlling the temperature mode of fast exothermal processes, in a reaction zone, by means of external heat removal. The quasi-plug flow mode formed in turbulent flows, when the 'torch' edges reach the heat exchange surfaces, can be used for thermostating fast chemical reactions by external heat removal. Developed quantitative correlations guarantee the possibility of scaling up this mode to industrial processes, with consideration of the reaction kinetic parameters and physical characteristics of the feedstock flow. The obtained equations are suitable for engineering calculations of the temperature profile in a reaction zone, under external thermostating conditions. It has formed the basis for the development of technologically acceptable methods

of process control. In particular, a good tool for the control of adiabatic temperature growth in a reaction zone and optimisation of the cooling zone length is the variation of the reactor radius, reaction mixture flow rate, and hydrodynamics. A quantitative correlation has been revealed for the heat transfer coefficient and reaction mixture hydrodynamics under convective heat exchange conditions.

The application of tubular turbulent devices is a mature concept, which is well developed on the basis of the macrokinetic approach applied to the electrophilic reaction of isobutylene polymerisation. The results of studying the behaviour of the turbulent mixing process in single- and two- phase systems, as well as the control of the temperature mode in the reaction zone of fast exothermal processes, has advanced the application range of tubular turbulent devices in the chemical industry. It is possible to provide a scientific background for the application of new technologies to fast polymerisation processes, and for the intensification of heat and mass transfer processes as well. All the aforementioned have made it reasonable to seek new solutions for fast turbulent chemical processes and therefore, for the development of continuous energy- and resource-efficient technologies on the basis of tubular turbulent devices for the synthesis of other products.

## References

1. V.M Barabash and N.N. Smirnov, *Zhurnal Prikladnoi Khimii*, 1994, **67**, 2, 196. [In Russian]

2. V.V. Konsetov and J.V. Kokotov, *Himicheskaya Promyshlennost*, 1990, **5**, 299. [In Russian]

3. J. Baldyga, J.R. Bourne and R.V. Gholap, *Chemical Engineering Science*, 1995, **50**, 12, 1877.

4. D.A. Bajzenberger and D.H. Sebastian in *Engineering Problems of Polymer Synthesis*, Khimiya, Moscow, Russia, 1988. [In Russian]

5. L.N. Braginskiy, V.I. Begachev and V.M. Barabash in *Agitation of Liquid Media: Physical Foundations and Engineering Methods of Calculation*, Khimiya, Leningrad, Russia, 1984. [In Russian]

6. V.V. Bogdanov, E.I. Hristoforov and B.A. Klocung in *Efficient Small Capacity Mixers*, Khimiya, Leningrad, Russia, 1989. [In Russian]

7. V.M. Barabash, *Teoreticheskie Osnovy Khimicheskoy Tekhnologii*, 1994, **28**, 2, 110. [In Russian]

8. J.V. Svetlov, *Teoreticheskie Osnovy Khimicheskoy Tekhnologii*, 1992, **26**, 6, 819. [In Russian]

9. A.N. Blaznov, V.A. Kunichan and D.V. Chashhilov, *Zhurnal Prikladnoi Khimii*, 2001, **74**, 4, 621. [In Russian]

10. E. Lang, P. Ortina, F. Streiff and M. Fleischli, *International Journal of Heat and Mass Transfer*, 1995, **38**, 12, 2239.

11. H.Z. Li, C. Fasol and L. Choplin, *Chemical Engineering Science*, 1996, **51**, 10, 1947.

12. D.M. Hobbs and F.J. Muzzio, *Chemical Engineering Science*, 1998, **53**, 18, 3199.

13. K.S. Minsker, V.P. Zakharov and A.A. Berlin, *Russian Polymer News*, 2000, **5**, 3, 18. [In Russian]

14. R.G. Tahavutdinov, G.S. Dyakonov, R.Ya. Deberdeev and K.S. Minsker, *Himicheskaya Promyshlennost*, 2000, **5**, 41. [In Russian]

15. R.G. Tahavutdinov, G.S. Dyakonov, V.P. Zaharov, R.Ya. Deberdeev and K.S. Minsker, *Bashkirskiy Khimicheskiy Zhurnal*, 2000, **7**, 2, 62. [In Russian]

16. B.E. Launder and D.B. Spalding in *Mathematical Models of Turbulence*, Academic Press, London, UK, 1972.

17. O. Zenkevich and K. Morgan in *Finite Elements and Approximation*, Mir, Moscow, Russia, 1986. [In Russian]

18. K.S. Minsker, V.P. Zakharov, R.G. Tahavutdinov, G.S. Dyakonov and A.A. Berlin, *Zhurnal Prikladnoy Khimii*, 2001, **74**, 1, 87. [In Russian]

19. K.S. Minsker, V.P. Zakharov, R.G. Takhavutdinov and G.S. Dyakonov, *Russian Polymer News*, 2000, **5**, 4, 9. [In Russian]

20. J. Villermaux and L. Falk, *Chemical Engineering Science*, 1994, **49**, 5127.

21. J. Baldyga, J.R. Bourne and S.J. Hearn, *Chemical Engineering Science*, 1998, **52**, 3, 457.

22. J. Balduga and J.R. Bourne, *Chemical Engineering Journal*, 1989, **42**, 83.

23. F.G. Galimzyanov and R.F. Galimzyanov, *The Theory of Internal Turbulent Motions*, Expert, Ufa, Russia, 1999. [In Russian]

24. M.C. Chaturvedi, *Journal of the Hydraulics Division. Proceedings of the American Society of Civil Engineers*, 1963, **89**, 61.

25. E. Turgeon, D. Pelletier and L. Ignat in *Proceedings of the 36th Aerospace Sciences Meeting and Exhibit*, American Institute of Aeronautics and Astronautics, Reston, VA, USA, 1998, p.1.

26. V.Z. Kompaniec, A.A. Ovsyannikov and A.S. Polak in *Chemical Reactions in Turbulent Gas and Plasma Flows*, Nauka, Moscow, Russia, 1979. [In Russian]

27. V.Z. Kompaniec, A.A. Konoplev and L.S. Polak in *Experimental and Theoretical Studies of Plasma Chemistry Processes*, Khimiya, Moscow, Russia, 1984. [In Russian]

28. V.M. Olevskiy and V.R. Ruchinskiy in *Rotor-Film Heat and Mass Exchange Devices*, Khimiya, Moscow, Russia, 1984. [In Russian]

29. V.P. Budtov and V.V. Konsetov in *Heat and Mass Transfer in Polymerization Processes*, Khimiya, Leningrad, Russia, 1988. [In Russian]

30. A.A. Berlin, V.Z. Kompaniec, A.A. Konoplev, K.S. Minsker, S.K. Minsker, J.A. Prochuhan, E.A. Ryabenko and N.S. Enikolopyan, *Doklady Akademii Nauk SSSR*, 1989, **305**, 5, 1143. [In Russian]

31. A. Prochuhan, K.S. Minsker, M.M. Karpasas, A.A. Berlin, R.H. Bahitova and N.S. Enikolopyan, *Vysokomolekulyarnye Soedineniya*, 1988, **30A**, 4, 1259. [In Russian]

32. M.G. Krehova, K.S. Minsker and S.K. Minsker, *Teoreticheskie Osnovy Khimicheskoy Tekhnologii*, 1995, **29**, 5, 496. [In Russian]

33. A.A. Berlin, K.S. Minsker and V.P. Zakharov, *Himicheskaya Promyshlennost*, 2003, **80**, 3, 36. [In Russian]

34. R.G. Tahavutdinov, A.G. Muhametzyanova, G.S. Dyakonov, K.S. Minsker and A.A. Berlin, *Vysokomolekulyarnye Soedineniya*, 2002, **44A**, 7, 1094. [In Russian]

35. K.S. Minsker and A.A. Berlin in *Fast Polymerization Processes*, Gordon and Breach Publishers, Amsterdam, Netherlands, 1996.

36. A.A. Berlin, K.S. Minsker and V.P. Zakharov, *Doklady Akademii Nauk*, 1999, **365**, 3, 360. [In Russian]

37. L.D. Landau and E.M. Lifshits in *Theoretical Physics. Volume 6: Hydrodynamics*, Nauka, Moscow, Russia, 1986. [In Russian]

38. A.G. Kasatkin in *Basic Processes and Machinery of Chemical Tehnology*, Khimya, Moscow, Russia, 1983. [In Russian]

39. K.S. Minsker, A.A. Berlin, R.G. Tahavutdinov, G.S. Dyakonov and V.P. Zaharov, *Doklady Akademii Nauk*, 2000, **372**, 3, 347. [In Russian]

40. R.G. Tahavutdinov, K.S. Minsker, G.S. Dyakonov, V.P. Zaharov and A.A. Berlin, *Trudy Akademii Nauk Respubliki Baskortostan*, 2001, **2**, 138. [In Russian]

41. K.S. Minsker, A.A. Berlin, R.G. Takhavutdinov, G.S. Dyakonov and V.P. Zakharov, *Russian Polymer News*, 2001, **6**, 2, 1.

42. K.S. Minsker, A.A. Berlin, V.P. Zakharov and R.G. Tahavutdinov, *Doklady Akademii Nauk*, 2001, **381**, 1, 78. [In Russian]

43. K.S. Minsker, A.A. Berlin, R.G. Tahavutdinov, G.S. Dyakonov and V.P. Zaharov, *Himicheskaya Fizika*, 2001, **20**, 5, 124. [In Russian]

44. V.P. Zaharov, R.G. Tahavutdinov, A.G. Muhametzyanova, G.S. Dyakonov, K.S. Minsker and A.A. Berlin, *Vestnik Bashkirskogo Universiteta*, 2001, **3**, 28. [In Russian]

45. K.S. Minsker, A.A. Berlin, V.P. Zakharov and G.E. Zaikov in *Fast Liquid-Phase Processes in Turbulent Flows*, Brill Academic Publishers, Amsterdam, Netherlands, 2004.

46. M.A. Belevickaya and V.M. Barabash, *Teoreticheskie Osnovy Khimicheskoy Tekhnologii*, 1994, **28**, 4, 342. [In Russian]

47. V.M. Barabash and M.A. Belevickaya, *Teoreticheskie Osnovy Khimicheskoy Tekhnologii*, 1995, **29**, 4, 362. [In Russian]

48. W. Podgorska and J. Baldyga, *Chemical Engineering Science*, 2001, **56**, 741.

49. L.N. Braginskiy and M.A. Belevickaya, *Teoreticheskie Osnovy Khimicheskoy Tekhnologii*, 1990, **24**, 4, 509. [In Russian]

50. L.N. Braginskiy and M.A. Belevickaya, *Teoreticheskie Osnovy Khimicheskoy Tekhnologii*, 1991, **25**, 6, 843. [In Russian]

51. V.V. Yaroshenko, L.N. Braginskiy and V.M. Barabash, *Teoreticheskie Osnovy Khimicheskoy Tekhnologii*, 1988, **22**, 5, 787. [In Russian]

52. A.W. Patwardhan and J.B. Joshi, *Industrial Engineering Chemical Research*, 1997, **36**, 3904.

53. N.S. Shulaev and I.H. Bikbulatov, *Bashkirskiy Khimicheskiy Zhurnal*, 1997, **4**, 2, 73. [In Russian]

54. V.N. Ivanec, S.N. Albreht and G.E. Ivanec, *Khimicheskaya Promyshlennost*, 2000, 11, 46. [In Russian]

55. M.A. Promtov and A.I. Zimin, *Pharmaceutical Chemistry Journal*, 2000, **34**, 10, 553.

56. J.V. Badikov, V.S. Piljugin and R.B. Valitov in *Application of Hydroacoustic Exposure Devices for Heterophase Processes*, Khimiya Moscow, Russia, 2004.

57. M.G. Krehova, S.K. Minsker, Y.A. Prochukhan and K.S. Minsker, *Teoreticheskie Osnovy Khimicheskoy Tekhnologii*, 1994, **28**, 3, 271. [In Russian]

58. A.A. Berlin, K.S. Minsker, A.G. Muhametzyanova, R.G. Tahavutdinov, G.S. Dyakonov, G.G. Aleksanyan, B.L. Rytov and A.A. Konoplev in *Transactions of Institute of Chemical Physics, Russian Academy of Sciences*, Moscow, Russia, 2003. [In Russian]

59. A.F. Vurzel and A.L. Suris, *Izvestiya Vuzov. Khimiya I Himicheskaya Tehnologiya*, 1997, **20**, 2, 116. [In Russian]

60. V.F. Popov and N.V. Vinogradova, *Himicheskaya Promyshlennost*, 1984, **1**, 53. [In Russian]

61. V.F. Popov and N.V. Vinogradova, *Himicheskaya Promyshlennost*, 1984, **5**, 49. [In Russian]

62. M. Nadler and D. Mewes, *International Journal Multiphase Flow*, 1997, **33**, 1, 55.

63. A.G. Muhametzyanova, V.P. Zaharov, R.G. Tahavutdinov, G.S. Dyakonov and K.S. Minsker, *Vestnik Bashkirskogo Universiteta*, 2002, **1**, 60. [In Russian]

64. A.G. Muhametzyanova, R.G. Tahavutdinov, G.S. Dyakonov, V.P. Zaharov and K.S. Minsker in *University Subject Collection 'Heat and Mass Exchange Processes and Machinery of Chemical Technology'*, Kazan State Technological University, Kazan, Russia, 2001.

65. K.S. Minsker, G.S. Dyakonov, R.G. Tahavutdinov, A.G. Muhametzyanova, V.P. Zaharov and A.A. Berlin, *Doklady Akademii Nauk*, 2002, **382**, 4, 509. [In Russian]

66. R.G. Tahavutdinov, G.S. Dyakonov, A.G. Muhametzyanova, V.P. Zaharov and K.S. Minsker, *Khimicheskaya Promyshlennost*, 2002, **1**, 22. [In Russian]

67. J.T. Kuo and G.B. Wallis, *International Journal Multiphase Flow*, 1988, **14**, 5, 547.

68. B.E. Launder and D.B. Spalding, *Computational Methods in Applied Mechanics and Engineering*, 1974, **3**, 269.

69. V. Yakhot and S.A. Orsag, *Journal of Science Computation*, 1986, **1**, 3.

70. V. Yakhot, S.A. Orsag, S. Thangam, T.B. Gatski and C.G. Speziale, *Physical Fluids*, 1992, **4**, 7, 14.

71. L.M. Smith and W.C. Reynolds, *Physical Fluids*, 1992, **4**, 2, 364.

72. P. Bradshow, B.E. Launder and J.I. Lumley, *AIAA Paper*, American Institute of Aeronautics and Astronautics, Reston, USA, 1991, p.97.

73. W. Haase, E. Chaput, E. Elsholz, M.A. Leschziner and U.R. Müller, *Notes on Numerical Fluid Mechanics*, 1996, **58**, 16.

74. A.N. Kolmogorov, *Doklady Akademii Nauk SSSR*, 1941, **32**, 1, 19. [In Russian]

75. V.P. Zaharov, A.G. Muhametzyanova, R.G. Tahavutdinov, G.S. Dyakonov and K.S. Minsker, *Zhurnal Prikladnoy Khimii*, 2002, **75**, 9, 1462. [In Russian]

76. V.M. Ramm in *Absorbciya Gazov*, Khimiya, Moscow, Russia, 1976. [In Russian]

77. D.N. Latypov and A.A. Ovchinnikov, *Izvestiya Vuzov. Khimiya I Himicheskaya Tehnologiya*, 2001, **44**, 2, 108. [In Russian]

78. E.D. Shhukin, A.V. Percov and E.A. Amelina in *Colloidal Chemistry*, Izdatelstvo MGU Moscow, Russia, [In Russian]

79. V.P. Zaharov and K.S. Minsker, *Khimicheskaya Promyshlennost*, 2003, **80**, 6, 38. [In Russian]

80. V.P. Zaharov, K.S. Minsker and F.B. Shevlyakov, *Vestnik Bashkirskogo Universiteta*, 2003, **3-4**, 26. [In Russian]

81. V.P. Zaharov and F.B. Shevlyakov, *Khimicheskaya Promyshlennost*, 2005, **82**, 3, 133. [In Russian]

82. V.P. Zaharov and F.B. Shevlyakov, *Zhurnal Prikladnoy Khimii*, 2006, **79**, 3, 410. [In Russian]

83. V.P. Zaharov, K.S. Minsker, F.B. Shevlyakov, A.A. Berlin, G.G. Aleksanyan, B.L. Rytov and A.A. Konoplev, *Zhurnal Prikladnoy Khimii*, 2004, **77**, 11, 1840. [In Russian]

84. A.A. Berlin, J.A. Prochuhan, K.S. Minsker and N.S. Enikolopyan, *Vysokomolekulyarnye Soedineniya*, 1991, **33A**, 2, 243. [In Russian]

85. N.V. Lisitsyn, *Khimicheskaya Promyshlennost*, 2003, **80**, 1, 47. [In Russian]

86. A.A. Berlin, K.S. Minsker and K.M. Djumaev in *Novel Unified Energy and Resource Efficient High Performance Technologies of Increased Ecological Safety Based on Tubular Turbulent Reactors*, Niitjehim, Moscow, Russia, 1996. [In Russian]

87. A.A. Berlin and K.S. Minsker, *Doklady Akademii Nauk*, 1997, **355**, 3, 346. [In Russian]

88. A.A. Berlin, J.A. Prochuhan, K.S. Minsker, J.A. Tumanyan, G.G. Aleksanyan and N.S. Enikolopyan, *Vysokomolekulyarnye Soedineniya*, 1988, **30A**, 11, 2436. [In Russian]

89. K.S. Minsker and J.A. Sangalov in *Isobutylene and its Polymers*, Khimiya, Moscow, Russia, 1986. [In Russian]

90. K.S. Minsker, A.A. Berlin, Ju.A. Prochuhan, Je.A. Tumanyan, M.M. Karpasas and N.S. Enikolopyan, *DAN SSSR*, 1986, **291**, 1, 114.

91. G.S. Dyakonov, R.G. Tahavutdinov and I.V. Averko-Antonovich, *Teoreticheskie Osnovy Khimicheskoy Tekhnologii*, 2001, **35**, 4, 429. [In Russian]

92. I.V. Averko-Antonovich, R.G. Tahavutdinov and G.S. Dyakonov, *Khimicheskaya Promyshlennost*, 1999, **5**, 52. [In Russian]

93. Y.A. Prochukhan, K.S. Minsker, A.A. Berlin, J.A. Tumanyan, and N.S. Enikolopyan, *Doklady Akademii Nauk SSSR*, 1986, **291**, 6, 1425. [In Russian]

94. I.V. Averko-Antonovich, R.G. Tahavutdinov and G.S. Dyakonov, *Khimicheskaya Promyshlennost*, 1999, **5**, 52. [In Russian]

95. V.Z. Kompaniec, A.A. Konoplev, A.A. Berlin, Y.A. Prochukhan, K.S. Minsker, M.M. Karpasas and N.S. Enikolopyan, *Doklady Akademii Nauk SSSR*, 1987, **297**, 5, 1129. [In Russian]

96. J.A. Prochuhan, K.S. Minsker, A.A. Berlin, M.M. Karpasas, V.Z. Kompaniec, A.A. Konoplev and N.S. Enikolopyan, *Doklady Akademii Nauk SSSR*, 1988, **298**, 6, 1428. [In Russian]

97. V.P. Zakharov, A.A. Berlin and G.E. Zaikov, *Bulgarian Chemistry and Industry*, 2005, **76**, 2.

98. J.B. Monakov, A.A. Berlin and V.P. Zakharov, *Izvestiya Vuzov. Khimiya I Himicheskaya Tehnologiya*, 2005, **48**, 9, 3. [In Russian]

99. A.A. Berlin, K.S. Minsker and V.P. Zaharov, *Doklady Akademii Nauk SSSR*, 2000, **372**, 4, 503. [In Russian]

100. K.S. Minsker, A.A. Berlin, V.P. Zaharov, G.S. Dyakonov, A.G. Muhametzyanova and G.E. Zaikov, *Zhurnal Prikladnoy Khimii*, 2003, **76**, 2, 272. [In Russian]

101. K.S. Minsker, V.P. Malinskaya, V.P. Zaharov and A.A. Berlin, *Zhurnal Prikladnoy Khimii*, 2000, **73**, 9, 1505. [In Russian]

102. V.P. Zaharov and K.S. Minsker, *Vestnik Bashkirskogo Universiteta*, 2000, **1**, 42. [In Russian]

103. V.P. Zaharov, A.A. Berlin, K.S. Minsker and V.P. Malinskaya, *Trudy Akademii Nauk Respubliki Bashkortostan*, 2001, **2**, 231. [In Russian]

104. J.G. Chesnokov, *Zhurnal Prikladnoy Khimii*, 1997, **70**, 1, 907. [In Russian]

105. B.V. Dzubenko, G.A. Dreitser and A.V. Kalyatka, *International Journal on Heat and Mass Transfer*, 1998, **41**, 3, 645.

106. B.V. Dzubenko, G.A. Dreitser and A.V. Kalyatka, *International Journal on Heat and Mass Transfer*, 1998, **41**, 3, 653.

107. J.K. Kalinin and G.A. Drejcer in *Mass Exchange Intensification in Channels*, Mashinostroenie, Moscow, Russia, 1990. [In Russian]

108. G.A. Drejcer, *Teplojenergetika*, 1995, **3**, 11. [In Russian]

109. A.A. Konoplev, G.G. Aleksanyan, B.L. Rytov and A.A. Berlin, *Teoreticheskie Osnovy Khimicheskoy Tekhnologii*, 2002, **36**, 2, 220. [In Russian]

110. E.K. Kalinin, G.A. Dreitser and E.V. Dubrovsky, *Heat Transfer Engineering*, 1985, **6**, 1, 44.

111. G.A. Drejcer in *Modern Problems of Hydrodynamics and Heat Transfer in Components of Power Generation Systems and Cryogenic Machinery*, VZMI, Moscow, Russia, 1988. [In Russian]

112. A.A. Konoplev, G.G. Aleksanyan, B.L. Rytov and A.A. Berlin in *Transactions of Institute of Chemical Physics, Russian Academy of Sciences*, Moscow, Russia, 2002. [In Russian]

113. K.S. Minsker, V.P. Zaharov and A.A. Berlin, *Doklady Akademii Nauk*, 2003, **392**, 6, 783. [In Russian]

114. V.P. Zaharov, K.S. Minsker, A.A. Berlin and F.B. Shevlyakov, *Teoreticheskie Osnovy Khimicheskoy Tekhnologii*, 2004, **38**, 5, 528. [In Russian]

115. A.A. Konoplev, G.G. Aleksanyan, B.L. Rytov and A.A. Berlin in *Transactions of Institute of Chemical Physics, Russian Academy of Sciences*, Institute of Chemical Physics, Moscow, Russia, 2000. [In Russian]

116. F. Balzereit and W. Roetzel, *Chemical Engineering and Technology*, 1997, **69**, 9, 2324.

117. J. Villermaux, *Chemical Engineering Science*, 1996, **51**, 10, 1931.

118. A.B. Golovanchikov, G.V. Ryabchuk and N.A. Dulkina, *Izvestiya Vuzov. Khimiya I Himicheskaya Tehnologiya*, 2001, **44**, 4, 87. [In Russian]

119. V.V. Kafarov and M.B. Glebov in *Mathematical Modeling of Basic Processes of Chemical Industry*, Vysshaya Shkola, Moscow, Russia, 1991. [In Russian]

120. A.P. Torres, F.A.R. Oliveira and S.P. Fortuna, *Journal of Food Engineering*, 1998, **35**, 2, 147.

121. A.M. Zhurba and S.V. Kurilov *Teoreticheskie Osnovy Khimicheskoy Tekhnologii*, 1991, **25**, 3, 440. [In Russian]

122. A.D. Martin, *Chemical Engineering Science*, 2000, **55**, 5907.

123. M.M. Gavrilenko, I.E, Maleev and V.I. Nikitin, *Khimiya i Himicheskaya Tehnologiya*, 1998, **41**, 3, 101. [In Russian]

124. A.M. Zhurba, S.V. Kurilov, L.L. Gerasimova and I.B. Vilchinskaya, *Teoreticheskie Osnovy Khimicheskoy Tekhnologii*, 1995, **29**, 1, 22. [In Russian]

125. O. Levenshpil in *Engineering Background for Chemical Processes*, Khimiya, Moscow, Russia, 1969. [In Russian]

126. P. Viitanen, *Applied Radiation Isotope*, 1997, **48**, 7, 893.

127. A.G. Muhametzyanova, R.G. Tahavutdinov, G.S. Dyakonov, V.P. Zaharov and A.N. Bergman, *Vestnik Kazanskogo Tehnologicheskogo Universiteta*, 2002, **1-2**, 260. [In Russian]

128. V.P. Zakharov, K.S. Minsker, I.V. Sadykov and A.A. Berlin, *Himicheskaya Fizika*, 2003, **22**, 3, 34. [In Russian]

129. K.S. Minsker, V.P. Zaharov, F.B. Shevlyakov and A.A. Berlin, *Doklady Akademii Nauk SSSR*, 2003, **392**, 4, 490. [In Russian]

130. V.P. Zaharov, F.B. Shevlyakov and K.S. Minsker, *Izvestiya Vuzov. Khimiya I Himicheskaya Tehnologiya*, 2005, **48**, 3, 79. [In Russian]

# 3 Fast Processes in Polymer Synthesis and Principles of Tailoring their Molecular Characteristics

## 3.1 Polymerisation Processes

During fast polymerisation processes in a liquid phase, upon the adiabatic heating of a reaction mixture, both the increase of average molecular weight (MW) and the narrowing of the molecular weight distribution (MWD) of the polymer being formed present a problem. High absolute values of temperature in a reaction zone result in the formation of low molecular weight products with a large polydispersity, i.e., with a wide MWD [1, 2]. In this regard, the task of making polymeric products with maximum $M_w$, $M_n$, $M_z$ values and accompanying narrow MWD is of great importance.

### *3.1.1 Isobutylene Polymerisation*

Isobutylene (2-methylpropene) is easily polymerised *via* a cationic mechanism in the presence of electrophilic catalysts to form a wide range of products – from lower oligomers (where the number of links is about 2–3) to polymers with a MW of more than several millions.

Isobutylene polymerisation, in the presence of metals halides (Lewis acids) combined with Bronsted acids (exemplified by a catalyst based on $MeX_n$ and $H_2O$), proceeds according to the following scheme:

Catalytic complex formation: $MeX_n + H_2O \rightarrow MeX_n{\cdot}H_2O \rightarrow H^{\delta+}, MeX_nOH^{\delta-}$

Initiation ($k_{in}$): $H^{\delta+}, MeX_nOH^{\delta-} + CH_2 = C(CH_3)_2 \rightarrow (CH_3)_3C^{\delta+}, MeX_nOH^{\delta-}$

Chain propagation ($k_p$): $(CH_3)_3C^{\delta+}, MeX_nOH^{\delta-} + CH_2 = C(CH_3)_2 \rightarrow (CH_3)_3C\text{-}CH_2\text{-}(CH_3)_2C^{\delta+}, MeX_nOH^{\delta-}$

Chain transfer reactions (mostly to monomer, $k_m$):

a) $\text{-}CH_2\text{-}(CH_3)_2C^{\delta+}, MeX_nOH^{\delta-} + CH_2 = C(CH_3)_2 \rightarrow \text{-}CH_2\text{-}C(CH_3) = CH_2 + (CH_3)_3C^{\delta+}, MeX_nOH^{\delta-}$

b) $\text{-}CH_2\text{-}(CH_3)_2C^{\delta+}, MeX_nOH^{\delta-} + CH_2 = C(CH_3)_2 \rightarrow \text{-}CH\text{-}C(CH_3)_2 + (CH_3)_3C^{\delta+}, MeX_nOH^{\delta-}$

Reactions of transfer of a proton to a counterion (possible reaction) can be ignored in many cases:

a) $-CH_2-(CH_3)_2C^{\delta+}, MeX_nOH^{\delta-} \rightarrow -CH_2-C(CH_3) = CH_2 + H^{\delta+}, MeX_nOH^{\delta-}$

b) $-CH_2-(CH_3)_2C^{\delta+}, MeX_nOH^{\delta-} \rightarrow -CH-C(CH_3)_2 + H^{\delta+}, MeX_nOH^{\delta-}$

Chain termination by the addition of a counterion fragment ($k_t$):

a) $-CH_2-(CH_3)_2C^{\delta+}, MeX_nOH^{\delta-} \rightarrow -CH_2-C(CH_3)_2-X + MeX_{n-1}OH$

b) $-CH_2-(CH_3)_2C^{\delta+}, MeX_nOH^{\delta-} \rightarrow -CH-C(CH_3)_2-OH + MeX_n$

It should be noted that the catalyst regeneration, due to fast reinitiation, is transformed into the reaction of chain transfer to counterion.

A convenient possibility to control the MW and MWD of polyisobutylene involves changing the method of catalyst loading into the reaction zone, in particular, the implementation of a stepwise catalyst loading into the reactor. This can be achieved using the process zone model [3, 4], which implies a series of separate sequentially connected reaction zones, with a reaction mixture, as well as a new portion of the catalyst solution (or catalyst and monomer) being fed into each downstream zone after process completion in the previous one. The temperature in each zone is maintained at a constant value and determined by the heat balance, by taking (or without taking) into account the boiling of a solvent (and a monomer), as well as the heat transfer through the outer wall.

In the case of fast isobutylene polymerisation, when macromolecule length is determined by the chain transfer reaction to monomer, the polymer has an average MW dependent on the temperature in the reaction zone. Fast polymerisation processes can be carried out with or without boiling of the reaction mixture (internal heat removal). In this case, the analysis of heat balance and reaction mixture motion hydrodynamic mode indicates that the boiling of a solvent and/or a portion of a monomer allows, on the one hand, the mass exchange to be intensified (the coefficient of eddy diffusion and heat transfer in the reaction zone both increase due to the formation of a two-phase flow). On the other hand, it shows that a large amount of heat (more than 50%), liberated during polymerisation, is consumed for the evaporation of a solvent and/or monomer and hence, the conditions of thermal mode stabilisation in the reactor are significantly improved [5, 6].

There are several requirements to be met for implementing the zone model in a real process [2]: 1) Reaction zones should not cross each other; therefore, the distance between adjacent points of catalyst loading should be:

$$L_i > V / k_g \tag{3.1}$$

2) The reactor should meet the requirement of forming radially uniform temperature and concentration fields, at a turbulent reacting flow, in the reaction zone, i.e.:

$$R \le R_{cr} = \sqrt{D_t / k_g} \tag{3.2}$$

Where $R_{cr}$ is the reactor radius which allows the polymerisation process to proceed in quasi-plug flow mode in turbulent flows.

3) The heat released in every zone, depending on the polymerisation rate and amount of a monomer reacting in the reaction zone is small, and heat exchange coefficients are such as to meet the requirement of temperature uniformity in every reaction zone. In accordance with this condition in the reaction zone, the polymer should be formed with a MWD and MW corresponding to the temperature determined by the heat balance. Calculations show that such conditions are performed for the following equation [3]:

$$\Delta T_i = \frac{\rho \delta V q \Delta M_i}{\lambda_c} << \Delta T_2 = \frac{R T_i^2}{E_M - E_p} \tag{3.3}$$

Where:

$\Delta T_i$ is a characteristic temperature difference in a reaction $i^{th}$ zone.

$\rho V q \Delta M_i$ is the heat release rate in the $i^{th}$ zone.

$V$ is the linear flow rate.

$q$ is the heat of polymerisation (reaction thermal effect) in a liquid phase.

$\Delta M_i$ is the amount of reacted monomer in the $i^{th}$ zone.

$\lambda_T \Delta T_i / \delta$ is the rate of heat transfer along the reactor.

$\lambda_c$ is the effective heat conduction coefficient.

$\delta$ is a characteristic dimension of the reaction zone.

$\Delta T_2$ is a characteristic temperature range for changing MW.

$E_m$ and $E_p$ are activation energies of the reaction of chain transfer to monomer and chain propagation, respectively.

$T_i$ is the average temperature in the $i^{th}$ zone.

$R$ is the universal gas constant.

$\rho$ is the reaction mixture density.

If the polymerisation heat is consumed for heating of a reaction volume and no heat transfer through the outer wall occurs, there will be a definite relationship between the average temperature $T_i$ in $i^{th}$ zone, the initial temperature $T_0$ and amount of monomer reacted in all previous zones including the $i^{th}$ zone:

$$T_i = T_0 + \frac{q}{C_p}\sum_{k=1}^{i}\Delta M_k \tag{3.4}$$

Since the polymer is formed independently in each zone, the distribution function is summarised from the MWD functions of the polymer formed in each zone:

$$\rho_w^i(j) = \sum_{k=1}^{i}\Delta M_k \rho_w^k(j) \Big/ \sum_{k=1}^{i}\Delta M_k \tag{3.5}$$

Where $\rho_w^i(j)$ is the MWD weight function of the entire polymer volume at the exit of the $i^{th}$ zone.

Average degrees of polymerisation, which determine the MW values for the cascade of n reactors (separate reaction zones), are represented by the following equations, respectively [3]:

$$(P_n^i)^{-1} = \sum_{k=1}^{i}\Delta M_k \times (P_n^k)^{-1} \Big/ \sum_{k=1}^{i}\Delta M_k \tag{3.6}$$

$$P_w^i = \sum_{k=1}^{i}\Delta M_k \times P_w^k \Big/ \sum_{k=1}^{i}\Delta M_k \tag{3.7}$$

$$P_z^i \times P_w^i = \sum_{k=1}^{i}\Delta M_k \times P_z^i \times P_w^k \Big/ \sum_{k=1}^{i}\Delta M_k \tag{3.8}$$

**Equations 3.6–3.8** are true whatever distribution the polymer has in each zone.

For further analysis, the only thing which is important is that the average MW and MWD are determined by the reaction of chain transfer to monomer. Taking into consideration that the reaction in every zone occurs practically at a constant temperature, the following expression is obtained:

$$\rho_w^k(j) = \frac{j}{(P_n^k)^2}\exp\left(-\frac{j}{P_n^k}\right) \tag{3.9}$$

$$\frac{1}{3}P_z^k = \frac{1}{2}P_w^k = P_n^k = \frac{k_p^0}{k_m^0}\exp\left(-\frac{E_p - E_M}{RT}\right) \tag{3.10}$$

Thus, we have a closed system of **Equations 3.4–3.10** which allow the MWD and average MW to be calculated for a random distribution of polymer yields in each zone ($\Delta M_i$). For determining the relationship between the polymer yield in a separate zone and the amount of catalyst loaded, knowledge of polymerisation kinetic mechanisms is necessary. In particular, using the cationic mechanism of isobutylene polymerisation, the following expressions may be derived [1]:

$$\Delta M_i = (M_0 - \sum_{k=1}^{i}\Delta M_k)\left\{1 - \exp\left(-\frac{k_p}{k_t}\times[A^*]_i\right)\right\} \tag{3.11}$$

$$\sum_{k=1}^{i}\Delta M_k = M_0\left\{1 - \exp\left(-\sum_{k=1}^{i}\frac{k}{k}[A^*]_k\right)\right\} \tag{3.12}$$

Where $[A^*]_i$ is the amount of catalyst fed to the $i^{\text{th}}$ zone: $M_0$ is the monomer concentration in the starting mixture. If both the $k_p$ and $k_t$ are temperature independent, which is particularly typical for the polymerisation of isobutylene (diffusion reaction region) [7, 8], **Equation 3.8** may be simplified to:

$$\sum_{k=1}^{i}\Delta M_k = M_0\left\{1 - \exp\left(-\frac{k_p}{k_t}\sum_{k=1}^{i}[A^*]_k\right)\right\} \tag{3.13}$$

**Equations 3.2–3.10** allow the opportunity to calculate the MW and MWD of a polymer at any given method of catalyst loading under adiabatic conditions of polymerisation, i.e., in the absence of heat removal.

In many cases, a solvent and/or monomer will boil, starting from a certain temperature. The boiling of a solvent and/or monomer allows fast polymerisation processes to occur in milder conditions, as well as achieving higher values of average MW and narrower MWD of the polymeric products formed [3, 6].

If the boiling temperature is achieved in one of the zones, a consequent zone separation does not naturally make sense because the polymerisation reaction proceeds further at a constant temperature. In this case, single-shot catalyst loading may result in the narrowest (exponential) MWD and the lowest average MW values of polymer formed [2]:

$$\frac{1}{3}P_z = \frac{1}{2}P_w = P_n = \frac{k_p^0}{k_M^0}\times\exp\left(-\frac{\varepsilon}{T}\right) = P_n^0\times\exp(-x_k) \tag{3.14}$$

$$x_k = \frac{\varepsilon(T - T_0)}{T_0^2} \tag{3.15}$$

$$\varepsilon = \frac{E_m - E_p}{R} \tag{3.16}$$

Intensification of heat and mass exchange, due to fast chemical processes, is concerned with the change in the $D_{\text{turb}}$ value. Typically, as a linear reaction flow rate $V$ at the fixed length of the reaction zone $L$ increases, the time needed for contact of the reacting system with the thermostated surface decreases. In turn, this should reduce the efficiency of external thermostatic control through the wall. However, the increase of $V$, in the case of fast liquid-phase polymerisation processes, results in significant $D_T$ growth, which defines the efficiency of heat and mass transfer in turbulent flow. Therefore, an increase in the $D_T$ for tubular turbulent reactors with $R < R_{cr}$, upon external heat removal, induces significant temperature reduction in the reaction zone. The fact that in the absence of heat removal at high $V$ values during the initial stages of a process ($L$ = 1 $v$, $\tau_{\text{chem}}$ = 0.5 s), the temperature in the reaction zone is lower than that at low flow rates, is also important. Hence, the so-called 'dispersion' of a reaction along the reaction zone occurs.

Taking into consideration the fact that fast polymerisation processes are characterised by inequality of chemical reaction time $\tau_{\text{chem}}$ and transfer time $\tau_{\text{mix}}$ ($\tau_{\text{chem}} < \tau_{\text{mix}}$), it is clear that an increase of $D_{\text{turb}}$ facilitates the decrease of $\tau_{\text{mix}}$, and both these processes are comparable in duration. The increase in linear flow rate $V$, i.e., the intensification of heat and mass exchange in the system, is equivalent to a 'slow down' of the polymerisation reaction itself, compared with the transfer process. Therefore, the conventional approaches to external heat removal, which normally have such a restrictive effect on conventionally designed fast polymerisation processes implemented in stirred tank reactors, play an essential role at both high $V$ and $D_{\text{turb}}$ values when quasi-plug flow tubular turbulent reactors are used. In this case, control of the external temperature can be significantly enchanced due to zone-type catalyst loading.

Multizone-type catalyst loading provides a range of opportunities to control the average MW and MWD width for the polymer being produced in the tubular turbulent reactor, without external heat removal. On the other hand, external heat removal allows, at a corresponding $D_{\text{turb}}$ value, the temperature field inside the reactor to be stabilised and controlled; allowing extra opportunities to control the quality of a product.

Heat removal through an external wall has an effect upon even single-shot catalyst loading, namely the MWD of the polymeric product significantly contracts and the number-average MW ($P_n$) slightly increases. However, provided that some

requirements are met, both the reaction and heat removal zones can be separated, and quasi-adiabatic conditions in the reaction zone can actually be met and, as a consequence, the average MW of the product formed in each reaction zone is determined by the temperature, which corresponds to the adiabatic heat evolution in the zone.

Thus, the zone model of a reactor implies a combination of sequentially connected adiabatic (autothermal) quasi-isothermal turbulent plug flow reactors and heat exchange elements with external heat removal.

In this case, the conditions defining the adequacy of the zone model of a reactor, with external heat removal to the real tubular turbulent reactor, should be achieved with: 1) the length of the heat removal zone should be more than that of the reaction zone, i.e., $L_i >> V/k_g$, and 2) the amount of heat removed, from the reaction zone through the wall, should be significantly less than that of the heat generated during polymerisation in that zone:

$$2\pi \times R \times \frac{V}{k_t} \times K_{bt} \times (T_i - T_{\text{cool}}) << \pi \times R^2 \times V \times \rho \times q \times \Delta M_i \tag{3.17}$$

Where:

$R$ is the radius of the tubular reactor

$K_{bt}$ is the coefficient of heat transfer through an external wall

$T_i$ is the temperature in the $i^{\text{th}}$ zone

$T_{\text{cool}}$ is the temperature of the coolant

$\rho$ is the average density of the reaction mixture

$\Delta M_i$ is the amount of polymer obtained in the $i^{\text{th}}$ zone

For average MW and MWD of the polymer obtained in the sequentially connected quasi-isothermal adiabatic turbulent plug flow reactors and heat exchangers with external heat removal, the following relations are true [2]:

$$\rho_w(j) = \frac{1}{\Delta M} \times \sum_{k=1}^{i} \rho_w^k(j) \times \Delta M_k \tag{3.18}$$

$$P_w = \frac{1}{\Delta M} \times \sum_{k=1}^{i} P_w^k \times \Delta M_k \tag{3.19}$$

$$P_n = \Delta M \times \left( \sum_{k=1}^{i} \frac{\Delta M_k}{P_n^k} \right)^{-1} \tag{3.20}$$

$$P_z \times P_w = \frac{1}{\Delta M} \times \sum_{k=1}^{i} P_z^k \times P_w^k(j) \times \Delta M_k \tag{3.21}$$

Where:

$\rho_w(j)$ and $\rho_w^i(j)$ are differential mass MWD functions of the polymer obtained in the entire reactor and in the i$^{th}$ zone respectively; and

$\Delta M$, $\Delta M_i$, $P_w$, $P_w^i$, $P_n$, $P_n^i$, $P_z$, $P_z^i$ are amounts of polymer, weight-average, number-average and z-average polymerisation degrees of the polymerisation product in the entire reactor and in the $i^{th}$ zone respectively.

As opposed to the model of a reactor with internal heat removal due to boiling, the temperature in each zone of the tubular turbulent reactors, with external heat removal, is determined not only by the heat balance inside the reaction zone, but also by the amount of reaction heat removed through the wall. For an estimation of the temperature change in the cooling zone of the reaction mixture at vigorous cross-sectional stirring (turbulent flow), the following equation is true [2]:

$$\frac{dT}{dL} = -\frac{2K_t}{R \times \rho \times C_p \times V} \times (T - T_{\text{cool}}) = h \times (T - T_{\text{cool}}) \tag{3.22}$$

By integrating this equation in the case of the temperature change in the cooling zone, the following relation may be obtained:

$$\Delta T_k = (T_{k-1} - T_{\text{cool}}) \times \left[1 - \exp(-h \times L_{\text{cool}})\right] = \xi \times (T_{k-1} - T_{\text{cool}}) \tag{3.23}$$

Where:

$T_{k\text{-}1}$ is the temperature in the previous reaction zone or at the inlet of the corresponding cooling zone;

$L_{cool}$ is the length of the cooling zone:

$$\xi = [1 - \exp(-h \times L_k)] \tag{3.24}$$

$\xi$ is the portion of heat removed in the cooling zone from the total thermal energy accumulated by the system at the inlet of this zone (taking into account both the polymerisation reaction and cooling process in all previous zones).

The temperature in $i^{th}$ zone will be then equal to:

$$T_i = T_0 + \alpha_1 \sum_{j=1}^{i} \Delta M_i - \sum_{j=1}^{i} \xi \times (T_{j-1} - T_{\text{cool}}) \tag{3.25}$$

Where:

$$\alpha_1 = q / C_p \tag{3.26}$$

However, the numbering of the cooling zones in the reactor is the cooling zone followed by the reaction zone and has a similar index. In turn, the amount of a polymer obtained in the $i^{th}$ zone, is related to the amount of catalyst fed in accordance with the kinetic mechanism of the polymerisation reaction. For example, in the case of isobutylene polymerisation, the following relation is true [3]:

$$\Delta M_i = (M_0 - \sum_{j=1}^{i-1} \Delta M_j) \times \left[ 1 - \exp\left( -\frac{k_p}{k_t} \times A_i^* \right) \right] \tag{3.27}$$

If the ratio $k_p/k_t$ is temperature independent, then:

$$\Delta M_i = M_0 \times \exp\left( -\frac{k_p}{k_t} \times \sum_{j=1}^{i-1} A_j^* \right) \times \left[ 1 - \exp\left( -\frac{k_p}{k_t} \times A_i^* \right) \right] \tag{3.28}$$

With the temperature value for each zone, the average MW values may be found:

$$\frac{1}{3} P_z^i = \frac{1}{2} P_w^i = P_n^i = \frac{k_p^0}{k_m^0} \times \exp\left( -\frac{E_p - E_m}{R T_i} \right) = \frac{k_p^0}{k_m^0} \times \exp\left( -\frac{\varepsilon}{T_i} \right) \tag{3.29}$$

By addition of **Equation 3.20** to **Equations 3.9–3.21**, the $P_w$, $P_n$, $P_z$ values may be calculated. **Equation 3.18** transforms in this case into the following form:

$$\rho_w(j) = \frac{1}{\Delta M} \times \sum_{k=1}^{i} \Delta M_k \times \frac{j}{(P_n^k)^2} \times \exp\left( -\frac{j}{P_n^k} \right) \tag{3.30}$$

Thus, depending on the polymerisation conditions, particularly on the number of reactors in the cascade and the amount (portion) of a catalyst fed to each reactor, it is possible to influence the MW characteristics of the polymer obtained, over a specific but sufficiently wide range. Upon quasi-plug flow mode formation in turbulent flows, in the case of fast polymerisation processes, external heat removal becomes efficient enough and, as a consequence, has a notable effect on the temperature field of a reaction, as well as on the MW and MWD width of the polymeric product obtained. The occurrence of heat exchange in such reactors gives real opportunities to improve

the quality of the polymeric product obtained (narrower MWD, increased average MW, increased polymer yield, and so on). It allows added opportunities to control fast exothermal polymerisation processes.

### 3.1.2 Pentadiene-1,3 Polymerisation

Among commercial methods of isoprene production, one of the main methods is the process of two-stage isopentane dehydrogenation. Isopentane and isopentene dehydrogenation is carried out at elevated temperatures followed by the formation of a number of by-products among which a great part is piperylene (pentadiene-1,3) [9, 10]. Piperylene yield is 10–15% of the sum of the diene monomers during isoprene production.

One of the applications of piperylene is in cationic oligomerisation, which is used for the production of liquid rubber using a synthetic drying oil based on a commercial oligopiperylene synthetic rubber. Application of the piperylene fraction of hydrocarbons, as the feed stock for synthetic drying oil production, allows decreasing the consumption of vegetable oils in the paint-and-varnish and other industries, along with solving the problem of the by-product disposal from isoprene synthesis [11, 12].

The use of different catalytic systems of both ionic [10] and ionic-coordination [13, 14] types in piperylene polymerisation has been proposed. Because of a high reaction rate of chain transfer to monomer (which grows as catalyst acidity increases) and to solvent (which drops as solvent polarity increases) in cationic polymerisation, a polymer with low MW is obtained. Some halides of metals of groups III-V were tested as catalysts of cationic piperylene polymerisation; the most suitable were $TiCl_4$ and $SnCl_4$. The application of $SbCl_5$ and $InCl_3$ does not ensure an acceptable polymerisation rate and in the case of using $AlCl_3$, the insoluble polymer is obtained.

In [15], on the basis of quantum-chemical calculations and experimental data, it was showed that the acidic strength of the electrophilic catalysts is the measure of activity and selectivity of their action in cationic polymerisation. An increase in the acidic strength of catalysts of the electrophilic polymerisation reactions facilitates an increase in their activity, but decreases process selectivity. In particular, the piperylene oligomerisation with titanium chloride and aluminium chloride etherates was studied in the work of Mardykin and co-workers [16]. Aluminium chloride etherate $AlCl_3 \cdot O(C_6H_5)_2$ provides a greater yield and MW of a product, with the obtained oligopiperylene exhibiting lower unsaturation.

Electrophilic (cationic) piperylene polymerisation may be schematised as follows:

$$n(CH_2 = CH\text{-}CH = CH\text{-}CH_3) + Cat \rightarrow - CH_2\text{-}CH = CH\text{-}CH(CH_3)-$$

The elementary steps of the cationic piperylene polymerisation process are similar to those for isobutylene.

The electrophilic catalysts used for cationic piperylene oligomerisation display different activity; which stipulates in principle, the ability of upgrading the commercial production of synthetic drying oil at the stage of cationic piperylene oligomerisation by selecting a catalytic system with corresponding activity and selectivity.

In the case of electrophilic piperylene polymerisation, the reaction rate was found to substantially depend on the catalyst used ($TiCl_4$, $TiCl_4$-(i-$C_4H_9)_3Al$, $C_2H_5AlCl_2 \cdot O(C_6H_5)_2$, $C_2H_5AlCl_2$, $AlCl_3 \cdot O(C_6H_5)_2$) [17]. At the same time, polymerisation in the presence of $AlCl_3$ and $AlCl_3 \cdot O(C_6H_5)_2$ can only be related to fast chemical processes.

For all the electrophilic catalysts examined, the piperylene oligomerisation reaction is a first-order reaction both for monomer and catalyst. In particular, it was exemplified by using $TiCl_4$ and $AlCl_3 \cdot O(C_6H_5)_2$ (**Figure 3.1**). Reaction rate constants were determined from the experimental relationships between the monomer conversion and time (**Figure 3.2**), with the following relation:

$$\Delta P = \Delta T C_P \rho / q = [M]_0 \times (1 - e^{-k_{ef}\tau}) \tag{3.31}$$

Where:

The heat of piperylene oligomerisation $q$ = 72.38 kJ/mol.

$\Delta P$ is the amount of oligomer obtained per reaction volume unit.

The average heat capacity of the reaction mixture $C_p$ = 1.757 kJ/mol·K.

The average medium density $\rho$ = 863 kg/m$^3$.

As can be seen from the figure, the activity of the catalysts examined varies over a broad range (**Table 3.1**), with practically no piperylene oligomerisation occurring in the presence of $Al(C_2H_5)_2Cl$ and $Al(i\text{-}C_4H_9)_2Cl$. Greater yields (70–80% and more) can be achieved in a time of 15–20 s using $AlCl_3 \cdot O(C_6H_5)_2$ as well as $AlC_2H_5Cl_2$ as catalysts, whereas in the presence of $TiCl_4$ the product yield is not greater than 0.5–1% over the same timescale (**Figure 3.2**). The addition of electron-donor compounds, particularly $(C_6H_5)_2O$, to an electrophilic aluminium-containing catalyst leads to a decrease in the reaction rate constant in the case of piperylene oligomerisation, which seems to be caused by a decrease in the acid strength of the catalytic complex. By using the principle of interrelation between the acidity and cationic activity of Friedel–Crafts catalysts in polymerisation processes [15], it may be assumed that $AlCl_3$ will demonstrate greater activity compared with $AlCl_3 \cdot O(C_6H_5)_2$. In this case however, the crosslinked polymer will be obtained due to high catalyst activity in electrophilic processes, which is impermissible.

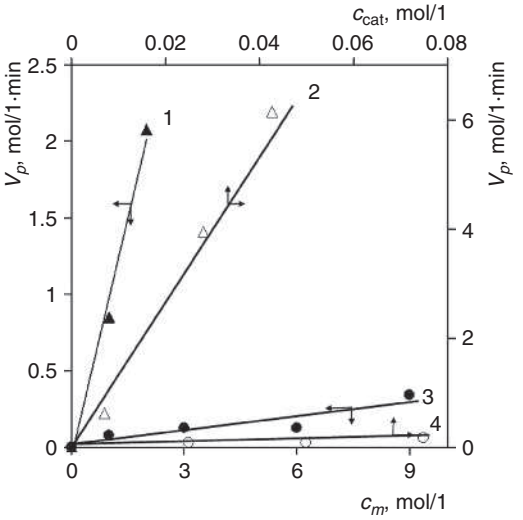


**Figure 3.1** Piperylene oligomerisation rate ($V_p$) as a function of monomer concentration (1, 3) and catalyst concentration (2, 4) in the presence of $AlCl_3{\cdot}O(C_6H_5)_2$ (1, 2) and $TiCl_4$ (3, 4). 1) $C_{Al}$ = 0.014 mol/l; 2) $C_M$ = 1 mol/l; and 3) $C_{Ti}$ = 0.025 mol/l, $T_0$ = 25 °C

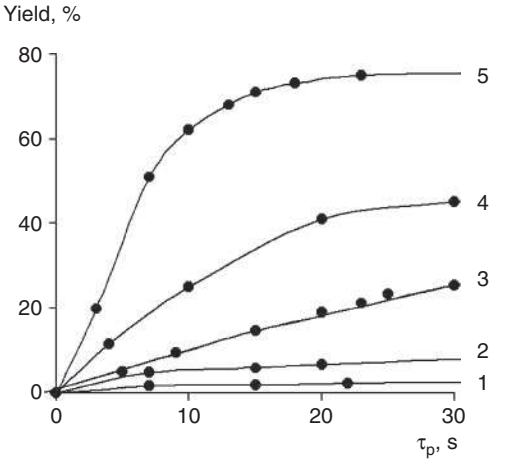


**Figure 3.2** Conversion curves of piperylene oligomerisation in the presence of different catalysts: $TiCl_4$ (1); $TiCl_4$-Al(*i*-$C_4H_9)_3$ (2); $AlC_2H_5Cl_2{\cdot}O(C_6H_5)_2$ (3); $AlC_2H_5Cl_2$ (4); and $AlCl_3{\cdot}O(C_6H_5)_2$ (5). $C_{Ti}$ = 0.025 mol/l (1, 2); $C_{Al}$ = 0.02 (3, 4) and 0.028 (5) mol/l; $C_M$ = 1.0 (1, 3–5); and 2.0 (2) mol/l. $T$ = 25 °C

| Table 3.1 Cationic piperylene oligomerisation in the presence of some electrophilic catalysts | | | | | |
|---|---|---|---|---|---|
| **τ, min** | $TiCl_4$ | $TiCl_4$- $Al(i\text{-}C_4H_9)_3$ | $AlC_2H_5Cl_2 \cdot O(C_6H_5)_2$ | $AlC_2H_5Cl_2$ | $AlCl_3 \cdot O(C_6H_5)_2$ |
| | **[η], decilitre/g** | | | | |
| 2 | - | - | 0.066 | - | 0.066 |
| 5 | - | 0.069 | - | 0.053 | - |
| 120 | 0.078 | - | - | - | 0.055 |
| 240 | 0.068 | 0.230 | 0.058 | 0.064 | - |
| **τ, min** | **Double bond content, mol% as per theoretical value** | | | | |
| 10 | - | - | 64.6 | 63.2 | 61.9 |
| 20 | 47.6 | 63.2 | - | - | - |
| 120 | - | - | - | 60.9 | 65.3 |
| 180 | 63.9 | 73.4 | - | - | - |
| 240 | - | - | 73.4 | - | - |
| ***Cis*-1,4/*trans*-(1,4+1,2) unit ratio** | | | | | |
| | 0.13 | 0.22 | 0.10 | 0.33 | 0.11 |
| **Effective piperylene oligomerisation rate constant $k_{ef}$, $min^{-1}$** | | | | | |
| Molecular weight type | 0.05 | 0.2 | 1.3 | 4 | 11.8 |
| **Oligopiperylene molecular characteristics** | | | | | |
| $M_w$ | 1347 | 3336 | 1729 | 1611 | 1889 |
| $M_n$ | 877 | 1153 | 1056 | 997 | 1075 |
| $M_w/M_n$ | 1.5 | 2.9 | 1.6 | 1.6 | 1.8 |

As in the case of the cationic polymerisation of other diene hydrocarbons [13], macromolecules of oligopiperylene synthesised in the presence of the studied catalysts, predominantly exhibited a *trans*-structure (**Table 3.1**); an increased concentration of *cis*-1,4-units is observed for samples prepared in the presence of $TiCl_4$- $Al(i\text{-}C_4H_9)_3$ and $AlC_2H_5Cl_2$.

Analysis of the double bond content of oligopiperylene macromolecules showed that there is little change in the unsaturation of the polymeric products obtained for all catalysts used in the synthesis (**Table 3.1**). The addition of ether, particularly $(C_6H_5)_2O$ in a 1:1 mol/mol ratio as a modifier to catalysts, decreases both the electrophilic catalyst activity (the effective oligomerisation rate constant $k_{ef}$ decreases) and the probability of gelation processes (crosslinking).

The MWD of oligopiperylene prepared in the presence of the catalysts studied, except for the $TiCl_4$-$Al(i\text{-}C_4H_9)_3$ system, is narrow (**Table 3.1**) and monomodal (**Figure 3.3**). In the presence of $TiCl_4$-$Al(i\text{-}C_4H_9)_3$, the curve of oligomer microchain MW distribution is shifted to a high MW (the curve takes a well-defined bimodal form). As a consequence, the MWD broadens which may be explained by the presence of several types of AC in a catalyst, particularly of cationic and ionic-coordinate nature, and are responsible for the formation of the corresponding mixture of low and high MW polymers. The formation of oligopropylene, with such molecular characteristics, seems to be technologically impracticable due to an increase in polymerisate viscosity as a result of using a high MW product, and the deterioration of synthetic drying oil performance characteristics.

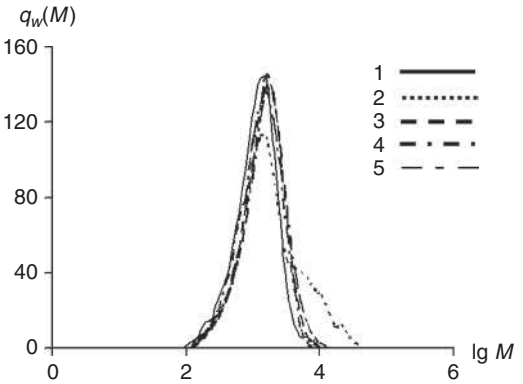


**Figure 3.3** MWD curves of oligopiperylene. $TiCl_4$ (1), $TiCl_4$-$Al(i\text{-}C_4H_9)_3$, (2) $AlC_2H_5Cl_2{\cdot}O(C_6H_5)_2$ (3), $AlC_2H_5Cl_2$ (4), $AlCl_3{\cdot}O(C_6H_5)_2$ (5) (Conditions may be seen in **Figure 3.2**)

Thus, the kinetic activity of the most commonly used electrophilic catalytic systems was found to be characterised by the following: $TiCl_4$ < $TiCl_4$-Al(*i*-$C_4H_9)_3$ < $AlC_2H_5Cl_2 \cdot O(C_6H_5)_2$ < $AlC_2H_5Cl_2$ < $AlCl_3 \cdot O(C_6H_5)_2$ for cationic piperylene oligomerisation. The catalysts studied demonstrate activity over a wide range, differing by two orders ($k_{ef}$ = 0.05–11.8 $min^{-1}$), without great differences in the molecular characteristics of the oligomeric products obtained. Using a two-component Ziegler–Natta catalytic system $TiCl_4$-Al(*i*-$C_4H_9)_3$ leads to the formation of a polymer blend with an increased average MW and a wide oligopropylene MWD, along with an insignificant increase in *cis*-1,4-unit content in the molecules.

Cationic piperylene oligomerisation used for producing liquid synthetic oligopiperylene rubber, in the presence of different catalytic systems, requires a variable approach to the process design according to the experimental data obtained (kinetic parameters). In particular, note should be taken of a sufficiently high value of the piperylene oligomerisation rate constant in the presence of $AlCl_3 \cdot O(C_6H_5)_2$ ($k_{ef} \approx 11.8$ $min^{-1}$) and $AlC_2H_5Cl_2$ ($k_{ef} \approx 4$ $min^{-1}$). In this case, using $AlCl_3 \cdot O(C_6H_5)_2$ as the catalyst of piperylene oligomerisation allows the synthetic drying oil preparation technique to be significantly simplified, and an energy- and resource-saving process to be developed using small-scale tubular reactors operating in a plug flow mode in turbulent flows.

The key parameter when selecting the type of reactor is the residence time and the reaction zone size which are necessary to achieve the required monomer conversion under isothermal conditions and, as a consequence, the optimum time of process running.

In the case of first-order polymerisation (when it is assumed that the concentration of AC is unchangeable during the process) for the plug flow reactor, the monomer concentration varies in accordance with the following equation [1]:

$$C_m = C_{m0} \exp\left( -k_{ef} \frac{\upsilon_r}{w} \right) \tag{3.32}$$

Where $C_{m0}$ and $C_m$, are the initial monomer concentration and outlet monomer concentration; w is volume flow rate of the reaction mixture; $\upsilon_r$ is the reaction zone volume.

The relationship between the reaction zone size $\upsilon_p$ and monomer conversion degree *x* may be obtained from **Equation 3.32**:

$$\upsilon_p = \frac{|ln(1-x)|w}{k_{ef}} \tag{3.33}$$

**Equation 3.33** allows the calculation of the optimum reaction zone size in the plug flow reactor, which is necessary to achieve the required degree of monomer conversion, as a function of the kinetic parameters of a chemical process $k_{ef}$ and the required monomer conversion degree x.

The calculation of a continuously operating stirred tank reactor used for polymerisation is based on the solution of the equation of material balance for the monomer [1]:

$$\frac{dC_m}{d\tau} = wC_{m0} - wC_{m1} - v_p V_n \tag{3.34}$$

Where $V_p = k_{ef}C_m$ – the rate of the second-order polymerisation process.

By transforming **Equation 3.26,** including the monomer conversion degree $x = (C_{m0}-C_m)/C_{m0}$, the expression for calculating the reaction zone size in a stirred tank reactor may be obtained:

$$v_p = \frac{xw}{(1-x)k_{ef}} \tag{3.35}$$

**Table 3.2** shows the effective rate constant values of piperylene polymerisation in the presence of different catalytic systems, as well as the required residence times in stirred tank reactors and plug flow reactors. It is evident that in the case of piperylene oligomerisation, in the presence of $TiCl_4$ and $TiCl_4$-Al($i$-$C_4H_9$)$_3$ as catalysts ($k_{ef}$ = 0.05–0.2 min$^{-1}$ at 25 °C), it is reasonable to use a conventional stirred tank reactor, or the cascade of such reactors, due to the high residence times the reaction mixture exhibits when in the reactor $\tau_{pass}$. In the case of oligopiperylene synthesis, in the presence of $AlCl_3 \cdot O(C_6H_5)_2$, $AlC_2H_5Cl_2$ and probably, $AlC_2H_5Cl_2 \cdot O(C_6H_5)_2$, the high rate constant values ($k_{ef}$ = 1.3–11.8 min$^{-1}$ at 25 °C) and correspondingly, the small geometry of the reaction zone determine the necessity of using small-scale tubular turbulent reactors which can operate in a quasi-plug flow mode. Moreover, low values of $\tau_{pass}$ (2–20 s) in this case, reduce the probability of slower side processes.

Since the quasi-plug flow mode, in turbulent flows, is formed at a strictly limited geometry of the reaction zone, it is necessary to examine the ratio of characteristic times of mixing $\tau_{mix}$ and chemical reaction $\tau_{chem}$, in the case of piperylene oligomerisation, in the presence of the studied catalysts in order to select the optimum reactor design.

In the absence of diffusion restrictions, the oligomerisation process in a divergent-convergent type reactor, in a self-similar mode of reaction mixture flow, is determined by the following condition [18]:

$$\tau_{mix} = \frac{17.427 f_E R_d^3}{f_c^2 f w} \le \tau_x = \frac{|ln(1-x)|}{k_{ef}} \tag{3.36}$$

**Table 3.2 Piperylene oligomerisation in a stirred tank reactor and a tubular plug flow reactor in the presence of various catalysts ($x$ = 0.95, $w$ = 4.4 m$^3$/hour, $C_{cat}$ = 0.15 mol/l, and $C_{M0}$ = 5.7 mol/l)**

| Catalyst | $K_{ef}$, min$^{-1}$ | $\tau_{pass}$, $c$ | | $R_d^{cr}$, m |
|---|---|---|---|---|
| | | Stirred tank reactor | Tubular turbulent reactor | |
| $TiCl_4$ | 0.05 | 3845.4 | 605.4 | 0.132 |
| $TiCl_4$-Al($i$-$C_4H_9$)$_3$ | 0.2 | 842.7 | 131.0 | 0.080 |
| $AlC_2H_5Cl_2 \cdot O(C_6H_5)_2$ | 1.3 | 122.7 | 18.8 | 0.042 |
| $AlC_2H_5Cl_2$ | 4 | 38.4 | 6.0 | 0.028 |
| $AlCl_3 \cdot O(C_6H_5)_2$ | 11.8 | 18.1 | 2.9 | 0.022 |

Where:

$R_d$ is the radius of a wide part of a reactor, where the uniform reagent concentration field or the required radius of a reactor (diffuser) should be created.

w is the volume flow of the reaction mixture.

$f$, $f_c$, and $f_E$ are numerical coefficients calculated according to **Equations 2.20**, **2.24**, and **2.25** respectively.

Using **Equation 3.36**, the equation for calculating a critical reactor radius $R_d^{cr}$, a criterion of quasi-plug flow mode formation at the ratio $\tau_{mix} \leq \tau_{chem}$ ($L_c/2R_d$ = 1.7, $R_d/R_c$ = 1.6, $\gamma$ = 45 $^0$), may be obtained:

$$R_d^{cr} \leq \sqrt[3]{\frac{w\left|ln(1-x)\right|}{k_{ef}\,318.93}} \tag{3.37}$$

Values of $R_d^{cr}$ (**Table 3.2**, **Figure 3.4**) for a rather fast piperylene oligomerisation reaction, in the presence of $AlCl_3 \cdot O(C_6H_5)_2$ and $AlC_2H_5Cl_2$ as catalysts, confirm the possibility and the practical necessity of using tubular turbulent reactors in which a vigorous turbulent stirring of the reaction mixture is achieved due to the energy of the hydrodynamic flow. A low reaction rate, in the case of piperylene oligomerisation in the presence of $TiCl_4$ and $TiCl_4$-Al($i$-$C_4H_9$)$_3$ as catalysts (**Table 3.2**), explains the practicability of using standard stirred tank reactors with a long radius (**Figure 3.4**).

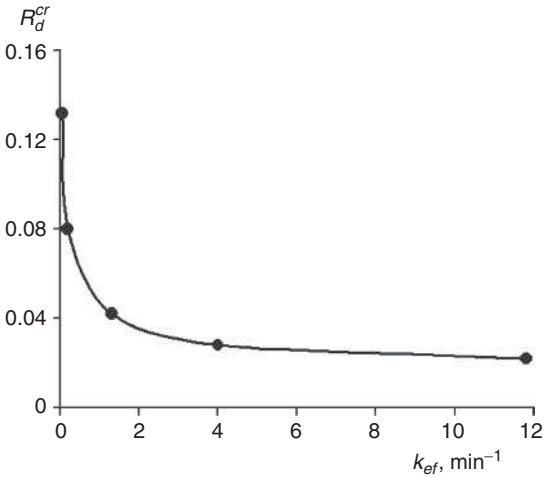


**Figure 3.4** The reactor radius $R_d^{cr}$ as a function of the kinetic parameters of piperylene oligomerisation in the presence of different catalytic systems (conditions may be seen in **Table 3.2**)

Use of the reactive catalyst, $AlCl_3{\cdot}O(C_6H_5)_2$, and tubular turbulent reactors for piperylene oligomerisation, compared with a stirred tank reactor and $TiCl_4$ as the catalyst, allows more than a 1000-fold decrease of the residence time for reagents in the reaction zone $\tau_{\text{pass}}$ [19].

When selecting a reactor to be used for any chemical process, including polymerisation, it is necessary to take into account the temperature distribution in the reaction zone and the possibility of controlling the thermal mode, in order to obtain a polymer with the MW and MWD close to the calculated ones. The lengthwise temperature field of the reactor, which has a geometry designed according to the kinetic parameters of piperylene oligomerisation (**Equation 3.29**), varies under adiabatic conditions according to **Equation 3.25**:

$$T = T_0 + T_{\text{ad}} = T_0 + \frac{qC_{m0}\left(1 - \exp\left(-k_{ef}\tau_{\text{pass}}\right)\right)}{C_p\rho} \tag{3.38}$$

For piperylene oligomerisation, the relation for calculating the lengthwise temperature in the reaction zone L, with external heat removal, may be obtained:

$$T = T_0 + T_{\text{ad}} - (T_0 - T_{\text{cool}} + T_{\text{ad}})\left(1 - \exp\left(-\frac{L}{(R_d^{cr})^{0.8} w^{0.2} 1302.2}\right)\right) \tag{3.39}$$

For the catalytic systems which have been studied, the temperature rise in the reaction zone exceeds the maximum temperature allowable for piperylene oligomerisation (120 °C), even in the case of external heat removal (**Figure 3.5**). A decrease of the temperature, i.e., heat removal in the reaction zone due to external cooling, in the case of using $AlCl_3 \cdot O(C_6H_5)_2$ and $AlC_2H_5Cl_2$ as catalysts, when the reaction rate is high enough, is observed practically as soon as the chemical process has finished (**Figure 3.5**, curves 6 and 7). This defines a low efficiency of external heat removal upon using a volume reactor where the reaction zone does not reach the heat exchange surfaces. At the same time, a significant lowering of temperature in the reactor can be gained by using tubular turbulent reactors operating in a quasi-plug flow mode, in the case of piperylene oligomerisation in the presence of $AlCl_3 \cdot O(C_6H_5)_2$, due to a small reactor radius $R_d$ = 0.022 m (**Figure 3.5**, curve 6). Only in this case will fast piperylene oligomerisation processes, in a jet flow in the presence of corresponding catalysts and without additional mechanical stirring, proceed in the optimum mode.

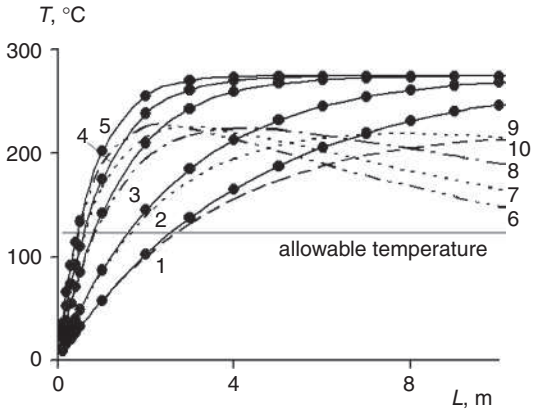


**Figure 3.5** Temperature in the reaction zone as a function of the length of tubular reactor in the case of piperylene oligomerisation under adiabatic conditions (1–5) and with external heat removal (6–10). Catalysts: $TiCl_4$ (1, 10), $TiCl_4$-$Al(i\text{-}C_4H_9)_3$ (2, 9), $AlC_2H_5Cl_2 \cdot O(C_6H_5)_2$ (3, 8), $AlC_2H_5Cl_2$ (4, 7), and $AlCl_3 \cdot O(C_6H_5)_2$ (5, 6). $T_0$ = 0 °C, $T_{cool}$ = 0 °C, $C_{m0}$ = 5.7 mol/l, $C_{cat}$ = 0.15 mol/l, and $R_d = R_d^{cr}$

Thus, differences in the kinetic parameters for the same chemical reaction occurring in the presence of catalysts differing in their activity, define the necessity of a variable approach to selecting a type and design of the main reactor. All other conditions being equal, the preference should probably be given to the more active catalytic system which allows high efficiency, energy- and resource-saving technologies, based on small-scale tubular turbulent reactors, to be developed. The possibility of the assured formation of the quasi-plug flow mode in turbulent flows in the reaction zone, as well as the use of the divergent-convergent design allows the problem of controlling

thermal conditions, in the case of piperylene polymerisation in the presence of $AlCl_3 \cdot O(C_6H_5)_2$, to be solved.

## 3.2 Polymer-analogous Transformations

The possibility of carrying out not only fast polymerisation processes in turbulent flows, but also polymer-analogous reactions of polymer modification [18, 20–22] was exemplified by butyl rubber (BR) chlorination in solution with molecular chlorine.

Halobutyl rubber is one of the BR species (chlorinated and brominated rubber) having the advantage of being able to be vulcanised with any type of rubber [23]. Due to this, the demand for halobutyl rubber is constantly growing, whereas the demand for BR has dropped. Halobutyl rubber is an excellent raw material for the tyre industry in the manufacture of tubeless tyres, high temperature and conveyor belts, and so on. [24]. Chlorinated rubber is generally produced on a commercial scale.

Macromolecules of chlorinated BR consist of fragments of isobutylene sequences (blocks) divided by the chlorine-containing isoprene units of various structures at random [8, 25]. BR chlorination results in a decrease of the total unsaturation of the macromolecules and particularly, the content of the internal C = C bonds, which is easily determined by split ozonolysis [26]. The reaction of BR chlorination proceeds as follows (**Figure 3.6**) [27, 28]:

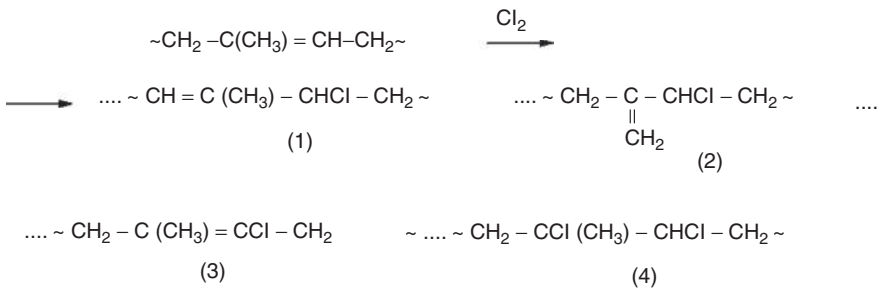


**Figure 3.6** BR chlorination reaction

Chlorinated BR macromolecules predominantly contain exomethylene groups [structure (2)], up to 90%. The content of endomethylene groups [structure (1)] is about 9%. Macromolecules may also include saturated groups [structure (4)], up to 1%, which are generally formed at low temperatures. The relative content of structures (2) to (1) defines the performance characteristics of chlorobutyl rubber particularly, the thermal load stability and processing stability. Before introducing one chlorine atom per one isoprene unit, in the case of chlorinating BR, an increase of the chlorine content in the polymer (linear relationship) is observed. BR contains up to 50 mol% of the added chlorine.

The chlorination of BR should be precisely monitored by the amount of chlorine atoms incorporated into the macromolecules. As one chlorine atom is introduced per C = C bond, the MW of a polymer decreases by not greater than 5–10%. If stronger chlorination occurs, a decrease in the C = C bond content in the macromolecules, as well as a high polymer degradation at the expense of the liquid products, is observed.

Less strict requirements can be imposed on the reaction temperature in the case of BR chlorination in solution because temperature variation in the reaction zone, in the range of 10–55 °C, has a slight effect on the preparation process and the quality of the chlorinated polymer produced. Above 55 °C, a fast degradation of chlorinated BR occurs.

Among the well-known methods of BR chlorination with molecular chlorine or chlorine-containing organic compounds, including in solution, water dispersion, and melt [8, 24, 25]; the most processable is chlorination with molecular chlorine in solution.

The process features are a highly viscous 10–15% solution of rubber (chlorobutyl rubber or BR) in an organic solvent (dynamic viscosity is about 0.3–0.6 Pa·s) and gaseous substances, namely the mixture of molecular chlorine and nitrogen (in a standard 1:6 – 1:5 ratio by volume), which is a characteristic of the process as the volume of the gaseous mixture is virtually 10 times greater than that of a highly viscous BR solution in an organic solvent. This requires specific attention while creating the optimum conditions of polymer chlorination in a liquid-gas system, including the fact that the fine bubble (foam) mode of stirring of the gas-viscous liquid flow is required in the reaction zone. Therefore, in order to make the BR chlorination process go faster in stirred tank reactors, a centrifugal pump is often used as an additional chlorination reactor, where the starting polymer solution is fed together with a chlorine-nitrogen mixture. To ensure the required residence time of the reaction mixture, recycling is necessary [26].

In view of the challenge to arrange a new continuous BR chlorination process, the principal issue is the numerical value of the characteristic time of a chemical reaction. According to [8], the time of chlorination in a temperature range of 17–52 °C is less than 60 s, but specifically in the case of a 15–16% BR solution chlorination in methylchloride (55 °C, molecular chlorine feed is 3–3.5 wt%) is 7.5 ± 2.5 s [25].

Close characteristic times of a chemical reaction also resulted from the experiments on producing chlorobutyl rubber by the reaction of BR with chlorine in a commercial 'Nefras' solvent within turbulent flows. Calculations of BR chlorination reactor geometry were performed according to the relationships of turbulent mixing in a self-similar mode of a highly viscous mixture flow. At a 0.21 $m^3$/h rate of feeding of the BR solution in a commercial 'Nefras' solvent, and a 2.1 $m^3$/h rate of feeding the

chlorine-nitrogen mixture (5:1 by volume) into a tubular reactor, the linear flow rate of reactants $V$, regardless of the volume taken by special packing, and the residence time $\tau_{pass} = L/V$ was found to be about 0.33 m/s and about 6.1 s respectively. Taking into account that no molecular chlorine breakthrough occurred after the reaction mixture had come out of the reactor, during plant operation, the chlorine conversion can be assumed to have been not less than 99% and the time of the chemical reaction $\tau_{chem}$ is comparable with the residence time $\tau_{pass}$ of the reaction mixture in the reactor.

Because of the low chemical reaction time ($\tau_{chem} \approx 6$ s), the process of liquid-phase BR chlorination with molecular chlorine in solution should be related to fast chemical reactions which have to be carried out according to fundamentally new technology using high efficiency, small-scale tubular turbulent jet reactors.

Pilot tests showed that BR chlorination, with molecular chlorine in solution, using a divergent-convergent-type tubular turbulent jet reactor as a chlorination reactor, resulted in a uniform distribution of gaseous chlorine throughout the reaction volume, ensuring stable composition of the polymer (**Table 3.3**). For example, the spread of chlorine content for chlorobutyl rubber produced in turbulent flows is not greater than 0.05 wt%. At the same time, for samples produced in stirred tank reactors *via* conventional technology this value reaches 0.14 wt%, i.e., the uniformity of chlorinated polymer samples increases practically by a factor of 3.

**Table 3.3 Elastomer halogenation in a turbulent mode**

| Elastomer | Halogenating agent | Halogen content (average value) | Halogen content spread, wt% | Mooney viscosity at 125 °C |
|---|---|---|---|---|
| BR | $Cl_2$ | 1.3 | 0.05 | 48 |
| BR | $Br_2$ | 1.9 | 0.05 | 46 |
| EPDM | $Cl_2$ | 1.5 | 0.08 | 38 |
| EPDM | $Br_2$ | 2.8 | 0.06 | 25 |
| BR* | $Cl_2$ | 1.2 | 0.14 | 46 |

*Halogenation was carried out in a column equipped with mechanical devices for creating turbulence in the reaction zone (a stirrer).

As seen from the results obtained (**Table 3.3**), the proposed method may also be used for bromobutyl rubber preparation. Moreover, other elastomers including copolymers of ethylene and propylene were halogenated in a turbulent mode.

Pilot tests showed that in spite of the high exothermicity of BR chlorination ($q$ = 184 kJ/mol), thermal conditions in the reaction zone did not create any problems, which has been confirmed by calculations. With both average heat capacity and density values of the reaction mixture being taken in the first approximation as equal to

those of the solvent, the adiabatic rise of the temperature in the reaction zone for a 23 kg/h pilot plant is:

$$\Delta T = q\Delta P / C_p \rho = 184 \times 1.6 / 0.17 \times 860 = 2^{\circ} \tag{3.40}$$

Thus, even in an adiabatic mode of tubular turbulent chlorination reactor operation (without heat removal), the temperature growth in the reaction zone in the case of BR chlorination (12–15% solution) with molecular chlorine in a tubular reactor, operating in the optimum plug-flow mode in turbulent flows, does not exceed 2 ± 1 °C. The process can be thought to proceed under quasi-isothermal conditions and does not require external or internal heat removal, or special stirring devices for heat and mass exchange intensification.

It should be pointed out that a jet-type tubular turbulent reactor of similar design, instead of stirred tank reactors with mechanical stirrers, can and should be used at other stages of the process of chlorinated BR production, in particular, for the neutralisation of the modified polymer solution (the rate constant of the interaction between mineral acids and alkalis is $k \approx 10^8$ l/mol·s), removal of salts and other substances from the chlorinated BR solution by water washing (extraction), removal of back solvent (extraction), and introduction of the stabiliser-antioxidant and adhesion reducing powder (mixing) into the polymer solution.

Thus, stages of BR chlorination in solution with molecular chlorine, neutralisation and washing of the polymerisate, as well as the introduction of the stabiliser into the polymer solution in chlorinated BR production, can be referred to as fast chemical and mass exchange physical processes to be carried out in turbulent flows. The possibility of using a self-similar mode in tubular turbulent reactors in relation to the viscosity, as well as revealed relationships of multiphase flows, allows the optimum design of reactors to be calculated for the development of a continuous energy- and resource-saving technology of chlorinated BR production. Moreover, the results obtained determine the possibility of using new technology not only for fast polymerisation processes, but also in the case of fast polymer-analogous reactions of polymer modification.

## 3.3 Reaction Mixture Formation *via* the Copolymerisation of Olefins and Dienes

The polymerisation process consists of a series of sequential stages with the main ones being initiation, propagation, and material chain termination. In order to produce a quality product it is necessary to provide optimum conditions for corresponding stages. These conditions include operation temperatures, pressure, concentrations of ingredients, and a sufficient degree of field uniformity for all characteristics. At the

same time, there are situations when the main chemical processes, in particular chain propagation stages, proceed slowly whereas the previous stages proceed rapidly [29]. Fast stages in a 'gross' process can either be the chemical reactions (initiation of the copolymerisation of olefins and dienes in the presence of Ziegler–Natta catalysts, formation of nucleation centres, and so on) or mass exchange physical reactions (saturation of a solvent with gaseous monomers in the case of the copolymerisation of ethylene and propylene, mixing of the monomer emulsion with the initiator in the case of the emulsion copolymerisation of butadiene and styrene, and so on). As stated previously, fast processes occur in the diffusion zone, which result in the nonuniform distribution of reaction mixture components at both micro- and macrolevels when chemical agents are fed directly into a stirred tank reactor. This defines the nonuniform composition of macromolecules, deterioration of the molecular characteristics of polymers obtained and, consequently, the loss of their quality.

Separation of fast (chemical or mass exchange physical) stages from the stage of copolymerisation of olefins and dienes in the presence of Ziegler–Natta catalytic systems proved to be reasonable. In this case, it was possible to ensure ideal (or almost ideal) conditions for carrying out the corresponding processes at each stage. For the first fast stage, it may be achieved using a turbulent divergent-convergent type prereactor, for the second slow stage a volume polymerisation reactor was used.

Taking into account the relationships of an increase in turbulence level in a divergent-convergent-type prereactor, the relation $\tau_{mix} \leq \tau_{chem}$ (for the fast stage of a chemical process) and $\tau_{mix} \leq \tau_{pass}$ (for the fast stage of a mass exchange physical process) are to be achieved. The separation of stages, in a multistage process, is exemplified by the copolymerisation of ethylene and propylene, as well as by the polymerisation of isoprene and butadiene in the presence of microheterogeneous Ziegler–Natta catalytic systems [30–36].

### 3.3.1 Synthesis of Ethylene and Propylene Copolymers

Studies on the optimisation of the physico-chemical processes of synthetic rubber production have been under consideration for many years. These investigations were initiated by the lack of agreement of results from the production scale and the level of existing machinery, the need to expand the range of rubber products, as well as imperfect technologies and, the most acute problem, the obsolete equipment of separate process stages. From this point of view, significant problems arise, particularly in developing a large-scale ethylene propylene rubbers (EPR) and ethylene propylene diene monomer (EPDM) rubber production because of the heterogeneity (the presence of liquid and gaseous phases) and complexity (ethylene, propylene, third monomer, hydrogen, catalyst, cocatalyst, and solvent) of the process.

Copolymerisation of ethylene and propylene is carried out using Ziegler–Natta catalysts in heavy hydrocarbon solvents or in liquid propylene: $CH_2 = CH_2 + CH_2 = CH\text{-}CH_3 \rightarrow - CH_2\text{-}CH_2\text{-}CH_2\text{-}CH(CH_3)\text{-}$.

Systems containing vanadium compounds ($VOCl_3$, $VCl_3$, $VCl_4$, and so on) and aluminium alkyls or aluminium halogenalkyls, such as triisobutylaluminum, diethylaluminium chloride, and ethylaluminium sesquichloride, found their practical application. No matter what catalytic system is used, the ethylene content in the copolymer is always higher than that in the starting mixture because of the relatively higher activity of this monomer during copolymerisation.

Dicyclopentadiene (DCPD) (I) or ethylidene norbornene (ENB) (II) are generally used as the third monomer, whereas hydrogen is used as the agent controlling the MW.

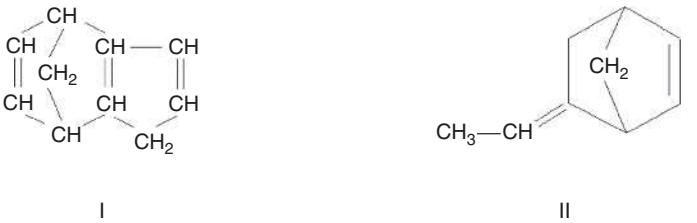


I II

**Figure 3.7** DCPD (I), and ENB (II)

The process of producing EPR rubbers in operating plants is normally carried out in a ~16 $m^3$ polymerisation reactor with vigorous mechanical stirring [25]. The reactor loading is 60% by height. Feeding of the reaction mixture components, directly into a large stirred tank reactor, cannot usually provide uniform saturation of the liquid products with monomers and hydrogen, which leads to broadening of the MWD of the polymer products obtained due to diffusion restrictions [37]. This is a result of performing the process in a two-phase system, with monomers being transported from a gaseous phase before reacting. Under real operating conditions, the phase equilibrium between the gas and liquid cannot be achieved at a polymer concentration of 8 to 14 wt%. This is due to the significant resistance to mass transfer in a liquid phase because of a high viscosity of the polymer solution opposing the catalysed EPR copolymerisation.

Like any other polymer, the EPR being produced in an uncontrolled process shows a nonuniform MWD. During copolymerisation, diffusion resistance affects the MWD of a polymer since the rate constant of hydrogen addition, used for MW control, is several orders less than the rate constants of the monomer copolymerisation. Ultimately, the monomer concentration to hydrogen ratios, change significantly through the

thickness of the diffusion boundary layer. As a result, the MW of the macromolecules formed at different points of the diffusion boundary layer throughout the reactor, differ significantly. Because of the high solution viscosity, a major part of a polymer is formed in the diffusion boundary layer, since its thickness grows as the viscosity increases, with the concentration of the two main monomers in the flow core being low. This factor substantially contributes to the MWD of the mean EPR. As the monomer copolymerisation rate constants are also significantly different, their concentration ratios through the thickness of the diffusion boundary layer also undergo significant variations. As a result, not only the MW but also the macromolecule compositions, prepared at different points of the reaction volume, differ.

Therefore, in the case of EPR production in particular, to improve the efficiency of the saturation of liquid products with monomers and hydrogen, it is necessary that the phase contact surface is maximised. Generally, it can be achieved by increasing the number of dispersion system elements (drops, bubbles) and by reducing their dimensions at a given dispersion phase volume. Therefore, it is advisable to use small-scale tubular turbulent divergent-convergent-type jet reactors in EPR production. In particular, tubular turbulent divergent-convergent-type reactors may be used at the stages of uniform liquid-gas mixture formation, with subsequent feeding of the mixture to large polymerisation reactors, run in parallel. In this case, the fast-slow stage separation technique is proposed, with the fast stage being the mass exchange physical process and the saturation of the solvent with the gaseous monomers, and the slow stage being the copolymerisation.

To estimate the efficiency of using tubular turbulent divergent-convergent-type reactors for the preparation of a uniform liquid-gas mixture with a developed phase contact surface, in the case of EPR production, it is advisable to study the quality of dispersion systems obtained in these types of reactors compared with stirred tank reactors.

Based on experimental data for stirred tank reactors, the following equations for calculating the mean diameter $d_{\text{disp}}$ of the dispersion phase particles in the mixing zone for the liquid-gas system were obtained [38]:

$$d_{\text{disp}} \approx 0.155 \times \left(\frac{\sigma}{\rho_1}\right)^{0.6} \times \left(\frac{\rho_1}{\rho_2}\right)^{0.2} \times \varepsilon_0^{-0.4} \tag{3.41}$$

$$\varepsilon_0 = \frac{N_g}{\rho_1 \times w_{\text{lg}}} \tag{3.42}$$

$$N_g = 0.706 \times \left(\frac{N_{\text{stir}}^2 \times n_{\text{stir}} \times d_{\text{stir}}^3}{G_2^{0.55}}\right)^{0.45} \tag{3.43}$$

Where:

$N_{stir}$ is the stirrer capacity consumed for stirring of a liquid

$n_{stir}$ is the rotary speed of a stirrer

$d_{stir}$ is the stirrer diameter

$G_2$ is the volume gas flow rate

$w_{lg}$ is the volume of the liquid-gas mixture in a reactor

$N_g$ is the stirrer capacity consumed for stirring of the liquid-gas mixture

In general, **Equation 3.32** truly represents the effect of stirring intensity on the dispersed phase size in the liquid-gas system. By order of value, the calculated values $d_{disp}$ are comparable with values calculated using an empirical equation [39]:

$$\frac{d_{disp}}{d_m} = (2.5\phi + 0.75) \times \left(\frac{\mathrm{Re}_c^2}{We_c}\right)^{-3/4} \times \left(\frac{\mu_1}{\sqrt{D\sigma\rho_1}}\right)^{1/2} \times \left(\frac{\mu_2}{\mu_1}\right)^{-0.4} \tag{3.44}$$

Where:

$D$ is the stirred tank reactor diameter

$\mathrm{Re}_c$ is the centrifugal Reynolds Number

$$\mathrm{Re}_c = \rho_1 n d_{stir} 2 / \mu \tag{3.45}$$

$We_c$ is the centrifugal Weber Number:

$$We_c = n_{stir}{}^2 d_{stir} \rho_1 / \sigma \tag{3.46}$$

At viscosity values $\mu_1$ = 0.001–0.0025 Pa·s of a continuous phase, a liquid in this case, the average gas content can be calculated by the equation [38]:

$$\phi = 0.33 \times \left(\frac{V'}{V_{flot}}\right)^{0.55} \times \left(\frac{N_g}{w_{lg}}\right)^{0.17} \times \left(\frac{V'}{V_{flot}}\right)^{-0.3} \tag{3.47}$$

Where $V'$ is the the reduced gas velocity.

It is assumed in the calculations that the gas bubble flotation rate $V_{flot}$ = 0.265 m/s.

The average diameter of the dispersed phase in the stirring area, calculated for the liquid-gas system according to **Equations 3.41** and **3.44**, was found to be 1.2 mm.

However, out of the stirring area, the average bubble diameter increases rapidly because of the decreasing degree of turbulence and, as a consequence, the fast coalescence of bubbles. The mean diameter of dispersed particles $d_{disp}$ in the peripheral part of a stirred tank reactor, for the liquid-gas system, can be calculated by the empirical relationship [80]:

$$d_{disp} = 4.15 \times \left( \frac{\sigma}{\rho_1} \right)^{0.6} \varepsilon_0^{-0.4} \phi^{0.5} + 0.0009 \tag{3.48}$$

In this area of a stirred tank reactor, the average bubble diameter significantly grows to be approxomately 8 mm.

Calculations show that the average dispersed particle size throughout the volume of the tubular turbulent reactor, intended for specific conditions of EPR (EPDM) commercial production, is about 0.127 mm, whereas in the case of using conventional stirred tank reactors, in bubbling mode, this value is 10-fold higher at 1.2 mm.

Thus, using small-scale tubular turbulent divergent-convergent-type reactors at the stage of uniform gas-liquid mixture formation, prior to feeding this mixture into a stirred tank polymerisation reactor, results in a notable (virtually by one order of magnitude) increase in the phase contact surface. A developed phase interface facilitates the uniform saturation of liquid products with monomers and hydrogen. In this case, it allows improved performance characteristics of the EPR in contrast to stirred tank reactors.

**Figure 3.6** shows the pressure relaxation time spectra for melts based on EPDM samples and DCPD derived under standard conditions, during the preparation of a gas-liquid mixture, in a tubular turbulent divergent-convergent-type reactor [33]. The method is based on using the experimental data of the pressure drop in the cylinder of the capillary viscosimeter, upon the nonstationary flow of the polymer melt in a capillary, after the piston has stopped (MPT Monsanto automatic capillary viscosimeter, capillary size $n$ = 1.5 mm, at 125 °C, and the starting shear rate of 3.6 $s^{-1}$) [40]. As it can be seen, this parameter for the copolymer obtained in the tubular turbulent reactor demonstrates a normal bell-shaped form, indicating rubber microuniformity.

Homogenisation of the flows entering the polymerisation reactor facilitates decreasing of the ethylene unit blockiness due to a (2.5-fold) decreasing content of the long units, with the content of the short units being retained, an increase of propylene unit blockiness also due to an increased content of long units, and an approximately 2-fold decreasing of the degree of macromolecule branching, and so on (**Table 3.4**).

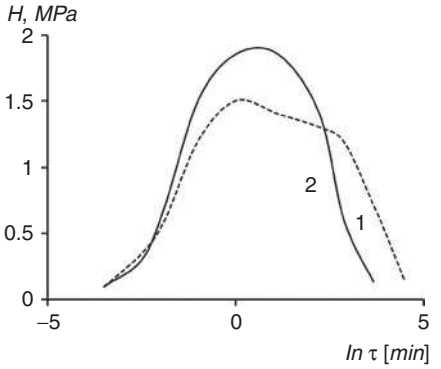


**Figure 3.8** Pressure relaxation time spectra of polymer melt based on a SKEPT-50 brand EPDM rubber and DCPD. 1 – standard preparation; and 2 – preparation of a gas-liquid mixture in a tubular turbulent reactor

**Table 3.4 Effect of turbulent stirring of gas-liquid flows on the composition of EPDM (ENB) macromolecules**

| EPDM molecular characteristics | Standard preparation | Preparation in a tubular turbulent reactor |
|---|---|---|
| Content of end vinyliden units, % | 0.29 | 0.19 |
| Content of long ethylene-based blocks, % | 0.17 | 0.06 |
| Content of short ethylene-based blocks, % | 1.1 | 0.9 |
| Long/short block ratio | 0.18 | 0.07 |
| Single propylene units, % | 0.35 | 0.028 |
| Fraction of propylene units in long blocks | 1.9 | 2.6 |
| Degree of macromolecule branching | 0.29 | 0.17 |

Moreover, step-by-step preparation of the liquid-gas mixture in tubular turbulent divergent-convergent-type reactors, as well as the mixture feed distribution for parallel polymerisation reactors, using a tubular turbulent spider-type distribution device, allowed copolymers with the same properties to be produced in different polymerisation reactors, run in parallel (**Table 3.5**).

| Table 3.5 Effect of homogeneous liquid-gas mixture feed distribution for polymerisation reactors run in parallel on EPDM rubber uniformity | | |
|---|---|---|
| **Liquid-gas mixture feed method** | **Polymerisation reactors run in parallel** | **Mooney viscosity** |
| Separate feeding | I<br>II | 49 ± 3<br>46 ± 1 |
| Feeding with tubular turbulent distribution device | I<br>II | 51 ± 1<br>51 ± 1 |

Thus, an increase in the degree of turbulence at the stage of stirring gaseous (ethylene, propylene, hydrogen, cycled gas) and liquid (solvent, DCPD or ENB) products during the production of EPR and EPDM (separation of fast and slow stages), ensures obtaining a copolymer with uniform composition.

A similar method of stage separation in a 'gross' process involving fast mass exchange physical processes in a tubular turbulent reactor was implemented for producing copolymers of butadiene and α-methylstyrene [2].

CKMC-30 APKM-15 brand rubber is produced by the continuous cold copolymerisation of butadiene and α-methylstyrene in an aqueous emulsion (5 °C, under atmospheric pressure), while a CKMC-30 50P brand rubber is produced by hot emulsion copolymerisation. At the stage of reaction mixture preparation, the emulsion containing a monomer, water and ingredients needed (emulsifier, and so on) is mixed with an aqueous cumene hydroperoxide solution together with an iron-trilon complex (initiating system), containing a rosin emulsifying agent. Due to insufficient mixing of the initiator, monomer and aqueous phase, which differ in density and viscosity, a nonuniform reaction mixture volume distribution of components takes place, which results in a copolymer with nonuniform composition.

The prepreparation stage of the reaction mixture, in a tubular turbulent reactor, leads to much greater efficiency of the mixing of flows with different densities, the formation of homogeneous fine emulsions, and substantially improved distribution of the initiator in emulsion droplets; as a consequence, a polymer fraction showing a wide variation range of the main quality characteristics (MW, MWD, and so on) decreases.

### *3.3.2 Synthesis of Stereoregular Polydienes*

Ziegler–Natta stereoregular polymerisation of α-olefins and dienes was discovered in 1954. This reaction opened opportunities for the synthesis of various stereoregular olefins and dienes. It occurs in the presence of catalytic systems, formed by organic

compounds of I-III Periodic Table group metals (aluminium is the most widely used in industry) and salts of groups IV-VIII transition metals, as well as lanthanides (the most widespread in industry are titanium chloride, vanadium, cobalt, and La-Lu metals).

Various metal complex systems of Ziegler type are widely applied within industry for the production of high-density polyethylene, isotactic polypropylene, 1,4-*cis*- and 1,4-*trans*-polymers of isoprene and 1,2-polybutadiene, and many other types of copolymers, such as ones based on ethylene and propylene, which could not be produced earlier based on traditional methods of synthesis.

Despite tremendous success in the development of scientific fundamentals for stereospecific polymerisation and the commercial production of stereoregular polymers, three key theoretical problems are still under discussion: a) the structure of AC; b) the mechanism of initiation and chain growth processes; and c) the reasons and factors responsible for the stereoregular products of $\alpha$-olefins and 1,3- diene polymerisation in the presence of Ziegler–Natta catalysts.

Stereospecific polymerisation of isoprene (2-methyl-butadiene-1,3) in the presence of *cis*-regulating catalytic Ziegler–Natta systems can be described by the following reaction:

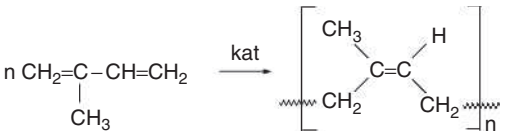


**Figure 3.9** Stereospecific polymerisation of isoprene (2-methyl-butadiene-1,3). The Russian industry has implemented technologies of *cis*-1,4-polyisoprene synthesis with Ti-Al Ziegler–Natta catalysts (synthetic *cis*-isoprene rubber SKI-3) and neodymium salts-based lanthanide catalysts SKI-5 grade synthetic rubber (TU 2294-051-16810126-96). SKI-3 rubbers contain up to 93 ± 1% of *cis*-1,4 links, while their content in SKI-5 grade rubber is 96 ± 1%

*In situ* catalyst preparation, variation of the catalytic system components ratio, its exposure time and so on, are known to exert a substantial influence on the polymerisation rate and molecular characteristics of synthesised polymers [13, 41]. Heterogeneity of Ziegler–Natta catalytic systems makes it possible to modify them using a hydrodynamic influence on the composition of the dispersed catalytic particles. The duration of the macrochain growth is known to be several orders of magnitude longer than the processes of AC formation (redox interaction of transition metal compounds with an aluminium-organic compound, surface structure formation, and so on). Therefore, a problem of modern interest is the development of a dienes

polymerisation process in the presence of Ziegler–Natta catalysts offering optimal conditions for constituent elementary stages: fast AC formation processes with intense mixing in a tubular turbulent prereactor and the growth of macrochains in a bulk device with a long pass time.

As Ziegler–Natta catalytic systems are microheterogeneous, it is necessary to analyse the motion characteristics of particles in a diffuser-confusor prereactor; such motion is accompanied by the formation of a separating effect [18]. According to literature data [13], pouring $TiCl_4$ and $Al(i\text{-}C_4H_9)_3$ solutions together results initially in the formation of thin flat rectangles with a $d_2$ average diameter of $(0.3–1)10^{-7}$ m. These particles, stored with the monomer, transform into secondary larger aggregates of about 30 micrometres in diameter. These values, taken for the size of catalyst dispersed inclusions, makes it possible to estimate the phase separation effect for the Ti-Al catalytic system in a reaction mixture passing through a tubular turbulent device. Calculations have shown, for isoprene polymerisation by a Ti-Al catalytic system (**Figure 3.10**), that an increase of catalyst particle diameter $d_{cat}$ and the linear flow rate $V_K$ of a reaction mixture, results in an increase of the relative difference between the volume fractions of the dispersed phase (catalyst) in the axial and peripheral zones of a device. However, heterogeneous catalyst particles are very small and thus the separating effect is insignificant $\Delta\alpha_2/\alpha_{2av} \sim 10^{-7}$.

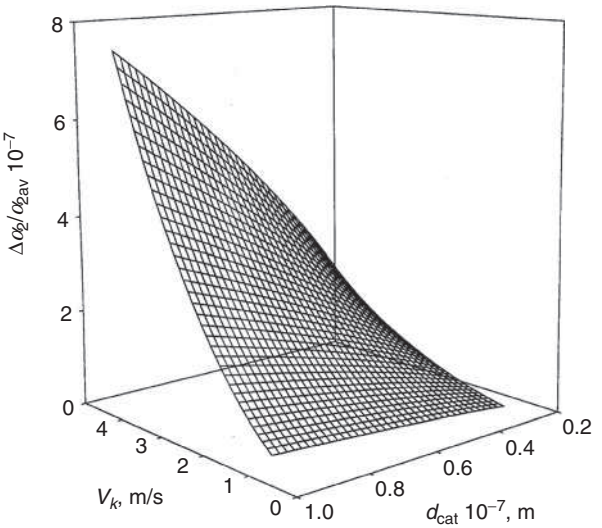


**Figure 3.10** Dependence of the relative difference $\Delta\alpha_2/\alpha_{2av}$ between $TiCl_4$-$Al(i\text{-}C_4H_9)_3$ catalyst volume fractions (isoprene polymerisation), in axial and peripheral zones of a tubular turbulent prereactor, on the particle diameter $d_{cat}$ and reaction mixture linear flow rate $V_K$. $\rho_1$ = 867 kg/m$^3$, $\rho_2$ = 2670 kg/m$^3$, and $\mu_1$ = 0.552 mPa·s

Thus, tubular turbulent diffuser-confusor prereactors provide a uniform distribution of catalyst particles in a reactor volume during the fast stages of macromolecule growth centre formation and the initiation reaction for the copolymerisation of olefins and dienes on microheterogeneous Ziegler–Natta catalysts. Equal conditions are provided in this case for the motion of all potential AC in a diffuser-confusor prereactor.

### *3.3.2.1 Modification of Microheterogeneous Ziegler–Natta Catalysts in the Turbulent Mode*

The cost price of synthetic products is determined by the cost of raw materials and energy consumption by the technological stage in a commercial production process. For example, the cost of residual catalyst extraction from a final product is about 30–40% of the total cost of a technological process. To make the production of polymers with catalytic technologies more profitable, reduction of expensive catalyst consumption is required. It will also reduce the overall cost as the process of catalyst removal from a polymer will become easier. It is demonstrated in [42], that the stereospecific isoprene polymerisation by Ziegler–Natta catalytic systems accelerates with mixing intensification, making it possible to reduce catalyst consumption. However, mechanical mixing alone is hardly sufficient for the creation of intense turbulent mixing in a reaction zone with highly viscous reactants. Small-sized tubular diffuser-confusor devices are a good alternative in this case as they are capable of forming a reaction mixture, in the processes of catalytic polymerisation of olefins and dienes, in conditions of intensive turbulent mixing.

The study of the influence of turbulent mixing on the modification of microheterogeneous Ziegler–Natta systems has been carried out in an experimental pulse-mode device (**Figure 3.11**), with a varied method of catalyst preparation. Isoprene polymerisation conversion curves have been obtained by gravimetric method.

Method 1: An additional reference experiment is carried out for each studied variant to model traditional process technology (initial reactants were fed into a reaction mixture, 4, without premixing in a prereactor, 3).

Method 2: The catalytic complex is prepared by the '*in situ*' method (two-component $TiCl_4$-Al(*i*-$C_4H_9)_3$ and three-component $TiCl_4$-Al(*i*-$C_4H_9)_3$-piperylene) and the solvent from tanks 1 and 2 (**Figure 3.8**) respectively, have been mixed in tubular turbulent device 3, at the minimal linear flow rate, in a diffuser of 0.5 m/s and the time of reactant passing through a reaction zone of 2–3 s (hydrodynamic impact on a catalytic system in the turbulent mode). The catalyst solution is then moved from device 3 to the vessel 4, where isoprene is then added and polymerisation is carried out.

Method 3: $TiCl_4$ and Al(*i*-$C_4H_9)_3$ solutions from 1 and 2 tanks respectively are moved from device 3 to vessel 4, where the resulting catalytic complex is kept for 30 min

at 0 °C, and a monomer is subsequently introduced (catalytic system formation in a turbulent mode).

Method 4: The solutions of preliminary prepared and matured catalytic complex and monomer in tanks 1 and 2 respectively, are mixed in device 3, and a reaction mixture is subsequently fed into device 4 (reaction mixture formation in a turbulent mode). Traditional conditions for isoprene polymerisation are provided in the volume device (flask) 4 with slow mixing by a magnetic stirrer (100 rpm). Tubular turbulent device 3 is a prereactor (**Figure 3.11**).

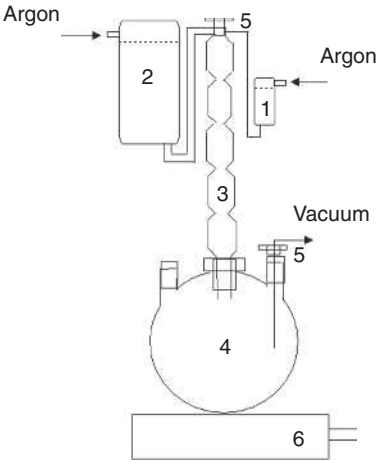


**Figure 3.11** An experimental device for isoprene polymerisation. 1 and 2) tanks for reactors; 3) tubular turbulent device; 4) vessel 500 $sm^3$; 5) three-way tap; and 6) magnetic stirrer

Variance analysis by gravity sedimentation has been carried out to estimate the quality of the resultant products after the preliminary hydrodynamic impact in a turbulent mode and in the reference experiment of microheterogeneous catalytic systems. Variance analysis data have been processed by the graphic differentiation of the precipitant accumulation curve. The results were used to determine the mass-averaged equivalent raduis r (the radius of a spherical particle with the same sedimentation rate) [35].

Preparation of a titanium-aluminium (Ti-Al) catalytic system without modifying diene additives (piperylene) results in the formation of relatively large catalyst particles (with an average radius of about 3–4 micrometres). The turbulent mode hydrodynamic impact on a two-component Ti-Al catalytic system does not influence the size of catalyst particles (and therefore its specific surface) compared with traditional process technology (**Figure 3.12,** curves 1 and 2). Preparation of Ti-Al with piperylene additives (three-component catalytic system) results in a decrease of the catalyst particles size to $r \approx 1.5$ micrometres

(**Figure 3.12,** curve 3). The hydrodynamic impact on a modified Ti-Al catalytic system, using piperylene additives in a turbulent mode, results in an additional decrease of catalyst particles size to $r \approx 1$ micrometre (**Figure 3.12,** curve 4). Catalyst formation with diene additives on the surface of the catalytically active precipitant would probably result in the growth of polypiperylene macrochains, which damages the morphological structure of a solid phase due to further grinding by the turbulent flow. The hydrodynamic impact on such precipitants, by a tubular turbulent prereactor, is equivalent to the grinding of Ziegler–Natta heterogeneous catalysts in polymerisation reactions.

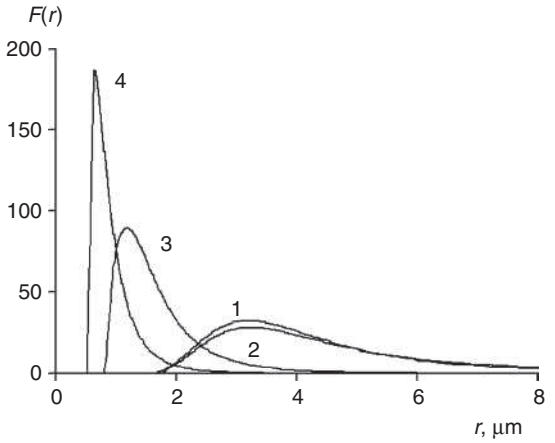


**Figure 3.12** Differential curves of radius $r$ distribution of $TiCl_4$-Al($i$-$C_4H_9)_3$ (1 and 2) and $TiCl_4$-Al($i$-$C_4H_9)_3$-piperylene (3 and 4) catalysts. 1 and 3 – traditional method; and 2 and 4 – hydrodynamic impact on catalyst particles in a turbulent mode (Method 2)

A similar dependency of catalyst dispersity can be observed in another microheterogeneous catalytic system based on the $VOCl_3$–Al($i$-$C_4H_9)_3$ compound, which is widely used in isoprene and butadiene polymerisation processes. A substantial change of particle size in a two-component (V-Al) catalytic system, and the hydrodynamic impact on a catalytic system in a turbulent mode, is not observed with traditional process technology. A substantial decrease of catalyst particle size is observed after modification of the V-Al catalyst using piperylene additives. The hydrodynamic impact on the modified catalytic system results in an additional reduction of catalyst particle size. In addition, the particle size distribution for the Ti-Al catalyst narrows as it does for the V-Al catalyst.

The size of V-Al particles in double catalytic systems is about 23% less than the size of the Ti-Al system particles (**Table 3.6**), all other things being equal. Ti-Al particle size in catalytic systems or catalysts modified using piperylene additives is 25%

less compared with the V-Al catalytic system. The modification of Ziegler–Natta microheterogeneous catalytic systems results in a decrease of catalyst particle size. Piperylene demonstrates altered dispersing properties upon the use of different transition metals in a catalytic system. For example, the size of Ti-Al catalyst particles decreases by almost 2-fold (for the traditional process method), while this value for the V-Al catalyst is only 26% [43].

Thus, modification using diene additives exerts a substantial influence on the dispersion characteristics of Ziegler–Natta microheterogeneous catalytic systems and therefore, on their activity. The effect is intensified by the preliminary hydrodynamic impact on an *in situ* prepared catalyst in a turbulent mode.

**Table 3.6 Modification of Ziegler–Natta microheterogeneous catalytic systems by piperylene additives in turbulent mode hydrodynamic impact conditions**

| Catalyst | The radius of catalyst particles | |
|---|---|---|
| | Traditional method | Hydrodynamic |
| $TiCl_4$–Al(*i*-$C_4H_9)_3$ | 3.5 | 3.5 |
| $TiCl_4$–Al(*i*-$C_4H_9)_3$- piperylene | 1.5 | 1.0 |
| $VOCl_3$–Al(*i*-$C_4H_9)_3$ | 2.7 | 2.7 |
| $VOCl_3$–Al(*i*-$C_4H_9)_3$- piperylene | 2.0 | 1.7 |

The aforementioned results on the modification of microheterogeneous Ziegler–Natta catalysts by the hydrodynamic impact on catalytically active particles, such as $TiCl_4$–Al(*i*-$C_4H_9)_3$ and $VOCl_3$–Al(*i*-$C_4H_9)_3$ catalysts, can be used for the polymerisation of dienes without the preliminary '*in situ*' preparation of catalysts. However, the *in situ* polymerisation method is also popular for the synthesis of stereoregular dienes. The catalytic system is in this case prepared in the reaction mixture itself by pouring its initial components together.

Interaction of the initial homogeneous components of Ziegler–Natta catalysts is fast and results in the formation of a solid phase (catalytically active particles).

$$TiCl_4 + AlR_3 \rightarrow TiCl_3\downarrow + AlR_2Cl$$

$$VOCl_3 + AlR_3 \rightarrow VCl_3\downarrow + Al(OR)R_2$$

These reactions are similar to the polycondensation method of dispersed system synthesis. The parameters of such systems are strongly influenced by the mixing efficiency during a reaction. Indeed, an increase of turbulent mixing intensity at the moment of V-Al catalyst formation, in a tubular turbulent device, results in a shift of the size distribution curve to lower values of particle size (**Figure 3.13**).

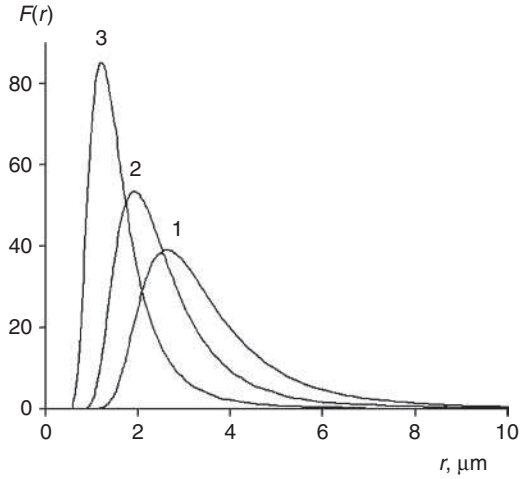


**Figure 3.13** Differential distribution curves of $VOCl_3$-Al($i$-$C_4H_9$)$_3$ (1, 2) and $VOCl_3$-Al($i$-$C_4H_9$)$_3$-piperylene (3) catalysts. 1, 3 – traditional method of catalyst synthesis, 2 – catalytic system formation in the turbulent mode (Method 3)

Obtained results provide vast opportunities for the modification of microheterogeneous Ziegler–Natta catalysts by changing their dispersion characteristics. This is achieved by turbulent mixing intensification both for synthesis (and *in situ* preparation method) and hydrodynamic impact on the preliminarily prepared and 'matured' catalyst ('separate' preparation).

The AC of stereospecific polymerisation are located on defects of the catalyst's crystalline structure; hence, the change of its dispersity (and therefore its specific surface) results in a respective change of the process rate.

### *3.3.2.2 Dienes Polymerisation Kinetics with Catalyst Formation in Turbulent Flows*

The hydrodynamic impact, on a separately prepared Ti-Al catalytic system, is almost negligible during isoprene polymerisation compared with a traditional process method (**Figure 3.11,** curves 1 and 2). The radius of catalyst particles is also unchanged (**Figure 3.12**) and so is the number of AC (**Table 3.7**). Catalyst activation can be carried out by the mixing of initial components directly in a tubular turbulent prereactor with subsequent maturing at 0 °C (Method 3) (**Figure 3.14,** curve 3). Dispersity analysis of the condensation-prepared suspensions demonstrates a reduction in the radius of the catalyst particles and an increase in the number of macromolecule growth centres (**Table 3.7**). Another shape of the conversion curves is observed during modification of the Ti-Al catalytic system by diene additives (piperylene). The introduction of a modified Ti-Al catalyst results in a substantial increase of the isoprene polymerisation

rate even in reference experiments (**Figure 3.14**, Curves 1 and 4), and is widely used in industry for the activation of Ziegler–Natta catalytic systems in dienes polymerisation processes. The hydrodynamic impact on a three-component catalytic system, during its mixture with a solvent in a turbulent mode (Method 2), favours a 10% increase of polymer product yield, compared with the reference experiment, in a polymerisation time of 1 h (**Figure 3.14**, Curve 5). Observed dependencies are also in correlation with the radius change of catalytically active precipitated particles and the concentration of AC (**Table 3.7**).

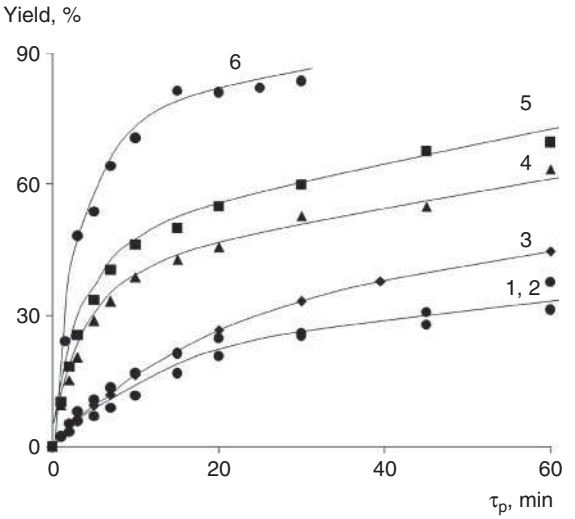


**Figure 3.14** Isoprene polymerisation in the presence of $TiCl_4$-Al(*i*-$C_4H_9)_3$ catalyst (1–3) and $TiCl_4$-Al(*i*-$C_4H_9)_3$-piperylene (4–6). Hydrodynamic impact on a catalytic system, in a turbulent mode (2, 5), catalyst formation (3) and reaction mixture (6); traditional method (1, 4). The concentration of titanium $C_{Ti}$ = 6 mmol/l, $C_M$ = 1.5 mol/l, Ti/Al/piperylene = 1/1.02/2, the catalyst is matured for 30 min at 0 °C

Experimental results demonstrate that an increase of the specific surface of the catalyst, in processes of stereospecific diene polymerisation (for example, isoprene polymerisation), is a good albeit, insufficient way to increase the process rate. A catalytic system obtains substantial activity when the catalyst and monomer solutions are mixed in a turbulent mode (Method 4) (**Figure 3.14**, Curve 6). In this case, there is the grinding process of catalyst particles (**Figure 3.12**, Curve 4) by the hydrodynamic impact, as well as its uniform distribution in a reaction mixture. In addition, the effect can be more substantial due to a decrease of the diffusion limitations for the addition of the first monomer molecule to the AC (fast initiation). A high polyisoprene (~80%) yield is, in this case, reached in around 20 min.

**Table 3.7 Isoprene polymerisation by $TiCl_4$-Al($i$-$C_4H_9)_3$ catalyst. $k_p$ is the chain growth reaction rate constant; $\sum C_a$ is the concentration of AC; $k_M^0$, $k_{Al}^0$ are chain-to-monomer and chain-to-aluminium-organic compound transfer reaction rate constants respectively, w is the initial polymerisation rate, method: 1) traditional, 2) hydrodynamic impact on a separately prepared catalytic system, 3) catalytic system formation in a turbulent mode, and 4) preliminary formation of a reaction mixture in a turbulent mode**

| Catalyst | Method | $w$, mol/l min | $k_p$, l/mol·min | $\sum C_a \times 10^5$, mol/l | $k_M^0$, l/mol·min | $k_{Al}^0$, l/mol·min |
|---|---|---|---|---|---|---|
| Ti-Al | 1 | 0.028 | 860 | 2.2 | 0.2 | 2.5 |
| | 2 | 0.029 | 840 | 2.3 | 0.2 | 1.4 |
| | 3 | 0.034 | 870 | 2.6 | 0.2 | 2.0 |
| Ti-Al-piperylene | 1 | 0.098 | 960 | 6.8 | 0.2 | 2.0 |
| | 2 | 0.120 | 1040 | 7.7 | 0.3 | 1.4 |
| | 4 | 0.190 | 1000 | 13 | 0.2 | 1.5 |

Similar change in the rate of stereospecific isoprene polymerisation by microheterogeneous Ziegler–Natta catalysts can also be observed for polyisoprene synthesis with a V-Al catalytic system (**Figure 3.15**).

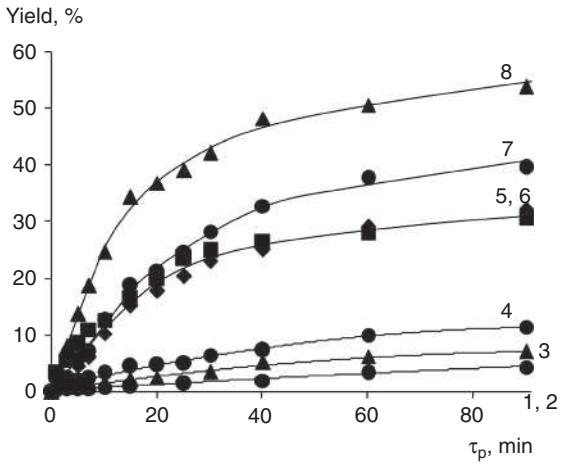


**Figure 3.15** Isoprene polymerisation in the presence of $VOCl_3$-Al($i$-$C_4H_9)_3$ (1–4) and $VOCl_3$-Al($i$-$C_4H_9)_3$-piperylene (5–8). Traditional process method (1, 5), catalytic system formation (3, 7) reactive mixture (4, 8) and hydrodynamic impact on catalyst particles (2, 6) in the turbulent mode. *V*/Al/piperylene = 1/2.4/5, $C_V$ = 6 mmol/l, $C_m$ = 1.5 mol/l, the catalyst is matured for 35 min at 0 °C

Therefore, the opportunity of preparing heterogeneous catalysts on the basis of $TiCl_4$-$Al(i\text{-}C_4H_9)_3$ and $VOCl_3$-$Al(i\text{-}C_4H_9)_3$, in a tubular diffuser-confusor prereactor operating in the turbulent mode, is a flexible way to control the isoprene polymerisation rate and reduce the catalyst consumption.

The fractional catalyst feeding and mixing rate have been studied in [42]. It has been shown that addition of a second and subsequent catalyst portions reduce the polymerisation rate, the reason is unsatisfactory mixing of the fresh monomer and catalyst portions in a viscous media. The authors demonstrated that the intensity of mixing in a reaction zone, at sufficiently high polymer concentrations (above 3 wt%), exerts a substantial influence on the polymerisation rate, which decreases at higher viscosities. Optimal catalyst-monomer mixing is required to achieve the maximum polymerisation rate, at least at the polymeriser input, where this effect can almost be achieved without a polymer. This circumstance is additional emphasis of the advantages of the installation of a tubular turbulent prereactor prior to a volume mixing device, with a long reactant pass time through the main stage (chain growth) of the reaction zone.

Altering the method of isoprene polymerisation in the presence of a Ti-Al catalyst, in particular, when a tubular turbulent prereactor is used, changes the kinetic parameters of the process (**Table 3.7**). Analysis of the change in the chain growth reaction rate constant reveals the fact that polymerisation conditions do not exert a substantial influence on this parameter, as observed $k_p$ changes are comparable to its determination error (~20%). In conditions of hydrodynamic impact for all the polymerisation methods, excluding the Ti-Al-piperylene catalytic system, (Method 2), $k_m^0$ does not change and its value is about 0.2 l/mol·min. Variation of the polymerisation method leads to the change of chain to $Al(i\text{-}C_4H_9)_3$ transfer reaction rate constant. Change from the traditional polymerisation method (Method 1) to a tubular turbulent prereactor (Methods 2–4) leads to a decrease of $k_{Al}^0$ in all the aforementioned cases.

Intensive initial mixing of a reaction mixture, in a tubular turbulent diffuser-confusor prereactor, leads to a change of the kinetic parameters of the butadiene polymerisation reaction with a $TiCl_4$-$Al(i\text{-}C_4H_9)_3$ catalyst. An increase of the mixing intensity of the reaction mixture, in a tubular turbulent prereactor, at the initial moment of polymerisation results in a higher butadiene yield (**Figure 3.16**). The chain growth reaction rate constant and AC concentration $C_a$ values have been analysed to explain this acceleration effect. Estimation methods are described in [41]. According to the calculations, an increase of the polymerisation rate is caused by a 1.7 times growth of AC concentration in the polymerisation system. The polymerisation method exerts practically no influence on the polymer chain growth reaction rate constant and the expected 4.6 times growth (not 1.7) of initial polymerisation rate is observed when a turbulent tubular prereactor is used. This effect can be explained by an AC concentration increase and a more uniform distrubution of microheterogeneous catalyst particles.

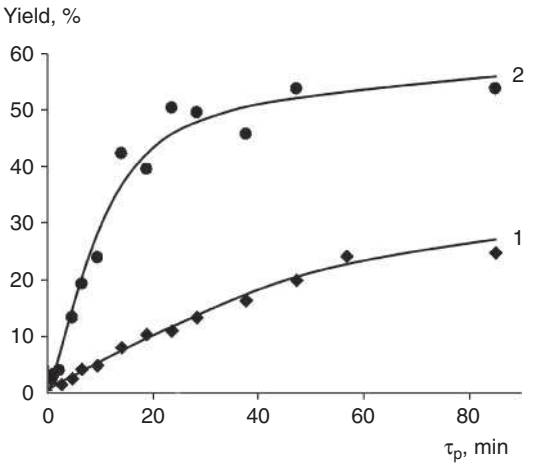


**Figure 3.16** Butadiene polymerisation conversion curves in the presence of a $TiCl_4$-$Al(i\text{-}C_4H_9)_3$ catalyst and traditional process method (1) and preliminary reaction mixture formation in a turbulent mode (2). Al/Ti = 1.8, $C_{Ti}$ = 5 mmol/l and $C_M$ = 1.5 mmol/l, catalyst is matured for 30 min at 0 °C

The change of reaction rate is well known to change with the intensity of mixing, indicating that elementary stages of the process are diffusion controlled. Preliminary turbulent mode mixing of a reaction mixture, for isoprene and butadiene polymerisation with a microheterogeneous titanium catalytic system, decreases the diffusion limitations when the surface structure of the catalyst is formed.

An increase of the AC concentration should result in the change of the average MW of polybutadiene according to the diene polymerisation kinetic chart; this assumption is confirmed by obtained experimental data.

### *3.3.2.3 The Influence of Preliminary Reaction Mixture Formation in the Turbulent Mode on Molecular Characteristics of Polydienes*

The change of polymerisation method exerts a substantial influence on the molecular characteristics of polyisoprene, synthesised in the presence of a $TiCl_4$-$Al(i\text{-}C_4H_9)_3$ catalyst, such as weight-average $M_w$ and number-average $M_n$ MW. The hydrodynamic impact (Method 2) on both two-component and three-component Ti-Al catalytic systems increases the $M_w$ (**Figure 3.17**) and $M_n$ (**Figure 3.18**). Similar changes of average MW can also be observed in the process of the catalytic system and reaction mixture formation, in a turbulent mode, when a tubular turbulent prereactor is used (Methods 3 and 4). The dependence of the polymer MW on the process method (such as preliminary turbulent mixing in a tubular prereactor at the formation stage of growth centres) is an additional way to control the molecular characteristics of polyisoprene.

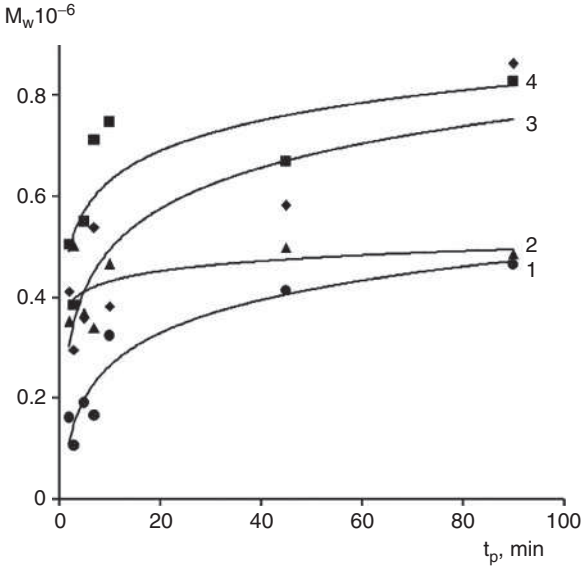


**Figure 3.17** The dependence of $M_w$ on isoprene polymerisation time in the presence of $TiCl_4$-Al($i$-$C_4H_9$)$_3$ (1, 3) and $TiCl_4$-Al($i$-$C_4H_9$)$_3$-piperylene (2, 4) catalytic systems. The traditional method (1, 2); and hydrodynamic impact on a catalytic system in the turbulent mode (3, 4)

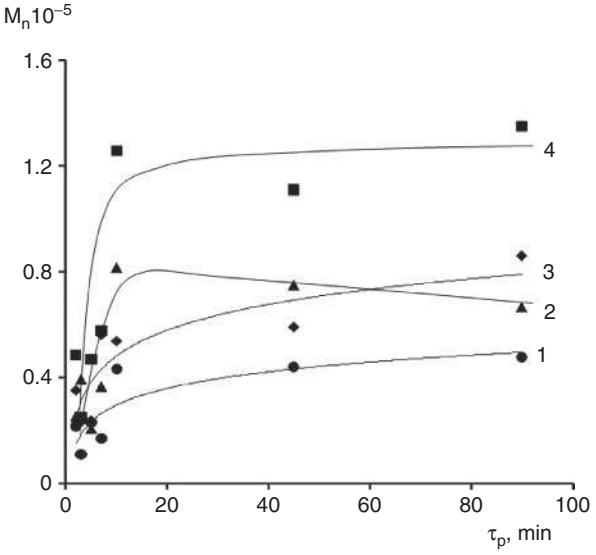


**Figure 3.18** The dependence of $M_n$ on isoprene polymerisation time in the presence of $TiCl_4$-Al($i$-$C_4H_9$)$_3$ (1, 3) and $TiCl_4$-Al($i$-$C_4H_9$)$_3$-piperylene (2, 4) catalytic systems. The traditional method (1, 2); and hydrodynamic impact on a catalytic system in the turbulent mode (3, 4)

One must note that the number of AC, $C_a$, increases in all studied cases, except in the hydrodynamic impact on a two-component Ti-Al catalytic system (**Table 3.7**). According to the process kinetic chart, it should decrease the average MW of *cis*-1,4-polyisoprene. A higher concentration of AC is observed in a reaction mixture forming in a turbulent mode (Method 4) (**Table 3.7**) than when a traditional polymerisation method is used (Method 1). It determines the fact that the average MW depends on the *cis*-1,4-polyisoprene yield, similar to the 'conversion' growth of MW (**Figure 3.16**). The polymer MW is seen to be practically identical for different polymerisation methods. The growth of AC concentration and respective polymerisation rate increase is not so considerable for other methods (Methods 2 and 3) using the tubular turbulent prereactor. Therefore, MW growth is observed in comparison with the traditional polymerisation method at comparable monomer conversions; it is a result of the prevailing influence of turbulent mixing. A general explanation of the higher MW of *cis*-1,4-polyisoprene, when a tubular turbulent prereactor is used, is a decrease of the chain to $Al(i\text{-}C_4H_9)_3$ transfer reaction rate constant (**Table 3.7**).

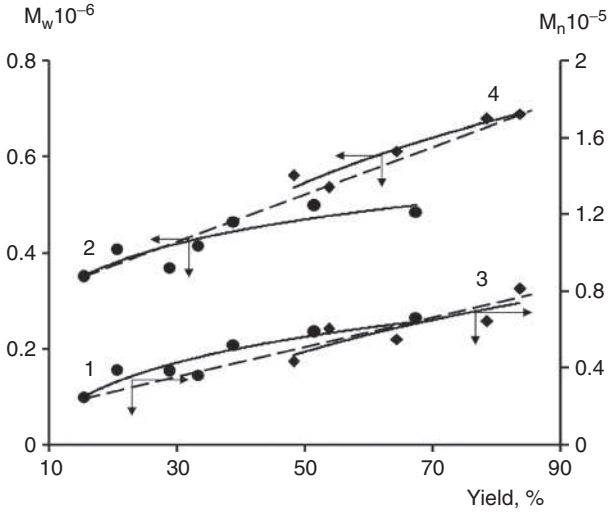


**Figure 3.19** Decrease of the number-average $M_n$ (1, 3) and weight-average MW (2, 4) MW of *cis*-1,4-polyisoprene with the $TiCl_4$-$Al(i\text{-}C_4H_9)_3$-piperylene catalyst. 1, 2 – the traditional method; and 3, 4 – reaction mixture formation in the turbulent mode

Changing the isoprene polymerisation method, in the presence of a titanium catalyst, exerts a different influence on the width of the MWD. The hydrodynamic impact on the double Ti-Al catalytic system, in the turbulent mode, results in the formation of

a polymer with a wider MWD than in traditional polymerisation processes. A similar MWD change is observed for the formation of a reaction mixture in the turbulent mode. However, the turbulent mode hydrodynamic impact on the diene modified Ti-Al catalytic system, leads to the formation of a polymer with a narrow MWD. The narrowest possible MWD of *cis*-1,4-polyisoprene is achieved in conditions of Ti-Al formation in a turbulent mode (**Figure 3.20**), when the initial homogeneous components ($TiCl_4$ and $Al(i\text{-}C_4H_9)_3$) interact in a tubular prereactor. It is determined by a higher number-average MW.

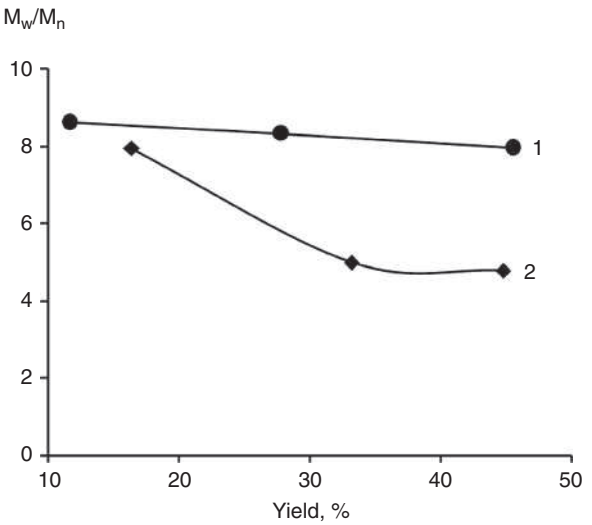


**Figure 3.20** Dependence of the $M_w/M_n$ during isoprene polymerisation in the presence of $TiCl_4$-$Al(i\text{-}C_4H_9)_3$-piperylene catalyst. 1 – the traditional method (Method 1); and 2 – catalytic system formation in turbulent streams (Method 3)

Preliminary formation of the reaction mixture for butadiene polymerisation, in the presence of $TiCl_4$-$Al(i\text{-}C_4H_9)$ catalysts in the turbulent mode, results in a substantial decrease of the weight-average MW (**Figure 3.21**). A slight change of the number-average MW will lead, in this case, to a polymer product with a narrow MWD (**Figure 3.22**). Products of the traditional polymerisation method provide multimodal MWD curves. The monomer conversion increase initiates their shift to the higher MW area without substantial changes of distribution width. A polymer with a monomodal MWD and MWD curves shifted in the low molecular area, with conversion growth, can be synthesised under the conditions of hydrodynamic impact on a reaction mixture in turbulent flows.

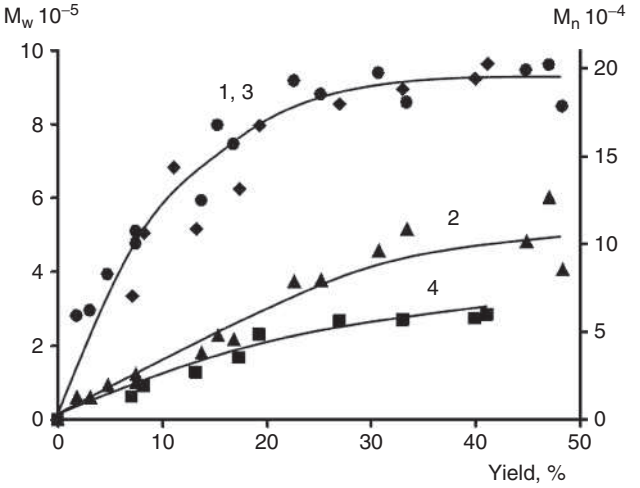


**Figure 3.21** Dependence of the weight-average $M_w$ (1, 2) and number-average $M_n$ (3, 4) MW on polybutadiene yield in the presence of the $TiCl_4$-Al(*i*-$C_4H_9)_3$ catalyst. Traditional method (1, 3),and preliminary formation of a reaction mixture in turbulent flows – 2, 4

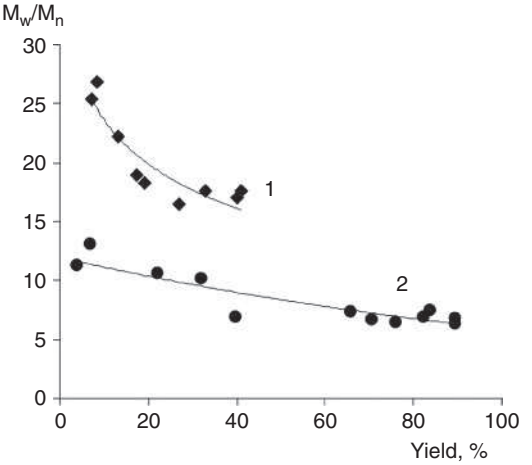


**Figure 3.22** Dependence of the polydispersity index $M_w/M_n$ on polybutadiene yield in the presence of a $TiCl_4$-Al(*i*-$C_4H_9)_3$ catalyst. Traditional method – 1, and preliminary formation of a reaction mixture in turbulent flows – 2

A substantial increase of the polymerisation rate of dienes, in the presence of Ziegler–Natta microheterogeneous catalysts, is an opportunity to decrease the consumption of the expensive catalyst and control the molecular characteristics of the polymer

products. In particular, butadiene polymerisation in the presence of a titanium catalyst with the initial rate of 0.0175 mol/l·min is obtained at a catalyst concentration of $C_{Ti}$ = 5 mmol/l. Turbulent prereactor technology provides a 1.7 times reduction of catalytic complex consumption (the rate of AC concentration increases). Redistribution of the type of AC leads to a polymer product with the same high weight-average MW and higher catalyst concentration ($C_{Ti}$ = 5 mmol/l) (**Figure 3.23**). The effect of a decrease of the polybutadiene polydispersity index, with a decrease of catalyst concentration, can be explained by a higher number-average MW when the reaction mixture is formed in the turbulent mode.

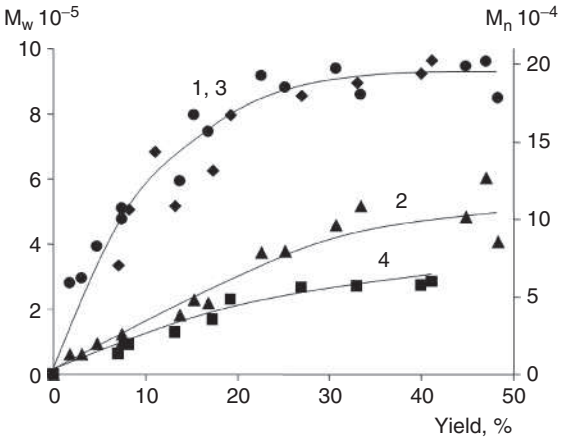


**Figure 3.23** Conversion change of weight-average (1, 3) and number-average (2, 4) MW of polybutadiene in the presence of a $TiCl_4$-Al($i$-$C_4H_9$)$_3$ catalyst. The traditional method ($C_{Ti}$ – 5 mmol/l – 1, 4); and preliminary formation of a reaction mixture in a turbulent mode ($C_{Ti}$ – 3 mmol/l – 2, 3)

SKI-3 grade synthetic isoprene rubber is largely produced on titanium-aluminium Ziegler–Natta catalysts. Its main application areas are the production of tyres, transporter belts, industrial and medical goods. Performance characteristics of *cis*-1,4-polyisoprene-based products and their applications are mainly determined by the molecular characteristics of the macrochains. These characteristics include, in particular, the content of the insoluble fraction (gel fraction) in a polymer, which reaches the value of 10–20% [44]. A decrease of the insoluble fraction content in *cis*-1,4-polyisoprene provides rubber blends capable of processability by moulding, while SKI-3 rubbers with a low gel-fraction content are more adhesive and less shrinkable.

It is assumed in [45, 46] that the insoluble polyisoprene fraction is not a crosslinked polymer with transversal bonds, but that it is a conglomerate of separate macromolecules. Polymer chain growth leads to either the moving of a macromolecule

into solution (depending on the thermodynamic properties of the polymer-solvent system), sinking in the solvent or partially remains at the catalyst surface (due to sorption) with the emergence of the so-called polymer-catalyst particle. If the size of catalyst particles is small enough, and the number of growing macromolecules is high enough, the high surface density of polymer chain ends is achieved and the crosslinking reaction becomes increasingly possible.

It is demonstrated in [47] that gel fraction formation in the stereospecific process of diene polymerisation in the presence of Ziegler–Natta catalysts is caused by secondary cationic processes, which occur near the solid surface of the catalyst and involve the polymer chain. The most probable reactions are the intramolecular interaction between the double bonds in a grown polymer chain; it is confirmed by the high activity of various catalysts (such as, $TiCl_4$-$AlR_3$ and so on) in the cationic reactions of the opening of isolated dienes. The direction of these reactions depends on the concentration of the polymer molecules: the reaction is intramolecular at small concentrations due to the partial cyclisation of a macromolecule; whereas, high concentrations lead to simultaneous cyclisation and random crosslinking of various macromolecules. Star-shaped olymers and statistically branched cluster structures are formed in the second case. Their existence is no longer limited by the presence of the initial catalyst core.

If the concentration of particles in a solution is small and the average distance between particles exceeds the average square root distance between the ends of the forming macromolecules, then only the initial polymer-catalyst particles exist during the polymerisation process [45]. If the size of the macromolecule is comparable to the distance between the particles, there is a probability of the free macromolecule end hitting another catalyst particle and binding with macromolecules grown on that particle. Secondary polymer-catalyst star-shaped particles form in this case. Formation of a distinct amount of macromolecules with high MW (300,000) occurs from the very beginning of polymerisation and is parallel to the process of the dispersion of the catalyst particles. Therefore, the probability of catalyst particles binding at the stage of dispersion is rather high as they are close to each other, leading to the formation of a crosslinked polymer. It is important to decrease the MW of the forming macromolecules at this stage to avoid binding of the catalyst particles.

Installation of a tubular turbulent prereactor before the volume polymerisation device leads to a change of the heterogeneous catalyst dispersity (such as a decrease of the size of catalytically active precipitant particles) in the process of $TiCl_4$-$Al(i\text{-}C_4H_9)_3$ polymerisation with a long pass time of reactants. This makes it possible to change the content of the insoluble fraction in *cis*-1,4-polyisoprene, develop a method to decrease the gel-fraction content in isoprene rubber, and increase the performance characteristics of respective products.

The catalyst deactivation method in [48] included the intensive mechanical impact both on a polymer solution and on a reaction mixture in a high molecular compound precipitation process. The physical 'gel' is destroyed in this case and the results of the insoluble *cis*-1,4-polyisoprene fraction analysis indicates the gel-fraction content is formed by chemically crosslinked molecules (a chemical 'gel'). This effect is confirmed by the data of the insoluble fraction content in polyisoprene, which has been synthesised using different methods (**Figure 3.24**). The results of dynamic and static measurements of the insoluble fraction content are comparable, thus indicating, the formation of chemically linked branched structures.

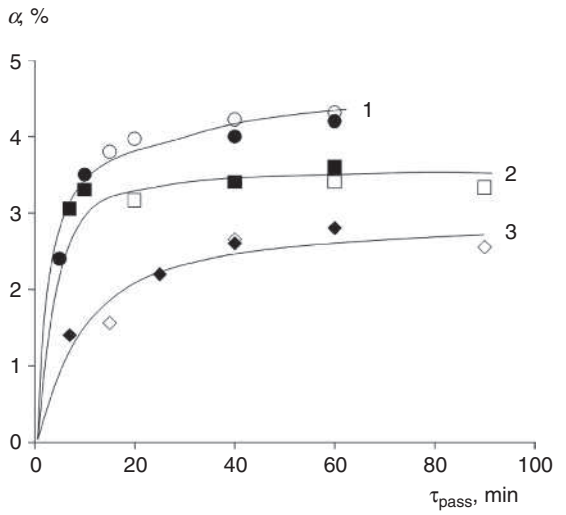


**Figure 3.24** Content of the insoluble α fraction in polyisoprene synthesised in the presence of the $VOCl_3$-Al($i$-$C_4H_9)_3$-piperylene catalyst. Traditional method (1), reaction mixture (2), and catalytic system (3) formation in a turbulent mode determined in static (●■◆) and dynamic modes (○□◇)

The polymer yield increase is caused by the growth of the insoluble fraction content in *cis*-1,4-polyisoprene (**Figure 3.25**). The hydrodynamic impact on the $TiCl_4$-Al($i$-$C_4H_9)_3$ catalyst particles in the turbulent mode (**Figure 3.25**, curve 2) results in a smaller decrease of the gel-fraction content in the polymer, compared with the traditional method (curve 1). The minimal amount of insoluble fraction in *cis*-1,4-polyisoprene is observed in the presence of the double $TiCl_4$-Al($i$-$C_4H_9)_3$ catalytic system, formed in the turbulent mode (**Figure 3.25**, curve 3). A catalytically active precipitant is formed in the tubular turbulent prereactor in the fast interaction of the initial homogeneous components. Modification of the $TiCl_4$-Al($i$-$C_4H_9)_3$ catalyst by diene additives (piperylene) leads to a decrease of the gel-fraction content, in similar polymerisation conditions, and polymer yield amount (**Figure 3.25**, curves 1 and 4;

2 and 5). In addition, the hydrodynamic impact on the modified catalytic system, in a turbulent mode, is more effective for the decrease of the gel-fraction content than the unmodified catalyst.

Depending on the polymerisation method employed, such as the installation of a tubular turbulent prereactor, it is possible to modify the MW of *cis*-1,4-polyisoprene, the number of macromolecule growth centres, and the polymerisation rate. The parameter, which explains these process characteristics, is the number of macrochains per active centre. Therefore, it is reasonable to estimate the correlation between the insoluble fraction content in the polymer with the number of macromolecules per active centre.

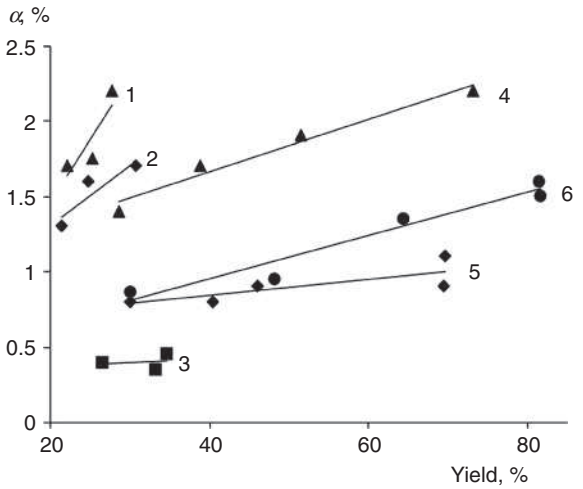


**Figure 3.25** Dependence of the gel-fraction α content on the *cis*-1,4-polyisoprene yield in the presence of $TiCl_4$-Al(*i*-$C_4H_9)_3$ (1–3) and $TiCl_4$-Al(*i*-$C_4H_9)_3$-piperylene catalysts (4–6). Traditional method (Method 1) (1, 4), hydrodynamic impact on the catalyst particles (Method 2) (2, 5), formation of the catalytic system (Method 3) (3) and reaction mixture (Method 4) (6) in the turbulent mode (Ti/Al/piperylene = 1/1.25/2 (molar)), toluene is used as the solvent, $C_{Ti}$ = 6 mmol/l, $C_M$ = 1.5 mol/l, 25 °C

The number of polymer chains in a reaction mixture ($N_{pol}$) is calculated in the following equation:

$$N_{pol} = \frac{C_m U}{P_n} \tag{3.49}$$

Where:

$C_m$ is the initial concentration of a monomer.

$U$ is the polymer yield.

$P_n$ is the number-average degree of polymerisation.

The number of polymer chains per active centre ($n_{AC}$) is therefore calculated by the following ratio:

$$n_{AC} = \frac{C_m U}{P_n C_a} \tag{3.50}$$

Where $C_a$ is the concentration of active centres.

In accordance with **Equation 3.38**, the increase of polymer yield leads to the growth of macrochain number and therefore, to a higher probability of secondary processes, such as crosslinking reactions. It finally leads to the experimentally proven effect of a polymer synthesised containing a high gel-fraction content (**Figure 3.25**). Generalisation of the insoluble fraction content data in *cis*-1,4-polyisoprene has been carried out for double $TiCl_4$-Al(*i*-$C_4H_9)_3$ and modified $TiCl_4$-Al(*i*-$C_4H_9)_3$-piperylene catalytic systems, and different polymerisation methods. It has revealed a correlation between the characteristics of this polymer and the number of macrochains per active centre, *n* (**Figure 3.26**).

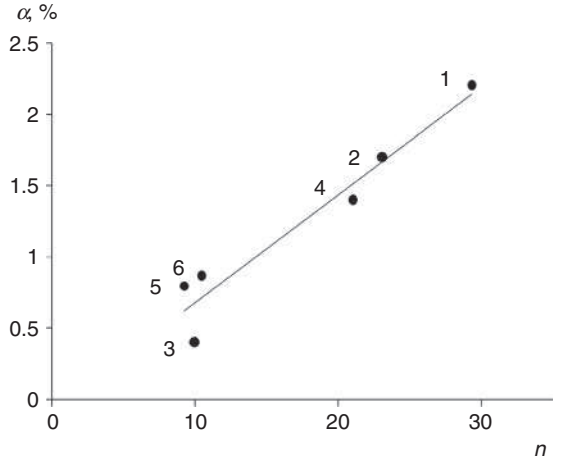


**Figure 3.26** Dependence of the gel-fraction α content in *cis*-1,4-polyisoprene on the number of macromolecules per active centre, n, during the polymerisation process in the presence of $TiCl_4$-Al(*i*-$C_4H_9)_3$ (1–3) and $TiCl_4$-Al(*i*-$C_4H_9)_3$-piperylene (4–6) catalysts. Traditional method (Method 1) (1, 4), hydrodynamic impact on catalyst particles (Method 2) (2, 5), formation of the catalytic system (Method 3) (3), and reaction mixture (Method 4) (6) in the turbulent mode (polymer yield is 30%)

The AC of the stereospecific isoprene polymerisation in the presence of $TiCl_4$ and Al(*i*-$C_4H_9)_3$ catalysts are known to be located on the crystal lattice defects, $\beta$-$TiCl_3$. According to **Equation 3.39**, it creates a correlation between the insoluble fraction

content in a polymer with the heterogeneous catalyst particle radius, as confirmed by the sedimentation analysis data (**Figure 3.27**). A decrease of the heterogeneous catalyst particle radius leads to a decrease of the insoluble fraction content in the *cis*-1,4-polyisoprene. In turn, the catalyst particle size and the content of the insoluble fraction of the polymer (according to **Figure 3.27**) can be controlled both by catalytic system modification, using diene additives, and by the formation of a $TiCl_4$-$Al(i\text{-}C_4H_9)_3$ catalyst in a turbulent mode. As **Figure 3.26** demonstrates, the minimal number of macrochains per active centre and the required gel-fraction content is achieved in the catalytic system formed in a turbulent mode, when the fast chemical reaction occurs and a finely dispersed catalytically active precipitant is formed. Obviously, further decrease of the catalyst particle size (**Figure 3.27**) will lead to a decrease of the insoluble fraction content in *cis*-1,4-polyisoprene. This fact is confirmed by the absence of the gel fraction in a polymer synthesised on pseudohomogeneous lanthanide catalysts.

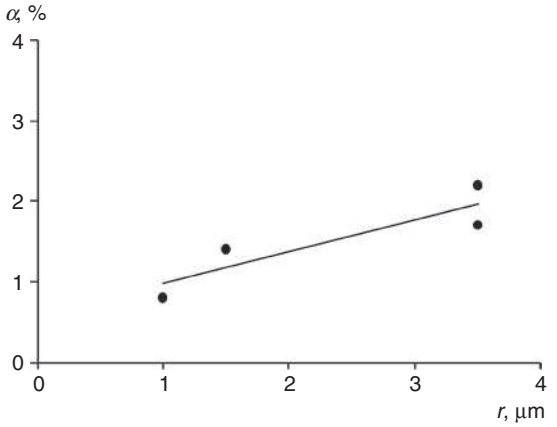


**Figure 3.27** The dependence of gel-fraction $\alpha$ content on the radius, $r$, of titanium-aluminium catalyst particles

It is obvious that the revealed dependence (**Figure 3.27**) can be explained by the effect of the catalyst particle size decrease, when the polymer shell on their surface becomes close to the monomolecular adsorption layer. There is less probability of a cationic reaction between the internal double bonds of neighbouring macromolecules on a solid catalyst surface, which leads to the formation of crosslinked structures. This fact is confirmed by results in [45, 46]: the smaller the size of the catalyst particle, the bigger the polymer shell becomes (the thickness of the adsorption layer in a monomolecular layer is similar to the length of a macromolecule). Growing molecules on these particles are linked with the surface of the heterogeneous catalyst by one chain end. Revealed behaviour of the gel fraction, formed by linked macromolecules (a chemical 'gel'), will evidently be valid for the insoluble fraction of the chemically bound macrochains (physical 'gel').

Formation of the $TiCl_4$-Al($i$-$C_4H_9)_3$ catalyst in the turbulent mode (excluding Method 3) does not change the polyisoprene microstructure (**Table 3.8**). A highly stereoregular polymer is formed in all cases. Isoprene polymerisation in the tubular turbulent prereactor, in the presence of the Ti-Al catalyst, leads to the formation of the polymer with an increased content of *cis*-1,4-links, (up to 96.8%) and a lower content of 1,4-*trans* and 3,4-links (1.7% and 1.5%, respectively).

Modern theoretical concepts of the polymerisation of dienes on Ziegler–Natta catalysts are based on the principle of their inherent polycentrism [49]. Substantial changes in the MW characteristics of polyisoprene and polybutadiene, due to the formation of a microheterogeneous titanium catalyst in the turbulent mode, make it reasonable to analyse the distribution of macromolecular growth centres on their kinetic activity.

**Table 3.8 The microstructure of polyisoprene synthesised with a Ti-Al catalyst**

| Catalyst | Polymerisation method | The content of links, % | | |
|---|---|---|---|---|
| | | 1,4-*cis* | 1,4-*trans* | 3,4 |
| Ti-Al | 1 | 94.9 | 3.2 | 1.9 |
| | 2 | 94.0 | 4.2 | 1.8 |
| | 3 | 96.8 | 1.7 | 1.5 |
| Ti-Al-piperylene | 1 | 94.8 | 3.3 | 1.9 |
| | 2 | 95.6 | 2.9 | 1.5 |
| | 4 | 94.4 | 4.0 | 1.6 |

### *3.3.2.4 Polycentrism of Catalytic Systems in Polymerisation Processes*

A key problem of the catalytic polymerisation theory is known to be that of the AC structure. Experimental studies and theoretical developments in the ionic and ionic-coordination polymerisation of unsaturated compounds revealed a considerable amount of new information about the nature of AC, for example [50–53]. The most important concept is the polycentrism of catalytic systems as this problem is currently becoming much more important [49]. Researches have advanced from single examples of active centre types, in some catalytic systems, to an awareness of the fact that in some rare cases, the catalytic system can be considered to include only one type of active centre.

There are several references to the confirmation of several types of AC existing on the surface of heterogeneous catalytic systems and having different stereospecificity [54–56]. Such a conclusion has been made from the study of polymerisation kinetic

aspects, change of the MW and MWD, stereoregularity and composite inhomogeneity of synthesised polymers [1, 13, 41]. These studies are mainly dedicated to the polymerisation of olefins on heterogeneous catalytic systems.

Heterogeneous catalytic systems, microheterogeneous and especially homogeneous catalysts do not provide clear evidence for several types of AC. However, the majority of theses assuming polycentrism of heterogeneous catalysts are applicable for these cases too, as they provide the same reasons for several types of AC to appear [57].

Revealing several types of AC, obtaining the functions of their distribution on kinetic inhomogeneity and stereospecificity, determining the number and kinetic parameters for each type of active centre, for specific polymerisation systems, will provide opportunities for more advanced theoretical understanding of ionic and ionic-coordination polymerisation mechanisms. In addition, this approach allows optimisation of the polymerisation processes to synthesise polymers with tailored molecular characteristics (microstructure, MW, MWD, and so on).

The present generalised understanding of the phenomena of the existence of several types of AC is provided in [49], revealing general regularities and specific peculiarities of the polycentrism in ionic and ionic-coordination polymerisation of unsaturated compounds.

First of all, it is necessary to determine the reasons for the inhomogeneity of the catalytic system in the ionic and ionic-coordination polymerisation of unsaturated compounds.

*Crystal lattice defects and the degree of dispersed distribution of particles in heterogeneous catalytic systems*: The presence of several types of AC in heterogeneous catalytic systems is first of all in good agreement with the concept that any solid surface cannot be equipotential [58]. In the heterogeneous polymerisation process with an ionic and ionic-coordination mechanism, the polymer chain is linked with the transition metal atom on the catalyst surface and the chain growth process is provided by penetration of the monomer molecules between the metal atom and growing polymer chain [59]. That is why the presence of defects on a crystal lattice and catalyst surface roughness cannot contribute to the complex kinetic activity of a catalyst.

Any heterogeneous catalytic system has a specific distribution of catalyst particles according to the degree of dispersity. Polymerisation systems for isoprene polymerisation in the presence of $MgH_2/TiC1_4$-$Al(C_2H_5)_3$, studied in [45], consisted of individual macromolecules and macromolecules linked with catalytic particles of a various size. In addition, the dispersity of the catalyst changed during polymerisation;

the polyisoprene had a broader MWD in the initial period of polymerisation. According to the authors, this effect was caused by various types of AC on the surface of big and small catalyst particles. The increased quantity of polymerised monomer led to an additional dispersing of the polymer-catalyst particles and levelling of the differences in their size; as a result, the polyisoprene MWD narrowed.

The growth of Ziegler–Natta catalyst activity with an increased specific surface of the $\delta$-$VCl_3$ component is mentioned in [60]. This effect was achieved by additional grinding on a ball mill.

The analysis of ethylene polymerisation peculiarities on the $MgH_2/TiC1_4$-$Al(C_2H_5)_3$ catalytic system [61] has revealed that the catalyst is the most active at a lower titanium content and larger specific surface of the catalyst (an increase of the polymerisation rate, AC concentration, and polymer yield is observed). An increase of the catalyst surface area leads to a decrease of the number of AC and therefore, to a substantial drop of catalyst activity. Hence, the authors emphasise that there is a correlation between the catalyst surface area, its activity, and the concentration of AC. However, a twofold drop of titanium content and surface area will result in almost tenfold drop of catalyst activity. According to the authors, this is an indication of an existing high number of active centres, which are the first to degrade, and centres which are incapable of fast polymerisation.

*Complex composition of catalytic systems*: Many real catalytic systems are complex. An ionic polymerisation process may form the following equilibrium structures in catalytic systems: two contact ionic pairs, solvent-separated ionic pairs, free ions, and aggregated particles. The presence of AC, of various reactivities, will influence the molecular characteristics of the forming polymers, especially their MWD curves.

The type of ionic particle is mostly affected by the nature of the solvent and its dielectric permittivity [62]. Solvents with low dielectric permittivity, such as hydrocarbons, can favour the association of ions: [63] provides a study of the stereoregular process direction and polymerisation kinetics of dienes in the presence of lithium alkyls and an initiator. It has been shown that only the monomer form of the lithium organic compound participates in chain growth. There is either no chain growth on associated particles, or it is very slow and accompanied by an associated equilibrium of particles $\leftrightarrow$ nonassociate ions. Small amounts of added electron donors provide a sharp increase of side 1,2- and 3,4- links content in the polydiene chain, while strongly solvating compounds lead to the formation of polymers with mainly 1,2- links. However, the study of isoprene polymerisation in toluene, in the presence of sodium organic and lithium organic compounds, indicates that chain growth occurred both on the monomer AC and on associated ones. According to the authors of [64], the complex correlation of polymerisation rate and initiator concentration (sodium ethylhexyl)

indicates the existence of several types of AC (the reaction order is fractional at 0.002–0.01 mol/l concentration of initiator and close to the first order at higher concentrations). In addition, chain growth during polymerisation in heptane occurs predominantly on associated forms of AC.

α-methylstyrene copolymerisation with styrene in hexane is described in [65] with a $Li(H\text{-}C_4H_9)$ initiator and in the presence of tetrahydrofuran (THF). It is assumed that the chain growth reaction is carried out by both individual AC and their complexes with one or two THF molecules. It is reported in [66], that there are four types of AC in the process of $\alpha$-methylstyrene polymerisation in cyclohexane with a $Li(H\text{-}C_4H_9)$ initiator and small amounts of added THF. The authors consider that the following types of AC are present in the system in an equilibrium state: monomers, dimers, and monomer complexes with one or two THF molecules. A study of the influence of the ethyl benzoate additive on the polymerisation process of a buten-1 mixture with isobutylene, using a $TiCl_3$- $Al(C_2H_5)_2Cl$ catalyst [67], leads to the conclusion that the catalyst contains both coordinative and cationic AC, which are independent of each other.

The presence of several different ionic particles and therefore, centres with different reactivity, should contribute to the values of the chain growth and chain termination reaction rate constants. The presence of associated, nonassociated and isomeric forms of catalyst particles, the influence of electrolytic dissociation, intramolecular and intermolecular interaction, leading to the formation of catalytic complexes is the reason for the presence of different centres in ionic catalytic systems.

It is well known [13, 50] that the stereospecificity of polymerisation by ionic-coordination catalytic systems is mainly determined by the nature of a transition metal and its valent state. It is confirmed today that complexes of transition metals with different oxidation levels can exist in a catalytic system [68]. It is obvious that catalytic centres formed by transition metals with different oxidation levels will demonstrate different stereospecificity.

The complicated nature of a catalytic complex is well demonstrated by compounds with 4f-elements. These compounds have a high coordination number – from 8 to 12. Free coordination sites can be occupied by molecules of a solvent, monomer, or electron-donating ligand cocatalyst. The probability of such interactions is confirmed by the different values of kinetic constants obtained upon variation of the polymerisation conditions, catalytic system components, its preparation method, and so on [69].

In addition to its function of an alkylation agent and chain transfer agent, the aluminium-organic compound participates in the formation of AC [11]. Variation of

the methods of component content, and temperature and catalytic system preparation exert a distinct influence on the MWD. These facts may indicate the existence of several types of AC forming in a ligand exchange process near the central lanthanide atom. We cannot also neglect the probability of the ligand redistribution reaction (and therefore redistribution of AC) during polymerisation.

The following factors are consequences of the presence of inhomogeneous AC in ionic and ionic-coordinative catalytic systems [49]: wide distribution of copolymers in composition and stereoregularity, nonuniform composition and stereoregularity of copolymers, nonuniform composition and stereoregularity of polyolefins, nonuniform composition and stereoregularity of dienes, and a wide MWD of polymers.

*Composition and stereoregularity distribution of copolymers*: The wide composition distribution of copolymers, and the presence of several polymer fractions with different stereoregularity, is an indication of diverse and polytypic AC. For example, the composition distribution of copolymers is discussed in [56] for polymerisation using heterogeneous catalysts, in terms of active centre distribution by their activity and stereospecificity. The fraction composition has been studied for ethylene-propylene copolymers synthesised in the presence of a $VC1_3$-$Al(C_2H_5)_3$ heterogeneous catalyst and a $V(Ac)_3$-$Al(i\text{-}C_4H_9)_2Cl$ homogeneous catalyst. There was a wide distribution of the content of ethylene links in the copolymer fractions, especially when the heterogeneous catalyst system was used. A proposal has been made regarding the correlation between the stereospecificity of catalytic centres and the kinetic parameters of copolymerisation on these centres.

The study of ethylene and propylene copolymerisation, on vanadium and titanium catalysts of various compositions [70], led to the conclusion that studied catalytic systems contain two or three types of AC. This conclusion has been made as a result of the analysis of the MWD curves, $^{13}$carbon nuclear magnetic resonance spectroscopy analysis, and copolymers composition fractionation data. The analysis of a large number of copolymer fractions, produced by their dissolution in several solvents at various temperatures, has indicated the existence of several types of AC different both in stereospecificity and in reactivity. According to the authors of [70], a combination of copolymer fractionation results with gel chromatography data indicates the presence of two or three types of AC.

The study of ethylene and hexane-1 copolymerisation has been carried out with the catalytic system formed by the interaction of $Mg(C_2H_5)Cl$, THF, and $TiCl_4$, in the presence of hydrogen. Two modifications have been synthesised; with deposition on $SiO_2$ and without deposition. Catalysts have been revealed to exhibit a wide distribution of active centre activity, which was characterised by the copolymerisation constant $r_1$; values varied from 5–7 to 2000 [71]. The narrowest distribution was

demonstrated using catalysts with deposition on $SiO_2$, while the widest distribution was observed for the catalysts synthesised with intermediate Ti:Mg values. It was proposed that there were several groups of AC, different in relative reactivity in copolymerisation processes, MW of synthesised polymers, and stability. The centres with the highest reactivity to the copolymerisation of specific monomers are fast to form and eliminate, thus they produce a low MW copolymer: on the contrary, kinetically stable centres produce high molecular weight linear chains. First-type centres are subject to predominant deactivation resulting in a decrease of $\alpha$-olefin links in a copolymer however, the MW of the copolymers increases in this case.

The study of propylene and butane-1 copolymerisation by $TiCl_3$ and $Al(C_2H_5)_3$ heterogeneous catalysts [72] indicates the presence of AC, which differ in forming isotactic structures. However, there is still an open-ended question; are there a different number of groups (types) or do their behaviour characteristics change during the reaction?

*Stereoregularity and MW nonuniformity of polyolefins and polydienes*: Polyolefins synthesised on complex Ziegler–Natta catalysts are products without uniform stereoregularity and MW. The reason for this effect is the existence of different types of AC with different stereospecificity. On the other hand, these catalysts are kinetically nonuniform (differ in reactivity).

The study of external and internal donors has been made in [73], in terms of their influence on the composition of polymer fractions and their stereoregularity in the process of propylene polymerisation on titanium-manganese catalysts. Three types of AC are assumed: aspecific centres with two coordination vacancies; isospecific centres with one coordination vacancy, and isospecific centres with a mixture of donor and coordination vacancies from an aspecific active centre.

In addition to polyolefins, there is also information regarding the correlation between kinetic nonuniformity and stereoregularity nonuniformity for polydienes. The correlation between the polymer microstructure and the MW has been revealed in [74] for polybutadiene fractions synthesised on π-allylic nickel complexes. It has been shown that the lower the MW of the fractions, the higher the content of the 1,4-*trans*- and 1,2- links, while the higher the MW, the higher the content of the 1,4-*cis*- links. The study of the MW and microstructure of polybutadiene has been carried out in the presence of a *cis*-regulating catalytic system [75]. The MW and stereoregularity have been proved to change in a similar way. Decrease of the MW and an increase of 1,4-*trans*-links content can also be achieved by the increase of nickel and aluminium concentration, increase of temperature, and decrease of butadiene concentration. Dolgoplosk has proposed an assumption that *anti-syn*-isomerisation of an active centre plays a certain role in the stereoregulation of dienes. The decrease

of butadiene concentration in polymerisation processes with $TiI_2Cl_2$-$AlR_3$, $CoCl_2$-$AlR_2Cl$, and $Ni(OCOCCl_2)_2$-Niπ-RCl catalytic systems, led to an increase of *trans*-links content in the polymer, due to a decrease of the chain growth reaction rate and a more important role of the *anti-syn*-isomerisation reaction. *Cis*-regulating structures of AC are characterised by a higher polymerisation rate and the formation of macromolecules with a higher MW [76].

The correlation between MW and polymer microstructure is also mentioned by the authors of [77] for fractions of dienes synthesised on complex Ziegler–Natta catalysts. The content of *cis*-1,4-links drops in fractions with a decrease of their MW. A substantial decrease of *cis*-1,4-links content was observed in the area of MW < $2 \times 10^4$ (from 90 to 70%). The authors assume that the heterogeneity of a catalyst is the basis for the formation of different types of AC with different growth reaction rates and *anti-syn*-isomerisation. More active centres tend to form macromolecules with an increased content of the *cis*-1,4-links and a higher MW.

The presence of such a correlation however, is not only a feature of heterogeneous catalytic systems. Confirmation of this assumption is the product of the *trans*-piperylene polymerisation on the *cis*-regulating catalytic system $NdCl_3 \cdot 3$ tributylphosphate-$Al(i\text{-}C_4H_9)_3$ in heptanes and toluene [76]. The catalyst used in this process was washed-out from individual triisobutylaluminium. The polymerisation system became homogeneous after the addition of a monomer, while the polypiperylene product had both a nonuniform MW and microstructure. In addition, the MW decrease led to a substantial drop of *cis*-1,4-links content, especially for the process in toluene. Such a correlation between microstructural nonuniformity and polymer MW has been observed for different stages of monomer conversion. The reason for the nonuniform composition of such polymers is the presence of simultaneously acting AC with different reactivity and stereoregulating capability.

*The effect of wide and polymodal MW distribution of the synthesised polymer*: Polymers synthesised in various ionic and ionic-coordination polymerisation reactions demonstrate a broader MWD and sometimes clearly indicated bimodal or trimodal distribution. Broad MWD may indicate the presence of AC with different reactivity. Ultraviolet-spectroscopy and adiabatic calorimetry methods have been used to study α-methoxystyrene cationic polymerisation kinetics in dichloromethane, with a $Ph_3C^+SnCl^-$ catalyst [78]. MWD curves of forming polymers have been found to be polymodal, while three of the four fractions revealed themselves at the very beginning of the process. Such a distribution has been concluded to be caused by chain growth on three types of AC.

The bimodal MWD has been determined for polyethylene samples synthesised on the $Cr/AlPO_4$ catalytic system in isobutene, in the presence of triethylboron as a

cocatalyst. It supplemented other data as an indication of a wider range of AC than for the $Cr/SiO_2$ catalyst [79]. The authors consider that some of the AC contained the less stable Cr-polymer bond. The resulting activity of such centres was higher in the reaction of chain transfer to cocatalyst and β-H-elimination.

Therefore, any specific type of active centre produces a polymer with a specific MWD and stereoregularity; observed characteristics of polymers are the superposition of numerous normal distributions [80] leading to broadening of the MWD.

*Mathematical modelling of polymerisation and copolymerisation processes with consideration of polycentrism of catalytic systems*: Nonuniformity of AC is assumed in various publications dedicated to the mathematical modelling of polymerisation and copolymerisation processes.

A kinetic model of polyolefins copolymerisation by Ziegler–Natta catalysts has been proposed in [81]. The model is based on a mechanism assuming a reaction pathway with different types of AC in the catalyst particle. The kinetic chart describes the formation and deactivation of AC, as well as the spontaneous reactions of chain transfer to hydrogen, monomer, or metal-organic compound. The model is suitable for calculations of copolymerisation rate, composition, and MWD of copolymers.

Modelling of the polymer particle growth process [82] has resulted in the conclusion that diffusion limitations are the single reason for the wide polydispersity of synthesised polymers. The model has demonstrated that the main transport limitations localise on the level of macroparticles. Modelling results are confirmed by data obtained in gas and liquid polymerisation experiments on titanium-magnesium catalysts. Authors also consider that the wide polydispersity of polymers can be explained by the existence of more than one type of active centre. Each specific type is responsible for a certain portion of polymer with a different MWD. However, the authors did not succeed in characterising the active centre [82] because it required the optimisation of many kinetic parameters.

The kinetic model developed in [83] describes the dependence of the conversion on time and MW for butadiene polymerisation on homogeneous catalysts. Compounds with Co, Al, and $H_2O$ are assumed to participate in the formation of AC. Computational and experimental data for the conversion of butadiene are proved to correlate well with each other when polymerisation is carried out with the cobalt octanoate – diethylaluminium chloride – water catalytic system. However, this model considers only one type of active centre and does not provide an explanation for the increase of polybutadiene polymerisation with conversion growth. The polymerisation diagram and mathematical model with two types of AC have been proposed for butadiene polymerisation in the presence of a $Li(H\text{-}C_4H_9)$ – diethylene glycol dimethyl ether catalytic system [84]. This approach is suitable for the calculation of changes

in the concentration kinetics of the polymerisation components, polybutadiene microstructure and its MWD, with various initial concentrations of monomer. The model demonstrates satisfactory agreement with experimental data.

Another mathematical model has been proposed for isoprene polymerisation kinetics. This model takes into consideration the nonuniformity of the AC [85]. It also provides tools for calculation of the monomer conversion time and the average MW of the polyisoprene for various concentrations of reactants, reaction times, and probability of various processes. The estimation of model kinetic parameters using experimental data is also provided.

The phenomenon of polycentrism is discussed in [86, 87], regarding the polymerisation of olefins and 1,3-dienes with Ziegler–Natta catalysts. Four research methods have been applied to study the formation of AC and the formation of stereoregular polymers [86]:

1) 'Atomic-atomic' potentials method, providing reliable results for the calculation of valent-unbound molecules [88], in particular, for the process of physical adsorption of the monomer and catalytic system components at the stage of the formation of AC.

2) CNDO/2 method, which is suitable for the reproduction of bond lengths, bond angles, and distribution of electrons in molecules [89]. The geometry of metal complexes and charge distributions in $MeCl_m$ and $R_nM$ molecules were calculated with geometry optimisation using the conjugate gradient method.

3) Modified method of the 'diatomic complexes in molecules', which provides a satisfactory prediction of the valent-bound atoms interaction at the stages of chemical adsorption of catalytic system components and monomer molecules, reactions of initiation and chain growth in a-olefins, and 1,3-dienes stereospecific polymerisation reactions.

4) Monte-Carlo method to complement the theoretical calculations determined using mathematical experimental data.

The study of the adsorption process of $R_nM$ (organic compounds of group I-III metals) on the $MeX_m$ surface (the salts of transition metals from groups IV-VIII) was based on the assumption that the molecule of a metal-organic compound is a solid body with Cartesian coordinates x,y,z = $\bar{X}$ and Euler's angles $\alpha$, $\beta$, $\gamma$. The Markovian chain consisted of 220000 configurations, each configuration corresponded to a certain minimum of the energy surface determined by 'atomic-atomic potentials'.

Interaction of various combinations of Ziegler–Natta catalytic system components results in the formation of potential AC [86]. This process depends on the chemical

structure of $R_nM$ and $MeX_m$ compounds at points of open metallic component on the $MeX_m$ crystalline surface.

An important effect is the formation of Me..R..M bridges, if the combination of $MeCl_m$ and $R_nM$ compounds is used. The homogeneous $R_nM$ component completes the real crystal lattice $MeX_m$ and forms potential AC. The M atom occupies the position equivalent to the position of the Me atom in a crystal, while the R-group occupies the anionic vacancy of $MeX_m$ equivalent to the position of X in the layered $MeX_m$ crystals.

Experimental confirmation of the formation of impurity crystals with surface electronic defects has been found in the process of alkylaluminium adsorption by titanium oxide, the alkylaluminium contained marked carbon atoms. Large $TiCl_3$ crystals have been studied microscopically. The polymerisation process was the propylene polymerisation in the presence of Ziegler–Natta catalysts and so on.

Study of the monomer interaction with a potential active centre has revealed the following fact: $R_nM$ exhibits different behaviour in the proximity of various minimums of the potential energy surface, at the stage of physical adsorption of the metal-organic $R_nM$ compounds on the surface of the $MeX_m$ crystal. There are three main cases:

1) The $R_nM$ molecule is strongly 'fixed' in the surface energy minimum and forms the physical adsorption centre PhAC-1. Orientation of the metal-organic compound molecule $R_nM$ is strongly fixed in an energy minimum in this case. This orientation is persistent at sufficiently high distances from the minimum. Migration of the $R_nM$ molecule on the crystal surface is hindered in the area of surface potential energy minimum (for example, for a, g, and d-$TiCl_3$ + $AlR_3$ systems). This fact is confirmed by the small Euler's angle dispersions indicating the $R_nM$ molecule orientation in the minimum neighbourhood, as well as by the effective radius values which indicate the degree of $R_nM$ molecule fixation on the $MeX_m$ surface. Strong fixation of the $R_nM$ molecule in the minimum is also confirmed by the extremum peak on the metal-organic compound distribution function histogram in the neighbourhood of the potential energy minimum [86].

2) The $R_nM$ molecule is strongly fixed in the surface energy minimum (PhAC-2); its surface migration is hindered. However, the $R_nM$ molecule orientation is not so strongly fixed in the surface energy minimum or its neighbourhood. Rotation of the metal-organic compound $R_nM$ molecule can be hindered and limited by only one coordinate axis, and the $R_nM$ molecule can be fixed in various positions relative to the $MeX_m$ crystal surface. The only difference between these positions is if the mutual 'rearrangement' of the R-groups of the metal-organic compound is at a fixed position of the central M atom in the $R_nM$ molecule.

3) The $R_nM$ molecule is not strongly fixed (PhAC-3) and can freely migrate on the crystalline surface, and change its spatial orientation in the area of the potential surface area minimum. An indication is a fuzzy contour of the $R_nM$ distribution function histograms and Euler's angles of dispersion in the minimum neighbourhood, and so on.

PhAC-1, PhAC-2, and PhAC-3 form AC AC-1, AC-2, and AC-3, respectively.

As a result of the interaction of the catalytic centres of the Ziegler–Natta catalyst components $R_nM$ and $MeX_m$, depending on their chemical structure, $R_nM$ and $MeX_m$, three main types of AC can be identified on a crystalline surface with open Me clusters $MeCl_m$: AC-1, AC-2, and AC-3. They differ in geometric structure, energy of configurations, and relative composition.

The combination of a-, g-, and d –modifications of $TiCl_3$ as well as $VCl_3$ and $CrCl_3$ compounds with Al, Be, Mg, and Li alkyls, mainly results in the formation of single-type AC-1 centres.

This group of Ziegler–Natta catalysts is stereospecific for the polymerisation of a-olefins and 1,3-dienes: the products are mainly isotactic polyolefins (polypropylene, polystyrene, and so on) and *trans*-1,4-polydienes (polybutadiene, polyisoprene, and so on).

The characteristic feature of an AC-1 centre is the formation of one bridge bond and a relatively weak interaction between Me and R, with a respective redistribution of charges. The specific arrangement of Me, M, C, and H atoms in the AC-1, on the layered surface of the $MeX_m$ crystal, favours the formation of a specific spatial 'tunnel'-like disposition of molecules. Figuratively speaking, it is a 'cave' or 'grotto' (**Figure 3.28**), which is very important for the orientation of the monomer molecule during its approach to the AC. According to quantum-chemical calculations and numerical experiment, this arrangement puts the monomer (both a-olefin and 1,3-diene) in a very specific position: vinyl group $CH_2$ = CHR is turned to the Me atom in the AC-1, while the R-group (for example, $-CH_3$, $-CH_2CH_2CH(CH_3)_2$, - CR = $CH_2$, and so on) is turned to the crystal surface. The molecule approach to AC-1 is only possible from the other side (from the entrance to a 'grotto').

Generally, monomer molecules can adsorb onto AC-1 with their other more bulky C = C-groups, however, both calculations and numerical experiment show that chain growth on AC-1 is not caused by the steric factor. For example, the dependence of AC-1 stereospecificity and *trans*-1,4-polydiene yield on the chemical structure of monomers can be observed experimentally. The more bulky substituent is in the 1,3-diene molecule, the lower the stereospecific polymerisation rate, the higher the content of *trans*-1,4-isomers of the respective polydienes.

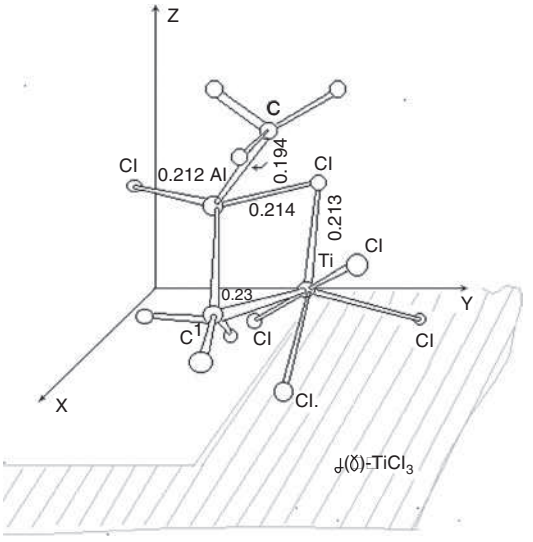


**Figure 3.28** The geometry of a model AC AC-1 for catalytic systems a(g)-$TiCl_3$-$Al(CH_3)_3Cl$ (Me - Ti, V, Cr; M - Al, Be, Mg, Li)

The AC-2 forms predominantly from combinations of Al, Be, Mg, and Li alkyls with *b*-modifications of $TiCl_3$ as well as Co, Fe, and Ni chlorides. The AC-2 type of AC form stereoregular *cis*-1,4-polydienes. The structure of AC-2 (**Figure 3.29**) is similar to the structure of AC-1, however, there is a significant difference in the interaction of the Me atoms with two R-groups and the formation of two bridge bonds.

As a result, AC-2 has a different spatial structure than AC-1, which enables the partial alkylation of the transition metal compound by the $R_nM$ metal alkyl. All Al-R bonds weaken, while one of them weakens significantly.

Two bridge bonds form: Ti...R-Al and Al...Cl-Ti. The Al atom interacts with Cl and the Cl atom of the $TiCl_3$ crystal, which is linked with only one Ti atom in the initial crystal.

Formation of AC-2 results in a more substantial transformation of bonds than the formation of AC-1. A different spatial structure of AC-2 is formed, which has the 'flower' shape and permits both mono and bidentate coordination of 1,3-dienes, as well as putting less restrictions on their coordination with a monomer for all the positions of substituent at the C = C bond, in relation to a crystal surface. This is the reason for AC-2 stereospecificity and the aforementioned possibility of stereo block copolymer formation during a-polymerisation in the presence of Ziegler–Natta catalytic systems. AC-2 can orient unsaturated C = C bonds of 1,3-dienes to bidentate coordination on the bidentate AC.

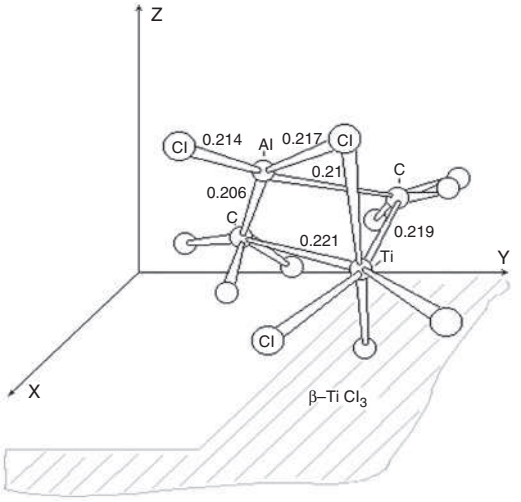


**Figure 3.29** The geometry of a model active centre. AC-2 in *b*-$TiCl_3$-$Al(CH_3)_2Cl$ (Me - Ti, Co, Fe; M -Al, Be, Mg, Li) catalytic systems

The possibility of 1,3-diene bidentate coordination and the energetically favoured formation of a polymer chain with *cis*-1,4-links enables the formation of *cis*-1,4-polydienes on AC-2. The p-allylic system can form on AC of this type in the form of an anticomplex, favouring the formation of *cis*-1,4- structures in 1,3-diene polymerisation. It is also important to note that the growth of *cis*-1,4 macromolecules on AC-2 AC (a 'flower') puts the least restrictions on monomer access to the catalytically AC of a transition metal.

$\alpha$, $\gamma$, $\delta$-$TiCl_3$, V, and Cr chlorides mainly form AC-3 types of AC in interactions with Zn and Na (**Figure 3.27**). These centres are not stereospecific in the polymerisation of a-olefins or 1,3-dienes.

The structure of AC-3 is different from AC-1 and AC-2. This type of active centre is characterised by the weak interaction between atoms in the $MeX_m$ - $R_nM$ complexation processes. The molecule of a $MeX_m$ metal-organic compound is almost coplanar to the crystal surface in AC-3 formation processes, while the Me-R distance is less than the Me-M distance, as opposed to AC-1 and AC-2 (**Figure 3.30**).

AC-3 has a more bulky spatial structure than AC-1 and AC-2. As we can conclude from the calculated results and Stuart–Briegleb models, an opportunity for the random coordination of the monomer molecules is the reason for the nonspecific polymerisation of a-olefins and 1,3-dienes.

This type of AC (AC-3) is called a 'wicket'; absence of steric restrictions typical both for AC-1 and AC-2, permits synthesis of more bulky 1,2-(3,4-) polydienes on AC-3.

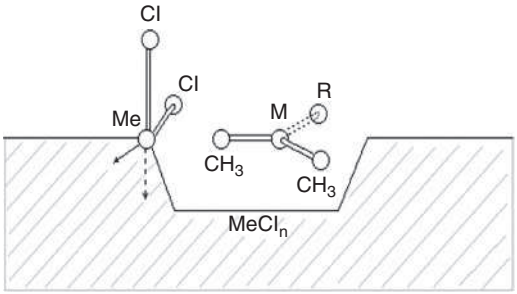


**Figure 3.30** AC-3 structure ('wicket') (Me - Ti, Co, Ni, Fe; M - Zn, Na, Al, Be, Mg, Li)

The aforementioned information demonstrates that the problem of several types of AC in various heterogeneous catalytic systems is put on the agenda over and over again. However, the true distribution of the polymerisation centres (the number, kinetic parameters, and stereospecificity of each type of active centre) is still a problem under discussion. Research in this area is mainly limited to the polymerisation of olefins. For example, propylene polymerisation was studied in [89] to obtain the quantitative characteristics of the kinetic inhomogeneity of a polymerisation system. These parameters, however, are strongly dependent on the model assumptions of the distribution shape of the macromolecule growth centre kinetic activity, which form the basis for the calculation algorithm. The following assumption has been made in [90]: the AC on the surface of the $MgCl_2/PhC(O)O(C_2H_5)$-$TiCl_4$-$Al(C_2H_5)_3$ catalytic system give different chain growth and chain termination reaction constants. This assumption made it possible to obtain the surface distribution function of the density of polymerisation centres. The number of AC was determined by catalyst poisoning using carbon monoxide (CO). Differential equations describing the distribution of growing and 'dead' chains have been derived for polymerisation systems with fast stages of initiation and polymerisation, occurring without elimination of the AC. A solution has been achieved with Laplace transformations; as a result, invariant MWD times have been obtained for the model with isotactic and atactic centres of chain growth.

Computer simulation has been used to study the polymerisation and copolymerisation of olefins on supported catalysts. The model is based on the assumption that AC have a distribution of reactivity on the catalyst surface. The $MgCl_2/TiCl_4$-$Al(C_2H_5)_3$ catalytic system is assumed to have two types of AC: highly active short-living centres and low activity, slowly deactivating centres. The ratio of Al:Ti < 10.7 is shown to provide a unimodal or bimodal distribution of AC with a predominant content (> 90%) of highly active short-living centres. The ratio of Al:Ti > 10.7 leads to the bimodal distribution of kinetic activity with a high content of low activity AC.

A new method is described in [91] for the study of the nonuniformity of AC. It is based on the mass-spectrometry control of temperature-programmed desorption of products, from the catalyst surface, at the initial stage of the gas-phase polymerisation of olefins. Polymerisation conditions have been selected in a way to favour the formation of low MW products (up to 14 monomer links in a chain). The authors report two definite maximums in the areas of 180–210 and 280–320 °C in the process of desorption from the $SiO_2/TiCl_4$-$Al(C_2H_5)_2Cl$ surface. Therefore, the catalyst contains at least two types of AC with different activation energies of thermal destruction of Ti-C bonds. This publication also contains calculations of the activation energy distribution of thermal Ti-C bond destruction for various types of AC.

It is proposed in [92], that the summary of polymer MWD can be used for the Tikhonov regularisation method [93, 94] to derive AC distribution by chain termination probability. No assumption has been made about the type of this distribution.

Polymer MWD width is known to be described by the general equation [95]:

$$u = \mathrm{PSX} \tag{3.51}$$

Where:

$u$ is the polymer polydispersity.

P is the ratio between the polymerisation reaction and diffusion limitations.

S is the factor depending on the kinetic activity distribution of polymerisation AC.

X is the parameter of the size distribution of the globules.

For P = 1 and X = 1, the MWD widening can only be determined by the kinetic activity distribution of polymerisation centres [86, 92, 95–99].

In the case of a narrow polymerisation increment, the differential numerical MWD of 'dead' chains $q_n(M)$ is described by the more probable Flory Distribution:

$$q_n(M) = \beta \exp(-\beta M) \tag{3.52}$$

Where $\beta$ is the inverse value of $M_N$ and the measure of chain termination probability. $\beta = 1/M\ r_0/r_p$ at the $r_p$ polymer growth rate and the total chain termination rate $r_0$, (M is the MW of a polymer).

Introduction of the $\phi(\beta)$ function for the distribution of AC, ($\beta = \Sigma W_n / W_p$) will give us the following differential equations for MWD:

$$q_w(M) = \int_0^\infty \phi(\beta)\, M\, \beta^2 e^{-\beta M}\, d\beta \tag{3.53}$$

Assuming:

$$s = ln\,\beta \tag{3.54}$$

$$x = ln\,M \tag{3.55}$$

$$U_\delta(x) = q_w(M) \tag{3.56}$$

**Equation 3.42** can be shown to correlate with the classical form of the first-order Fredholm Equation:

$$U_\delta(x) = \int_0^\infty Z(s)\,K(x,s)\,ds \tag{3.57}$$

Where:

$K(x, s)$ is the core of the integral in **Equation 3.58**:

$$K(x,s) = \exp(x + s + \exp(x + s)) \tag{3.58}$$

$Z(s)$ is the required integrand:

$$Z(s) = e^{2s}\phi(e^s) \tag{3.59}$$

and the $\delta$ index in the left part of the equation is the error of the experimental $U(x)$ function value.

The complexity of **Equation 3.43** in relation to $Z(s)$ is because it falls into the category of improperly posed problems in this case. The numerical solution of **Equation 3.43** has been obtained by the Tikhonov regularisation method: the following conditions are required to obtain an approximate $Z(s)$ solution by approximation of the right part $U_\delta(x)$: firstly, the $Z(s)$ value must give the residual norm not exceeding the experimental data error:

$$\int_c^d \left[ \int_a^b K(x,s)\,Z(s)\,ds - U_\delta(x) \right]^2 dx \le \delta^2 \tag{3.60}$$

Secondly, it is necessary to provide $Z(s)$ minimisation of Tikhonov's functional:

$$M_\alpha[Z] = \int_c^d \left[ \int_a^b K(x,s)\,Z(s)\,ds - U_\delta(x) \right]^2 dx + \alpha \int_a^b \left[ Z^2(s) + \left( \frac{dz}{ds} \right)^2 \right] ds \tag{3.61}$$

Where $\alpha$ is the numerical parameter of regularisation, $\alpha > 0$.

The minimum of the Tikhonov functional is achieved with the optimal value of the α regularisation parameter $\alpha = 9.4 \times 10^{-5}$, while the residual norm value was $1.07 \times 10^{-4}$. This method allows the variation of the error value in the integral equation core selection process. However, as the model core was the Schulz–Flory function, the error h was assumed to be $h \rightarrow 0$.

The selection of the regularisation parameter has been carried out in accordance with the generalised principle of misalignment: experimental data errors have been used to obtain α values from **Equation 3.61**. The correction method for experimentally obtained chromatograms has been developed to solve the problem of 'equipment-caused widening', emerging due to the nonideal and nonuniform process of chromatographic separation. The regularisation method has also been used to solve Tung's equation. The 'equipment-caused widening' function was approximated by the Pearson distribution. The resulting error of the chromatographic experiment was reduced to 1%. Solution algorithms have been found for the inverse problem of MWD derivation, based on Tikhonov's regularisation method.

The results are demonstrated graphically in $\psi(ln\ \beta) - ln\ M$ coordinates, as such the representation is a good demonstration of the correlation between the MW and kinetic inhomogeneity of a catalytic system.

For example, **Figure 3.31** demonstrates $\psi(ln\ \beta)$ - $ln\ M$ functions, obtained for isoprene polymerisation with a $NdCl_3 \cdot 3TBF\text{-}Al(i\text{-}C_4H_9)_3$ catalytic system. Demonstrated curves are seen to be polymodal; each point on the distribution curve characterises the fraction of AC with the chain termination probability of $\beta_i$, which produce macromolecules with $M_i$ MW. The presence of a $\psi(ln\ \beta)$ distribution indicates kinetic inhomogeneity of a catalytic system. Such inhomogeneity appears at small conversions (1–5%) and does not depend on the nature of the catalytic system components, its preparation method or polymerisation conditions, meaning that a catalytic system is initially kinetically inhomogeneous.

Assuming a statistical nature of the deviation of AC from the maximum, the distribution can be subdivided into separate 'Gaussian' functions (**Figure 3.32**). The area occupied by each 'Gaussian' curve corresponds to the numerical fraction of polymer synthesised on a respective centre or the fraction of monomer consumed by this type of active centre. Therefore, the area inside the 'Gaussian' curves corresponds to the kinetic activity of this type of active centre.

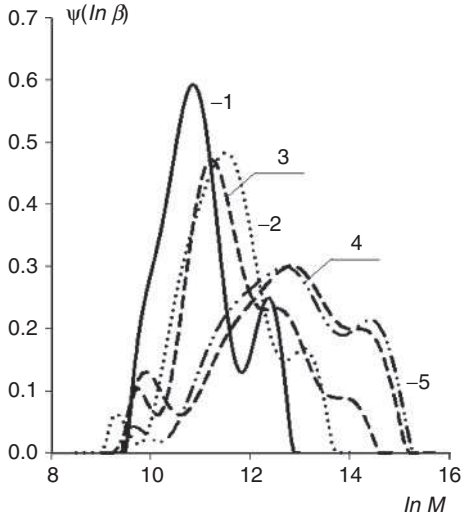


**Figure 3.31** Kinetic activity distribution of the $NdCl_3 \cdot 3TBF\text{-}Al(i\text{-}C_4H_9)_3$ catalytic system in the isoprene polymerisation reaction; conversions %: 1 – 2.6; 2 – 6.4; 3 – 7.5; 4 – 32.7; and 5 – 53.4. Polymerisation conditions: toluene, $T_{\text{polymerisation}}$ = 25 °C, $C_m$ = 1.5; $C_{Nd} = 3.0 \times 10^{-3}$ mol/l, and Al/Nd = 30, $T_{\text{melt}}$ = 25 °C

An optimisation procedure was used to split the complex function into 'Gaussian' functional elements. The task can be reduced to the search of the target $\Phi(z)$ function minimum in the space of 2n variables:

$$\Phi(z) = \sum_{i=1}^{m}\left[\phi(h_i) - \sum_{k=1}^{n}\frac{1}{\sqrt{2\pi\sigma_k}}\exp\left(-\frac{(h_i - h_k)^2}{2\sigma_k^2}\right)\right]^2 \tag{3.62}$$

Where:

$n$ is the number of curve maximums.

$\sigma_k(h)$ are the respective normalised elementary functions.

$h_i$ and $h_k$ are the coordinates of their maximums.

Visual selection of $h_k$ values was used to reduce the calculation time, these values could be found in the area of the $k^{\text{th}}$ peak maximum. The parameter of 'Gaussian' function width $\sigma_k$ was assumed to be constant for all $k$ = 1.

The optimal values of $h_k$ and $\sigma_k$ were found using the alternating variable descent method. The 'golden section' method was used to the find one-dimensional minimum along the axis. The procedure was considered to be completed at $\Phi(z) < \delta = 10^{-4}$.

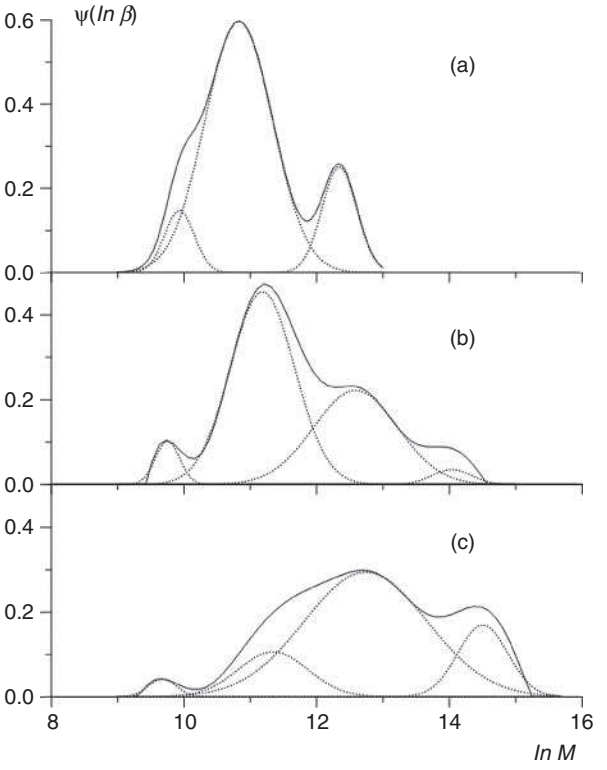


**Figure 3.32** Kinetic inhomogeneity distribution curves obtained for AC of the $NdCl_3 \cdot 3TBF\text{-}Al(i\text{-}C_4H_9)_3$ catalytic system in the process of isoprene polymerisation. Monomer conversions, %: a – 2.6; b – 7.5; and c – 53.4. The solid line represents the total distribution, the dashed line demonstrates splitting into separate 'Gaussian' functions

**Figures 3.33** and **3.34** demonstrate the kinetic activity distribution functions obtained from monomodal MWD curves for $PrCl_3 \cdot 3$(tributylphosphate)-$Al(i\text{-}C_4H_9)_3$ and $GdHal_3 \cdot 3$(tributylphosphate)-$Al(i\text{-}C_4H_9)_3$ catalytic systems in the isoprene polymerisation process. The functions demonstrated in the figures are also seen to be polymodal. The initial stage of isoprene polymerisation demonstrates that the activity of AC, formed by both neodymium and praseodymium catalytic systems, is predominant in the maximum of the low molecular weight area of the $\psi(ln\ \beta)$-$ln\ M$ distribution curves (**Figure 3.32**).

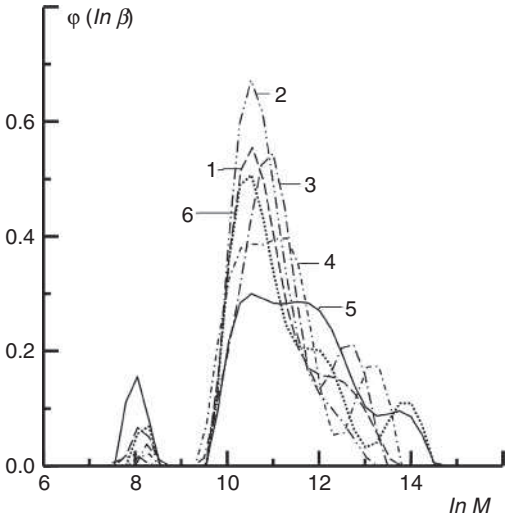


**Figure 3.33** $PrCl_3 \cdot 3TBF–Al(i\text{-}C_4H_9)_3$ catalytic system kinetic activity distribution curves in the process of isoprene polymerisation. Isoprene conversion %: 1 – 1.9; 2 – 2.4; 3 – 3.1; 4 – 3.6; 5 – 19.7; and 6 – 89.6

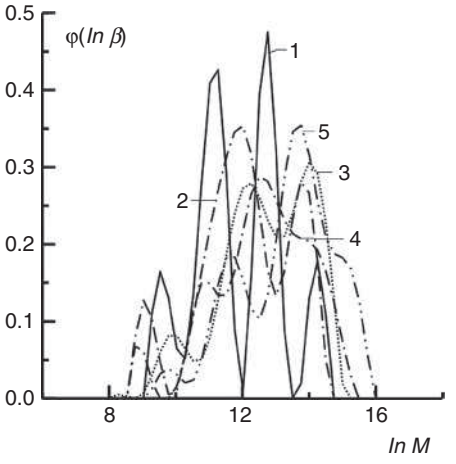


**Figure 3.34** $GdCl_3 \cdot 3TBF–Al(i\text{-}C_4H_9)_3$ catalytic system kinetic activity distribution curves in the process of isoprene polymerisation. Isoprene conversion %: 1 – 0.9; 2 – 1.1; 3 – 4.4; 4 – 7.6; and 5 – 16.6

The low molecular weight peak becomes less predominant with an increase of the monomer conversion and the intensities of peaks are levelled (**Figure 3.32**). The $GdCl_3 \cdot 3TBF\text{-}Al(i\text{-}C_4H_9)_3$ catalytic system demonstrates high activities of AC corresponding to the second and third peaks. The domination of these peaks is

sustainable in the other stages of polymerisation and probably explains the high MW values of polyisoprene synthesised with the aforementioned catalytic system.

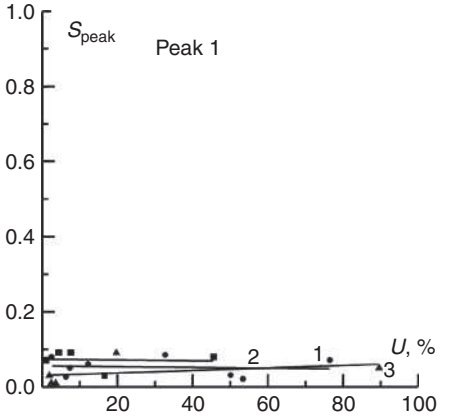


**Figure 3.35** Kinetic activities of various types of AC in isoprene polymerisation with the $LnCl_3 \cdot 3$(tributylphosphate)- Al($i$-$C_4H_9$)$_3$ catalytic system at different monomer conversion rates. Polymerisation conditions: toluene, $C_m$ = 1.5, $C_{Al}$ = 4.5 × $10^{-3}$ mol/l, $T_{polymerisation}$ = 25 °C, and Al/Ln = 30. Ln: Nd (1), Gd (2) and Pr (3). Peak 1

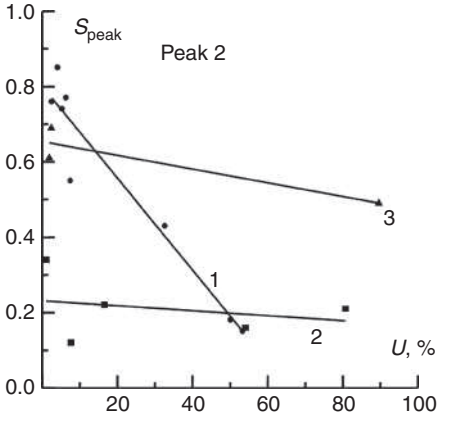


**Figure 3.36** Kinetic activities of various types of AC in isoprene polymerisation with the $LnCl_3 \cdot 3$(tributylphosphate)- Al($i$-$C_4H_9$)$_3$ catalytic system at different monomer conversion rates. Polymerisation conditions: toluene, $C_m$ = 1.5, $C_{Al}$ = 4.5 × $10^{-3}$ mol/l, $T_{polymerisation}$ = 25 °C, and Al/Ln = 30. Ln: Nd (1), Gd (2) and Pr (3). Peak 2

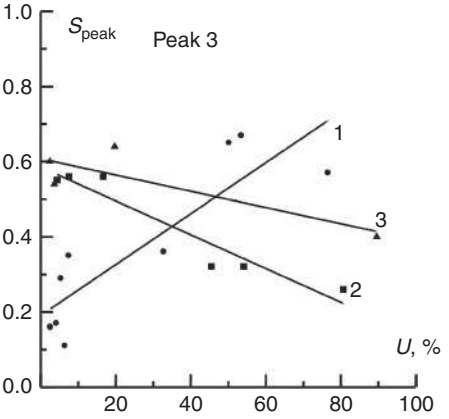


**Figure 3.37** Kinetic activities of various types of AC in isoprene polymerisation with the $LnCl_3 \cdot 3$(tributylphosphate)- Al($i$-$C_4H_9$)$_3$ catalytic system at different monomer conversion rates. Polymerisation conditions: toluene, $C_m$ = 1.5, $C_{Al} = 4.5 \times 10^{-3}$ mol/l, $T_{polymerisation}$ = 25 °C and Al/Ln = 30. Ln: Nd (1), Gd (2) and Pr (3). Peak 3

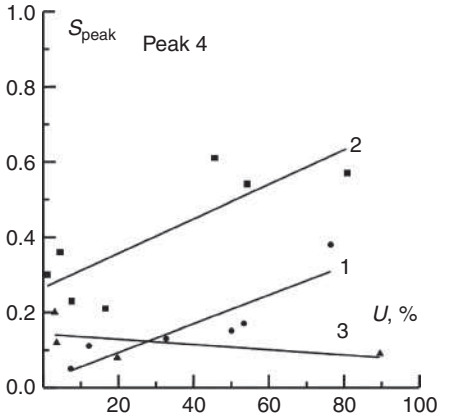


**Figure 3.38** Kinetic activities of various types of AC in isoprene polymerisation with the $LnCl_3 \cdot 3$(tributylphosphate)- Al($i$-$C_4H_9$)$_3$ catalytic system at different monomer conversion rates. Polymerisation conditions: toluene, $C_m$ = 1.5, $C_{Al} = 4.5 \times 10^{-3}$ mol/l, $T_{polymerisation}$ = 25 °C and Al/Ln = 30. Ln: Nd (1), Gd (2) and Pr (3). Peak 4

Separation of the distribution curves (**Figure 3.39**) reveals that maximum peaks shift toward higher MW only at the initial moment of polymerisation and then stay constant throughout the polymerisation process. Therefore, each type of active centre synthesises macromolecules of a specific length.

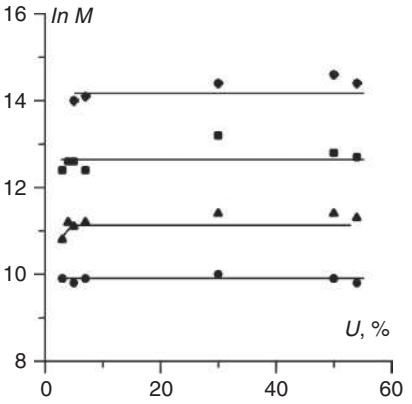


**Figure 3.39** The maximum positions of the $NdCl_3 \cdot 3TBF\text{-}Al(i\text{-}C_4H_9)_3$ catalytic system kinetic inhomogeneity distribution curves in the isoprene polymerisation process

Thus, the inverse task of the MWD method helped to reveal peculiarities of the macromolecule growth centre distribution on their kinetic activity, for a wide range of catalysts and monomers, in the processes of stereospecific polymerisation of dienes [100]. Another important problem to solve is obtaining distributions of AC by their stereoregularity in diene polymerisation reactions. Stereoregulating activity and kinetic inhomogeneity distributions are reported [101] for the AC of ionic-coordinating titanium-containing catalytic systems in butadiene polymerisation processes. Butadiene polymerisation was studied with a $TiCl_4\text{-}Al(i\text{-}C_4H_9)_3$ catalytic system; this system can synthesise polybutadiene with a microstructure varied over a wide range, depending on the polymerisation conditions [102].

Polybutadiene samples were fractioned to obtain the stereospecificity distribution of AC. All the extracted fractions are sufficiently narrowly dispersed ($M_w/M_n < 2$) and their yield was at least 95–96% (**Table 3.9**). There is satisfactory correlation between the average MW data of initial samples obtained from the MW of fractions and gel-permeating chromatography data, confirming successful fractionation [102].

Correlation between the MW and stereospecificity of fractions has been revealed; for the studied samples, an increase of 1,4-*cis*-links content and a decrease of 1,4-*trans*-structures is observed with an increase of MW. The fraction of the 1,2-links is insignificant and constant during the polymerisation process. The most intensive changes of the microstructure can be observed in the low MW area (~$10^3$–$10^4$), where all the fractions are seen to have a mixed microstructure. There are no fractions with a strictly regular 1,4-*cis*- or 1,4-*trans*-stereostructure of macromolecular chains. Such a nonuniform stereospecificity indicates the existence of several types of AC with different stereoregulating capabilities [102].

**Table 3.9 Polybutadiene sample fractionation results. The catalytic system used was $TiCl_4$-Al(*i*-$C_4H_9)_3$ (toluene, 25 °C, 26 % yield)**

| Fraction number | Sample mass, g | Weight fraction, % | Molecular weights and polydispersity | | | Microstructure, % | | |
|---|---|---|---|---|---|---|---|---|
| | | | $M_w10^{-3}$ | $M_n10^{-3}$ | $M_w/M_n$ | 1,2- | 1,4-*trans* | 1,4-*cis* |
| Initial sample | 0.5 | - | 125 | 5 | 21 | 4 | 66 | 32 |
| 1 | 0.0263 | 5.5 | 320 | 160 | 2 | 2 | 28 | 70 |
| 2 | 0.0484 | 10.2 | 245 | 130 | 1.8 | 3 | 34 | 63 |
| 3 | 0.0607 | 12.7 | 215 | 110 | 1.9 | 2 | 36 | 62 |
| 4 | 0.0965 | 20.4 | 185 | 115 | 1.6 | 3 | 39 | 58 |
| 5 | 0.0285 | 6.0 | 160 | 90 | 1.9 | 3 | 42 | 55 |
| 6 | 0.0397 | 8.3 | 140 | 40 | 2 | 2 | 42 | 56 |
| 7 | 0.0441 | 9.2 | 125 | 80 | 1.6 | 3 | 51 | 46 |
| 8 | 0.0437 | 9.1 | 90 | 60 | 1.6 | 3 | 59 | 38 |
| 9 | 0.0222 | 4.7 | 75 | 45 | 1.6 | 3 | 67 | 30 |
| 10 | 0.0156 | 3.3 | 50 | 34 | 1.5 | 3 | 65 | 32 |
| 11 | 0.0101 | 2.1 | 30 | 16 | 1.9 | 2 | 75 | 23 |
| 12 | 0.0096 | 2.0 | 20 | 9 | 2.1 | 3 | 76 | 21 |
| 13 | 0.0312 | 6.5 | 7 | 3 | 2.2 | 3 | 81 | 16 |
| Total amount extracted | ~96 % | | | | | | | |

Indeed, diagrams of fractions of the microstructural distribution plotted using fractionation data, demonstrate several maximums corresponding to the types of AC with different stereospecificities. There are at least three types of centres with different stereospecific capability: Type 1 forms macromolecules with the content of 1,4-*cis*-structures up to 55–70%; Type 2 synthesises chains with the percentage of 1,4-*cis*-links in the range of 30–45%; Type 3 forms macromolecules with a low content of 1,4-*cis*-structures (15–25%). Variation of polymerisation conditions does not affect the number of forming AC. It shifts, however, the position of maximums in the AC stereospecificity distribution diagram. An increase of monomer conversion and a decrease of catalyst concentration shift the maximums to the area with a higher content of 1,4-*cis*-structures.

Comparison of the kinetic inhomogeneity and fraction microstructure distributions reveals that the third type of centre (which produces polymers with the highest MW) synthesises macromolecules with a higher content of 1,4-*cis*-links (55–70%). The

second type of centre forms macromolecules with a MW ~$10^5$ and a content of *cis*-links of 30–45%. Finally, the first type of AC forms the lowest MW macromolecules with a 15–25% content of *cis*-structures. Centres with a higher reactivity are also more *cis*-stereospecific in this case.

The study of Ti-Al catalytic systems used for isoprene polymerisation revealed three types of AC responsible for the formation of a polymer fraction with a specific MW: Type I - *ln M* = 6.1–9.8; Type II - *ln M* = 10.5–11.8; and Type III - *ln M* = 12.3–15.0 (**Figure 3.40**). The hydrodynamic impact on the Ti-Al catalytic systems, in the turbulent mode, leads to the redistribution of the macromolecule growth centres between various types of AC and a higher activity is demonstrated by the centres responsible for the high MW polyisoprene fraction.

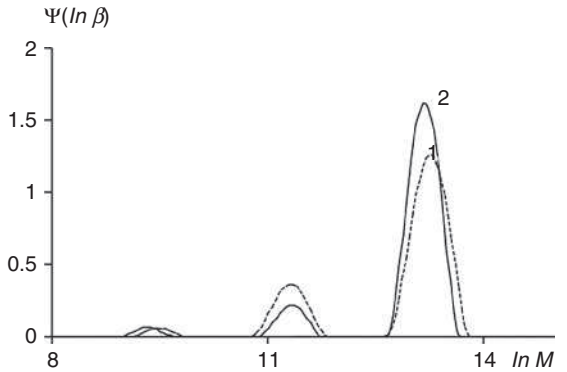


**Figure 3.40** Kinetic activity distribution of macromolecule growth centres in the isoprene polymerisation process with $TiCl_4$-Al($i$-$C_4H_9)_3$-piperylene. 1) traditional method, and 2) hydrodynamic impact on the catalytic system. The yield is 20%

The kinetic activity of the macromolecule growth centres of a specific type is characterised by the S area under the 'Gaussian function' in the distribution curve calculation process (**Figure 3.34**). This area is contributed to by both the concentration of AC and the chain growth reaction rate constant (activity ~ $C_a \times k_p$). Evidently, the kinetic activity value of specific types of macromolecule growth centres depends on their concentration in varied polymerisation conditions. The dependence of the kinetic activity S upon polymer yield, in the isoprene polymerisation process with $TiCl_4$-Al($i$-$C_4H_9)_3$, demonstrates (**Figure 3.41**) a reduction in the fractions of Type I and Type II centres, which produce polymers of low and medium MW. Significant changes of the S value are observed at monomer conversion below 10%. The fraction of Type III centres, responsible for the high MW polymer fraction (*ln M* = 12.3–15.0), grows with process continuation, thus increasing the average MW. In addition, the hydrodynamic impact on a two-component $TiCl_4$-Al($i$-$C_4H_9)_3$ catalytic system, in the turbulent mode, leads to the redistribution between polymerisation centres, which is already observed at low polymer conversions. The

initially formed catalyst has a majority of Type III centres with high catalytic activity, which are responsible for the synthesis of the high MW fraction (*ln M* = 12.3–15.0) and a low number of Type I (*ln M* = 6.1–9.8) and Type II (*ln M* = 10.5–11.8) centres, which form polymer fractions with a lower MW. It results in an increase of the average MW, although the initial total concentration of AC stays constant.

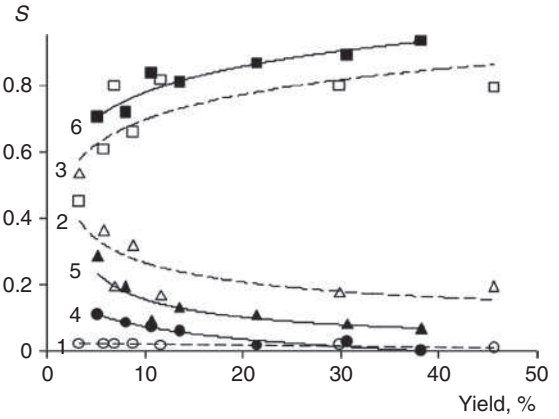


**Figure 3.41** The change of the kinetic activity *S* of different types of macromolecule growth centres I (1, 4), II (2, 5), and III (3, 6) in the isoprene polymerisation process with $TiCl_4$-Al(*i*-$C_4H_9)_3$. 1–3 – traditional method; and 4–6 – hydrodynamic impact on a catalytic system in the turbulent mode (Method 2)

Similar changes of kinetic activity, S, can be observed after the turbulent mode hydrodynamic impact on the modified three-component $TiCl_4$-Al(*i*-$C_4H_9)_3$-piperylene catalytic system. However, an increase of the Type III centre catalytic activity and resulting growth of the average MW is accompanied by an increase of the total number of AC. The tubular turbulent prereactor modification, for the process using the $TiCl_4$-Al(*i*-$C_4H_9)_3$-piperylene catalyst, leads to the growth of the molecular *cis*-1,4-polyisoprene MW due to an increase in the total number of AC. This effect is explained by the grinding of the heterogeneous catalyst and simultaneous redistribution between different types of AC.

A relatively small increase in the total concentration of AC formed by the two-component $TiCl_4$-Al(*i*-$C_4H_9)_3$ catalytic system, prepared in the turbulent mode (Method 3), provides substantial changes in the kinetic activity of the macromolecule growth centres (**Figure 3.41**). The fraction of centres responsible for the high MW polymer fraction also increases, in this case, with the simultaneous reduction of AC responsible for low MW fractions.

The plot of the dependence of the kinetic activity of the macromolecule growth centre, *S*, on monomer conversion (**Figure 3.42**) is similar to the plot describing the 'conversion' growth of MW at a high polymerisation rate and concentration of AC, when a reaction mixture is formed in the turbulent mode (Method 4). The kinetic activity of

the macromolecule growth centres of various types is constant for each polymerisation method used (Methods 1 and 4). However, it requires 15–20 min to get a polymer product with an 80% yield and a MW of $M_w \approx 600000$, $M_n \approx 25000$, when a reaction mixture is formed in the turbulent mode. It requires over 2 h to synthesise a polymer with the aforementioned characteristics using a traditional polymerisation method (without the installation of a turbulent prereactor, it is 8 times more).

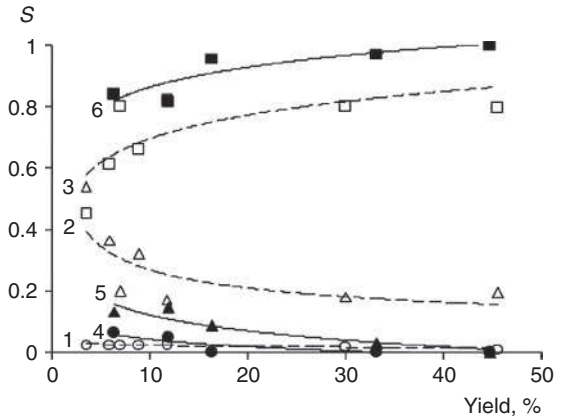


**Figure 3.42** The change of kinetic activity, *S*, of different types of macromolecule growth centres I (1, 4), II (2, 5), and III (3, 6) in the isoprene polymerisation process with the $TiCl_4$-Al(*i*-$C_4H_9)_3$ catalyst. 1–3 – traditional method; and 4–6 – formation of a catalytic system in the turbulent mode (Method 3)

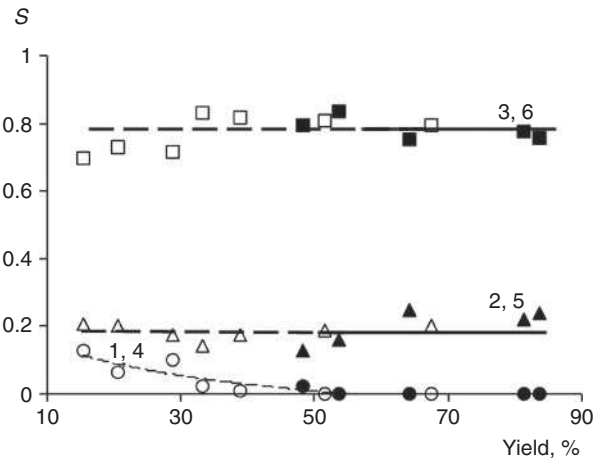


**Figure 3.43** The change of kinetic activity, *S*, of different types of macromolecule growth centres I (1, 4), II (2, 5), and III (3, 6) in the isoprene polymerisation process with the $TiCl_4$-Al(*i*-$C_4H_9)_3$-piperylene catalyst. 1–3 – traditional method; and 4–6 – formation of a catalytic system in the turbulent mode (Method 4)

The solution of the inverse MWD problem using the Tikhonov regularisation method has revealed that the traditional polybutadiene polymerisation process with $TiCl_4$-$Al(i\text{-}C_4H_9)_3$ occurs in the presence of four types of AC. The location of the maximums on the kinetic inhomogeneity curves corresponds to the following intervals of MW values (each type synthesises different polymer fractions): *ln M* = 9.2–10.4 - Type I; 11.2–11.4 - Type II; 12.9–13.2 - Type III; and 14.1–14.7 - Type IV.

The concentration of macromolecule growth centres of Type I and II decreases with conversion growth when the traditional polymerisation method is used, while high molecular weight centres of Type III and IV demonstrate the opposite behaviour (**Figures 3.44–3.47**). Reaction system formation in the turbulent mode (Method 4) results in the elimination of Type I AC, responsible for the synthesis of the low MW polybutadiene fraction (*ln M* = 9.2–10.4). The concentration of Type II AC is significantly higher when a reaction system is formed in the turbulent mode. The fraction of Type III centres changes insignificantly, while the Type IV AC concentration does not change during polymerisation and is lower than when the traditional method is used.

Each type of active centre is characterised by a specific ratio of chain termination and chain growth reaction rates, meaning that it synthesises macromolecules of a specific length. Therefore, the possible explanation of the tubular turbulent prereactor effect on a reaction mixture is that the increase of AC total concentration is not the only reason for polybutadiene MW and MWD changes. Another factor is the change in the number of types of active centre, each having a specific set of kinetic constants. The presence of the low MW fraction in a polymer (which makes the main contribution to the number-average MW value) is caused by the chain-to-monomer and chain-to-aluminium-organic compound transfer reactions, with the maximum values of constants observed for Types I and II AC. The aforementioned types of AC have comparable values of chain transfer reaction rate constants, however, they are significantly different in chain growth reaction rate constants. The hydrodynamic impact on a reaction system leads to a significant increase of Type II active centre concentration, which provides a higher chain growth reaction rate constant than Type I centres (which are eliminated). According to the kinetic chart of the process, this effect results in sustainable values of the number-average MW of polybutadiene in polymerisation processes based on a different method.

The presence of a high MW fraction in a polymer is mainly caused by AC of Types III and IV, their initial concentration in the polymerisation system reduces after the preliminary hydrodynamic impact on a reaction mixture. In addition, the concentration of Type IV centres does not change with conversion of a monomer after the hydrodynamic impact on a reaction mixture in turbulent flows, while the fraction of this type of centre increases when the standard polymerisation method is used (**Figures 3.44–3.47**). Therefore, preliminary formation of a reaction mixture in a turbulent mode leads to the synthesis of a polymer with a lower number-average MW.

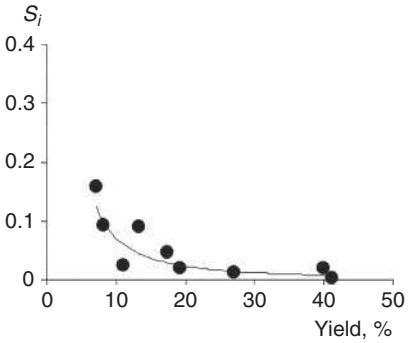


**Figure 3.44** The dependence of kinetic activity of Type I macromolecule growth centres on the yield of polybutadiene synthesised with a $TiCl_4$-Al($i$-$C_4H_9$)$_3$ catalyst. 1) Traditional method; and 2) reaction mixture preliminary formation in turbulent flows (Method 4)

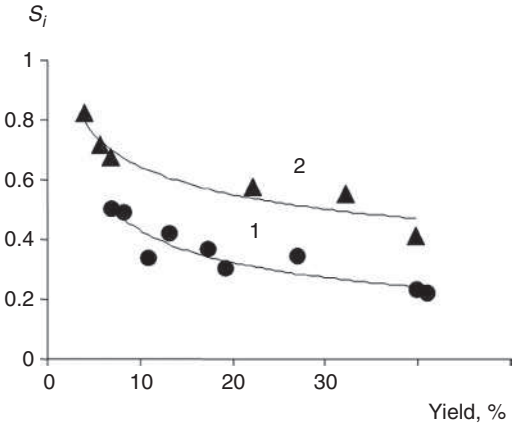


**Figure 3.45** The dependence of kinetic activity of Type II macromolecule growth centres on the yield of polybutadiene synthesised with a $TiCl_4$-Al($i$-$C_4H_9$)$_3$ catalyst. 1) Traditional method; and 2) reaction mixture preliminary formation in turbulent flows (Method 4)

Changes in the kinetic activity distribution of the macromolecule growth centres can be observed in the butadiene polymerisation process when a titanium catalyst is prepared *in situ*. The function $\Psi(ln\ \beta)$ of the studied catalytic system has several maximums, indicating different types of AC in the butadiene polymerisation process and catalytic complex prepared *in situ*, which is directly in the monomer solution. The number of maximums depends on the conversion (**Figure 3.48**). Five different types of AC have been identified for the studied system; each of them is responsible for the synthesis of the polymer fraction with a specific MW: Type I - $ln\ M$ = 7.1–7.8; Type II - $ln\ M$ = 9.4–9.9; Type III - $ln\ M$ = 11.0–12.0; Type IV - $ln\ M$ = 12.7–13.2; and Type V - $ln\ M$ = 14.6–14.8.

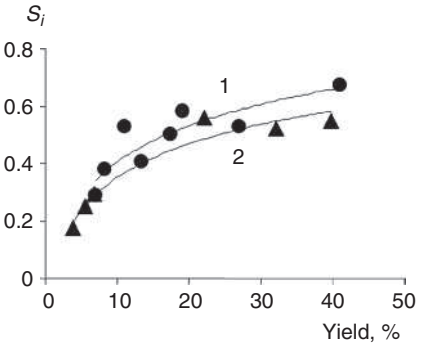


**Figure 3.46** The dependence of kinetic activity of Type III macromolecule growth centres on the yield of polybutadiene synthesised with a $TiCl_4$-$Al(i\text{-}C_4H_9)_3$ catalyst. 1) Traditional method; and 2) reaction mixture preliminary formation in turbulent flows (Method 4)

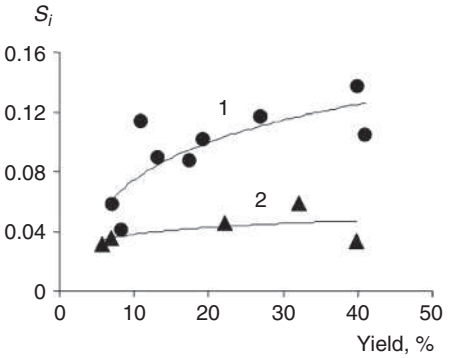


**Figure 3.47** The dependence of kinetic activity of Type IV macromolecule growth centres on the yield of polybutadiene synthesised with a $TiCl_4$-$Al(i\text{-}C_4H_9)_3$ catalyst. 1) Traditional method; and 2) reaction mixture preliminary formation in turbulent flows (Method 4)

Peak analysis of the active centre kinetic inhomogeneity distribution curves reveals that Type I AC (responsible for the polybutadiene fraction with a MW in the range of 2400) only exist in traditional polymerisation processes; disappearing by polymerisation time $\tau_{pol}$ = 20 min. Type II AC are also deactivated by this time. Type V AC (which are responsible for the high MW fraction of a polymer) become active by the polymerisation time of 60 min (~15% conversion). The pattern of the polybutadiene MWD curves is evidently influenced by the wide range of different types of AC, which affect the polymerisation process at all stages.

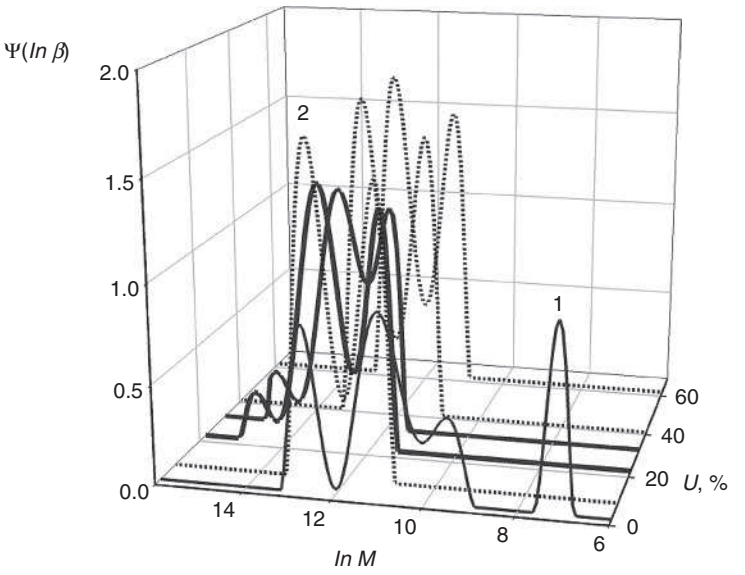


**Figure 3.48** The curves of active centre distribution by kinetic inhomogeneity in the butadiene polymerisation process. 1) Traditional polymerisation method; and 2) formation of AC in turbulent flows

A catalytic system formed in turbulent flows includes AC of Types III and IV (**Figure 3.48**). The polycentrism model of an ionic-coordinative catalytic system predicts that each active centre type is responsible for the synthesis of polymer fractions with the most probable Flory distribution of $M_w/M_n = 2$. Taking this into consideration, we can prove that such a narrow MWD at the initial polymerisation stage is provided by the presence of only two types of AC, formed after the hydrodynamic impact, a situation opposite to the traditional method of polymerisation.

The area of the Gaussian curve obtained when splitting the distribution curves into separate peaks of active centre kinetic activity, corresponds to a multiplication of the AC concentration by the chain growth reaction rate constant (**Figure 3.49**). Formation of AC directly in the reaction mixture volume leads to an increase of activity of the centres responsible for low MW (Types I, II and III), while the activity of growth centres producing macromolecules with high MW (Types IV and V) increases with conversion growth. The mixing intensification, in the fast chemical reaction of the interaction of catalytic system components during polymerisation, leads to a decrease in activity of Type III centres and growth in the activity of Type IV centres.

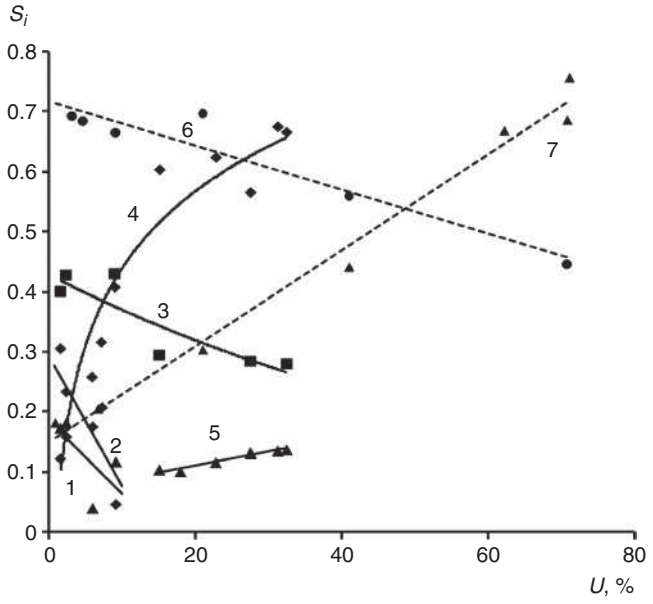


**Figure 3.49** Changes of kinetic activity of macromolecule growth centres. 1 – Type I, 2 – Type II, 3, 6 – Type III, 4, 7 – Type IV, and 5 – Type V. 1, 2, 3, 4, 5 – traditional method; and 6, 7 – formation of AC in turbulent flows

According to the results published in [101, 103], there must be a correlation between the stereospecificity of the catalytic system and changes in the kinetic inhomogeneity of the titanium catalytic system, with an increase of the local level of turbulent mixing at the stage of active centre formation. The hydrodynamic impact on a reaction system at the stage of active centre formation is known to decrease the content of 1,4-*cis*-links and increase the content of 1,4-*trans*-links, compared with the traditional method (**Figure 3.50**). In addition, the proposed polymerisation method leads to a twofold decrease of the 1,2-links content (from 3% to 1.5%) in synthesised polybutadiene. The analysis of kinetic activity distribution changes, obtained for macromolecule growth centres, reveals the possible reason for the effect of the polymerisation method on the stereoregularity of polybutadiene. In particular, the preliminary turbulent mixing of the components of the catalytic complex, increases the fraction of Type III AC, which are most probably responsible for the 1,4-*trans*-addition. The effect is intensified by the absence of Type V centres, which are most probably responsible for the *cis*-addition.

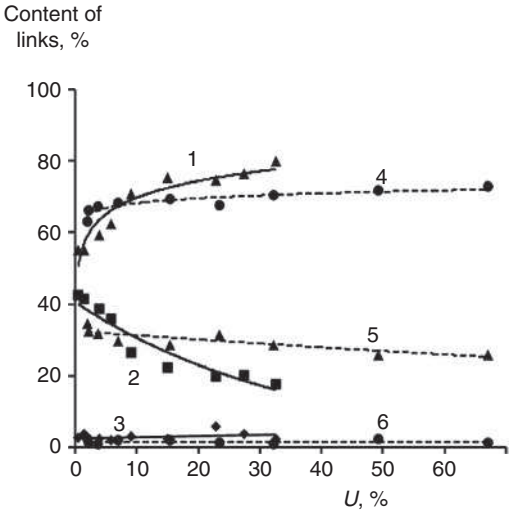


**Figure 3.50** Polybutadiene microstructure. 1, 4 – 1,4-*cis*-links; 2, 5 – 1,4-*trans*-links; and 3, 6 – 1,2-links. 1, 2, 3 – traditional method, and 4, 5, 6 – formation of AC in turbulent flows

A catalyst prepared using the traditional method of mixing, increased the number of *trans*-links at the beginning of the polymerisation process due to a reduced number of *cis*-sequences. The maximum activity at sufficient catalyst exposure (30 min at 0 °C), using traditional polymerisation, corresponds to the following polybutadiene composition: 1,4-*cis* – 78%, 1,4-*trans* – 1%, 1,2-links – 3%. The following explanation can be proposed for this distribution: the initial stage of polymerisation is catalysed by titanium compounds formed in the slowed down process of the formation of three-valent metal compounds in bimetallic AC. This assumption is confirmed by polybutadiene microstructure data obtained during a cationic polymerisation process with various initiators ($TiCl_4$, $SnCl_4$, $AlCl_3$). The polybutadiene product contained a significant number of 1,4-*trans* and 1,2-links. Preparation of the $TiCl_4$-Al(*i*-$C_4H_9)_3$ catalytic complex *in situ* (when the catalytic system components are mixed directly in a reaction mixture at the initial stages of polymerisation) would probably favour the superposition of cationic and stereospecific polymerisation, which explains the unusual microstructure of polybutadiene. From the viewpoint of the polycentrism approach, this effect can be caused by Types I and II AC, responsible for the formation of low molecular weight fractions of polybutadiene and favouring predominant 1,4-*trans*-addition. Further growth of the 1,4-*cis*-sequences content in polybutadiene can be caused by Type V AC. This effect emerges when 15% conversion ($\tau_{pol}$ = 60 min) is reached.

In addition to traditional methods of influencing the catalytic activity and stereospecificity of Ziegler–Natta catalysts in butadiene polymerisation processes (*in situ* and 'separate' preparation, addition of modifiers, and so on), there is an

opportunity to change the hydrodynamic conditions at the stage of *in situ* formation of the titanium catalyst. The fast interaction of the initial catalytic system components, in conditions of intensive turbulent mixing, decreases the duration of the AC formation period, which is slow. Micromixing intensification boosts the nucleation rate in forming a catalytically active precipitate and therefore, decreases the size of the microheterogeneous catalyst particle and increases its specific surface. The growth of active centre concentration and redistribution between their different types, decreases the weight-average and number-average MW, and results in the synthesis of finely dispersed polybutadiene ($M_w/M_n \approx 5–7$). The revealed correlation between the kinetic activity distribution of macromolecule growth centres and their stereospecificity explains the changes of polybutadiene stereoregularity. Direct mixing of the catalyst component provides five different types of growth centres. Types I ($ln\ M = 7.1$) and II AC (lnM = 9.4) (which are responsible for the low MW fraction of a polymer and obviously react *via* the cationic mechanism) produce a polymer with an increased content of 1,4-*trans* links (up to 50–60%). Type III ($ln\ M = 11.0–12.0$) and Type IV centres ($ln\ M = 12.7–13.2$) synthesise a higher MW fraction of polybutadiene with about 70% 1,4-*cis*-links. Finally, Type V AC produce a polybutadiene fraction with the highest MW and maximum content of 1,4-*cis*-links (85–90%). Therefore, the polybutadiene microstructure is affected by the change in the composition of the macromolecule growth centres caused at the initial moment of polymerisation.

Thus, an unconventional method has been revealed for influencing the process behaviour, molecular characteristics and quality of a polymerised dienes (isoprene and butadiene), and ethylene-propylene copolymerisation with Ti-Al, Nd-Al, and V-Al Ziegler–Natta catalytic systems. It is reasonable to separate the fast stage of the formation and initiation of the macromolecule growth centres from the slow stage of olefins or dienes copolymerisation. It can be achieved in the new type of chemical technology equipment: jet-type tubular turbulent reactors, used separately from the volume mixing devices (used for the slow stage) to provide a substantial increase of turbulence level for the fast stage. Such an approach provides a substantial increase of desired molecular characteristics of the formed polymer products and offers opportunities for controlling the types and concentrations of AC participating in polymer synthesis and therefore, reduces catalyst consumption.

The fundamental analysis of fast polymerisation processes in turbulent flows has been carried out in this chapter. Kinetic parameters of polymerisation and polymer-analogous processes become available for calculation as the decrease of diffusion limitations in polymer synthesis reactions is achieved by turbulent mixing intensification in the reaction zone. This approach also opens ways to optimise the molecular characteristics of the forming polymer products, as well as tools to control the entire process. Results of the theoretical description of the turbulent mixing process of a reaction zone in a diffuser-confusor-type reactor provide opportunities for control of fast polymerisation processes.

## References

1. A.A. Berlin and S.A. Volfson in *Kinetic Methods in Polymer Synthesis*, Khimiya, Moscow, Russia, 1973. [In Russian]

2. A.A. Berlin, K.S. Minsker and K.M. Djumaev in *Novel Unified Energy and Resource Efficient High Performance Technologies of Increased Ecological Safety Based on Tubular Turbulent Reactors*, Niitjehim, Moscow, Russia, 1996. [In Russian]

3. A.A. Berlin, J.A. Prochuhan, K.S. Minsker and N.S. Enikolopyan, *Vysokomolekulyarnye Soedineniya*, 1991, **33A**, 2, 243. [In Russian]

4. A.A. Berlin, J.A. Prochuhan, K.S. Minsker, G.G. Aleksanyan, S.V. Grobov and N.S. Enikolopyan, *Vysokomolekulyarnye Soedineniya*, 1988, **30A**, 11, 2441. [In Russian]

5. A.A. Berlin, J.A. Prochuhan, K.S. Minsker, J.A. Tumanyan, G.G. Aleksanyan and N.S. Enikolopyan, *Vysokomolekulyarnye Soedineniya*, 1988, **30A**, 11, 2436. [In Russian]

6. K.S. Minsker, A.A. Berlin, Ju.A. Prochuhan, Je.A. Tumanyan, M.M. Karpasas and N.S. Enikolopyan, *DAN SSSR*, 1986, **291**, 1, 114.

7. K.S. Minsker and A.A. Berlin in *Fast Polymerization Processes*, Gordon and Breach Publishers, Amsterdam, Netherlands, 1996.

8. K.S. Minsker and J.A. Sangalov in *Isobutylene and its Polymers*, Khimiya, Moscow, Russia, 1986. [In Russian]

9. Z.M. Borovkova, L.V. Kosmodemyanskiy and E.P. Kopylov in *Synthesis and Properties of Piperylene-Based Polymers*, Cniitjeneftehim, Moscow, Russia, 1983. [In Russian]

10. F.N. Kapuckiy and V.P. Mardykin in *Cationic Oligomer of Piperylene: Synthesis, Properties and Application*, Izd. BGU, Minsk, Belorussia, 1997.

11. I.R. Mullagaliev and J.B. Monakov, *Vysokomolekulyarnye Soedineniya*, 2002, **44C**, 2251. [In Russian]

12. R.M. Livshits and L.A. Dobrovinskiy in *Vegetable Oil Substitutes in Paint and Varnish Industry*, Khimiya, Moscow, Russia, 1987. [In Russian]

13. J.B. Monakov and A.G. Tolstikov in *Catalytic Polymerization of 1,3-Dienes*, Nauka, Moscow, Russia, 1990.

14. N.N. Sigaeva, V.G. Kozlov, K.V. Nefediev, O.I. Kozlova, T.S. Usmanov, E.A. Shirokova and J.B. Monakov, *Bashkirskiy Khimicheskiy Zhurnal*, 1998, **5**, *5*, 31. [In Russian]

15. V.A. Babkin, G.E. Zaikov and K.S. Minsker in *Quantum Chemical Aspects of Cationic Polymerization of Olefins*, Gilem, Ufa, Russia, 1996. [In Russian]

16. V.P. Mardykin, S.G. Morozova, L.V. Gaponik and L.D. Chuprakova, *Zhurnal Prikladnoy Khimii*, 1998, **71**, 6, 1041. [In Russian]

17. K.S. Minsker, V.P. Zakharov, I.R.Mullagaliev, J.B. Monakov and A.A. Berlin, *Zhurnal Prikladnoy Khimii*, 200, **73**, 11, 1895. [In Russian]

18. K.S. Minsker, A.A. Berlin, V.P. Zakharov and G.E. Zaikov in *Fast Liquid-phase Processes in Turbulent Flows*, Brill Academic Publishers, Amsterdam, Netherlands, 2004.

19. V.P. Zakharov, A.A. Berlin, Y.B. Monakov and G.E. Zaikov, *Journal of the Balkan Tribological Association*, 2005, **11**, 1, 65.

20. K.S. Minsker, A.A. Berlin, R.Y. Deberdeev and S.R. Ivanova, *Khimicheskaya Promyshlennost*, 2000, **11**, 26. [In Russian]

21. A.A. Berlin, K.S. Minsker and R.Y. Deberdeev, *Doklady Akademii Nauk*, 2000, **375**, 2, 218. [In Russian]

22. V.M. Busygin, R.T. Shiyapov, N.I. Uhov, A.S. Ziyatdinov, K.S. Minsker, V.P. Zaharov, A.A. Berlin, G.S. Dyakonov and R.Y. Deberdeev, K*himiya v Interesah Ustojchivogo Razvitiya*, 2003, **11**, 843. [In Russian]

23. I.V. Garmonov in *Synthetic Rubber*, Khimiya, Leningrad, Russia, 1983. [In Russian]

24. A.A. Doncov, G.Ya. Lozovik and S.P. Novickaya in *Chlorinated Polymers*, Khimiya, Moscow, Russia, 1979. [In Russian]

25. P.A. Kirpichnikov, V.V. Beresnev and L.M. Popova in *Flowcharts of Major Industrial Technologies of Synthetic Rubber Production*, Khimiya, Leningrad, Russia, 1986. [In Russian]

26. L.A. Oshin in *Industrial Chlorine-Organic Products*, Khimiya, Moscow, Russia, 1978. [In Russian]

27. K.S. Minsker, R.F. Gataullin, V.V. Lisickiy, I.S. Beresneva, S.B. Salnikov and V.S. Shmarlin, *Vysokomolekulyarnye Soedineniya*, 1983, **25A**, 8, 1686. [In Russian]

28. K.S. Minsker, R.F. Gataullin, V.M. Yanborisov, T.A. Krasnova, S.B. Sal'nikov and V.S. Shmarlin, *Vysokomolekulyarnye Soedineniya*, 1984, **26**, 4, 781. [In Russian]

29. K.S. Minsker, V.P. Zaharov, A.A. Berlin and J.B. Monakov, *Vestnik Bashkirskogo Universiteta*, 2004, **2**, 8. [In Russian]

30. K.S. Minsker, A.A. Berlin, R.H. Rakhimov, P.I. Kutuzov and V.P. Zakharov, *Zhurnal Prikladnoy Khimii*, 1999, **72**, 6, 996. [In Russian]

31. R.G. Tahavutdinov, A.G. Muhametzyanova, G.S. Dyakonov, K.S. Minsker and A.A. Berlin, *Vysokomolekulyarnye Soedineniya*, 2002, **44A**, 7, 1094. [In Russian]

32. R.G. Tahavutdinov, G.S. Dyakonov, A.G. Muhametzyanova, V.P. Zaharov and K.S. Minsker, *Khimicheskaya Promyshlennost*, 2002, **1**, 22. [In Russian]

33. K.S. Minsker, V.P. Zaharov, A.A. Berlin and J.B. Monakov, *Doklady Akademii Nauk*, 2001, **381**, 3, 373. [In Russian]

34. V.P. Zaharov, I.V. Sadykov, K.S. Minsker, A.A. Berlin and J.B. Monakov, *Vysokomolekulyarnye Soedineniya*, 2004, **46B**, 10, 1765. [In Russian]

35. V.P. Zaharov, I.V. Sadykov, K.S. Minsker, A.A. Berlin and J.B. Monakov, *Zhurnal Prikladnoy Khimii*, 2004, **77**, 2, 302. [In Russian]

36. K.S. Minsker, V.P. Zaharov, I.V. Sadykov, I.A. Ionova, A.A. Berlin and J.B. Monakov, *Vestnik Bashkirskogo Universiteta*, 2003, **3-4**, 26. [In Russian]

37. A.G. Muhametzyanova, G.Z. Sahapov, G.S. Dyakonov, R.G. Tahavutdinov and L.M. Kurochkin in *Interuniversity Subject Collection 'Heat and Mass Exchange Processes and Machinery of Chemical Technology'*, KGTU, Kazan, Russia, 1995. [In Russian]

38. L.N. Braginskiy, V.I. Begachev and V.M.Barabash in *Agitation of Liquid Media: Physical Foundations and Engineering Methods of Calculation*, Khimiya, Leningrad, Russia, 1984. [In Russian]

39. V.P. Budtov and V.V. Konsetov in *Heat and Mass Transfer in Polymerization Processes*, Khimiya, Leningrad, Russia, 1988. [In Russian]

40. V.I. Kimelblat, M.G. Hakimov, I.G. Chebotareva and S.I. Volfson, *Mechanics of Composite Materials*, 1998, **34**, 4, 531. [In Russian]

41. N.M. Chirkov, P.E. Matkovskiy and F.S. Dyachkovskiy in *Polymerization with Complex Metal Organic Catalysts*, Khimya, Moscow, Russia, 1976. [In Russian]

42. S.A. Buder, G.A. Perlin, V.V. Solodskiy and L.S. Jegova, *Promyshlennost SK*, 1983, **7**, 9. [In Russian]

43. V.P. Zakharov, A.A. Berlin, Y.B. Monakov and G.E. Zaikov, *Journal of the Balkan Tribological Association*, 2005, **11**, 1, 145.

44. T.V. Bashkatov and Y.L. Zhitalin in *Synthetic Rubber Technology*, Khimiya, Leningrad, Russia, 1987. [In Russian]

45. V.A. Grechanovskiy, L.G. Andrianova, L.V. Agibalova, A.S. Estrin and I.Y. Poddubniy, *Vysokomolekulyarnye Soedineniya*, 1980, **22A**, 9, 2112. [In Russian]

46. V.A. Grechanovskiy and I.Y. Poddubniy, *Vysokomolekulyarnye Soedineniya*, 1974, **15B**, 12, 875. [In Russian]

47. A.S. Muzhaj, L.S. Bresler, V.A. Grechanovskiy and I.Y. Poddubniy, *Doklady Akademii Nauk SSSR*, 1968, **180**, 4, 920. [In Russian]

48. V.P. Zaharov, A.A. Berlin and J.B. Monakov, *Zhurnal Prikladnoy Khimii*, 2005, **78**, 5, 779. [In Russian]

49. J.B. Monakov and N.N. Sigaeva, *Vysokomolekulyarnye Soedineniya*, 1974, **43C**, 9, 1667. [In Russian]

50. B.A. Dolgoplosk and E.I. Tinyakova, *Vysokomolekulyarnye Soedineniya*, 1994, **36A**, 10, 1653. [In Russian]

51. L. Porri, A. Dzharusso and D. Richchi, *Vysokomolekulyarnye Soedineniya*, 1994, **36A**, 10, 1698. [In Russian]

52. Z.M. Sabirov, V.N. Urazbaev, V.P. Efimov, I.R. Mullagaliev and J.B. Monakov, *Doklady Akademii Nauk*, 2000, **372**, 5, 635. [In Russian]

53. Z.M. Sabirov, V.N. Urazbaev and J.B. Monakov, *Vysokomolekulyarnye Soedineniya*, 1997, **39A**, 1, 150. [In Russian]

54. G. Natta, *Journal of Polymer Science*, 1959, **34**, 21.

55. W.R. Schmeal and J.R. Street, *Journal of Polymer Science, Part C: Polymer Physics Edition*, 1972, **10**, 2173.

56. E.I. Vizen and J.V. Kissin, *Vysokomolekulyarnye Soedineniya*, 1969, **11A**, 8, 1774. [In Russian]

57. J.A. Fushman, A.D. Margolin, S.S. Laloyan and V.J. Lvovskiy, *Vysokomolekulyarnye Soedineniya*, 1995, **37B**, 9, 1589. [In Russian]

58. J.G. Frolov in *Colloidal Chemistry Course: Surface Phenomena and Disperse Systems*, Khimya, Moscow, Russia, 1989. [In Russian]

59. B.A. Dolgoplosk and E.I. Tinyakova in *Metal Organic Catalysis in Polymerization Processes*, Nauka, Moscow, Russia, 1985. [In Russian]

60. D. San, H. Siew, P. Courtine, J.C. Yannel, D. Lalart and K. Buyadoux, *European Polymer Journal*, 1986, **22**, 89.

61. I.A. Yaber, K. Hauschild and G. Fink, *Macromolecular Chemistry*, 1990, **191**, 9, 2067.

62. J.P. Kennedy and E. Marechal in *Carbocationic Polymerization*, Wiley, New York, NY, USA, 1982.

63. A. Hernandez, J. Semel, H.C. Broecker, H.G. Zachman and H. Sinn, *Macromolecular Chemistry, Rapid Communications*, 1980, **1**, 2, 75.

64. L.V. Shcheglova, N.I. Pakuro and A.A. Arest-Yakubovich, *Macromolecular Chemistry Physics*, 1998, **199**, 1025.

65. M. Camps, R. Ait-Hamouda, S. Boilean, P. Hemery and R.W. Lenz, *Macromolecules*, 1988, **21**, 4, 891.

66. F. Chen and S. Ying in *Mechanics and Kinetics of Polymer Reactions and their Use in Polymer Synthesis: International Symposium Honored Professor Pierre Sigwalt Occas*, Paris, France, 1990.

67. L. Liang, S. Guo and S. Ying, *Gaodjen Sjujeslo Huasjuje Sjujebao, Chimia Universal*, 1988, **9**, 4, 384.

68. V. Bussio, R. Corradini, A. Ferraro and A. Proto, *Macromolecular Chemistry*, 1986, **187**, 5, 1125.

69. V.G. Kozlov, K.V. Nefediev, Y.G. Marina, J.B. Monakov, A.V. Kuchin and S.R. Rafikov, *Doklady Akademii Nauk SSSR*, 1988, **299**, 35, 652. [In Russian]

70. S. Cozewith and G. Verstate, *Macromolecules*, 1971, **4**, 4, 482.

71. T.E. Nowlin, Y.V. Kissin and K.P. Wagner, *Journal of Polymer Science*, 1988, **26**, 3, 755.

72. P. Locatelli, M.C. Socchi, I. Tritto and G. Zannoni, *Macromolecular Chemistry, Rapid Communications*, 1988, **9**, 8, 575.

73. J.C. Chudwiyek, A. Miedema, B.I. Rusch and O. Sudmeiyer, *Macromolecular Chemistry*, 1992, **193**, 6, 1463.

74. Y. Wu, X. Jing, H. Hu and W. Zhang, *Chinese Journal of Applied Chemistry*, 1987, **4**, 3, 70.

75. A.G. Azizov, F.A. Nasyrov and B.C. Aliev, *Vysokomolekulyarnye Soedineniya*, 1987, **29A**, 2, 388. [In Russian]

76. P.M. Hairullina, N.G. Marina, O.I. Kozlova, N.V. Duvakina, N.N. Sigaeva, V.G. Kozlov and J.B. Monakov, *Vysokomolekulyarnye Soedineniya*, 1991, **33A**, 6, 463. [In Russian]

77. V.I. Valuev, A.S. Iestrin, R.A. Shlyahter, I.V. Garmonov, A.S. Hachaturov and E.E. Avstriyskaya, *Vysokomolekulyarnye Soedineniya*, 1978, **20B**, 7, 512. [In Russian]

78. G. Sauvet, M. Moreau and P. Sigwalt, *Macromolecular Chemistry, Macromolecular Symposium*, 1986, **3**, 33.

79. M.P. McDaniel and M.M. Johnson, *Macromolecules*, 1987, **20**, 4, 773.

80. E.I. Vizen and F.I. Yakobson, *Vysokomolekulyarnye Soedineniya*, 1978, **20A**, 4, 927. [In Russian]

81. A.V. De Carvalho, P.E. Gloor and A.E. Hamielec, *Polymer*, 1989, **30**, 2, 280.

82. F. Bonini, G. Storti, M. Morbidelli and S. Carra, *Gazzetta Chimica Italiana*, 1996, **126**, 2, 75.

83. J.A.J. Honing, P.E. Gloor, J.F. Macgrigor and A.E. Hamielec, *Journal of Applied Polymer Science*, 1987, **34**, 2, 829.

84. A.L. Zak, B.A. Perlin, P.P. Shpakov, I.I. Ermakova, B.C. Ryahovskiy, B.T. Drozdov and M.A. Eremina, *Zhurnal Prikladnoy Khimii*, 1986, **59**, 1, 227. [In Russian]

85. J.A. Prochuhan, K.S. Minsker, A.A. Berlin, M.M. Karpasas, V.Z. Kompaniec, A.A. Konoplev and N.S. Enikolopyan, *Doklady Akademii Nauk SSSR*, 1988, **298**, 6, 1428. [In Russian]

86. K.S. Minsker, M.M. Karpasas and G.E. Zaikov, *Uspehi Himii*, 1986, **55**, 1, 29. [In Russian]

87. K.S. Minsker and M.M. Karpasas, *Teoreticheskaya i Eksperimentalnaya Khimiya*, 1986, **22**, 2, 160. [In Russian]

88. K.S. Minsker, J.A. Sangalov, O.A. Ponomorev and V.M. Yanborisov, *Vysokomolekulyarnye Soedineniya*, 1980, **22A**, 10, 2259. [In Russian]

89. K.S. Minsker and M.M. Karpasas, *Doklady Akademii Nauk SSSR*, 1985, **283**, 5, 1201. [In Russian]

90. T. Keii, *ProcLamations of International Symposium 'Recent Developments in Olefin Polymer Catalysis'*, 1990, p.1.

91. L.A. Novokshonova, N.Y. Kovaleva, U.A. Gavrilov, V.A. Krasheninnikov, I.O. Leipunskii, A.N. Zhigach, M.N. Larichev and M.V. Chebunin, *Polymer Bulletin*, 1997, **39**, 59.

92. V.P. Budtov, Y.G. Zotikov, E.L. Ponomareva and M.I. Gandelsman, *Vysokomolekulyarnye Soedineniya*, 1985, **27A**, 5, 1094. [In Russian]

93. A.N. Tihonov and V.Y. Arsenin in *Methods of Solution of Improperly Posed Problems*, Nauka, Moscow, Russia, 1986. [In Russian]

94. A.N. Tihonov, A.V. Goncharskiy, V.V. Stepanov and A.G. Yagola in *Chislennye Metody Resheniya Nekorrektnyh Zadach*, Nauka, Moscow, Russia, 1986. [In Russian]

95. S.Y. Frenkel in *Introduction to a Statistic Theory of Polymerization*, Nauka, Moscow, Russia, 1986. [In Russian]

96. N.N. Sigaeva, T.S. Usmanov, E.A. Shirokova, V.P. Budtov, S.I. Spivak and J.B. Monakov, *Doklady Akademii Nauk*, 1999, **365**, 2, 221. [In Russian]

97. N.N. Sigaeva, T.S. Usmanov, V.P. Budtov, S.I. Spivak and J.B. Monakov, *Vysokomolekulyarnye Soedineniya*, 2000, **42B**, 1, 112. [In Russian]

98. N.N. Sigaeva, E.A. Shirokova, I.R. Mullagaliev, I.A. Ionova, V.P. Budtov and J.B. Monakov, *Vysokomolekulyarnye Soedineniya*, 2000, **42A**, 8, 1269. [In Russian]

99. K.S. Minsker, O.A. Ponomarev, M.M. Karpasas, G.S. Lomakin and J.B. Monakov, *Vysokomolekulyarnye Soedineniya*, 1982, **24A**, 7, 1360. [In Russian]

100. Y.B. Monakov, N.N. Sigaeva and V.N. Urazbaev in *Active Sites of Polymerization. Multiplicity: Stereospecific and Kinetic Heterogeneity*, Brill Academic Publishers, Leiden, Netherlands, 2005.

101. A.R. Gareev, N.N. Sigaeva, I.R. Mullagaliev, E.A. Gluhov and J.B. Monakov, *Doklady Akademii Nauk*, 2005, **404**, 5, 646. [In Russian]

102. N.G. Marina, J.B. Monakov, S.R. Rafikov and V.I. Ponomarenko, *Uspehi Himii*, 1983, **52**, 733. [In Russian]

103. N.N. Sigaeva, A.R. Gareev, I.R. Mullagaliev, E.A. Gluhov and J.B. Monakov, *Vysokomolekulyarnye Soedineniya*, 2007, **49A**, 1, 1. [In Russian]

# 4 Synthesis of Low Molecular Weight Compounds through Fast Reactions in Turbulent Flows

As mentioned previously, fast liquid-phase polymerisation processes are characterised by the reaction time, which may be equal to or shorter than the mixing time of the initial components. One of the most important results of the investigation of these processes is evidence of several macroscopic process modes. Each of the modes is characterised by certain temperature field structures and reactant concentrations and therefore, different reaction fronts and rates [1–3].

The mechanisms of fast processes, during polymer synthesis, are the same for all low molecular weight (MW) compounds, including the chlorination and hydrochlorination of ethylene, sulfuric acid alkylation of paraffins by olefins, neutralisation of acid and alkali media, and so on. Thus, the formation of different macroscopic types, during fast chemical reactions, is a common phenomenon which can be observed in almost all fast chemical processes, including the interaction of low MW compounds.

## 4.1 Formation of Mixing and Reaction Front Macrostructures

It is possible to observe the formation of five macroscopic reaction fronts (**Figure 4.1**) [4–6] in a tubular turbulent reactor, during the low MW reaction of KSCN and $FeCl_3$ ($k = 10^4$ l/mol·s) aqueous solutions, with the formation of a coloured product.

The torch is similar to the local torch mode, where the boundaries of the reaction front broaden while flowing along the reactor axis from the introduction point of the axis flow (**Figure 4.1a**).

The planar reaction front is a macroscopic structure, which is perpendicular or inclined to the reactor axis. This structure is similar to the quasi-plug flow mode in turbulent flows (**Figure 4.1b**).

The drift is formed due to the stagnation regions before the reactant introduction point; in this case, the process takes place in the whole reactor volume due to the strong reverse diffusion of the reactant flows (**Figure 4.1c**).

The wave is a stable structure which spreads from the introduction point of the main flow into the mixing zone, along the *x*-coordinates, in the form of a wave without any transversal diffusion (**Figure 4.1d**).

The cord is a macrostructure in the form of double reflex waves oscillating at a high frequency and spreading along the *x*-axis, with the amplitude exceeding the diameter of the main flow supply branch pipe (**Figure 4.1e**); it is here that the intensive axial rotation occurs.

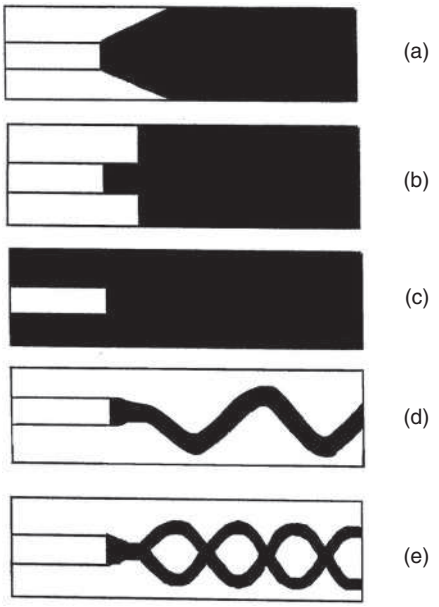


**Figure 4.1** Formation of reaction front macroscopic structures during the synthesis of low MW compounds; a – torch; b – plane front; c – drift; d – wave; and e – cord

It is important to note that the method of reactant introduction (**Figure 4.2**) and the ratio of the linear rates of the $V_1$ central and $V_2$ side flows (**Table 4.1**) play a key role in the reaction front formation.

The plane front is the most favourable type for fast chemical reactions with low MW compounds. This mode is intermediate between the torch and drift, due to the strongly developed turbulence in reactant mixing zone 1 (coaxial supply) and zone 2 (radial supply). The plane front is characterised by the homogeneity of the reaction flow composition along the reactor radius, which is typical of the quasi-plug flow mode in turbulent flows.

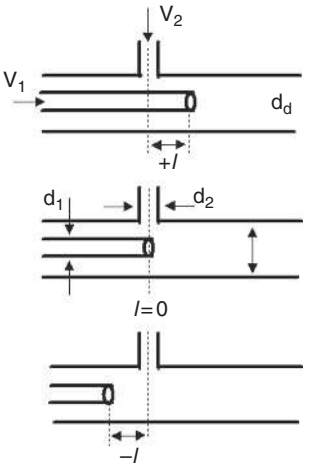


**Figure 4.2** Flow chart of the introduction of two liquid flows into a tubular turbulent reactor

**Table 4.1 Reaction fronts depending on reactant introduction method**

| Reactant introduction method | $V_1/V_2$ | Reaction front type |
|---|---|---|
| *+l* | 0.5–1.5 | Torch |
| | 1.5–2.0 | Mixed (torch and plane front) |
| | 2.0–5.0 | Torch |
| | 5.0–8.0 | Mixed (plane front and drift) |
| | >8.0 | Drift |
| *l = 0* | >1.5 | Plane front |
| | 1.5–2.0 | Mixed (plane front and drift) |
| | >2.0 | Drift |
| *-l* | 0.5–25 | Drift |

The quasi-plug flow mode (plane front of reaction) is the most important condition for commercial production. The conditions of its creation were analysed and the mixing process of the two reacting liquids, within the $K$-$\varepsilon$ turbulence model, was mathematically simulated [7]. The results showed that during fast chemical reactions, the quasi-plug flow mode in turbulent flows is obtained due to the carry-over of the initial component mixture and/or reaction products into the reactant introduction

zone. This carry-over occurs because of the stationary vortex which appears due to the difference in the flow rates (pressure gradients). Indeed, comparison of the ratio rates in the $V_1$ central and $V_2$ side flow branch pipes, and conditions for the formation of macrostructures (fronts of mixing) shows that with an increase of the $V_2$ side flow rate, the transition between the modes occurs in the following order: drift → torch → plane front. With an increase of $V_2$, the distance from the end of the central branch pipe $l$ increases, starting from negative values for the drift mode, moving through zero, and finally, obtaining positive values for the torch mode. An increase of the central flow rate leads to the reverse sequence of transition between the modes and change of distance $l$.

The pattern of the liquid flow motion in tubular turbulent reactors, of the described construction, can be represented in the form of a central jet (the flow introduced through the central branch pipe) flushing either into the 'dead leg' or the plane perpendicular to the reactor axis (**Figure 4.3**). In this case, the reverse currents form a plane front perpendicular to the reactor axis. The increase of the side flow rate is equal to the movement of the 'dead leg' along the reactor axis, away from the point of the central flow introduction. In this case, the reverse currents attenuate and the transition between the fronts occurs in the following order: drift → plane front→ torch. Any further increase of $V_2$ (the movement of the 'dead leg' away from the point of the central flow introduction) leads to the formation of 'wave' and 'cord' type macrostructures in the reactor, and eventually to unstable macroformations. This assumption is confirmed by the approach of the reactor mode to plug flow (the values of the Bodenstein number, Bo, increase). An increase of the central flow rate is comparable to the 'dead leg' approaching the reactant introduction point along the reactor axis.

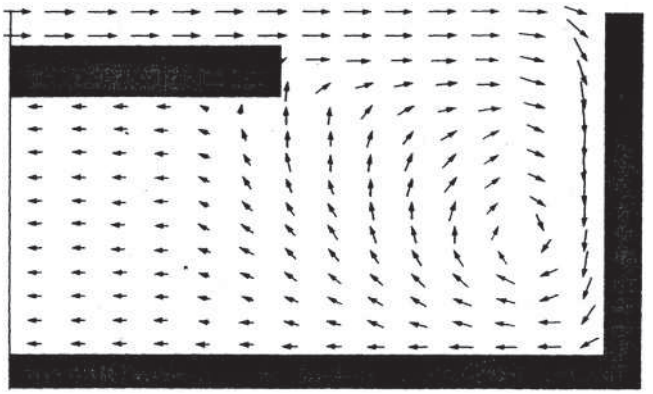

**Figure 4.3** Vector field of rates ($V$ = 40 m/s) for a stationary turbulent flow, flushing into the 'dead leg', at 180° turning

At the same time, we should not ignore the possibility of the quasi-plug flow mode formation in turbulent flows, during fast chemical reactions, due to the 'cut-out' of the central part of the torch, the lateral dimensions of which are much larger than the reactor diameter (**Figure 4.4**) [6].

The 'torch' front and 'plane' front are also formed during the simple mixing of coloured flows without any chemical reactions [8–11]. Thus, these fronts of liquid flow mixing can appear both during fast chemical reactions and without any reactions. This fact led to further investigation into the influence of the reaction rate constant on the conditions of quasi-plug flow mode formation in turbulent flows (plane front of reaction). Solutions of reactants were prepared which interacted with each other, at different rate constants, with the formation of coloured products; these solutions were introduced into the tubular reactor for the formation of reaction front macrostructures. The second-order reactions, which occur at rate constants in the range of $k = 10^2$–$10^8$ l/mol·s, were studied:

$$HCl + NaOH \rightarrow NaCl + H_2O\,(k = 10^8\,l/mol \cdot s)$$

$$3KSCN + FeCl_3 \xrightarrow{H^+} Fe(SCN)_3 + 3KCl\,(k = 10^4\,l/mol \cdot s)$$

$$3KSCN + FeCl_3 \rightarrow Fe(SCN)_3 + 3KCl\,(k = 10^2\,l/mol \cdot s)$$

$$K_4[Fe(CN)_6] + FeCl_3 \rightarrow KFe[Fe(CN)_6] + 3KCl\,(k = 10^2\,l/mol \cdot s)$$

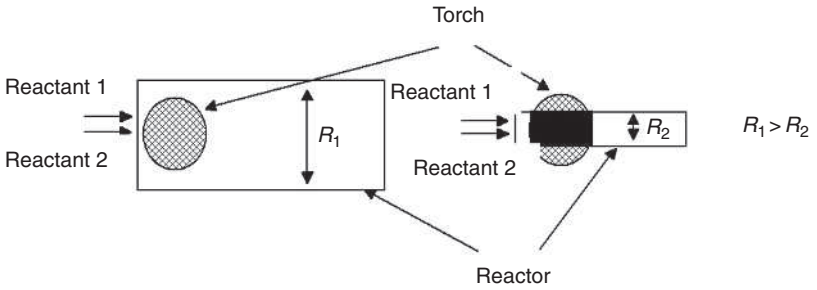


**Figure 4.4** Formation of a 'plane' front of reaction during 'cut-out' of the central part of the torch, the lateral dimensions of which are much larger than the reactor diameter

The chemical process appeared to make a substantial contribution to the conditions of the corresponding macroscopic reaction front formation, during the mixing of the

reaction flows [12]. Therefore, the requirements for the hydrodynamic conditions of the macroscopic structure formation decrease: an increase of the chemical reaction rate is similar to an increase of the turbulence level in the reaction zone, which improves the mixing of the reactants (**Figure 4.5**). Consequently, the lower boundaries of the macrostructures are characterised by the lower values of $V_1/V_2$. Quantitatively, for the lower boundary of the quasi-plug flow mode formation, during fast chemical reactions of the second order, the following ratio is correct (at $d_1/d_d = 0.44$):

$$V_1 / V_2 = -0.07 \lg k + 1.6 \quad (2 < \lg k < 8) \tag{4.1}$$

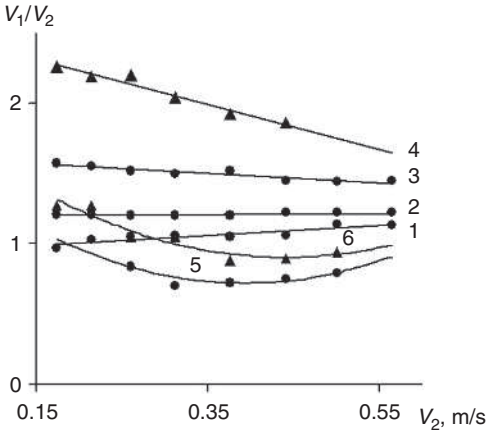


**Figure 4.5** Conditions for formation of plane front (1–4) and torch (5, 6) during the following reactions: neutralisation (1); interaction of potassium thiocyanate and iron chloride in acid (2) and neutral (3, 5) media; mixing of methyl green solution and water (4, 6). ($d_1/d_d = 0.44$, $d_1$ is the diameter of the central branch pipe, $d_d$ is the diameter of the cylindrical turbulent reactor)

Analysis of the conditions for the transition from torch mode to quasi-plug flow mode during the reaction of low MW compounds:

$$R_{cr} = \sqrt{D_{\text{turb}} / k[C]^{n-1}} \tag{4.2}$$

reveals that upon increasing the chemical reaction rate constant value k, and the reactant concentration, the $R_{cr}$ values decrease. The decrease of $R_{cr}$ as the quasi-plug flow formation criterion, in turbulent flows, provides the decrease of the $D_{\text{turb}}$ value defined by the linear rate of the reaction flow motion and the $V_1/V_2$ ratio.

An increase of the reaction order can change the requirements of the plane front formation in both directions: the $R_{Kr}$ values decrease at [C] >1 and increase at [C] < 1.

Fast chemical reaction conditions also change the conditions of the reaction torch front lower boundary formation (**Figure 4.5**, points 5, 6). With an increase of the chemical reaction constant value k, the ratio of the linear rates of the reactant supply to the reactor, necessary for the torch mode lower boundary formation, decreases. The kinetic parameters of the chemical reaction, in this case, the rate constants, do not change the area where the corresponding macrostructures are formed. The ratio of rates $V_1/V_2$, necessary for torch mode and quasi-plug flow mode formation, shifts to the area of their smaller values.

It is interesting to note that calculations of turbulent flows during fast chemical reactions, predicted that the chemical reaction rate constant influences the effective diffusion coefficient and accelerates micromixing, due to an increase of the local reactant concentration gradients [13]. The dependence of the lower boundaries of the reaction front macrostructure formation, in particular, the plane and the torch front, which characterise different scales of liquid flow mixing, on the values of the chemical reaction constants is experimental evidence of the correlation between the kinetic and diffusive parameters of the process. At the same time, one can suppose that the formation of the characteristic reaction front macrostructures is defined by the mixing at the macro- and microlevels.

Changes in the density and viscosity of the liquid flow, introduced into the tubular turbulent reactor, influence the conditions of the reaction plane front formation. An increase in the density of at least one of the reactants or solvent results in a decrease of the required ratio of the linear rates $V_1/V_2$, necessary for the quasi-plug flow mode formation in turbulent flow (**Figure 4.6**). An increase in the viscosity of the liquid flow is accompanied by an increase of the $V_1/V_2$ ratio, i.e., for effective mixing in the tubular turbulent reactor and its optimal operation, reactants with different viscosities should be introduced at a higher $V_1$ axial flow rate (**Figure 4.7**). The influence of the density and viscosity of the mixing (reacting) flow on the formation of the reaction plane front, which defines the stability of the process in turbulent flow, can be described by the following dependencies:

$$V_1 / V_2 = -5.9 \times \rho + 8.2 \tag{4.3}$$

$$V_1 / V_2 = 1.07 \times \mu + 6.2 \tag{4.4}$$

Where:

$\rho$ = 1–1.2 g/sm$^3$

$d_1/d_d$ = 0.44

$\mu$ = 1–6 mPa·s

$d_1/d_d$ = 0.13

As opposed to the kinetic parameters of the chemical process, changes in the density and viscosity of the liquid flow do not influence the conditions of the reaction plane front formation (**Figures 4.6** and **4.7**). An increase in the density of the flow due to a decrease of the lower boundary of the $V_1/V_2$ ratio, necessary for plane front formation, and the constancy of the $V_1/V_2$ ratio, necessary for the torch front lower boundary formation, result in the shrinkage of the low efficient torch mode formation area, thus expanding the opportunities for the application of tubular turbulent reactors in the optimal mode of quasi-plug flow (quasi-isothermal mode). In general, an increase in the density of the liquid flow results in the tubular turbulent reactors working in a more stable manner during the highly efficient quasi-plug flow mode.

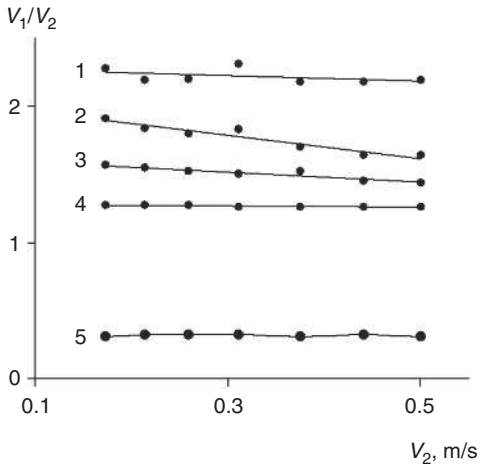


**Figure 4.6** Conditions for the formation of the reaction torch front (5) and plane front (1–4) depending on the flow density: 1.02 (1); 1.07 (2); 1.12 (3); 1.19 (4); and 1.02, 1.07, 1.12, 1.19 (5), g/sm$^3$ ($d_1/d_d$ = 0.44)

These observations can be explained by the influence of the liquid flow density and viscosity on the turbulence level, defined in the first approximation by the Reynolds Number (Re). In particular, an increase of the density value for the reactant flow in motion, leads to an increase of the Re values, i.e., the hydrodynamic similarity of the system changes. In order to form the quasi-plug flow mode in the reactor after a change in the reactant density, it is necessary to reach the previous Re values, which may be possible due to a decrease in the linear rate of the liquid motion $V$, or due to a decrease of the reactor diameter $D$, and increase of the system viscosity. The hydrodynamic similarity of the system and the quasi-plug flow mode are reached due to the decrease of the $V_1/V_2$ ratio (a decrease of the axial flow rate). In much the same way, it is possible to explain the influence of viscosity on the conditions of plane front formation.

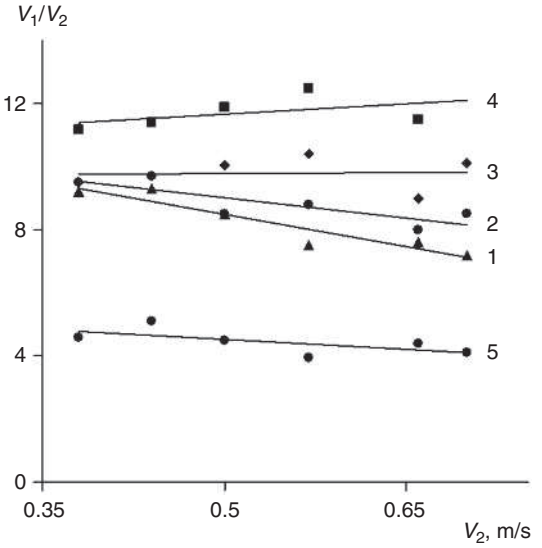


**Figure 4.7** Conditions for the formation of the reaction torch front (5) and plane front (1–4) depending on the flow viscosity: 1, 3 (1); 2, 5 (2); 3, 8 (3); 6 (4); and 1, 3, 2, 5, 6 (5), mPa·s. ($d_1/d_d$ = 0.13)

The use of cylinder tubular turbulent reactors with different diameter ratios $d_1/d_d$, showed [3] that a decrease of $d_1/d_d$ leads to quasi-plug flow mode formation at a lower consumption of reactant, introduced through the $d_1$ diameter axis branch pipe. In particular, upon the decrease of $d_1/d_d$ from 0.44 to 0.13, the axial volume flow rate, at which the quasi-plug flow mode starts to form, decreases by 60%. This allows us to use more concentrated reactant solutions in the chemical process.

Thus, **Equations 4.1–4.3**, in the case of the homogeneous mixing of liquid flows, characterised by density and viscosity, provide an efficient commercial application of tubular turbulent reactors at almost any stage limited by mass exchange. The optimal operation conditions of the tubular turbulent reactors in the quasi-plug flow mode can be calculated due to the changes of the physical characteristics of the liquid flow, the kinetic parameters of the fast chemical reactions and the reaction construction parameters.

Moreover, the influence of the chemical reaction rate constant and some other physical parameters of the liquid flow (density, viscosity) on the conditions of macroscopic front formation in turbulent flows, allow us to make an assumption about the differences in the nature of the reaction front and mixing front formation. In the first case, the key parameters of the process are the kinetic and diffusion parameters; in the second case, however, the key parameters of the process are the convective and turbulent transfer. The influence of density and viscosity, i.e., the parameters which define the hydrodynamic motion mode of the liquid flow in the tubular channels, on the

conditions of the plane front formation during the reaction and mixing stages, shows the importance of the hydrodynamic constituent in the formation of the corresponding macrostructures.

For fast chemical reactions and effective mass exchange, during many physical processes (mixing, dispersion, extraction, and so on), it is necessary to form a macroscopic structure in the tubular turbulent reactor, which defines the quasi-plug flow mode in the high turbulence flow. The macroscopic mode conditions provide all the advantages necessary for the practical realisation of all chemical reactions and physical processes, which are defined by the effective mass exchange. The guaranteed synthesis of low MW compounds in the quasi-plug flow mode defines the optimal process conditions for high quality products. This is demonstrated below, in a number of typical processes for different model systems.

## 4.2 Fast Chemical Reactions in a Single-phase Reaction Mixture (Neutralisation of Acid and Alkali Media)

A typical example of fast chemical reactions in a one-phase reaction mixture is the neutralisation of acid and alkali media. The neutralisation stage of the acid medium in the liquid-phase flow is an integral part of the commercial production of synthetic compounds. The wastewater released into the sewage system is permitted only at pH $\geq 7$ therefore, acid medium neutralisation is the key stage during wastewater treatment and the production of many synthetic compounds (neutralisation of amine chlorine hydrates during ethylene diamine synthesis, ammonation of phosphoric acid during ammophos production, neutralisation and saponification of alkyl sulfuric acid during alkyl sulfates production, and so on). During the commercial neutralisation stage it is necessary to consider the specific features of the process. The neutralisation reaction is very fast (the reaction rate constant $k = 10^8$ l/mol·s and therefore, the length of the reaction zone is very short, constituting $L_{chem} \approx 2 \times 10^{-10}$ m). Accordingly, the reaction occurs in the diffusion mode of classical bulk mixing reactors, even at small concentrations of reactants. At the same time, the neutralisation reaction is a highly exothermic process (the thermal effect of the strong acid and base reaction $q$ = 57.2 kilojoules/mol). The process occurs in an aggressive medium therefore, at high temperatures, anticorrosive materials are required. For efficient process optimisation, solutions of the initial reactants are mixed within $\tau_{cm}$, the time comparable to the chemical reaction time $\tau_{chem}$, i.e., at $\tau_{mix} \approx \tau_{chem}$. Moreover, the devices should have no mechanical apparatus in motion and a small specific surface of the reaction medium in contact with the reactor walls; there should be no drastic temperature increase in the introduction zone of the neutralising agent.

The experience of using small-scale tubular reactors [1], which operate in a quasi-plug flow mode, for fast chemical and many mass exchange physical processes, together with the results of laboratory research and mathematical modelling for processes of

liquid flow mixing, enable efficient maintenance for acid wastewater neutralisation. In this case, of particular importance is the opportunity to guarantee the formation of the reaction plane front in the zone where the reactants mix. The plane front should correspond to the quasi-plug flow mode in turbulent flow and provide a quasi-isothermal mode in the reaction zone. This enables efficient mixing of the initial reactants before their interaction and accessibility of the reaction zone to the heat exchange surfaces, as well as the opportunity to control the thermal mode of the reaction *via* external cooling.

In accordance with the experimental data, the transition from the flare front of a reaction to the quasi-plug flow mode in turbulent flow (plane front of reaction) is observed at a certain ratio of the linear rates $V_1/V_2$ of the reactant supply to the tubular reactor [14]. With an increase of the radial flow rate $V_2$, in order to form the reaction plane front, it is necessary to increase the rate of the axial flow supply $V_1$ (**Figure 4.8**). The conditions of the quasi-ideal mode formation do not depend on the strength of the acid and/or base, introduced to the tubular reactor during neutralisation.

The results of the experimental tests gave the following dependence of the conditions of quasi-plug flow mode formation in a tubular turbulent reactor ($V_1$, $V_2$ = 0.1–0.8 m/s, and $d_1/d_d$ = 0.44):

$$V_1 / V_2 = 0.28 \times V_2 + 0.96 \tag{4.5}$$

The fast neutralisation reaction in conditions of guaranteed formation of the quasi-plug flow mode in the zone where reactants mix, with the use of the **Equation 4.5**, at a device radius:

$$R \leq \sqrt{D_T / k[C]} \tag{4.6}$$

allows achieving the ideal ratio $\tau_{mix} \approx \tau_{chem}$ and a decrease of the reaction mixture time in the device $\tau_{pass}$.

Formation of the quasi-plug flow mode in the reaction zone in turbulent flows, due to the intensive convective heat exchange in proximity to the reactor walls and resulting quasi-isothermal conditions, allows efficient control of the thermal mode of the neutralisation process by external cooling. In order to decide whether it is reasonable to use external cooling for the neutralisation reaction in a tubular turbulent reactor of cylinder form, it is necessary to estimate the amount of heat which is released in the reaction zone $\Delta T_{ad}$ under conditions of adiabatic heating. If the density and thermal capacity of the reaction mixture in the first approximation correspond to the values for water, then [15]:

$$\Delta T_{ad} = \frac{q \times \Delta P}{C_p \rho} = 13.67 \times \Delta P \tag{4.7}$$

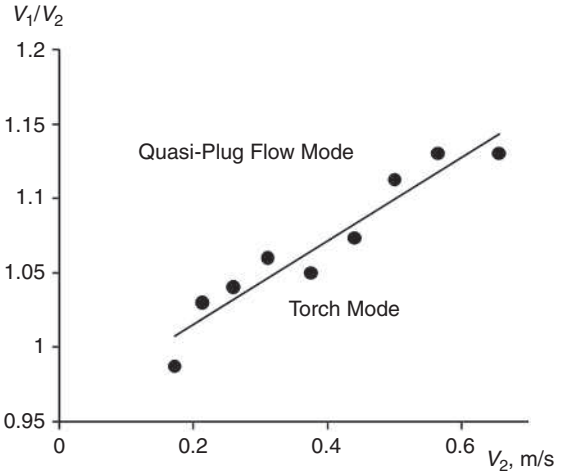


**Figure 4.8** Conditions of transition from torch mode to quasi-plug flow mode during neutralisation reactions ($d_1/d_d$ = 0.44, $\rho$ = 1.2 g/sm$^3$, and $\mu$ = 1 mPa·s)

Where:

$q$ = 57.2 kilojoules/mole.

$\rho$ = 1000 kg/m$^3$.

$C_p$ = 75.2 joules/mol·K.

**Equation 4.7** proves that during neutralisation of a 30% aqueous solution of HCl by a 20% aqueous solution of NaOH, the temperature increase $\Delta T_{ad}$ is 50 °C; at the same time, during neutralisation of a 30% acid solution by a solid base, $\Delta T_{ad}$ will be much higher, and reach a value of around 130 °C (**Table 4.2**).

The results show that acidic media can be neutralised (up to a 30% aqueous solution of acid) by an aqueous solution of alkali (up to 20 wt%), without any additional external heat removal at the initial temperature of acidic wastewaters not higher than 30 °C. In this case, the increase of temperature $\Delta T_{ad}$ in the reaction zone will not exceed 30–50 °C.

In the case of concentrated reactant solutions, we can observe a sharp temperature increase during acidic media neutralisation. The temperature field in the reaction zone can be adjusted by using small tubular turbulent reactors of cylinder or diffuser-confusor design. There are several options for temperature adjustment [16], e.g., the change of the device radius and reactant flow rate, allows the application of the zone model for fast chemical processes and the use of shell-and-tube reactors with pipe columns of small radius comprising the same reactor cross section in total [17].

**Table 4.2 Temperature increase $\Delta T_{ad}$ during neutralisation of hydrochloric acid aqueous solution by sodium hydroxide**

| $C_{HCl}$, %vol | $C_{NaOH}$, %vol | | | | | |
|---|---|---|---|---|---|---|
| | 10 | | 20 | | 100 | |
| | $C_{NaCl}$, mole/l | $\Delta T_{ad}$ | $C_{NaCl}$, mole/l | $\Delta T_{ad}$ | $C_{NaCl}$, mole/l | $\Delta T_{ad}$ |
| 0.01 | 0.0027 | 0.04 | 0.0027 | 0.04 | 0.0027 | 0.04 |
| 0.02 | 0.0055 | 0.08 | 0.0055 | 0.08 | 0.0055 | 0.08 |
| 0.05 | 0.0136 | 0.19 | 0.0137 | 0.19 | 0.0137 | 0.19 |
| 1 | 0.2500 | 3.40 | 0.2699 | 3.7 | 0.2748 | 4 |
| 5 | 0.9169 | 12 | 1.1185 | 15 | 1.3699 | 19 |
| 10 | 1.4105 | 19 | 1.9528 | 27 | 2.8712 | 39 |
| 30 | 2.1433 | 29 | 3.7043 | 51 | 9.4438 | 129 |

It should be noted that in order to mix the reactants efficiently and to prevent acid from weeping, due to the fact that the industrial wastewater flow is much higher than the neutralising agent flow, the reaction should be carried out in a tubular turbulent reactor of diffuser-confusor design. In this case, the reactor diameter in the broad part (diffuser) should be from 0.05 to 0.4 m, with a length of up to 2 m (device volume of around 0.016–0.12 $m^3$); this corresponds to the capacity of a small reactor of around 7–460 $m^3$/h (at a linear flow rate of 1 m/s) and higher. The holes in the branch pipe for the supply of the alkali solution to the reactor (in alignment to the flow) should provide the supply of the reactant to the reaction zone at a rate of $V_1$ >1.1 m/s, so as to support the ratio $V_1/V_2 \geq 1.2$.

Therefore, the neutralisation reaction of acidic and alkali media is a fast chemical process which should be carried out in the new type of reactors, i.e., low energy- and resource-efficient tubular turbulent reactors of cylinder or diffuser-confusor design, which provides the jet mode of reaction mixture flow, quasi-isometric conditions in the reaction zone, complete conversion of reactants, and so on. Industrial wastewaters with an acid content of up to 30 wt% can be neutralised in a tubular turbulent reactor by a 10% or 20% aqueous solution of alkali, without any additional external heat removal.

The production of ammonium phosphate fertilisers is an example of acidic and alkali media neutralisation under commercial plant conditions [1]. During the production of ammonium phosphate, at the liquid ammonium and phosphoric acid reaction stage, a six-section tubular turbulent reactor of diffuser-confusor design is used. The reactor maintains turbulence along its length, with a reactor diameter of 220 mm and confusor diameter of 105 mm; the reactor operates in a normal mode at a

supply of around 20 $m^3$/h of phosphoric acid, 35 $m^3$/h of ammonium and 4 $m^3$/h of wash liquid; the final product corresponds to industrial regulations. As a result, the content of ammonium in wastewaters decreases and the range of changes in nutrients, including nitrogen and phosphorus, increases.

## 4.3 Fast Chemical Reactions in 'Liquid-liquid' Systems (Sulfation of Olefins)

The interaction of olefin hydrocarbons and sulfuric acid is widely used in commercial production, in particular, in the production of synthetic detergents, methyl ethyl ketone, gasoline fractions of hydrocarbons [1], higher fatty alcohols [18] and so on:

$$R\text{-}CH = CH_2 + H_2SO_4 \rightarrow R\text{-}CH(CH_3)\text{-}O\text{-}SO_3H + Q$$

Anionic surfactants, based on alkyl sulfates, are widely used as the basis for synthetic detergents, emulsifiers, stabilisers, and so on. Alkyl sulfates $ROSO_3Me$ (where Me is Na, K and so on) under the conditions of commercial production, in particular, during the synthesis of detergents, can be produced by the interaction of the $\alpha$-olefins of the unsaturated hydrocarbon fractions $C_8$–$C_{18}$ (olefin content no less that 97 wt%) and 98% sulfuric acid at the ratio of $\alpha$-olefin/$H_2SO_4$ = 1/1.2–1.4 mole, with further neutralisation of the unreacted $H_2SO_4$ and saponification of the synthesised alkyl sulfur acid:

$$R\text{-}CH(CH_3)\text{-}O\text{-}SO_3H \rightarrow R\text{-}CH(CH_3)\text{-}O\text{-}SO_3Na + H_2O$$

The choice of the reactor for the sulfation of $\alpha$-olefins is complicated due to the peculiarities of the chemical process. The reaction is fast (the reaction time, according to [18], is less than 30 s) and highly exothermic. In particular, the sulfation heat is around $q \approx 502.1 \times 10^3$ kilo joules per 1 $m^3$ of $\alpha$-olefins [19]. Therefore, the temperature increase in the reaction zone reaches 190 ± 5 °C. Due to the significant difference in values of viscosity ($\mu$) and density ($\rho$) of the initial reactants: $\mu_{H_2SO_4} / \mu_{olefin} \approx 75.1$; $\rho_{H_2SO_4} / \rho_{olefin} \approx 2.63$, the flows mix poorly; at the same time, the initial stage of the reaction occurs on the phase contact surface in the 'liquid-liquid' system. This results in a slowdown of the chemical reaction, despite the fact that this reaction is a fast chemical process. In this case, an increase of the turbulent mixing level in the reaction zone leads to an increase of the chemical process rate (**Figure 4.9**). Therefore, the technological process of alkyl sulfuric acid synthesis during the production of alkyl sulfates should include

intensive turbulent mixing of the initial reactants in the reaction zone, and enable removal of the reaction heat. Moreover, the secondary processes (synthesis of dialkyl sulfates, resinification of $\alpha$-olefins, hydrolysis and alkoholysis of dialkyl sulfates, and so on) make it necessary to decrease the time of the reaction mixture presence in the reaction zone $\tau_{pass}$, and to impose strict limitations on the highest temperature level in the reaction zone (reactor). This requires intensive turbulent mixing of liquid flows in the device, a larger specific surface to improve external heat removal and a jet mode of reaction to enable an adjustable residence time of reactants $\tau_{pass}$ [20].

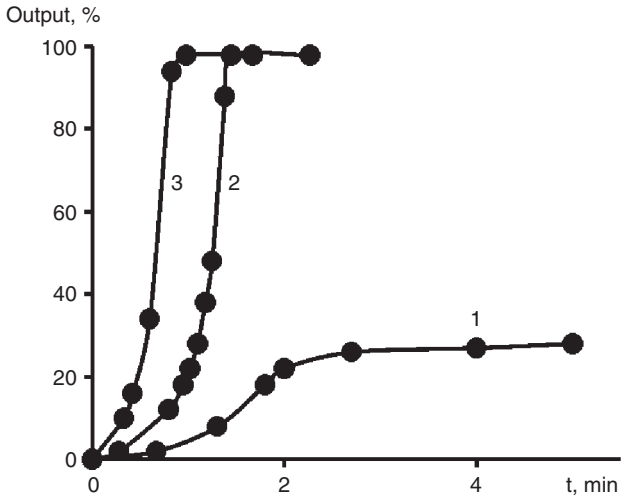


**Figure 4.9** Conversion curves for the sulfation of $\alpha$-olefins, fractions $C_8$–$C_{16}$ (~97 wt%), concentrated (95 wt%) by sulfuric acid in bulk mixing reactors. Ratio of α-olefins/$H_2SO_4$ = 3.9:1 vol. 25 °C. Rate of mixing, rpm: 100 (1), 500 (2), and 1000 (3)

An efficient method for the substantial decrease of the adiabatic temperature rise in the reaction zone $DT_{ad}$ during the sulfation of a-olefins by sulfuric acid, is the dilution of the initial reaction mixture by a high thermal capacity inert solvent (saturated hydrocarbons, e.g., decane) (**Table 4.3**); in this case, the length of the cooling zone $L_{cool}$ also decreases (**Figure 4.10**). The low boiling point solvent, for the dilution of the initial reaction mixture, provides efficient internal heat removal. In this case, gas formation in the volume of the reaction mixture provides additional flow turbulence, while high linear rates block the formation of gas locks. The process is compact, efficient, and easily controllable.

**Table 4.3 The influence of α-olefin dilution by decane on the thermal mode of sulfation in a tubular turbulent reactor without internal heat removal ($T_0$ = –20 °C, $T_{chem}$ = –20 °C, $R$ = 0.014 m, and $V$ = 0.35 m/s, reactor length 14 m)**

| Consumption of components, $m^3/h$ | | | α-olefin/ decane ratio, vol | $\Delta T_{ad}$ | Temperature in reaction zone, °C | |
|---|---|---|---|---|---|---|
| α-olefin (fractions $C_8$–$C_{18}$) | Decane | $H_2SO_4$ (98% vol) | | | $T_{ad}$ | $T_r$ |
| 0.62 | - | 0.160 | - | 189 | 169 | 112 |
| 0.34 | 0.34 | 0.088 | 1:1 | 112 | 92 | 53 |
| 0.24 | 0.48 | 0.062 | 1:2 | 81 | 61 | 30 |
| 0.18 | 0.55 | 0.470 | 1:3 | 64 | 44 | 17 |
| 0.15 | 0.59 | 0.038 | 1:4 | 53 | 33 | 10 |
| 0.12 | 0.62 | 0.032 | 1:5 | 46 | 26 | 4 |
| 0.11 | 0.64 | 0.031 | 1:6 | 39 | 19 | 0.6 |

The reaction of the sulfation of α-olefins by concentrated sulfuric acid results in the emission of heat $\Delta q_{ad}$ in the reaction volume:

$$\Delta q_{ad} = q w_{olefin} \tag{4.8}$$

Where $w_{olefin}$ is the volume flow rate of the α-olefin hydrocarbon fractions.

The adiabatic heating of the reaction mass to the reaction temperature defined by the solvent boiling temperature $T_{boil}$, consumes $q_{ad}$ of heat:

$$Q_{ad} = q w_{\Sigma} \rho (T_{boil} - T_0) \tag{4.9}$$

Where $w_{\Sigma}$ is the reaction mixture flow rate.

The amount of the readily boiling solvent $w_{solv}$, necessary for the removal of the remaining heat due to boiling, is defined by the formula:

$$w_{solv} = \frac{\Delta q_{ad} - q_{ad}}{q_{evap}} \tag{4.10}$$

where $q_{evap}$ is the evaporation heat of the solvent.

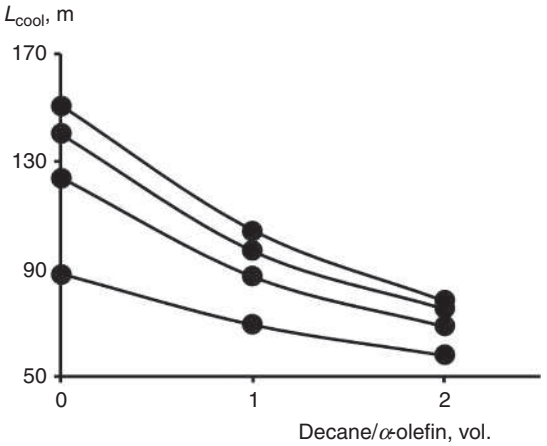


**Figure 4.10** The dependence of cooling zone length $L_{cool}$ on dilution of the initial reaction mixture for the case of the 'zone' model. Supply of equal quantities of $H_2SO_4$ to 1 (1); 2 (2); 3 (3); and 4 (4) reaction zones in the absence of internal heat removal; ($T_0$ = 30 °C, $T_r$ = 5 °C, $T_{cool}$ = -20 °C, $R$ = 0.014 m, $w_{olefin}$ = 0.62 $m^3$/h, and $w$ = 0.16 $m^3$/h)

For example, if the initial reaction mixture is diluted by petroleum benzine with $T_{boil} \approx 343$ K at the ratio of α-olefin/solvent = 1/1.24 vol., due to adiabatic heating of the reaction mixture from $T_0$ = 293 K to $T_{boil}$ = 343 K ($\Delta T$ = 50 °C) in a tubular turbulent device at $w_{olefin}$ = 0.62 $m^3$/h, $W_{H_2SO_4} = 0.16\,m^3$/h and $R$ = 0.014 m, 1.5 × $10^5$ kilojoules of heat is removed, that is around 48% of the total heat. Due to the solvent (petroleum benzine) boiling at atmospheric pressure, the remaining 52% of the heat, i.e., 1.6 × $10^5$ kilojoules, is also removed. If the initial reaction mixture is diluted at the ratio α-olefin/petroleum benzine = 1/1 vol., then due to the adiabatic temperature increase and solvent boiling, around 86% of the heat will be removed, and due to autothermal heating, the temperature in the sulfator will rise by 15–17 °C above the solvent boiling temperature, which is acceptable. In the latter case, after the removal of the main portion of petroleum benzine from the gas phase, the procedure of alkyl sulfur acid treatment for the residual solvent in a commercial process is simplified due to its complete boiling.

There is an alternative method for the efficient decrease of the adiabatic temperature rise at the point of the reactant introduction. This is the 'zone' model of the process due to the distribution of a specified amount of sulfuric acid along the length of the tubular turbulent reactor of cylinder construction. In particular, due to the

increased number of zones for the partial introduction of lower amounts of $H_2SO_4$, a sharp decrease of $\Delta T_{ad}$ at the introduction points is possible, and a temperature increase above the allowable value in the reaction zone can be prevented (**Figure 4.11**). Therefore, if the number of reactant introduction zones in the tubular reactor increases, the fast reaction slows down, and the temperature profile in the reactor approaches the temperature of the chemical process at $\tau_{chem} \approx \tau_{pass}$ in an ideal mixing mode. In this case, even in the absence of external heat removal, the temperature of the reaction mixture is equal throughout the whole volume of the reactor, i.e., the process mode is quasi-isothermal.

However, in the case of the 'zone' model, the process flowsheet is complicated, in particular, because of the necessity to use several cooling devices between the reaction zones, and an increase of the total cooling zone length $L_{cool}$ and therefore, the reactor size.

In the case of the sulfation of $\alpha$-olefins by sulfuric acid, it is reasonable to use a shell-and-tube turbulent jet type reactor with a bundle of small diameter tubes, washed by a coolant. Division of the flow for $N$ tubes of a smaller diameter r, operating in the quasi-plug flow mode, at the same flow cross section, $S$, as in the singular tubular reactor for the conventional and zone models, provides an $N^{0.6}$ times decrease of the cooling zone length $L_{cool}$, and a more compact process. A combination of the partial introduction of sulfuric acid and multitube cooling devices, provides additional reduction of the adiabatic temperature increase in the reaction zone $\Delta T_{ad}$ and considerable shortening of the cooling zone during sulfation of the $\alpha$-olefins (**Figure 4.12**).

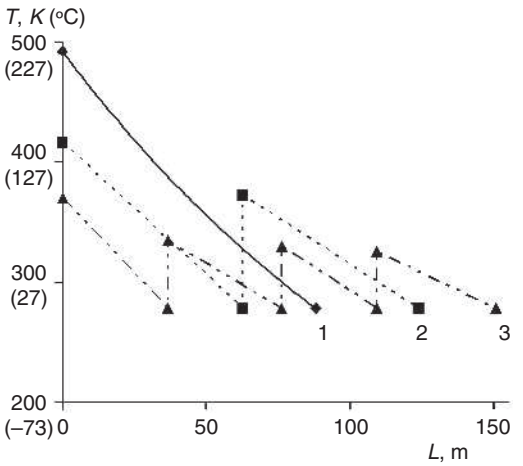


**Figure 4.11** Temperature profile along the length of the tubular turbulent reactor for the 'zone' model. Introduction of equal $H_2SO_4$ quantities to 1 (1); 2 (2); and 4 (3) reaction zones (see conditions in **Figure 4.10**)

Therefore, the sulfation reaction of $\alpha$-olefins by concentrated sulfuric acid is a fast chemical reaction. For guaranteed prevention of a sharp temperature increase in the reaction zone during $\alpha$-olefin sulfation, it is reasonable to use tubular turbulent reactors of cylinder and shell-and-tube construction. At the same time, the initial reactants are to be diluted by low boiling point solvents, or the 'zone' process model is to be implemented (partial introduction of reactants along the reactor length).

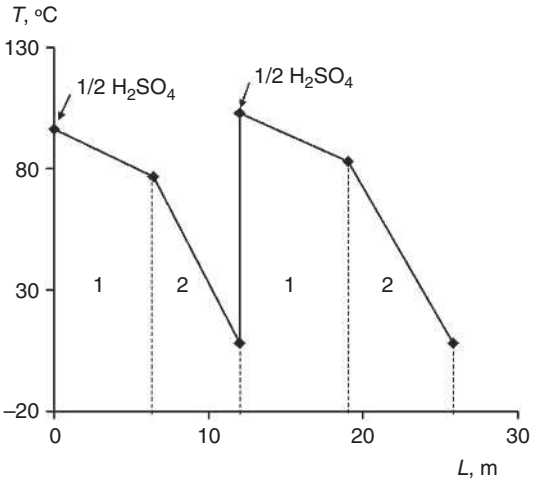


**Figure 4.12** Temperature profile along the tubular turbulent reactor length at a two-stage introduction of equal $H_2SO_4$ quantities. Reaction zone (1) – cylinder tubular turbulent reactor ($R$ = 0.014 m); cooling zone (2) – shell-and-tube turbulent reactor ($N$ = 31, r = 0.0025 m). $T_0$ = -20 °C; $T_r$ = 5 °C; $T_{chem}$ = -20 °C; $W_{olefin}$ = 0.62 $m^3$/h; and $W_{H_2SO_4} = 0.16\,m^3$/h )

The sulfation reaction process was used for the commercial production of methyl ethyl ketone [1]. At the stage of butyl sulfuric acid production, bulk mixing reactors or leakproof pumps for chemically aggressive media, were used. Turbulent reactors, operating in the quasi-plug flow mode, were used at the stage of butyl sulfuric acid production during the sulfation of butylenes from the butane-butylene fraction. The advantages of the process were as follows: stable and efficient operation of the turbulent reactor, which provides improved operating conditions for maintenance and repair, and the exclusion of pumps from the technological cycle; reduction of expense for frequent replacement, repair and preventive maintenance of pumps because of the aggressive media; reduction of wastewaters and atmospheric emissions, and the decrease of energy consumption due to decommissioning of electric drive mixing pumps (up to 100,000 kw/h per year); and nonstop operation of the butylene sulfation block in the butane-butylene fraction during maintenance of the tubular turbulent reactor. In general, this is an environmentally friendly resource- and energy-efficient process.

## 4.4 Fast Chemical Reactions in 'Liquid-gas' Systems (Liquid-phase Oxidation)

There are a large number of processes in chemical technology, which occur in 'liquid-gas' systems, in particular, halogenation, hydrohalogenation, oxidation, and so on, where the main problem is obtaining a reaction mixture with a well-developed phase contact surface. Diffusion constraints are of special importance at high rates of chemical reactions. In this case, it is necessary to decrease the dimensions of devices to a dimension equal to the reaction zone size (intensive dispersion zones) in order to eliminate any dead zones.

The work of Zaharov and co-workers [21] describes the laws of mass transfer intensification for liquid-gas flows in tubular turbulent reactors and the dependencies of the gas absorption rate on reactor geometry and reactant introduction method; the atmospheric oxygen dissolution in water is given as an example.

In order to estimate the efficiency of the mass transfer in gas-liquid flows, a sulfite method [22], based on the catalytic oxidation of sodium sulfite by atmospheric oxygen, was used:

$$Na_2SO_3 + 1/2O_2 \xrightarrow{CuSO_4} Na_2SO_4$$

Interaction of sodium sulfite and atmospheric oxygen occurs in the diffusion zone, i.e., the process rate is completely defined by the stage of oxygen transfer from the gas phase to the liquid phase. Due to the poor solubility of oxygen in water, the mass transfer coefficient is defined by the mass delivery coefficient in a liquid phase (the stage of oxygen diffusion from the phase boundary to the liquid volume). Therefore, the change in the rate of sodium sulfite oxidation is related to the intensification of the mass delivery in the liquid phase.

The value which defines the intensity of gas dissolution in the gas-liquid reaction mixture flow in the device is the 'sulfite number of the reactor', i.e., the amount of oxygen absorbed by a unit of reaction volume per unit of time:

$$SuR = 0.127 \frac{\Delta C_{Na_2SO_3}}{\Delta \tau} \frac{V_\Sigma}{V_r} \tag{4.11}$$

where $V_r$, $V_\Sigma$ are the volume of the reactor and the volume of the reaction mixture, respectively; $\Delta C_{Na_2SO_3}$ is the change of the sodium sulfite concentration in the time $\Delta\tau$.

Increasing the ratio of the gas- and liquid-phase introduction volume rates, $w_g/w_l$ (the gas multiplicity of the disperse system), in the tubular turbulent reactor of diffusion-confusion construction to the value of 0.1, we observe an increase in the

sulfite number of the reactor *SuR*, and therefore, the efficiency of the oxygen mass transfer from the gas phase to liquid (**Figure 4.13**). This is obviously related to the increase of the rate of oxygen approach to the reactor and therefore, the increase of its concentration in the reaction mixture, which results in an acceleration of the oxidation process. It should be noted that in this case, the process visually occurs in the bubble mode, and the oxidation rate increases despite the fact that an increase of the $w_g/w_l$ ratio promotes the growth of the gas bubble average size ($d_{32}$) to 1.4 mm. No further increase of the gas content in the reaction mixture (gas consumption $w_g$) can lead to changes in the sulfite number of the reactor, and this is related to the transfer of the two-phase mixture flow to the densely packed bubble (foam) mode, while the volume surface diameter of the dispersed spots, remains constant at $d_{32} \approx 1.4$ mm. Thus, there is an optimal $w_g/w_l$ ratio, which apparently depends on the physical characteristics of the reacting components of the two-phase mixture, and it is not reasonable to exceed this ratio. This fact is of special importance for aggressive gases, with no possibility of bypassing the unreacted gas, in particular, for the chlorination of butyl rubber in a hydrocarbon solvent by molecular chlorine [23].

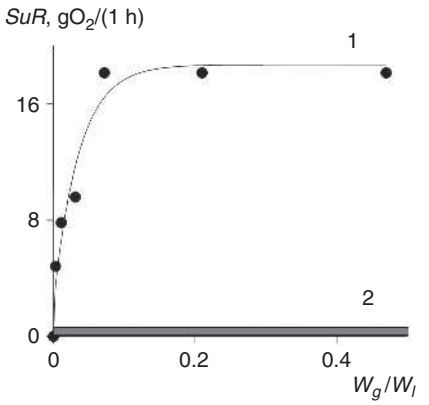


**Figure 4.13** Dependencies of the sulfite number of the reactor SuR, on $w_g/w_l$ in a tubular turbulent reactor (1) ($w_l$ = 170 ± 10 sm$^3$/s, $N$ = 5, $d_1$ = 10 mm, $d_2$ = 3 mm, $d_K$ = 15 mm) and bulk mixing reactor (2) at mixer rotation rate 1700 rpm ($w_l/w_g$ = 3.3)

The specific rate of the atmospheric oxygen absorption in water, for a tubular turbulent reactor of diffuser-confusor design (**Figure 4.13**, curve 1), is more than one order of magnitude higher than for the volume reactor with a high-speed mechanical mixer (~1700 rpm) (curve 2). This can be explained by the fact that during gas bubbling in the reactor volume upon mechanical mixing, the efficient dispersion zone, which determines the high rate of oxygen transfer, is much smaller than the reaction volume. The gas bubbles coalesce and the phase contact surface decreases in the reactor areas remote from the mixer rotation zone, where dispersion is efficient. Moreover, in this case, the two-phase mixture circulation zones, which determine

the intensive turbulent pulsations in the liquid phase, are missing. Therefore, the tubular turbulent diffuser-confusor design reactors are characterised by higher values of the reactor sulfite number, due to the possibility of intensive dispersion throughout the whole volume of the reactor, and the presence of circulation zones in the diffuser-confusor sections. The small dimensions of the tubular reactor ($v_r$ ~ 0.1 l), in comparison with the bulk mixing reactor ($v_r$ ~ 4 l), provide metal efficiency and high (over 40 times higher) capacity without any decrease in the duration of the oxidation process.

A significant increase of the *SuR* value is observed upon increasing the reaction mixture flow rate at a fixed gas content of the flow (**Figure 4.14**, curve 2). In this case, the shift deformations for gas bubbles are intensified due to the hydrodynamic energy of the flow, which results in the grinding of the dispersed phase particles and an increase of the phase contact surface area. In addition, there is almost no gas absorption, during the laminated mode of the reaction mixture flow, at low rates (in this case, below 97 $sm^3/s$), which is the lowest limit of the reactor capacity. At the same time, at high $w_l$ values, no maximum (plateau) of the $SuR = f(w_l)$ dependence can be reached, i.e., a maximum limit of the reactor capacity does not exist. A characteristic feature of the chemical and mass exchange physical processes, in tubular turbulent reactors, is the dependence of the process rate on the residence time of reactants in the reactor. The atmospheric oxygen dissolution in water also shows that with a decrease of the reaction mixture residence time in the reactor, the *SuR* value increases (**Figure 4.14**, curve 1). In this case, the reaction zone is packed, which is a consequence of the process behaviour in the diffusion area.

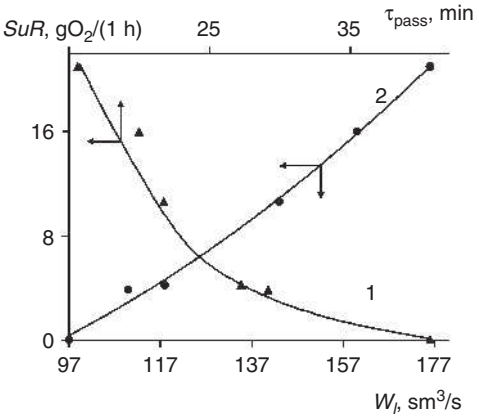


**Figure 4.14** Dependencies of the sulfite number of the reactor SuR, on the liquid residence time in the reactor $\tau_{pass}$ (1) and liquid rate $w_l$ (2) ($w_l/w_g$ = 3.3; $N$ = 5; $d_1$ = 10 mm; $d_2$ = 3 mm; and $d_c$ = 15 mm)

It is possible to influence the size of the dispersion spots in 'liquid-gas' systems (specific phase contact surface) and therefore, the mass transfer efficiency, by changing the method of reactant introduction. During the motion of the gas-liquid flows in tubular turbulent reactors, an increase of the gas supply branch pipe diameter results in a slight decrease of the sulfite number of the reactor (**Table 4.4**), which can be seen from the decrease of the phase contact surface as $d_{32}$ grows by 15%. Similarly, with the decrease of the coaxial liquid-phase supply branch pipe diameter $d_1$ from 10 to 5 mm, *SuR* equals 13.5 and 14 $gO_2$/h, respectively. Thus, there is almost no dependence of the rate of sodium sulfite oxidation in aqueous solution, by atmospheric oxygen, on the method of reactant introduction. This is related to the fact that changes in the method of the liquid- and gas-phase introduction, in particular, the diameters of the feeding branch pipes, do not influence the mass delivery coefficient in the liquid phase.

**Table 4.4 Influence of gas supply branch pipe diameter $d_2$ ($d_d/d_c$ = 2) and ratio $d_d/d_c$ ($d_2$ = 3 mm) on the sulfite number of the reactor ($w_l/w_g$ = 3.3, $w_l$ = 140 $sm^3/s$ and $d_1$ = 10 mm)**

| $d_d/d_c$ | *SuR*, $gO_2$/h | $d_2$, mm | *SuR*, $gO_2$/h |
|---|---|---|---|
| 1.0 | 2.2 | 0.8 | 13.5 |
| 1.6 | 8.7 | 1.5 | 13.0 |
| 2.0 | 12.0 | 3.0 | 10.4 |
| 3.0 | 20.0 | 7.0 | 9.0 |

The geometry of the tubular turbulent reactor, in particular, the $d_d/d_c$ ratio, unlike the method of reactant introduction, influences the sodium sulfite oxidation rate (**Table 4.4**). When the reactor construction changes from a cylinder type ($d_d/d_c$ = 1) to a diffuser-confusor design with $d_d/d_c$ = 3, the sulfite number of the reactor increases by at least one order of magnitude. This can be seen from an increase of the mass delivery coefficient in the liquid phase, due to the growth of the turbulent diffusion coefficient in the circulation zones of the diffuser-confusor sections, with an increase of the channel profile depth from $d_d/d_c$ = 1 to $d_d/d_c$ = 3. Moreover, in this case, we can observe a decrease of the dispersion spots of over 70%. An increase of the efficiency of oxygen solubility in water, with the change of the reactor type from a cylinder to diffuser-confusor design, can be seen from an increase of the turbulent flow energy. This can be observed in the high values of the pressure fall at the reactor output; this increases the energy consumption required for the reaction mixture to flow at the required linear rate. However, due to the short length of the tubular turbulent reactor, necessary for the fast chemical reaction under the conditions of a phase separation surface with a high output, and high efficiency of mass transfer, the cost of the energy required to move the reaction mixture is insignificant. The optimal ratio for efficient oxygen absorption in water and optimal pressure fall at the reactor output is $d_d/d_c$ = 2.

It should be noted that acceleration of the oxygen dissolution in water and sodium sulfate oxidation process, depending on the intensity of the mixing in the tubular turbulent reactor, looks like a curve with saturation. In particular, an increase of the longitudinal mixing coefficient by any of the above given methods, results in the growth of the specific rate of atmospheric oxygen dissolution in water and therefore, in the acceleration of the liquid-phase oxidation (**Figure 4.15**). Under the experimental conditions, there is no need to increase the rate of longitudinal mixing above $E$ [(2–3)$10^{-2}$ $m^2$/cs].

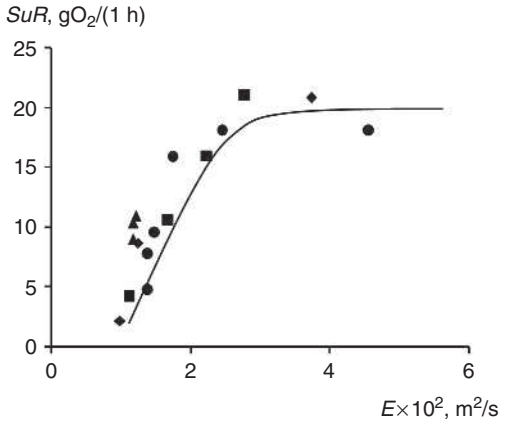


**Figure 4.15** Summarised dependence of the sulfite number of the reactor *SuR*, on the coefficient of longitudinal mixing *E*, in liquid phase (18 °C) during the motion of gas-liquid flow (water-air) in a tubular turbulent reactor. ● – $SuR = f(w_g/w_l)$; ♦ – $SuR = f(w_l)$; ■ – $SuR = f(d_d/d_c)$; and ▲– $SuR = f(d_2)$

Thus, the tubular turbulent reactors of diffuser-confusor design, in comparison with the bulk mixing reactors (bubbling during mechanical mixing) are characterised by a higher (more than one order of magnitude) specific rate of atmospheric oxygen dissolution in water. An efficient method to influence the rate of oxygen absorption is to increase the rate of the two-phase reaction mixture flow (reactor capacity) and to increase the depth of the channel profile, expressed by the ratio $d_d/d_c$. The obtained results allow us to recommend the use of tubular turbulent reactors in wastewater treatment for the oxidation of wastewaters by atmospheric oxygen or ozone. Moreover, the patterns of mass transfer intensification in 'liquid-gas' systems enable the efficient use of tubular turbulent reactors, of diffuser-confusor design, as reactors for: fast chemical reactions, prereactors, remote dispersion devices to increase the phase contact surface in a two-phase reaction mixture, as inner circulation tubes in bubbling air lift (gas lift) devices, as absorbers, and so on.

## 4.5 Fast Chemical Reactions in 'Liquid-solid' Systems (Condensation Method of Suspension Synthesis)

The processes of suspension production by condensation, during chemical reactions with sedimentation, are widespread in chemical technology. In many cases, the goal is to obtain homogeneous finely dispersed suspensions, in particular, during the formation of highly active heterogeneous and microheterogeneous Ziegler–Natta catalytic systems for the polymerisation of olefins and dienes, antiagglomerators for synthetic rubbers, pigments for dyes, and so on.

Baldyga and co-workers [24] showed the correlation between mixing at different levels (macro-, meso-, and micromixing) and the process of crystallisation in reactors with a batch mixer. The influence of mixing intensity, reactant concentration and their volume ratio on particle size, during chemical reactions with sedimentation, was studied. With an increase of the mixing rate during the reaction, the size of the particles decreases, while their number increases; the mixing rate, however, has a very small influence on particle size in the treatment of ready-made suspensions (an example being yttrium oxalate production [25]). Kim and Tarbel [26] showed that before the mixer rotation rate reaches 400 rpm, the size of the dispersed phase particles increases, any further increase of the mixing rate (>400 rpm) results in a decrease of the sedimentation particle size. A decrease of the specific surface area with an increase of the mixing intensity (up to 400 rpm) can be explained by the fact that in this case, the diffusion growth (reactant supply to the crystal surface) dominates the micromixing rate growth [27], which results in an increase of the number of new phase nuclei.

When using fast chemical reactions in commercial production, it is popular to produce suspensions during the mixing of the initial homogeneous reactants in the turbulent mode, due to the movement of the centrifugal pump blades. In this case, however, there is a probability that the moving elements of the pumps can be broken, moreover for aggressive media, special anticorrosive coatings are applied to the operating surfaces of the device. Due to the fact that the suspension is finely dispersed, chemical reactions used in production are usually ion exchange reactions which occur at high rates, it may be reasonable to use tubular turbulent reactors.

### *4.5.1 Synthesis of Barium Sulfate*

In order to study the prospects of the application of diffuser-confusor designed tubular turbulent reactors for the production of homogeneous finely dispersed suspensions, by condensation in fast chemical reactions, and to compare their operating efficiency with volume reactors, a model reaction, which occurs at high rate, was chosen [28]:

$$H_2SO_4 + BaCl_2 \xrightarrow{fast} BaSO_4 \downarrow + 2HCl$$

There are three methods employed to synthesise this suspension [28]: interaction of barium chloride with sulfuric acid in a bulk mixing reactor (three-necked flask with a volume of 500 $sm^3$, 70% full) with a rotating mixer, operating according to the centrifugal pump principle and creating intensive turbulent flows in the axial direction of the reaction volume. The second method is similar to the first method however, there is a baffle wall in the volume of the reaction mixture, which together with an increase of the power used for mixing, intensifies the turbulent mixing of the flows [29]. According to the third method, the interaction of the initial reactants (aqueous solutions of $H_2SO_4$ and $BaCl_2$) occurs directly in the six-sectioned tubular turbulent reactor of diffuser-confusor design (diffuser diameter 24 mm, confusor diameter 10 mm, section length 48 mm) at a linear rate of reactant flow of $V \approx 0.5$ m/s.

It is well known [30], that in order to synthesise highly dispersed systems, it is necessary to create a high supersaturation at a limited growth rate of the synthesised particles. This can be achieved for barely soluble substances, where high concentrations correspond to significant supersaturation. The most highly dispersed systems can be synthesised by mixing a comparably high concentration of a solution of one substance, with a very dilute solution of another substance, which in combination with the first substance, forms a barely soluble compound. The high concentration of the first substance provides a sufficient supersaturation and a high rate of nucleation, while the low concentration of the second substance limits the growth rate of the germs due to the slow diffusion from the diluted solution. Thus, in order to increase the germ formation rate/crystal growth rate ratio and therefore, to synthesise the utmost highly dispersed system, aqueous solutions of $BaCl_2$ and $H_2SO_4$ respectively, were used.

The dispersion analysis of the synthesised $BaSO_4$ suspensions was performed using the method of sedimentation in a gravitation field with the standard use of the torsion balance [28]. In order to decrease the probability of particles interacting during sedimentation, diluted solutions of $BaSO_4$ suspensions (~0.35 wt%) were obtained. The sedimentation analysis data was processed using the graphical differentiation of the sediment accumulation curve (**Figure 4.16**). For this purpose, the sediment dependencies of the obtained sediment mass $m$ on time $\tau$ were approximated using the sigma three-parameter function:

$$m(\tau) = \frac{a}{1 + \exp\left(-\frac{\tau - x_0}{b}\right)} \tag{4.12}$$

Coefficients $a$, $b$ and $x_0$ in (**Equation 4.12**), and the degree of error during the approximation of sedimentation experimental curves (**Figure 4.16**), are given in **Table 4.5**.

| Table 4.5 Approximation characteristics | | | | |
|---|---|---|---|---|
| **Mixing rate $N_{rpm}$** | ***a*** | ***b*** | $x_0$ | **Correlation coefficient *R*** |
| **Bulk mixing reactor with baffle walls** | | | | |
| 300 | 295.1 ± 2.1 | 6.6 ± 0.2 | 32.4 ± 0.2 | 0.99 |
| 1500 | 289.8 ± 3.2 | 14.2 ± 0.6 | 72.8 ± 0.8 | 0.99 |
| 2500 | 293.3 ± 1.8 | 19.1 ± 0.6 | 88.9 ± 0.8 | 0.99 |
| **Tubular turbulent reactor** | | | | |
| | 303.2 ± 2.6 | 30.7 ± 1.1 | 138.7 ± 1.4 | 0.99 |

In this case, in accordance with the Svedberg–Oden equation, the mass $m_i$ of the fraction of suspended particles with the radius $r > r_i$, settled by the time $\tau_i$, can be calculated:

$$m_i = \frac{a}{1+\exp\left(-\frac{\tau_i - x_0}{b}\right)} - \tau_i \frac{\exp\left(-\frac{\tau_i - x_0}{b}\right)a}{b\left(1+\exp\left(-\frac{\tau_i - x_0}{b}\right)\right)^2} \tag{4.13}$$

The microscopic analysis of the synthesised suspensions showed that the $BaSO_4$ particles are anisometric (rods with a ratio of length to diameter of 4:1, which explains the sigmoidal appearance of the sedimentation inflection curves). At the initial phase of sedimentation, the rod-like particles may rotate, which provides additional resistance to their movement (similar to an increase in viscosity), and decelerates the sediment accumulation rate. Moreover, during free sedimentation, the aspherically formed particles provide maximum resistance to their own motion. This also decreases the sedimentation rate of the solid particles and complicates the definition of their true size. Therefore, the equivalent radius *r* (radius of spherical particle, settling at the same rate) was defined according to the results of sedimentation analysis.

The sedimentation curves show (**Figure 4.16**) that with an increase of the mixing rate, the curves shift to the area of smaller sized particles (longer sedimentation time), i.e., with an increase of turbulent mixing in the reaction zone, the average particle radius decreases. Due to the fact that the differential distribution of the dispersed phase particles, according to their size $F(r)$, is a typical random value distribution function, the following expression was used for the calculation of the most probable (average integral) suspension particle radius *r*:

$$r = \frac{\int_0^\infty rF(r)dr}{\int_0^\infty F(r)dr} \tag{4.14}$$

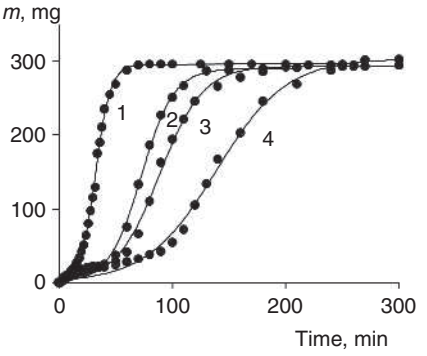


**Figure 4.16** Curves of the sedimentation of $BaSO_4$ particles. Rotation rate of mechanical mixer in volume device: 300 (1); 1500 (2); 2500 (3) rpm; and tubular turbulent device (4). Points – experiment; lines – approximation function

In the case of bulk mixing reactors, including reactors with turbulence stimulation, we can observe the decrease of r with an increase of the mixing rate $N_{rot}$ (from $r$ = 4.6 μm in the absence of mixing to $r$ = 1.2 μm at $N_{rot}$ = 5000 rpm) (**Figure 4.17**). In this case, the reaction mixture, according to the experimental conditions, is significantly diluted and an increase of turbulent mixing does not considerably intensify mass transfer and therefore, does not increase the crystal growth rate or size of the crystals. The dispersed phase particle radius decreases significantly due to the high rate of micromixing, the intensity of the latter increases with the growth of the turbulence specific kinetic energy dissipation ε and increase of the mixing rate [26]. At a high rate of micromixing, the germ formation rate/crystal growth rate ratio increases, which leads to an increase in the number of new phase germs and a decrease of their size. This, in particular, can be observed in the case of the baffle wall, which increases the intensity of turbulent mixing in the volume reactor. In this case, the relative rate of the r value decrease, with an increase of the mixer rotation $N_{об,}$ is higher than that in the first synthesis method. It should be noted that with an increase of the mixing rate in the volume reactor (flask) up to the highest possible *in vitro* rate ($N_{rot} \approx$ 5000 rpm), the r value tends to $r \approx 1.1$ μm, corresponding to the size of suspension particles obtained in a tubular turbulent reactor where the high level of turbulent mixing is created exclusively due to the channel geometry and hydrodynamic energy of the flow [31].

In order to estimate the polydispersity degree of the synthesised suspensions, the average weight $r_w$ and average numeric radii $r_n$ of particles were calculated along the sedimentation curve:

$$r_w / r_n = \frac{\sum r_i n_{wi}}{\sum r_i n_{ni}} \tag{4.15}$$

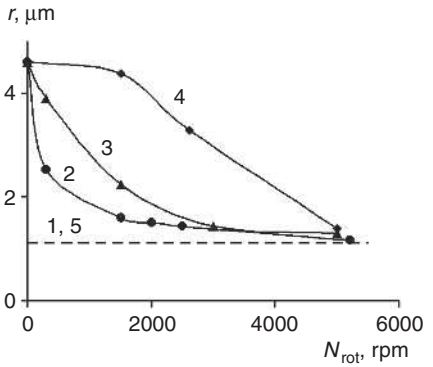


**Figure 4.17** Dependence of the average radius r of $BaSO_4$ suspension particles obtained *in situ* (1–3) and 'separately' (90 min) (4, 5), on mixing rate. Tubular turbulent reactor (1, 5); bulk mixing reactor (3) with turbulence stimulator (2, 4)

Where $n_{wi}$, $n_{ni}$ are the weight and numeric share of particles with radius $r_i$. For a homogeneous suspension, the polydispersity index $r_w/r_n = 1$. With an increase of the mixing intensity during the formation of the solid particles in the volume reactor, the polydispersity index decreases from $r_w/r_n = 2.8$ in the absence of mixing to $r_w/r_n = 1.55$ at $N_{rot} = 5000$ rpm (**Figure 4.18**). The homogeneity of the suspension synthesised with the application of an additional turbulising device, changes very slightly with an increase of the turbulent mixing intensity and $r_w/r_n \approx 1.77$. A fast chemical reaction with sedimentation, in a tubular turbulent reactor, provides a highly homogeneous suspension $r_w/r_n \approx 1.48$.

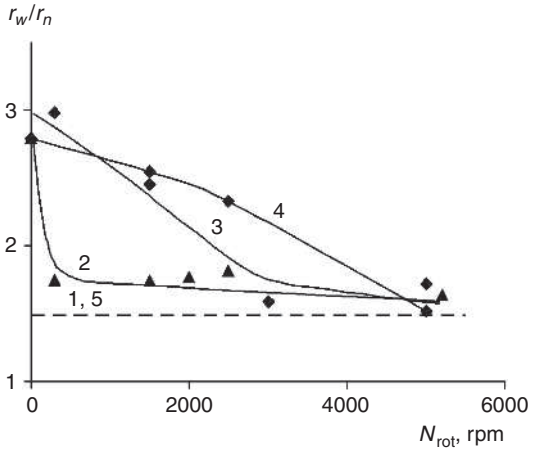


**Figure 4.18** Dependence of the polydispersity index $r_w/r_n$ of $BaSO_4$ suspension particles obtained *in situ* (1–3) and 'separately' (90 min) (4, 5), on mixing rate. Tubular turbulent reactor (1, 5); and bulk mixing reactor (3) with turbulence stimulator (2, 4)

During the course of the work undertaken by Zaharov and co-workers [28], it was considered necessary to study the characteristics of suspensions which were under a hydrodynamic influence not at the moment of their formation, but after preliminary storage in the absence of mixing. For this purpose, the initial reactants ($H_2SO_4$ and $BaCl_2$ aqueous solutions) were allowed to interact without mixing, stored for 90 min and the obtained suspensions were exposed to further turbulent mixing in the volume reactor with an additional turbuliser, within the tubular turbulent reactor. It appeared that in this case, the average particle radius did not grow during storage (**Figure 4.17**). With an increase of the turbulent mixing intensity of the mixture, containing the preliminarily formed suspension, no sharp decrease in the radius of the solid particles was observed in comparison with the suspension formed at different rates of mixer rotation. This was also shown in the work of Sung and co-workers [25]. However, finely dispersed particles with $r$ = 1.2 μm were formed during an intensive hydrodynamic influence in the volume reactor ($N_{rot}$ = 5000 rpm). Use of the tubular turbulent reactor in order to influence the suspension, which was preliminarily stored for 90 min, allows dispersed systems with an even smaller particle size ($r \approx$ 1.1 μm) to be obtained. The picture is similar for the polydispersity index $r_w/r_n$ of the obtained suspensions. Use of the tubular turbulent reactor, both at the moment of suspension formation and during the influence on the preliminarily obtained system and the dispersed system stored for 90 min, results in the formation of considerably homogeneous particles with a polydispersity index $r_w/r_n \approx 1.48$ (**Figure 4.18**).

Thus, the tubular turbulent reactors are efficient not only for suspension synthesis, but also for treatment of the preliminarily obtained suspensions. Therefore, it is necessary to use tubular turbulent reactors for: the synthesis of Ti-Al, V-Al, Nd-Al, and other highly active Ziegler–Natta catalytic systems in the copolymerisation processes of olefins and dienes (*cis*-1,4-isoprene, ethylene propylene, *cis*-1,4-butadiene and other rubbers); antiagglomerators ($Me^{2+}$ stearates) for synthetic rubbers; pigments, in particular, on the basis of $TiO_2$, and other homogeneous highly dispersed suspensions, formed during the interaction of homogeneous liquid flows. It is obvious that reactors of this type are no less efficient for suspension synthesis than any other pumping and high energy-consuming equipment.

### *4.5.2 Synthesis of an Antiagglomerator for Synthetic Rubbers Based on Calcium Stearate*

Polymer separation is an essential part of any large-scale production of synthetic rubbers by solution polymerisation [32, 33]. In order to remove the residual solvent and the unreacted monomer, the reaction mixture is treated by direct steam at the water degassing stage, after the necessary conversion and catalyst decomposition. To avoid adhesion of the polymer flakes and to decrease the viscosity of technological flows, an antiagglomerator in the form of a diluted aqueous suspension is introduced into

the reaction mixture at the degassing stage. Due to the formation of unconsolidated sediments, the most popular antiagglomerators are, in particular, slightly soluble calcium carboxylates and calcium stearate. Due to the formation of a structural mechanical barrier at the boundary of the liquid phase and the polymer, the antiagglomerator particles prevent the adhesion of the polymer flakes and provide their safe transportation to the drying stage. The antiagglomerating characteristic of the calcium stearate aqueous suspension, and therefore, its consumption and content in the final product (for the consumption of 7.5 kg of stearic acid and 1.5–2.5 kg of calcium chloride per 1 ton of polymer, the antiagglomerator content in the polymer should not exceed 1.1 wt%) are defined by the granulometric composition of the active substance.

During large-scale production, calcium stearate is formed directly before its introduction into the polymer solution (fresh antiagglomerator) according to a two-stage scheme ($St - C_{17}H_{35}COO^-$):

$$HSt + KOH \rightarrow KSt + H_2O$$

Then:

$$2KSt + CaCl_2 \xrightarrow{fast} CaSt_2 \downarrow + 2KCl$$

During the second stage, an irreversible ion exchange reaction with a solid-phase separation occurs (condensation method synthesis of a dispersed system). Therefore, it is possible to influence the granulometric composition of the antiagglomerator suspension by varying the reaction conditions of the calcium stearate and calcium chloride interaction.

In commercial production, the antiagglomerator based on calcium stearate, is formed directly in the circulation water pipeline. The concentration of stearic acid is 4.3–5.3 wt%, the average volume flow rate is 3 $m^3$/h at temperatures of up to 75 °C. The content of calcium chloride in aqueous solution is 2–3 wt%, with an average volume flow rate of 1.8 $m^3$/h, at temperatures of 20–25 °C; the concentration of the obtained aqueous solution of calcium stearate is no more than 5 wt%. The low flow rates of the initial solutions during their mixing in the pipeline (no more than 0.1 m/s at a total flow rate from 1.2 to 8 $m^3$/h) determine the inefficient mixing of the reactants and result in the production of rather large dispersed particles (diameter of around 100–500 μm).

The work of Zaharov [34] describes the laws governing the granulometric composition of the suspended particles of calcium stearate under the changing conditions of the calcium stearate aqueous solution and calcium chloride reaction, in particular, for tubular turbulent reactors.

In the case of using condensation methods to obtain dispersed systems, an important role belongs to the oversaturation of the local concentration of the barely soluble final product, where the centres of the solid-phase germ formation are located. An increase of the calcium chloride concentration at fixed calcium stearate content in aqueous solution, results in a decrease of the particle size (**Figure 4.19**). It should be noted that the diameter changes significantly in the range of $CaCl_2$ content in water up to 2–3 wt%. In addition, the suspension particle size changes during its synthesis: volume reactor → tubular reactor of cylinder construction → tubular reactor of diffuser-confusor design, and this correlates to the increase of the turbulent mixing intensity [3].

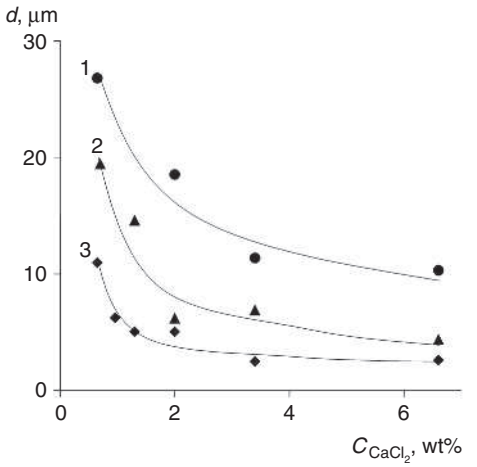


**Figure 4.19** Dependence of the diameter d, of the suspension particles on $CaCl_2$ concentration. Volume reactor (1), tubular turbulent reactor of cylinder (2) and diffuser-confusor (3) construction. $C_{StK}$ = 5 wt%

The change of potassium chloride aqueous solution concentration has a similar influence on the granulometric composition of the antiagglomerator (**Figure 4.20**). However, in this case, the dependencies are smoother, without any prominent bends, and the particle diameter decreases with the growth of the initial reactant concentration. This is obviously related to the increased viscosity of potassium stearate, which also explains the extremely low value of the reactant concentration of no more than 15 wt%. At a fixed ratio of the initial reactant concentration, an increase of the solid-phase content of the obtained calcium stearate suspension, results in the growth of the particle size. In all cases, particles of minimal experimental diameter can be obtained in the reaction within a tubular turbulent reactor of diffuser-confusor design.

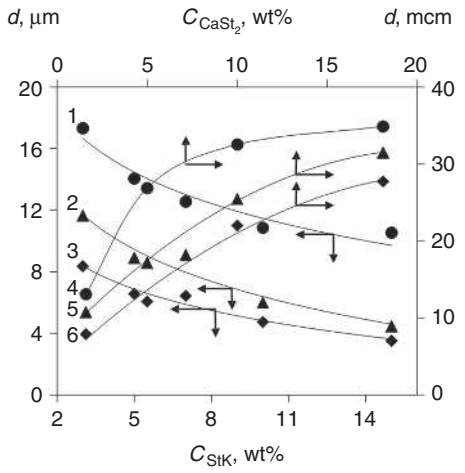


**Figure 4.20** Dependence of the suspension particle diameter on the concentration of StK $C_{StK}$ (1–3) ($C_{CaCl_2}$ = 2 wt%) and $CaSt_2$ (4–6). Volume reactor (1, 4), tubular turbulent reactor of cylinder (2, 5) and diffuser-confusor (3, 6) construction

Obtained dependencies can be explained by the change in the ratio between the germ formation rate and crystal growth rate. An increase in the concentration of one of the reactants, at a fixed low value of the other reactant, results in an increase of the solid-phase germ formation rate, due to the creation of local oversaturation zones in the reaction mixture, which act as a driving force for new phase formation. A decrease in the concentration of the second reactant provides a low rate of particle growth, due to the diffusion limits of the motion of the molecules from the aqueous phase volume to the crystal surface, which results in a decrease of the suspension particle size. It is obvious that in the commercial production of synthetic rubbers it is reasonable to use potassium stearate solutions with concentrations of up to 5 wt% and a concentrated solution of calcium chloride. Due to the fact that the solubility of $CaCl_2$ in water is around 50 wt% (at 30 °C), in order to obtain a finely dispersed suspension of antiagglomerate and to prevent early crystallisation of calcium chloride on the walls of the process equipment, it is reasonable to work with a concentration of up to 40 wt%. The use of a low-tonnage tubular turbulent reactor of diffuser-confusor design, due to the formation of intensive micromixing in the reaction zone, provides a higher germ formation rate than crystal growth rate, which in the long run results in a significant change of the suspension granulometric composition.

All the dispersed systems, due to a well-developed interphase surface and uncompensated surface energy, possess low aggregation stability. Moreover, under commercial production conditions, calcium stearate, before its introduction directly

into the polymer solution at the de-gassing stage, passes through a number of process units (pipeline, averaging vessel and so on), which is accompanied by the partial exfoliation of the reaction mixture and unavoidable agglomeration of particles. During the storage of a calcium stearate suspension, the solid-phase particles are enlarged despite the low concentration of the obtained dispersed systems (no more than 5 wt%) (**Figure 4.21**). The size of the particles, formed in the bulk mixing reactor, increases by around 30% within 40 min of storage in the absence of mixing. Almost no further changes of calcium stearate granulometric composition can occur. Due to the small initial size of the suspension particles, formed in tubular reactors of cylinder and diffuser-confusor design, they show an almost fourfold increase in size within 60 min. However, the final size of the particles, preliminarily formed in a tubular reactor of diffuser-confusor design and stored in the absence of suspension mixing, remains smaller than that of the particles synthesised by other methods. Thus, during the flow of the freshly formed antiagglomerator suspension through the process units to the degassing stage, the solid-phase particles may agglomerate. Furthermore, due to a decreased antiagglomerating capacity of the roughly dispersed suspension of calcium stearate, this can result in an unacceptable increase of antiagglomerator content in the final product. The experimental data shows the need for additional grinding of calcium stearate-based antiagglomerator particles directly before the exposure of the suspension to polymer grain stabilisation in the degasser.

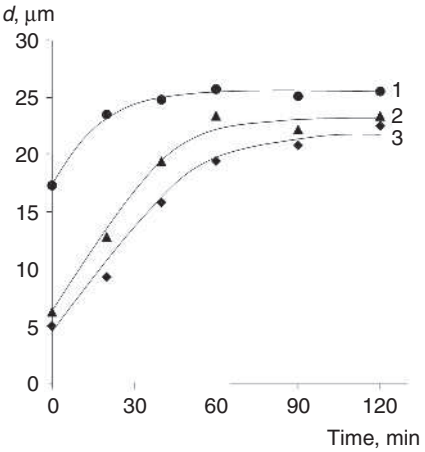


**Figure 4.21** Dependence of the suspension particle diameter on storage time in the absence of mixing $\tau$. Volume reactor (1), tubular turbulent reactor of cylinder (2) and diffuser-confusor (3) construction. $C_{StK}$ = 5 wt% and $C_{CaCl_2}$ = 2 wt%

The hydrodynamic impact on the preliminarily formed and stored (for a certain period of time) $CaSt_2$ suspension, in a volume reactor with an additional turbulising device,

does not significantly change the particle size of the dispersed phase (**Figure 4.22**). A decrease of the particle diameter can be observed during the hydrodynamic influence of the tubular devices of cylinder construction. The suspension treated in this way has an active component size comparable to the size of the components *in situ* (freshly made without preliminary storage) in a volume reactor with an additional turbulising device (**Figure 4.22**, curve 5). The flow of the preliminarily stored suspension in the tubular turbulent reactor of diffuser-confusor construction, due to the intensive shift deformations from the solid phase, leads to the formation of particles, the size of which does not exceed the size of the particles formed in the volume reactor *in situ* (**Figure 4.22**, curve 3).

The hydrodynamic influence on the suspension stored at different time intervals in different reactors, results in a similar decrease of the particle size. This can be observed in the parallel shift of the graphs showing the dependence of the particle diameter of calcium stearate upon storage time under different synthesis conditions (**Figure 4.22**, curves 1–3), relative to the dependence of antiagglomerator 'ageing' (**Figure 4.22**, curve 4). This proves the defining influence of shift deformations, from the solid phase, on the grinding process of preliminarily formed and stored suspension particles. The intensity of the hydrodynamic impact, for the reactors under consideration, is maximal for the tubular reactor of diffuser-confusor design.

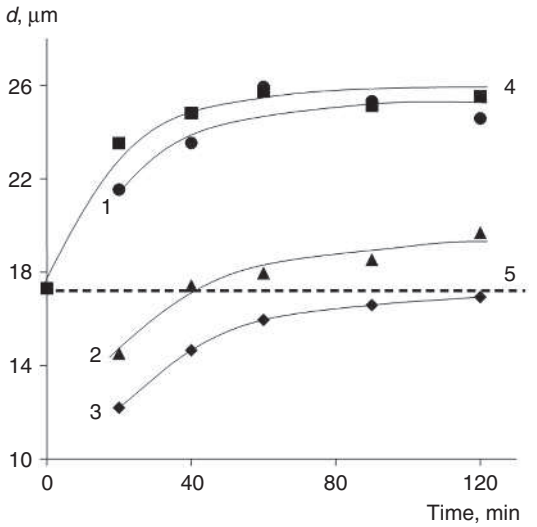


**Figure 4.22** Dependence of the particle diameter, formed in a volume reactor, on suspension storage time in the absence of mixing (4). Influence on the particles, preliminarily formed in a volume reactor (1), tubular turbulent reactor of cylinder (2) and diffuser-confusor (3) construction, and *in situ* (5)

Maintenance of the commercial parameters of the process, during the synthesis of the calcium stearate antiagglomerator in tubular turbulent reactors, allows an aqueous suspension with pH = 10.5–12 to be obtained. The hydrogen indicator of the solution is optimal both for the stabilisation of polymer grains and for the separation of the unreacted monomer and solvent from the reaction mixture at the degassing stage.

Thus, optimisation of the initial reactant concentrations during the production of an antiagglomerator for synthetic rubbers, on the basis of calcium stearate, provides an efficient impact on the granulometric composition of the active substance. *Ceteris paribus*, a suspension containing the smallest solid-phase particle size can be obtained under experimental conditions in a low-tonnage tubular turbulent reactor of diffuser-confusor design. Variation of the reactant concentrations, together with an improvement of the reactor type and construction, defines the possibility of the maximal ratio between the germ formation rate and the crystal growth rate, and therefore, the formation of calcium stearate particles of a high antiagglomeration capacity. The opportunity to obtain a high-quality product, the absence of mechanical mixing devices and moving elements, prove the advantages of tubular turbulent reactors of diffuser-confusor design for the production of calcium stearate-based antiagglomerators for synthetic rubbers.

## References

1. A.A. Berlin, K.S. Minsker and K.M. Djumaev in *Novel Unified Energy and Resource Efficient High Performance Technologies of Increased Ecological Safety Based on Tubular Turbulent Reactors*, Niitjehim, Moscow, Russia, 1996. [In Russian]

2. K.S. Minsker and A.A. Berlin in *Fast Polymerization Processes*, Gordon and Breach Publishers, Amsterdam, Netherlands, 1996.

3. K.S. Minsker, A.A. Berlin, V.P. Zakharov and G.E. Zaikov in *Fast Liquid-Phase Processes in Turbulent Flows*, Brill Academic Publishers, Amsterdam, Netherlands, 2004.

4. S.K. Minsker, T.V. Golubeva, A.A. Konoplev, V.Z. Kompaniec, A.A. Berlin, K.S. Minsker and N.S. Enikolopyan, *Doklady Akademii Nauk SSSR*, 1990, **314**, 6, 1450. [In Russian]

5. S.K. Minsker, A.A. Konoplev, K.S. Minsker, Y.A. Prochukhan, V.Z. Kompaniec and A.A. Berlin, *Teoreticheskie Osnovy Khimicheskoy Tekhnologii*, 1992, **26**, 5, 686. [In Russian]

6. K.S. Minsker, K.M. Dyumaev, A.A. Berlin, N.P. Petrova, S.K. Minsker and A.Y. Fedorov, *Bashkirskiy Khimicheskiy Zhurnal*, 1995, **2**, 3-4, 41. [In Russian]

7. A.Y. Fedorov, B.L. Rytov, A.A. Berlin and G.G. Aleksanyan, *Doklady Akademii Nauk*, 1995, **342**, 4, 494. [In Russian]

8. K.S. Minsker and V.P. Zakharov, *Teoreticheskie Osnovy Khimicheskoy Tekhnologii*, 2000, **34**, 2, 221. [In Russian]

9. K.S. Minsker, V.P. Zakharov, A.A. Berlin and G.E. Zaikov, *Polymer News*, 1999, **24**, 7, 249.

10. K.S. Minsker and V.P. Zakharov, *Bashkirskiy Khimicheskiy Zhurnal*, 1997, **4**, 3, 32. [In Russian]

11. K.S. Minsker, V.P. Zaharov, A.A. Berlin and G.E. Zaikov, *Himicheskaya Fizika*.1999, **18**, 5, 53. [In Russian]

12. K.S. Minsker, V.P. Zakharov, A.A. Berlin and G.E. Zaikov, *Chemical Physics Reports*, 1999, **18**, 5, 897.

13. V.A. Kaminskiy, A.Y. Fedorov and V.A. Frost, *Teoreticheskie Osnovy Khimicheskoy Tekhnologii*, 1994, **28**, 6, 591. [In Russian]

14. V.P. Zakharov, K.S. Minsker, F.B. Shevlyakov and M.M. Muratov, *Himicheskaya Promyshlennost*, 2003, **80**, 3, 30. [In Russian]

15. K.S. Minsker, V.P. Malinskaya, V.P. Zaharov and A.A. Berlin, *Zhurnal Prikladnoy Khimii*, 2000, **73**, 9, 1505. [In Russian]

16. V.P. Zakharov, A.A. Berlin and G.E. Zaikov, *Bulgarian Chemistry and Industry*, 2005, **76**, 2.

17. K.S. Minsker, A.A. Berlin, Y.M. Abdrashitov, J.K. Dmitriev, V.D. Shapovalov, V.P. Malinskaya and N.V. Alekseeva, *Himicheskaya Promyshlennost*, 1999, **76**, 6, 41. [In Russian]

18. S.M. Loktev, V.L. Klimenko, V.V. Kamzoskin and A.T. Menyajlo in *Fatty Alcohols*, Khimya, Moscow, Russia, 1970. [In Russian]

19. B.R. Serebryakov, T.K. Plaskunov, V.R. Nizheles and M.A. Dalin in *Higher Olefins*, Khimya, Leningrad, Russia, 1984. [In Russian]

20. K.S. Minsker, V.P. Zakharov, A.A. Berlin and R.Y. Deberdeev, *Himicheskaya Tehnologiya*, 2003, **3**, 30. [In Russian]

21. V.P. Zaharov, K.S. Minsker, F.B. Shevlyakov, A.A. Berlin, G.G. Aleksanyan, B.L. Rytov and A.A. Konoplev, *Zhurnal Prikladnoy Khimii*, 2004, **77**, 11, 1840. [In Russian]

22. I.S. Pavlushenko, L.N. Braginskiy and V.N. Brylov, *Zhurnal Prikladnoy Khimii*, 1961, **34**, 5, 805. [In Russian]

23. A.A. Berlin, K.S. Minsker and R.Y. Deberdeev, *Doklady Akademii Nauk*, 2000, **375**, 2, 218. [In Russian]

24. J. Baldyga, W. Podgorska and R. Pohorecki, *Chemical Engineering Science*, 1995, **50**, 8, 1281.

25. M-H. Sung, I-S. Choi, J-S. Kim and W-S. Kim, *Chemical Engineering Science*, 2000, **55**, 2173.

26. W.S. Kim and J.M. Tarbel, *Chemical Engineering Communications*, 1999, **176**, 89.

27. J. Chen, C. Zheng and G. Chen, *Chemical Engineering Science*, 1996, **51**, 10, 1957.

28. V.P. Zaharov, K.S. Minsker, I.V. Sadykov, A.A. Berlin and J.B. Monakov, *Zhurnal Prikladnoy Khimii*, 2003, **76**, 8, 1302. [In Russian]

29. A.G. Kasatkin in *Basic Processes and Machinery of Chemical Tehnology*, Khimya, Moscow, Russia, 1983. [In Russian]

30. E.D. Shhukin, A.V. Percov and E.A. Amelina in *Colloidal Chemistry*, Izdatelstvo MGU Moscow, Russia, [In Russian]

31. V.P. Zakharov, K.S. Minsker, I.V. Sadykov, G.E. Zaikov and Y.B. Monakov, *Journal of the Balkan Tribological Association*, 2003, **9**, 4, 585.

32. T.V. Bashkatov and Y.L. Zhitalin in *Synthetic Rubber Technology*, Khimiya, Leningrad, Russia, 1987. [In Russian]

33. P.A. Kirpichnikov, L.A. Averko-Antonovich and Y.O. Averko-Antonovich in *Chemistry and Technology of Synthetic Rubber*, Khimya, Moscow, Russia, 1975. [In Russian]

34. V.P. Zaharov, *Zhurnal Prikladnoy Khimii*, 2006, **79**, 11, 1865. [In Russian]

# 5 Novel Approaches to the Instrumentation of Fast Technological Processes

Reactors are the essential elements of any technological process and flow sheet connected with the chemical transformation of substances. Equipment efficiency in terms of reliability, susceptibility, production and economic efficiency, and ecological safety are very important for any successful technological process. Industrial chemical equipment is available in different shapes, which complicates their classification. Generally, they are divided into continuous or batch models, perfect mixing and plug flow reactors, or their empirical combinations.

## 5.1 Plug Flow Reactors

There are different tubular and column plug flow reactors as well as screw reactors [1]. Plug flow reactors are used for various gas-phase reactions occuring within industrial-scale production, particularly for the reactions of nitrogen oxide oxidation, ethylene chloration, and high-pressure ethylene polymerisation. They are also used for some liquid-phase and gas-liquid reactions, e.g., styrene polymer production in a column, plastic and rubber production, synthesis of ammonia and methanol, and sulfation of olefins [2].

In continuous plug flow reactors there is no longitudinal mixing of fluids [1]. Therefore, the appropriate approximation of the reactor parameters is the plug flow model. This model is characterised by the following points:

1. Plug flow of reaction mixture.
2. Volume flow rate and fluid properties (pressure, temperature, and composition) are homogeneous at any cross section which is normal to the fluid motion. Therefore, the plug flow reactor is characterised by the narrow residence time distribution of reactants in a vessel. The average residence time $\bar{\tau}_{pass}$ may be calculated from the equation given below [3]:

$$\bar{\tau}_{pass} = \frac{L}{V} \tag{5.1}$$

Where:

$L$ is the reactor length

$V$ is the flow rate

3. There are gradients of temperature, reactant concentration, and chemical reaction rate along the reactor length due to the absence of longitudinal mixing (diffusion is negligible in comparison with the volume flow rate).

If the process occurs under laminar conditions, as typically takes place during polymerisation in plug flow reactors (particularly in the processes of casting polymerisation [4]), the cross dimensions of a plug flow reactor are limited by the transfer rate in the transversal direction, which have a molecular nature and therefore small values. At the same time, the prolonged period of many industrial processes (prolonged period of the chemical reaction $\tau_{chem}$) results in a long length of the plug flow reactor and the creation of high driving forces.

It is impossible to create an isothermal process in plug flow reactors as it requires the variation of thermal transfer, along the reactor length, according to the kinetics of heat emission. Therefore, plug flow reactors run under adiabatic conditions or at least under nonisothermal mode conditions with external heat removal. The heat balance equation for steady state conditions for the micro volume of a reactor can be written in the form [4]:

$$Q = -C_p \frac{dT}{dt} dv_p + q \frac{dP_{vol}}{dt} dv_p - 2\pi R dL K_T (T_{ad} - T_{cool}) \tag{5.2}$$

Where:

$v_r$ is the reactor zone volume.

$q$ is the reaction thermal effect.

$P_{vol}$ is the product yield per volume unit.

$C_p$ is the constant pressure heat capacity.

$K_{bt}$ is the heat transfer through a wall.

It should be noted that any deviation from ideal plug flow reactor behaviour is called back mixing. The opposite unit of the plug flow reactor is a continuous perfect or ideal mixing reactor.

## 5.2 Perfect Mixing Reactors

According to the construction of perfect mixing reactors, or cascade of flow mixing reactors, they can be classified as vertical and horizontal tanks equipped with different

agitators: blade, impeller, ribbon, disk, screw, and the agitators enable the mixing of a highly viscous media [5].

The fluid in the mixing reactor is perfectly mixed which distinguishes it from the plug flow reactor. It allows maximal use of the reaction volume without the formation of dead fluid zones. A wide residence time distribution of reactants is observed in this type of reactor.

Typically, the steady state mode of a mixing reactor is characterised by isothermal conditions. Therefore, the temperature field in the reaction zone can be changed during the process (generally for the cascade mixing reactors).

In mixing reactors, the heat balance is characterised by a temperature increase, due to the adiabatic heating of the reaction mixture, and the heat removal rate (without taking into account the boiling process) [4]:

$$Q_T = G_r \rho C_p (T_r - T_0) + C_T F (T_r - T_{\text{cool}}) \tag{5.3}$$

Where:

$G_r$ is the reactive mixture flow rate

$F$ is the heat transfer surface

The ideal models presented here allow us to study the processes at constant values of temperature and concentration in a reactor, i.e., under steady state conditions. Under the real conditions of chemical production, the physical processes of heat and mass transfer (heat conduction, diffusion, convection, turbulence, and so on) play an essential role.

The parameter which takes into account the heat and mass transfer, for the analysis of different chemical processes, is the relationship between the characteristic chemical reaction time ($\tau_{\text{chem}}$) and the heat or mass transfer; first of all, the mixing time:

$$\tau_{\text{chem}} < \tau_{\text{mix}} \tag{5.4}$$

One of the ways of influencing the chemical reaction behaviour in the diffusion region (chemical reaction rate, process selectivity, product characteristics, temperature mode, and so on) is the intensification of turbulent mixing in the chemical vessel. The most effective solution to this problem is the use of continuous plug flow tubular

turbulent reactors, which are not presented in the classification of continuous devices for chemical technology.

Small-sized tubular turbulent flow reactors of high capacity have been designed to create an effective process for rapid liquid-phase reactions in a turbulent mode. The units combine the best technological and engineering advantages of mixing and plug flow reactors, as well as having special characteristics which differ from other types of reactors.

## 5.3 Plug Flow Tubular Turbulent Reactors

Four designs of tubular turbulent reactors have been developed for creating rapid chemical reactions and mass exchange liquid-phase processes on an industrial scale (**Figure 5.1**): the cylindrical reactor (with a constant diameter along the reactor length); the tubular reactor (with a tube bundle surrounded by a coolant); the divergent-convergent reactor (with several sections connected in parallel with local hydrodynamic resistance), and the zone reactor (with independent adiabatic reaction zones connected in parallel and separated from each other by cooling zones). These reactor designs are principally different from the conventional industrial mixing and plug flow devices.

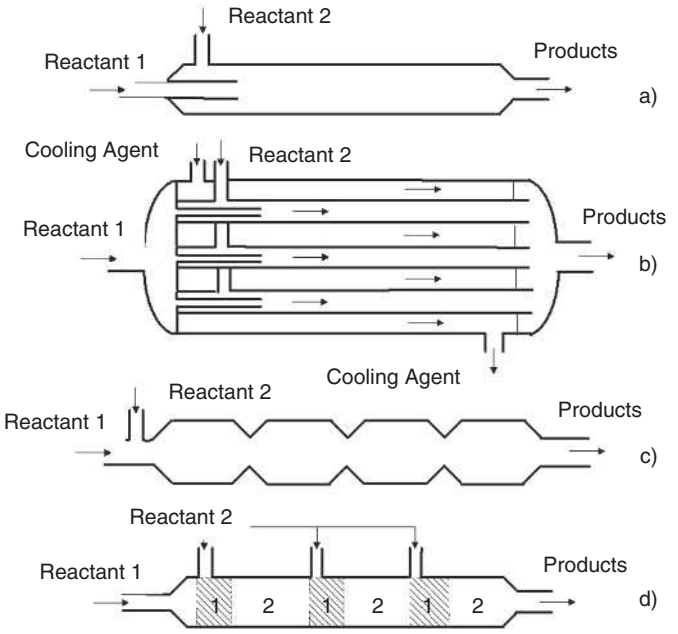


**Figure 5.1** Tubular turbulent reactor designs: cylindrical (a), tubular (b), divergent-convergent (c), and zone (d) (1 – reaction zone, 2 – cooling zone)

The relative disadvantage of small-sized tubular turbulent reactors of first generation (cylindrical design) is the rapid drop of the turbulence diffusion coefficient $D_{\text{turb}}$, which leads to a decreased mixing efficiency of the reaction mixture in the reactor when moving away from the area of reactant feeding, as well as low efficiency of external heat withdrawal. Tubular turbulent reactors have been designed to increase the efficiency of heat withdrawal. The design of the tube bundle, surrounded by the coolant, significantly increases the external heat withdrawal efficiency for the process occurring under quasi-isothermal conditions, whilst retaining the required productivity. If effective heat withdrawal cannot be provided for rapid chemical reaction processes based on both turbulent designs, the zone reactor can be used to avoid overheating of the reaction mixture in the areas of reactant feeding. A fixed amount of a reactant is fed to each zone where the reaction takes place. As the reactant amount defines the permissible temperature rise in this reactor zone, a greater number of reaction zones demands greater control of the rapid chemical reactions. In the case of polymer synthesis, it improves the control of the molecular characteristics.

The divergent-convergent reactors, the second generation tubular turbulence devices, show the best technical characteristics for rapid liquid-phase processes, in comparison with other chemical technology vessels. In particular, they provide the required level of turbulence, which results in an intensification of the mixing and heat transfer processes at essentially low values of flow rate, practically maintain a constant high level of turbulence throughout the reactor volume, form an automodelling mode related to viscosity, Reynolds number, and so on. Therefore, these reactors are essential devices when working with different products, including high viscosity polymer solutions. The divergent-convergent reactors, working with multiphase systems, are characterised by high efficiency. Due to local hydrodynamic resistance, the fine grinding of phases, which produces homogeneous emulsions and foams, occurs here. In comparison with bubbling or rapid mechanical mixing, the divergent-convergent reactors show a higher dissolution rate and amount of gas in liquid (an order of magnitude greater), as well as higher heat transfer coefficients through the outer wall compared with devices of cylindrical design. Under the relation:

$$\tau_{\text{chem}} > \tau_{\text{turb}} > \tau_{\text{meso}} > \tau_{\text{micro}} \tag{5.5}$$

The rapid processes occur in optimal mode and therefore, decreasing the reactor radius $R$ leads to a reduction of the characteristic mixing time, which is the main aspect for rapid processes occurring under optimal conditions. The only effective way of influencing the dispersing performance and quality of the desired emulsions and suspensions is to change the construction and $d_d/d_c$ ratio. The divergent-convergent reactors can work both in plug flow and mixing modes, which is possible due to the change of device geometry and the ratio of reaction mixture rates.

Thus, divergent-convergent tubular turbulent reactors which can be used for the formation of both a quasi-plug flow mode in turbulent flow (the main condition of any chemical process:

$$\tau_{mix} \leq \tau_{chem} \tag{5.6}$$

is met), and an automodelling liquid flow mode, related to the Reynolds number and viscosity, have become novel small-sized highly efficient industrial flow devices. They combine the best technical and technological characteristics of mixing and plug flow reactors and may be included in the classification of devices for the chemical industry.

Tubular turbulent units, used for creating rapid chemical processes during industrial production, provide continuous energy- and resource-saving technologies, meeting ecological requirements.

## 5.4 Continuous Energy- and Resource-saving Technologies Based on Tubular Turbulent Reactors

Small-sized tubular turbulent units are used in the production of:

- Low and medium molecular weight polymers and copolymers such as isobutylene, butylene, propylene, and so on, at the stage of cationic homo copolymerisation.
- Synthetic butadiene methylstyrene rubber of various grades. Butadiene-$\alpha$-methylstyrene rubbers ('hot' and 'cold' free radical copolymerisation of butadiene with $\alpha$-methylstyrene), at the stages of emulsion formation, emulsion mixing with an initiator, and introducing a terminator to the reaction mixture.
- Stereoregular polyisoprene at the stages of formation of growth centres of macromolecules (prereactor). The following grades of rubber can be produced: synthetic *cis*-isoprene rubber SKI-3 synthesised on a titanium-aluminum (Ti-Al) catalytic system and synthetic *cis*-isoprene rubber SKI-5 synthesised on a neodymium-aluminium (Nd-Al) catalytic system, neutralising and decomposition of isoprene hydrochlorides, and water washing of isoprene-isopenthane fractions of hydrocarbons.
- Synthetic ethylene-propylene rubber (EPM) and synthetic ethylene-propylene rubber modified by dicyclopentadiene (EPDM) at the stages of formation of a homogeneous gas-liquid mixture, during its uniform feed into the polymerisers running in parallel, formation of growth centres of macromolecules (prereactor),

decomposition and washing of Ziegler–Natta catalysts, and introduction of the stabilisers into the polymer.

- Halobutyl rubbers at the stages of halogenation of butyl rubber, neutralising and washing of the polymerisate, and the introduction of stabilisers.
- Mixed gasoline at the stage of compounding.
- The products of alkylation of isoparaffins by olefins.
- Ammonium phosphate fertilisers at the stage of interaction of liquid ammonia with phosphorous acid.
- Dichloroethane, chloroethane, and chlorobenzene at the stage of chlorination and hydrochlorination of hydrocarbons.

Novel methods and devices for these processes guarantee maintaining the key principles of the current flow sheet, namely: reducing the production area with no requirement for capital construction; more than a 2–4-fold increase in total productivity; (a 1,000-fold and more) increase in specific reactor capacity; high quality of end products; using a wide range of raw material composition, as well as off-grade materials without extra purification; decreasing the unit consumption of raw materials (by 10–15%) and catalysts (by a factor of 1.5–2); decreasing the specific amount of metal per structure and the reactor size (by a factor of 1,000–10,000); decreasing the cost per unit of water (by up to 15–20% and more); decreasing the power consumption (by up to 15–20% and more); staff reduction; a high level of ecological compatibility of the technological processes; narrowing the molecular weight distribution of the polymers ($M_w/M_n$ from 8–12 and still further to 2.5–3.5); process versatility (production of a broad spectrum of polymers with a molecular weight from 200 up to 60,000 by using a single reactor), and so on.

The general characteristics of novel energy- and resource-saving technology being able to meet the requirements of ecological safety, based on the tubular turbulence reactors, have been confirmed by the pilot-scale testing of the production of:

- 'Dneprol' an additive based on polyisobutylene [6].
- Isobutylene-styrene copolymer INH-388 [6].
- Piperylene oligomers (cationic oligomerisation, process terminating, and polymerisate washing) [7].
- Butadiene chlorination [6].

- Decomposition of Ziegler–Natta catalysts or chlorine-containing electrophilic catalysts using water, alcohol, steam, and so on [8, 9].
- Stabilised rubbers during the coupling of a rubber solution (polymerisate) with a stabiliser solution, and so on [10].
- Adhesion reducing powder for synthetic rubbers (interaction of potassium stearate with calcium chloride) [11].
- Acyclic, cyclic, di- and polyamines (dichloroethane ammonation and neutralising aminohydrochloride) [12].
- Detergents (neutralisation, washing, and alkylsulfate extraction) [13].
- Terephthalic acid (*p*-xylene oxidation with atmospheric oxygen) [12].
- Isopentene (isoprene hydrogenation) [12].
- Butene-1 (formation of a catalytic system of ethylene dimerisation).
- Synthetic rubbers (water washing of the butylene-isobutylene fraction and divinyl from ammonia, and isoprene from carbonyl- and nitrogen-containing compounds).
- Stereoregular polybutadiene rubber (formation of homogeneous macromolecule growth centres).

A detailed review of the commercial introduction of tubular turbulence reactors realised before 1996 is presented in the work of Berlin and co-workers [6].

### *5.4.1 Oligoisobutylenes and Polyisobutylenes*

For the first time, tubular turbulence devices of cylindrical design have been used in the commercial production of different polymer brands – butylenes (**Table 5.1**) in the Russian cities of Sumgayit, Salavat, Samara, Grozny, and Kremenchuk. A detailed review of the technological aspects in the production of oligo- and polyisobutylenes is presented in the work of [6]. Average parameters of a tubular reactor in comparison with conventional mixing devices are shown in **Table 5.2**.

**Figure 5.2** shows the interaction between the input and output parameters of rapid isobutylene polymerisation, occurring in the tubular turbulence reactor, demonstrating the possibility of automated reaction operation.

| Table 5.1 Commercial brands of oligoisobutylenes and polyisobutylenes | | | | | | | | | | | | |
|---|---|---|---|---|---|---|---|---|---|---|---|---|
| Product $M_w$ | | | | | | | | | | | | |
| 300–500 | 600–800 | 800–1,200 | 700–1,600 | 2,000–3,500 | 4,000–6,000 | 9,000–15,000 | 16,000–25,000 | 40,000–55,000 | 70,000–99,000 | 100,000–134,000 | 135,000–174,000 | 175,000–225,000 |
| Low $M_w$ | | | | | Medium $M_w$ | | | | | High $M_w$ | | |
| Commercial brands | | | | | | | | | | | | |
| Octol-300 | Condensing octol | Octol -1,000 | Octol -C | Octol -600 | П-5 | П-10 | П-20 | П-50 | П-85 | П-118 | П-155 | П-200 |

| Table 5.2 Technical and economic running of a tubular turbulent reactor under quasi-plug flow conditions in turbulent flows in comparison with a perfect mixing reactor | | | | |
|---|---|---|---|---|
| **Parameters** | **Tubular turbulent reactor** | **Mixing reactor, Russian company 'Lenniihimmash'** | **Mixing reactor, US company Stratco** | **Mixing reactor, US company Amoco** |
| Reactor volume, $m^3$ | 0.04 ± 0.02 | 1.5–4.0 | Up to 29 | 20–30 |
| Specific amount of metal, tonnes | 0.05 | 7.5 | Up to 40 | 50 |
| Energy consumption, relative unit | 0.08–0.085 | 1 | 1 | 1 |
| Response time (after shutting down), h | 0.01 | 5.5 ± 0.5 | 4±1 | 4±1 |
| Residence time, h | 0.003 | 1.5 ± 0.5 | 1 | 1 |
| Productivity, ton/h | More than 10 | 2 ± 1 | Up to 5 | Up to 10 |
| Relative productivity, relative unit | More than 1000 | 1 | 1 | 1.5 ± 0.5 |
| **Cost per unit of material, relative unit** | | | | |
| Water | 0.8 | 1 | 1 | 1 |
| Raw material | 0.75 | 1 | 0.9 | 1 |
| Catalyst | 0.55 | 1 | 1 | 1 |
| Adapted from A.A. Berlin, K.S. Minsker and K.M. Djumaev in *Novel Unified Energyand Resource Efficient High Performance Technologies of Increased Ecological Safety Based on Tubular Turbulent Reactors*, Niitjehim, Moscow, Russia, 1996 [6] | | | | |

### *5.4.2 Halobutyl Rubber*

Nowadays, over one million tons of butyl rubber is produced worldwide every year. Highly technological developments define the required properties of new butyl rubber and, in order to meet them, there is a rapid growth in the production of halobutyl rubber. Conventional technologies are based on the partial or complete addition of chlorine, bromine, iodine, and their mixtures, to the butyl rubber molecule. Such technologies use mixing reactors made from metals and alloys with high corrosion resistance. The distinguishing characteristic of this process is that halogenation agents may be in different aggregative states, e.g., chlorine may be in a gas form or in aqueous solution; bromine and iodine are in solution, and so on.

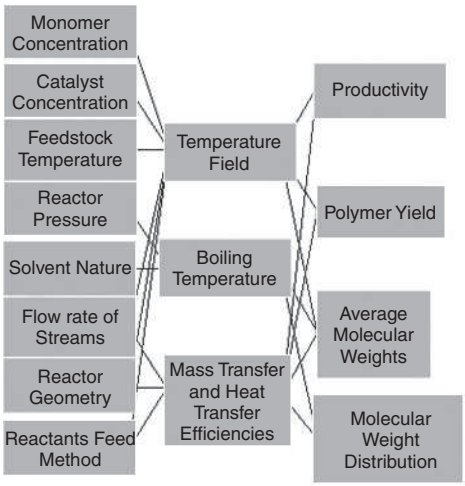


**Figure 5.2** The influence of chemical and technological factors on the quality and yield of polyisobutylene

From an engineering point of view, the commercial production of chlorobutyl rubber is an energy-consuming and complex process. The appropriate commercial process for chlorobutyl rubber production is butyl rubber chlorination with molecular chlorine in a highly viscous solution. The process consists of: 1) preparing a 10–15 wt% butyl rubber solution in aliphatic or chlorinated hydrocarbons; 2) liquid-phase chlorination of butyl rubber with molecular chlorine in solution; 3) neutralisation of the formed chlorobutyl rubber solution in a hydrocarbon solvent; 4) washing the salts from the chlorobutyl rubber solution with water (extraction); 5) introducing the stabiliser (calcium or zinc stearate powder) to the chlorobutyl rubber which acts as an antioxidant and adhesion reducer; 6) aqueous degassing of the polymer; 7) extraction and drying of the polymer; and 8) washing of the solvent, azeotropic drying and distillation of the solvent.

Standard reactors (6 $m^3$ and more), columns, mixing tanks, and so on, equipped with powerful agitators and heat exchangers are used at practically each stage of technological processes worldwide (**Figure 5.3**). There are some problems which must be solved during the process: 1) creating an effective mass transfer in a 'viscous liquid-gas' system with the accompanying formation of small bubbles in the reaction zone, and preventing the formation of a slug mode during the motion of the gas mixture through the viscous liquid; 2) providing the conditions for butyl rubber chlorination where the mixing time is equal or less than the chemical reaction time $\tau_{mix} \leq \tau_{chem}$. For the intensification of butyl rubber chlorination in mixing reactors, a centrifugal pump is typically used as an additional unit (chlorinator), where the butyl rubber solution and chlorine-nitrogen mixture are delivered. Recycling is used to provide the required residence time of the reaction mixture.

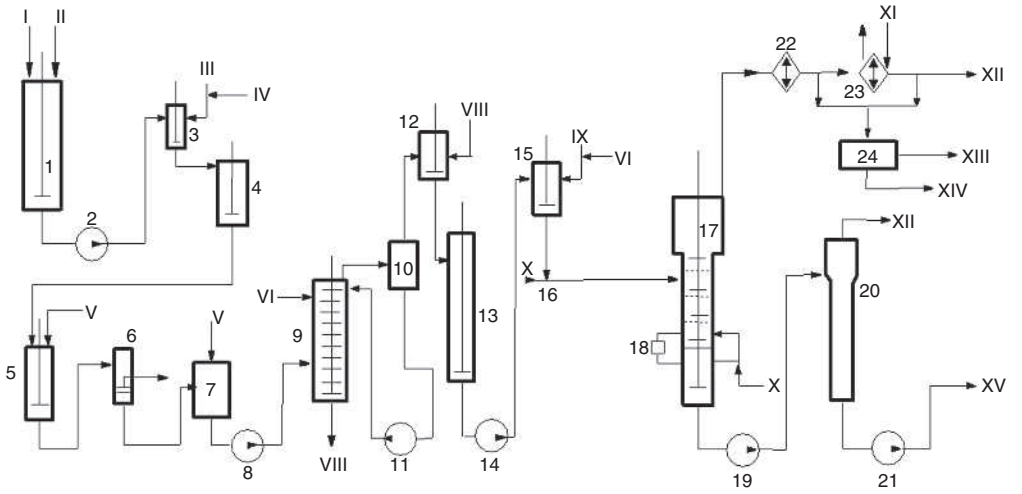


**Figure 5.3** Conventional chlorobutyl rubber production flow sheet: 1 – device for the production of butyl rubber solution; 2, 8, 11, 14, 19, 21 – pumps; 3,12,15 – stirred tanks with mechanical agitators; 4 – mixing reactor – chlorator; 5 – mixing reactor – neutraliser; 6 – filter; 7 – receiver; 9 – washer-column with agitator; 10, 24 – settlers; 13 – balance tank; 16 – injector; 17 – degasifier; 18 – expansion device; 20 – vacuum degasifier; and 22, 23 – condensers. Flows: I – solvent; II – butyl rubber chips; III – chlorine; IV – nitrogen; V – alkali water; VI – water; VII – washing water; VIII – stabiliser-antioxidant solution; IX – suspension of adhesion reducing powder; X – steam; XI – coolant; XII – to vacuum line; XIII – gasoline for drying; XIV – water for steaming out the organic compounds; and XV – pulp slurry to the concentrator

Based on the study of butyl rubber chlorination with molecular chlorine in the solution, the formation conditions of an automodel flow mode of high viscosity polymer solutions, and the fundamentals of the two-phase flow motion through tubular pipes, a principally new commercial continuous process for the production of chlorobutyl rubber has been proposed. The originally designed small-sized tubular turbulent devices, running in highly turbulent flows, can be used in at least four stages of the flow sheet (**Figure 5.4**) [10, 14, 15]. There is no mixing reactor, where the process of chlorobutyl rubber saturation with chlorine takes place. The mixing reactors are replaced with tubular reactors at the stages of butyl rubber chlorination (position 4), neutralising (position 5), introducing the stabilisers and adhesion reducing powder to the polymer (positions 12, 15). It is possible to replace the washer with a tubular device (position 9), where water washing of the solution occurs.

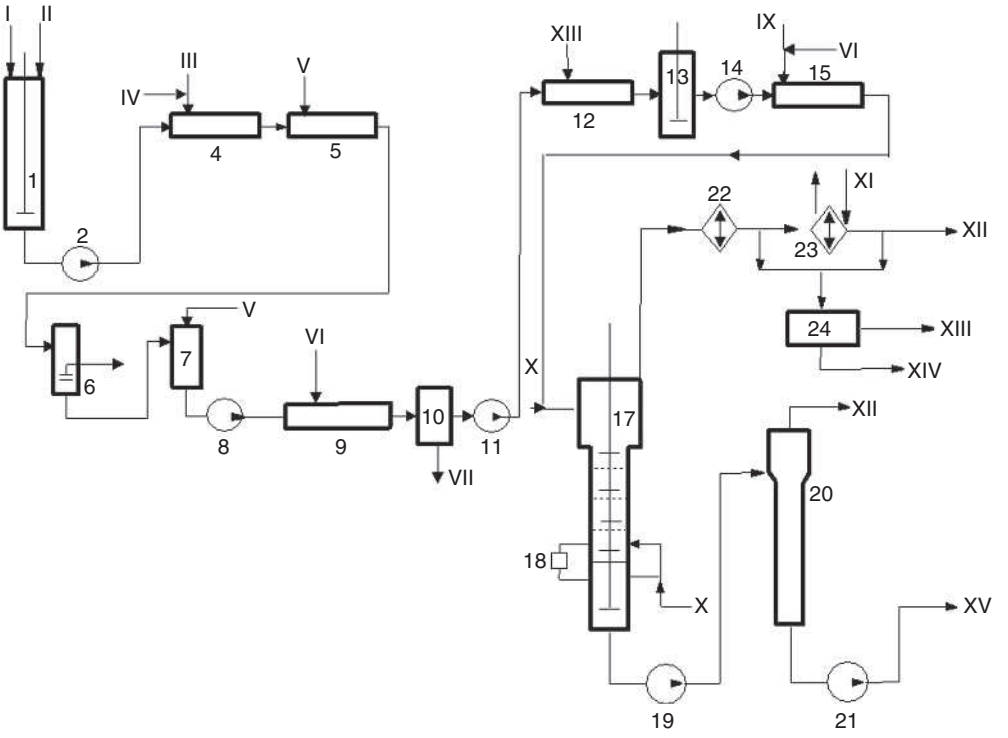


**Figure 5.4** Chlorobutyl rubber production flow sheet using flow tubular turbulent reactors at stages: 12, 15 – introducing the stabiliser-antioxidant and adhesion reducing powder to chlorobutyl rubber, respectively; 4 – chlorination; 5 – neutralising; and 9 – water washing of the solvent

The principal reaction of the interaction between a halogen and elastomer solution depends mainly on the aggregative state of the halogen. If the halogen is in a gaseous state, it is necessary to rapidly form a fine gas-liquid suspension and start mixing it intensively along the flow motion. Intensive mixing of the fine suspension enables the developed interphase of the suspension to be maintained and, along with the rapid reaction due to the addition of chlorine, makes the formation of a slug mode of gaseous media impossible. It should be taken into account that the differences in density and amount of interacting components are very high; therefore, it is the most complicated stage of the process.

To realise this stage a small-sized tubular turbulent reactor-chlorator, equipped with a novel packing, has been developed [12, 16] (**Figure 5.5**).

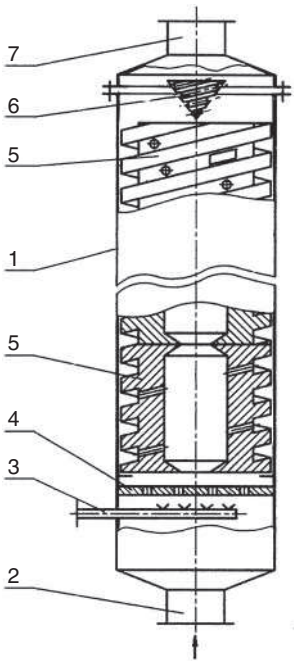


**Figure 5.5** General drawing of a divergent-convergent tubular turbulent reactor with packing for butyl rubber chlorination. 1 – casing; 2 – input connection for the butyl rubber solution; 3 – input connection for the gaseous mixture or gas; 4 – spreader; 5 – packing; 6 – static mixer; and 7 – output connection for the gas-liquid mixture

The gas mixture volume in this process exceeds the volume of the elastomer solution. Therefore after premixing, it is necessary to divide the flow in the packing into at least 2 parts: peripheral and axial. The peripheral flow passes through the spiral channel, which is formed by grooves on the external surface of the packing and the internal surface of the tubular reactor vessel. Due to the spiral motion, turbulisation of the gas-liquid mixture and an intensive mixing process occurs, leading to suspension formation. Increasing the turbulisation flow results in smaller suspension particles; increasing the interphase boundary leads to a more intensive interface renewal and chemical reaction rate.

The axial flow runs within the packing where the flow turbulisation occurs, as in the case of peripheral flow, which is attainable due to the cone shape of the internal end-face packing surface. The packing interconnects and forms a system of divergent-convergent sections, within the sections the flow continuously narrows and expands, causing flow turbulisation, and enables the rapid and thorough mixing of media and the intensification of the chemical reaction.

Taking into account that the halogenation process in the two flows may occur with different intensities, it is necessary to provide special spaces in the packing for interconnection and mixing of the two flows along the reactor length. Complete mixing of the two flows occurs along the flow motion as they leave the last packing. The packing may have porous separation layers, settled at regular intervals, for additional mixing intensification of the interacting peripheral and axial flows.

The processes of washing, neutralisation, and stabilisation of the halogenated elastomer also occur in turbulent flow motion by the introduction of an appropriate agent.

The continuous technological process of halogenated elastomer production, using small-sized tubular turbulent reactors, may be realised by a more compact flow sheet (**Figure 5.6**) [17].

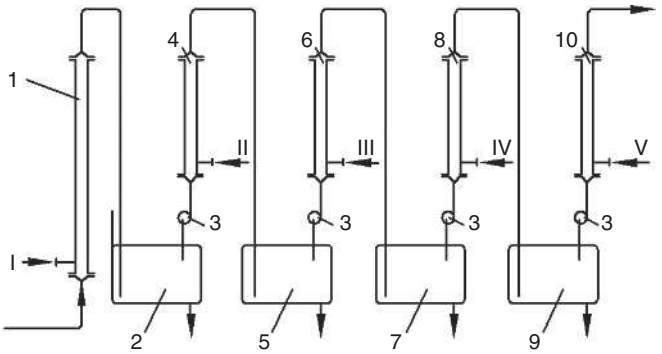


**Figure 5.6** Diagram of the principle of chlorobutyl rubber production based on small-sized tubular turbulent reactors. 1 – chlorator; 4 – basic washing reactor; 6 – neutraliser; 8 – additional washing reactor; 10 – stabilisation reactor; 2, 5, 7, 9 – separation chambers; and 3 – pump. Flows: I – halogen; II and IV – water; III – neutraliser; and V – stabiliser

The process may easily be transformed for the synthesis of other elastomers and copolymers with a double bond in the backbone of the monomer unit. Therefore, the range of elastomers is extensive: isoprene, butadiene, butadiene-styrene rubbers, ethylene-propylene terpolymer, and so on.

The process is compact, energy and resource effective, environmentally safe and easy to operate. It guarantees an increase in productivity (100-fold), an essential decrease in floor space, and high quality of products [17]; in addition, a decrease in product and investment cost. The equipment is made from low cost alloys, which is a significant advantage of the process.

### 5.4.3 Ethylene Propylene Rubber

The continuous solution copolymerisation of ethylene and propylene in the presence of a third unsaturated monomer (ethyledennorbornen or dicyclopentadiene), using Ziegler–Natta catalysts, is a delicate process. The parameters of the produced rubber differ from the parameters set for the respective polymerising batteries. It is connected to an insufficient stability of the gas-liquid mixture, containing the gaseous and liquid products, which leads to demixing during motion in the pipes. There is a possibility of inhomogeneity in the activity of the catalytic complex, which can occur during the mixing of the initial components. As a rule, this process occurs in the first reactor volume of a polymerising battery.

Based on the study of process characteristics and predicting the possible results of technological flow intensification, the advanced technological flow sheet for the synthesis of saturated copolymers of ethylene and propylene, and unsaturated copolymers of ethylene, propylene, and a third monomer, have been proposed.

During the first stage of the gas-liquid mixture (charge), containing a hydrocarbon solvent (nefras, hexane, heptane, diaromatic fractions $C_6$–$C_8$ or their mixtures), monomers (ethylene, propylene, dicyclopentadiene, ethylidennorbornen), and hydrogen, the recirculating gas enters the manifold and then the divergent-convergent tubular reactor. Due to the turbulent motion, there is complete and rapid mixing, and saturation of the liquids containing the gaseous products with the formation of a fine gas-liquid suspension.

The laminar gas-liquid flow in the tubes is divided into a gas and fluid medium, which leads to a change of the fractional composition of the flow entering the first reactor-polymerisator. To provide the required product quality, the suspension composition must be kept at an appropriate level during its motion to the reactor.

Another problem during production is obtaining copolymers with equal composition when using different polymerisation batteries. In this case, a reactor is used to distribute the monomer solution. Here, the additional developed turbulent motion is created using special sections, of divergent-convergent design, as packing. Subsequently, the gas-liquid mixture is distributed, under these conditions, through the outlet of the reactor-distributor to the distributing pipes; *via* this method, the gas-liquid mixture is delivered to the reactors under equal conditions. At the last stage, the gas-liquid mixture is again subjected to turbulisation before it enters the reactor.

According to the processes mentioned above, during the formation of a homogeneous gas-liquid mixture (**Figure 5.7**), a certain amount of cooled components are delivered, under pressure, to the manifold (position 7) and to the tubular turbulent divergent-convergent reactors (positions 8 and 9), where a turbulent flow motion is developed,

which leads to preliminary mixing. In a tubular turbulent reactor-distributor (position 10), the gas-liquid mixture is mixed again under the conditions of turbulent flow. The gas-liquid mixture travels to the distributing pipes (position 11) without changing the flow conditions. Then, the gas-liquid mixture, *via* the tubular turbulent divergent-convergent reactors (position 12), is forced directly into polymerisers working in parallel.

The gradual preparation of the gas-liquid mixture in tubular turbulent reactors, and its distribution to polymerisers working in parallel, results in the production of copolymers with equal properties in various reactors. Under equal polymerisation conditions, an increase in total process productivity is observed, and the productivities of separate polymerisers become identical [18].

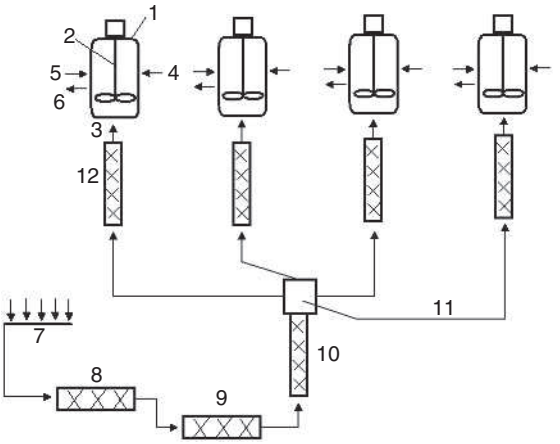


**Figure 5.7** The reactor-distributor and method of continuous solution copolymerisation. 1 – polymeriser; 2 – drive of the mixing device; 3 – connection pipe for the introduction of the gas-liquid mixture; 4, 5 – connection pipe for the separate introduction of the catalytic complex components; 6 – connection pipe for taking off the copolymer; 7 – manifold; 8, 9, 12 – tubular turbulent divergent-convergent reactors; 10 – tubular turbulent reactor-distributor; and 11- distributing pipes

There are three methods of catalytic complex production at the formation stage of the macromolecule growth centres, during monomer copolymerisation in the presence of the vanadium-aluminium (V-Al) catalytic complex (separation of the rapid stage of active centre formation and initiation, from the slow stage to copolymerisation):

1. Separate turbulent mixing of the catalytic complex components (catalyst and cocatalyst) and their introduction by separate flows, in gas or liquid phase, to the volume of the first reactor-polymeriser. (**Figure 5.8a**) [19].

2. Concurrent turbulent mixing of the catalytic complex components in a tubular reactor and their introduction into the reaction mixture volume of the first reactor-polymeriser (**Figure 5.8b**) [20].

3. Catalytic complex formation over the surface of the reaction mixture of the first reactor-polymeriser (**Figure 5.8c**) [21].

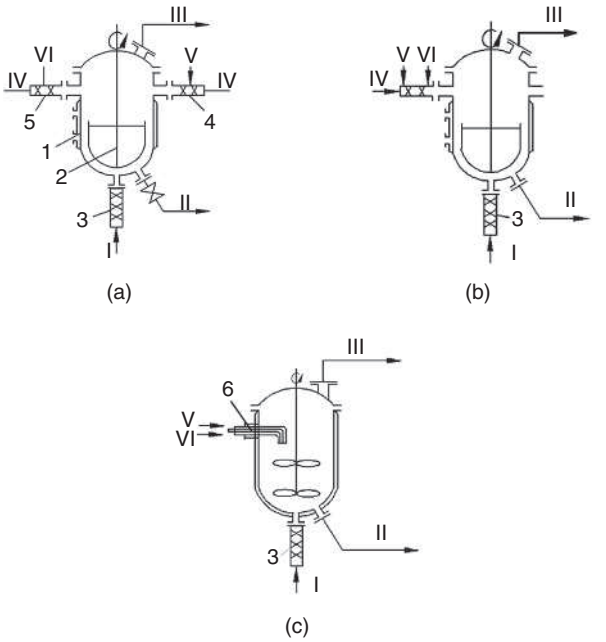


**Figure 5.8** Different technological schemes for the catalytic complex formation of ethylene and propylene copolymerisation. 1 – polymeriser; 2 – mixing device; 3 – tubular vessel for preparing the gas-liquid mixture; 4 – tubular vessel for preparing the cocatalyst solution; 5 – tubular vessel for preparing the catalyst solution; and 6 – tubular turbulent sprayer. I – gas-liquid mixture; II – polymer solution; III – recirculating gas; IV – solvent; V – cocatalyst; and VI- catalyst

Depending on the mixing conditions of the catalyst and cocatalyst, the tubular turbulent sprayer may be designed and divided into three technological schemes (**Figure 5.9**). In this case, the catalyst is delivered into fitting pipe 1, inside canal 2 of the prereactor (**Figure 5.9**); the solvent is introduced into fitting pipe 3. The flow, going through the turbulence section, position 4, equalises the catalyst concentration over the flow volume and enters position 5. The flow enters divergent-convergent section 6 through the inside canal, where turbulisation is provided. Then the flow goes to nozzle 7, where additional unstable hydrodynamic conditions are provided. Leaving the head of nozzle 7, the flow has a value of Veber Number 0.5 and as a result of the

interaction with the gas medium the flow loses its continuity. The breaking process does not start earlier than 50 mm from the nozzle head.

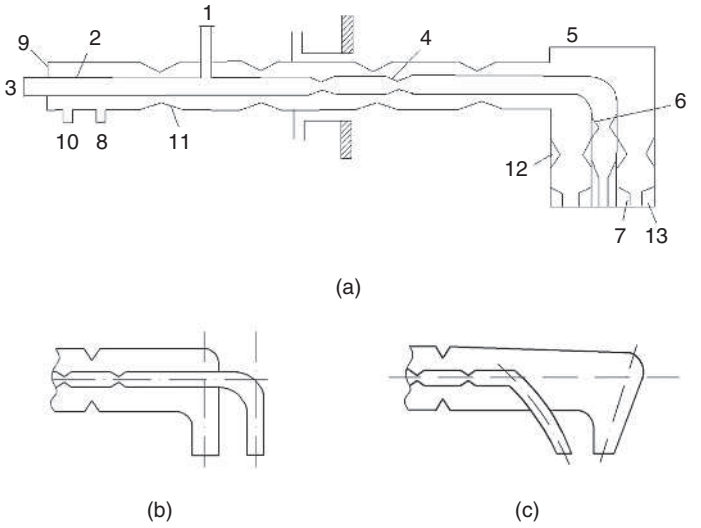


**Figure 5.9** Various schemes of tubular sprayers for the formation of homogeneous fine macromolecule growth centres during ethylene and propylene copolymerisation: a – coaxial; b – uniaxial; and c – intersecting

The cocatalyst is introduced *via* pipe 8 to the outside canal, position 9, where the solvent is preliminary added *via* pipe 10. The flow, going through turbulisation section 11, equalises the cocatalyst concentration over the volume of the reactor and is introduced outside canal 5. Outside the canal, the flow is subjected to preliminary turbulisation in divergent-convergent section 12, and then *via* nozzle 13 is introduced into the gaseous medium. The flow from the head of nozzle 13, has the value of Veber Number 0.5, and as a result of the interaction with the gaseous medium starts breaking, but not earlier than 50 mm from the nozzle head.

The rapid dissolving of the catalytic complex components is provided by turbulisation of the mixed flows, which is realised by the configuration of the inside surface of each canal of the tubular turbulent prereactor. Herein, the flow is subjected to sequential narrowing and expansion, providing the formation of turbulent eddies, which result in the complete and rapid mixing of liquids with different densities, over the flow volume; complete mixing is provided in at least two convergent-divergent sections.

The rapid reaction of the V-Al catalyst formation, proceeds *via* the mixing of the catalytic complex components. As a rule, the growing active crystal sites of high activity are precipitated onto the metallic surface of a device, used for component

mixing. Gradually, the thickness of the deposited layer increases, due to the formed polymer layer, resulting in the plugging of the holes used to introduce the catalytic complex solution. Moreover, under these conditions the catalytic complex, due to the absence of steric limitations, forms large crystals of perfect structure, covering most of the active sites on the solid surface. Hence, providing a separate introduction of the catalyst components, into a tubular turbulent designed prereactor (**Figure 5.9**), excludes the deposition of crystals on the device surface. Moreover, on the one hand, conditions of flow interaction, mainly over the surface of the reactive mass, allow the rapid mixing of catalytic complex components, with the formation of small particles of catalyst. On the other hand, these crystals form in the gaseous medium, containing a large amount of gaseous monomers, which are precipitated on the active sites of the growing crystal faces, preventing the formation of large crystals.

The results of active site formation of the V-Al catalytic system, in turbulent mode, for the copolymerisation of ethylene and propylene are presented in **Table 5.3**.

**Table 5.3 Formation of active sites in turbulent mode for ethylene and propylene copolymerisation in the presence of a $VOCl_3$-$Al(C_2H_5)_2Cl$ catalytic system**

| # | Copolymer | Time interval between measurement, hours | Flowrate of catalytic complex per copolymer ton | Copolymer yield, kg/h | Mooney viscosity |
|---|---|---|---|---|---|
| 1 | Synthetic ethylene-propylene rubber | 0 | 3.0 | 920 | 49 ± 2 |
| 2 | | 24 | 3.2 | 950 | 49 ± 2 |
| 3 | Synthetic ethylene-propylene rubber (modified by dicyclopentadiene) | 0 | 2.9 | 1020 | 51 ± 2 |
| 4 | | 24 | 3.1 | 1010 | 51 ± 2 |
| 5 | | 48 | 2.9 | 1020 | 51 ± 2 |
| 6 | Synthetic ethylene-propylene rubber | 0 | 3.5 | 800 | 46 ± 2 |
| 7 | | 24 | 3.5 | 750 | 44 ± 2 |
| 8 | | 48 | 3.5 | 780 | 46 ± 2 |

1–5: Formation of active sites in turbulent mode using a tubular turbulent prereactor (**Figure 5.9**).
6–8: Separate introduction of catalytic system components directly into the large-scale reactor-polymeriser.

The preparation and introduction of catalytic complex components to the polymeriser, using a tubular turbulent prereactor, enables the synthesis of copolymers (styrene-propylene (SSP) and styrene-ethylene-propylene (SSEPT)) which demonstrate high stability and durability. According to the laboratory results, obtained from the commercial production of ethylene and propylene copolymerisation, during separation of the active site formation and initiation of isoprene polymerisation on a Ti-Al catalytic system, an increase in copolymer yield and its molecular weight, as well as a decrease in catalyst rate were observed.

A six-sectional tubular turbulent device of optimal construction ($d_d$ = 150 mm, $d_c$ = 75 mm, and $L_c$ = 500 mm) is used in the production of the ethylene propylene copolymer. It is installed at the stage of catalyst decomposition and washing, after the ethylene and propylene copolymerisation, as well as at the introduction of the stabiliser into the ethylene propylene rubber solution. This intensifies the vanadium salt washing from the polymer and guarantees the production of rubber with a content of vanadium and ash, in the end products, which is within the required limits.

The flow sheet of a continuous solution copolymerisation of ethylene and propylene (**Figure 5.10**) has been proposed. Here, tubular turbulent reactors are used at the following stages [8, 9, 12]: 1) preparation of the homogeneous gas-liquid mixture and its introduction to the polymerisers working in parallel; 2) formation of macromolecule growth centres; and 3) decomposition of the catalyst with water and the introduction of the stabiliser to the polymer.

The intensification of technological processes in the production of SSEPT is very important and covers practically all stages of the flow sheet. Novel technology enables distributing and introducing gas-liquid mixtures of similar composition to the polymerisers, guarantees homogeneity of the end-product quality in different devices, essentially decreases the yield of low-quality rubber, and allows economic use of electric power (more than 250,000 kW/h), water (not less than 10 mass%), and catalyst (20 ± 5 mass%).

### *5.4.4 Isoprene Rubber*

According to classical concepts, rubber quality (macromolecule stereoregularity, molecular mass distribution, and so on) is determined by the chemical nature of the catalytic system employed and the conditions of its formation (nature and relation of catalytic system components, exposure conditions, and temperature of its preparation) [22].

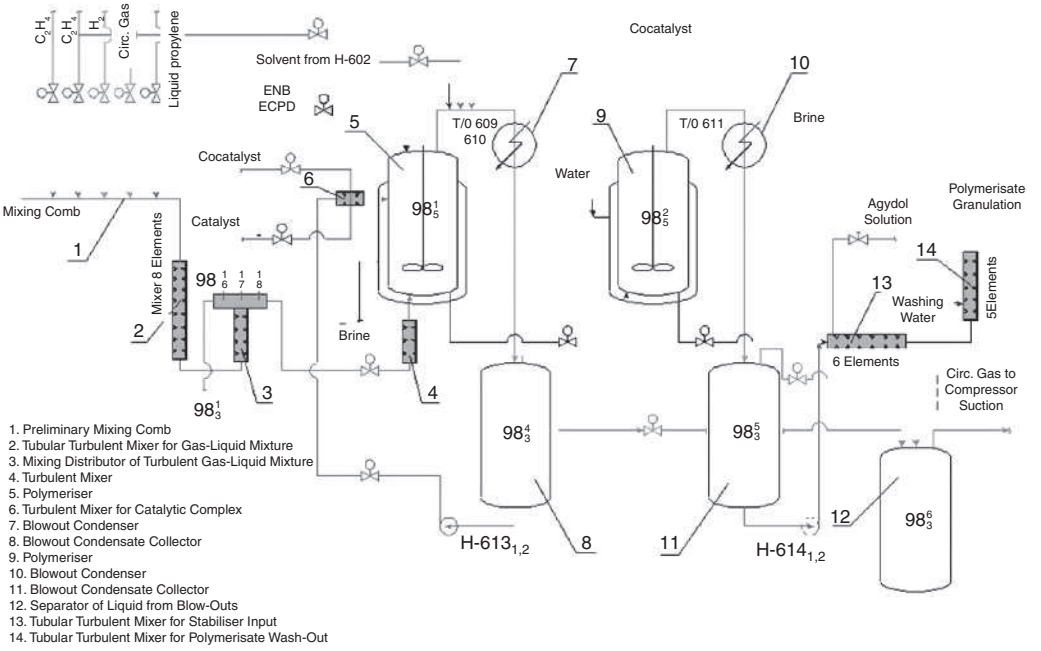


**Figure 5.10** The principal scheme of EPDM production. 1 – pipe manifold for preliminary mixing; 2, 3, 4, 6, 13, 14 – tubular turbulent devices; 5, 9 – polymerisers; 7, 10 – blowing condenser; 8, 11 – receiver of blowing condenser; and 12 – separator for blowing liquid phases

According to the conventional technology for both Ti-Al and Nd-Al catalytic systems, the introduction of the catalyst and monomer to the reaction mixture occurs in the first large-scale reactor-polymeriser of the cascade. Reactant mixing and catalytic system formation are inefficient processes due to the high viscosity of the reaction mixture. However, the formation conditions and catalyst distribution in the reaction zone are very important for the stereospecific *cis*-1,4-polymerisation of isoprene to provide a high polymerisation rate, low amount of catalyst, formation of similar active sites, and finally, high-quality rubber. It requires an essential increase in the mass transfer efficiency, i.e., a high level of turbulence for the rapid reactions of active site formation and initiation.

An unusual method has been created for improving the quality of *cis*-1,4-isoprene rubber during polymerisation, in the presence of both titanium and lanthanide (neodymium groups) Ziegler–Natta catalysts, under the conditions of commercial production. A tubular turbulent prereactor of divergent-convergent design (6 sections, with a volume less than 0.1 $m^3$) working on the principle of conservation of the turbulence level $D_{turb}$, over the volume of the device [23, 24] used in this

method, increases the turbulence level $D_{turb}$ by a factor of 5–10 or more. Using a tubular turbulent prereactor, at the reaction mixture formation stage, is necessary as information regarding the initiating rate constant is absent, due to the process of adding the first monomer molecule to an active site (initiating), during the diene polymerisation on Ziegler–Natta catalysts, differs from the addition of the next monomer molecules (chain growth) and occurs at a high rate. The high rate of active site formation and the initiating process in large-scale devices defines the diffusion limitations and inhomogeneity of the distribution of formed active sites, both on micro- and macrolevels, and therefore, it has an effect on the molecular and operating characteristics of the end products.

Commercial results were reproduced in a laboratory based on stereospecific isoprene polymerisation in the presence of: $NdCl_3 \cdot 3C_3H_7OH$-Al(*i*-$C_4H_9)_3$ and $TiCl_4$-Al(*i*-$C_4H_9)_3$ in toluene (298 °C). The mixing characteristics of typical (100 rev/min) and rapid (≈ 2000 rev/min) mixing devices were compared. The rapid mixing device created a high turbulence level ($D_{turb} > 10^{-3}$ m$^2$/s) in the mixing zone, which is close to the turbulent diffusion coefficient for a tubular turbulent divergent-convergent reactor. Effective mixing occurred during the first minute after the combination of catalytic complex solutions and isoprene (prereactor model); then polymerisation took place under the conditions which were identical for the reaction with both types of catalysts. The results are presented in **Table 5.4**. With the increased turbulence level, after the introduction of the catalyst to the reaction mixture, an increase of the average molecular weight and narrowing of the molecular weight distribution of the polymer at a comparable monomer conversion, both for titanium and lanthanide catalysts, was observed. Moreover, some reduction of the 3,4-unit content in the samples obtained using intensive mixing, in the case of the titanium catalyst, was observed.

**Table 5.4 The influence of mixing intensity on the stereospecific polymerisation of isoprene in combination with a catalytic complex and monomer solution in toluene**

| Catalyst | Mixing rate, rev/min | Yield, % | $M_w \times 10^{-5}$ | $M_n \times 10^{-4}$ | $M_w/M_n$ |
|---|---|---|---|---|---|
| $NdCl_3 \cdot 3C_3H_7OH$ - Al(*i*-$C_4H_9)_3$-piperylene | 100 | 47 | 2.8 | 4.5 | 6.1 |
| | 2,000 | 47 | 2.7 | 7.7 | 3.5 |
| $TiCl_4$-Al(*i*-$C_4H_9)_3$-piperylene | 100 | 46 | 3.5 | 8.3 | 4.2 |
| | 2,000 | 42 | 4.2 | 12.6 | 3.4 |

**Figure 5.11** presents the scheme of a tubular turbulent prereactor for the mixing stage of the catalytic complex with the monomer solution. The tubular turbulent reactor

consists of two series-connected devices. The parameters of device 1 (working in an optimal mode at an isoprene solution rate ranging between 32 $m^3$/h to 60 $m^3$/h) are: section number – 5, total length – 2.25 m, opening angle of diffuser – 45 ± 5°. The parameters of device 2 (working in an optimal mode at an isoprene solution rate ranging between 60 $m^3$/h to 112 $m^3$/h) are: section number – 4, total length – 2.4 m, the opening angle of diffuser is the same.

The isoprene flow into the solvent is introduced into device 1 axially; the catalytic complex solution flow is introduced radially.

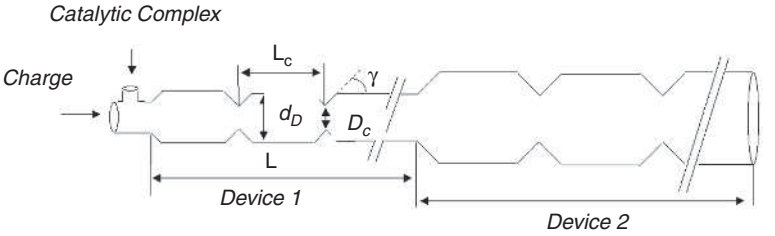


**Figure 5.11** General drawing of a tubular turbulent prereactor at the combination stage of the catalytic complex solution with the isoprene solution for polyisoprene production

Use of a tubular turbulent prereactor at the stage of preparing the reaction mixture for isoprene rubber production: decreases the catalyst rate in the actual process (by 25 ± 5% for SKI-3 and up to 50–80% for SKI-5); increases the reactor-polymeriser load; decreases oligomer formation (by a factor of 2–3 for SKI-3), oligomers do not form in the production of SKI-5; increases the process sensibility to the chain transfer agent ($Al(i\text{-}C_4H_9)_3$); and improves the correlation between the plasticity and Mooney viscosity (particularly for SKI-5), which was impossible in earlier commercial production. **Table 5.5** presents the characteristics of a tubular turbulent device working in an intensive turbulence mode, in comparison with the basic technology of SKI-3 production.

Small-sized tubular turbulent devices of convergent-divergent design, used for isoprene rubber production, are also effective at the mixing stages of the isoprene-isopenthane fraction with the catalyst suspension in toluene and chain transfer agent, as well as at the stage of water-alkali washing of the recycled isoprene-isopenthane fraction for the production of SKI-3 and SKI-5.

Tubular turbulent convergent-divergent reactors are the most appropriate devices at the stage of adhesion reducing powder preparation for synthetic rubber production by solution polymerisation including ethylene propylene, isoprene, and chlorobutyl rubbers (polymer solution modification).

**Table 5.5 Characteristics of a tubular turbulent device (TTD) at the stages of catalyst formation and its mixing with a monomer for the production of isoprene rubber under the conditions of commercial production**

| Parameters | Natural rubber | Synthetic *cis*-1,4-isoprene rubber | | | |
|---|---|---|---|---|---|
| | | Synthetic *cis*-isoprene rubber SKI-3 (Ti-Al catalytic system) | | Synthetic *cis*-isoprene rubber SKI-5 (Nd-Al catalytic system) | |
| | | Base | TTD | Base | TTD |
| Average molecular weight, $M_w \times 10^{-6}$ | 1–5 | 0.7–1.1 | - | 9 –11 | - |
| *Cis*-1,4-link content in molecules, % | 98.5–99 | 90–93 | Up to 96–97 | 95–97 | 98–99.5 |
| Width of molecular weight distribution, $M_w/M_n$ | 2.2–6.1 | 2.5–4.0 | - | 5.3–6.5 | 3.0–4.5 |
| Catalyst flow rate, relative unit | - | 1 | 0,5 | 1 | 0.3 |
| Oligomer content in rubber, % | 0 | 13 ± 1 | 5 ± 1 | 0 | 0 |

The design of the tubular turbulent convergent-divergent device for the stage of the interaction of calcium chloride with potassium stearate (**Figure 5.12**) was developed based on the results of the laboratory synthesis of a finely divided suspension. It consisted of the cascade of three series-connected minireactors of jet type. The proposed device design is characterised by a high value of the specific turbulent kinetic energy density dissipation, and consequently, by a minimum characteristic micromixing time. This determines the possibility of creating local shear deformation and the production of a fine suspension.

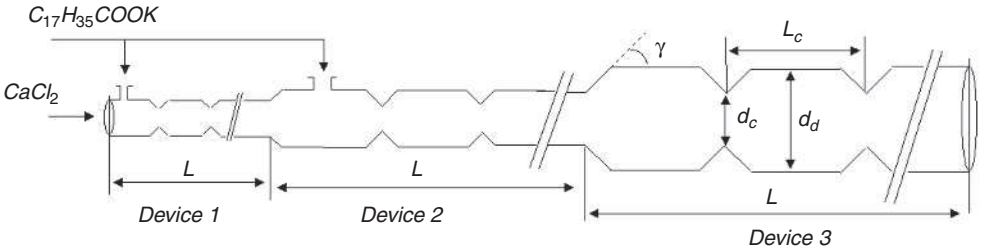


**Figure 5.12** General view of a tubular turbulent reactor for the stage of the interaction between potassium stearate and calcium chloride. Device 1 – *L* = 0.9 m, section number 10; device 2 – *L* = 1.4 m, section number 12; and device 3 – *L* = 3 m, section number 20

Each section of the turbulent device is calculated for optimal mode at various process productivities: device 1 – up to 2.5 $m^3$/h of total liquid flow; device 2–2.5–5 $m^3$/h; and device 3 – 5–10 $m^3$/h. The proposed design is applicable for the synthesis of adhesion reducing powder over a wide range of process productivity (2.5–10 $m^3$/h).

The interaction process between aqueous solutions of potassium stearate with calcium chloride, in tubular turbulent devices, provides a stoichiometric reaction leading to a reduction of the reaction mixture residence time in the device, which prevents particle deposition on the technological equipment walls, and consequently: increases the run between repairs; reduces the specific amount of metal per structure due to the small size of the reactor; reduces the process power capacity due to the removal of the mechanical mixing devices from the flow sheet; and produces a finely divided suspension of the adhesion reducing powder.

### *5.4.5 Liquid Oligopiperylene Rubber*

Irrespective of the catalytic system activity, the conventional flow sheet of liquid oligopiperylene rubber production [25, 26] includes an ideal mixing reactor (12 $m^3$) or a cascade of ideal mixing reactors (each reactor 1.5 $m^3$) as the main device, equipped with mechanical mixing devices as well as outside and inside condensers (coolant – recirculated water) (**Figure 5.13a**).

Kinetic calculation of the reactor, depending on the catalytic system used, shows that a tubular turbulent reactor is the most appropriate device for piperylene oligomerisation in the presence of $AlCl_3 \cdot O(C_6H_5)_2$. The low dynamic viscosity of liquid oligopiperylene rubber at the outlet of the reactor (at 283 °C, $\mu$ = 1 mPa·s) allows improvement of the catalyst deactivation stage using propylene oxide or water (**Figure 5.13b**).

The novel flow sheet of piperylene oligomerisation (**Figure 5.13b**) guarantees maintaining the main principles of current flow sheets, whilst increasing the specific output of the main reactor, and decreasing the specific weight of side reactions and secondary processes due to the significant decrease of $\tau_{pass}$.

### *5.4.6 Polymer-polyol*

Intensification of the technological flow motion, during various production processes, leads to increasing the process rates. This is especially true for the chemical interaction occurring in ideal mixing reactors. If it is impossible to replace them with small-sized devices and maintain the intensive mixing of the reaction mixture, an external circuit system may be used to pump the reaction mass (**Figure 5.14**). Multiplicity of the reaction mixture is defined by specific chemical reaction conditions and the required parameters of the end products.

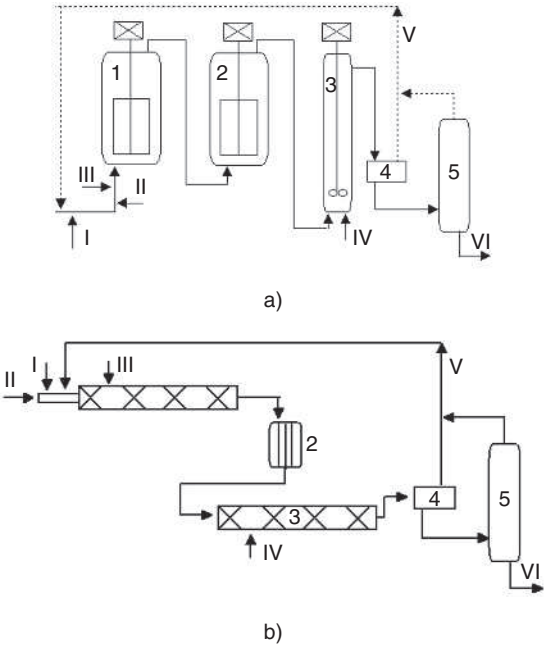


**Figure 5.13** The scheme of SSOP liquid oligopiperylene rubber synthesis. 1, 2 – reactor-polymeriser with gate agitators and condensers, 3 – degasator (a); 1, 3 – small-sized tubular turbulent devices for oligopiperylene synthesis and catalyst deactivation, 2 – condenser (b), 4 – receiver, 5 – degasator. I – solvent, II – catalyst, III – piperylene fraction, IV – deactivator, V – recycle, and VI – SSOP to stock

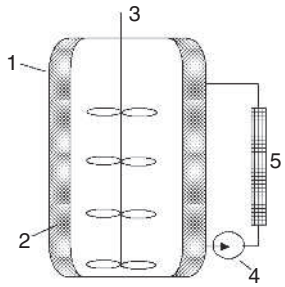


**Figure 5.14** Scheme of synthesis in an ideal mixing device with an external circuit for circulation of the reaction mixture through the tubular turbulent divergent-convergent device. 1 – ideal mixing reactor; 2 – cooling jacket; 3 – mechanical mixing device; 4 – pump; and 5 – tubular turbulent device

Installation of an external circuit in the system of a tubular turbulent divergent-convergent device causes changes in the conditions of the reaction mass motion. Firstly, in addition to the transporting pump, a turbulent flow is formed and persists

after the end of pump operation. This leads to the intensification of reaction mass mixing and the creation of a fine emulsion or suspension. Secondly, heat removal occurs through the walls of the tubular device.

An example of this tubular turbulent reactor application is the process of polymer-polyol production, which is the dispersion of a solid polymer in a liquid polyol (polyester or polyester mixture). Polymer-polyol preparation is a lengthy process of component mixing, which in some cases is complicated by chemical interaction. Typically, polymer-polyol production occurs in ideal mixing reactors, where the flow of the chemical agents is laminar. The larger the reactor volume, the more time is needed for the formation of a homogeneous reaction mass throughout the volume, and consequently, the process expenses are higher. In the case of chemical interaction, low rates of process flow do not provide the appropriate end-product yield, in spite of the high rate of chemical reaction in the case of polymer-polyol. In this case, rapid mixing may only occur in the external circuit with turbulent flow motion. Turbulent flow is created by the delivery pump and the tubular device is equipped with static turbulisation devices, which are an external circuit of the ideal mixing reactor.

Rapid and intensive mixing, and a combination of turbulent and laminar flows, enables the acceleration of monomer polymerisation, an increase in its depth, and exclusion of large particle formation in the polyester. This defines the dispersing stability not only for polymer-polyol but for other compositions of polyol dispersions, and results in highly flexible polyurethane foam processability and a high quality of moulded articles. Some properties of polymer-polyol and flexible polyurethane foam are given in **Tables 5.6** and **5.7** [27].

**Table 5.6 Polymer-polyol properties**

| Conditions* | Synthesis period, h | Viscosity, Pa·s | Solid residual, % | Average size of polymer particle, μm | Gravitational stability of dispersion, 24 h ($T$ = 45 °C) | Monomer odour (acrylnitrile) |
|---|---|---|---|---|---|---|
| 1 | 25 | 2080 | 34 | 6.4 | 28 | faint |
| 2 | 5.5 | 3140 | 40 | 2.9 | >60 | - |

*1:Mixing device.
2: Mixing devices equipped with a tubular turbulent divergent-convergent device (8 sections) in an external circuit.

Analysis of the properties of polymer-polyol and flexible polyurethane foam shows that the process flow turbulisation in polymer-polyol production enables the manufacturing of products with high-quality properties and reduces process time considerably.

| **Table 5.7 Characteristics of flexible polyurethane foam, prepared under the same conditions and compositions used in Table 5.6** | | |
|---|---|---|
| **Characteristics** | **Conditions*** | |
| | **1** | **2** |
| Density, kg/m$^3$ | 23 | 21 |
| Elasticity, % | 33 | 35 |
| Strain compression under load, kPa | | |
| 10% | 0.6 | 0.7 |
| 20% | 1.5 | 1.7 |
| 40% | 2.0 | 2.3 |
| *1: Mixing device.<br>2: Mixing devices equipped with a tubular turbulent divergent-convergent device (8 sections) in an external circuit. | | |

### *5.4.7 Detergents based on Alkylsulfates*

Sulfonated organic compounds are used for the production of surfactants which can be applied as an active base of detergents, emulsifiers, blowing agents, and so on.

The conventional flow sheet of alkylsulfate production includes the following stages (**Figure 5.15a**) [28]: sulfation of α-olefin with strong sulfuric acid (positions 1a and 1b); neutralisation of nonreacted $H_2SO_4$ and alkylsulfuric acid (positions 2a and 2d); and the two-stage washing of alkylsulfates, from unsaponified hydrocarbon products, with gasoline (positions 4a, 4b and 5).

A sulfation reaction refers to rapid reactions with the main goal being the formation of a rapid homogeneous distribution of the reacting media throughout the reactor volume. Taking into account that organic reactants and sulfoagents have significant differences in density, viscosity, and surface tension, this problem may be solved using turbulent flow.

The unmixed organic-inorganic flow is turbulent due to the static and dynamic devices, or their combination, in a tubular device, where the interacting media is distributed rapidly and homogeneously throughout the flow volume. Here, the flows mix continuously leading to the rapid chemical interaction of media. Multiple repeated flow turbulisation ensures maximum completeness of the chemical reaction.

Taking into account that the basic chemical reaction under these conditions occurs for a short period of time and is accompanied by significant heat emission, the heat is removed just after the beginning of the exothermic chemical reaction.

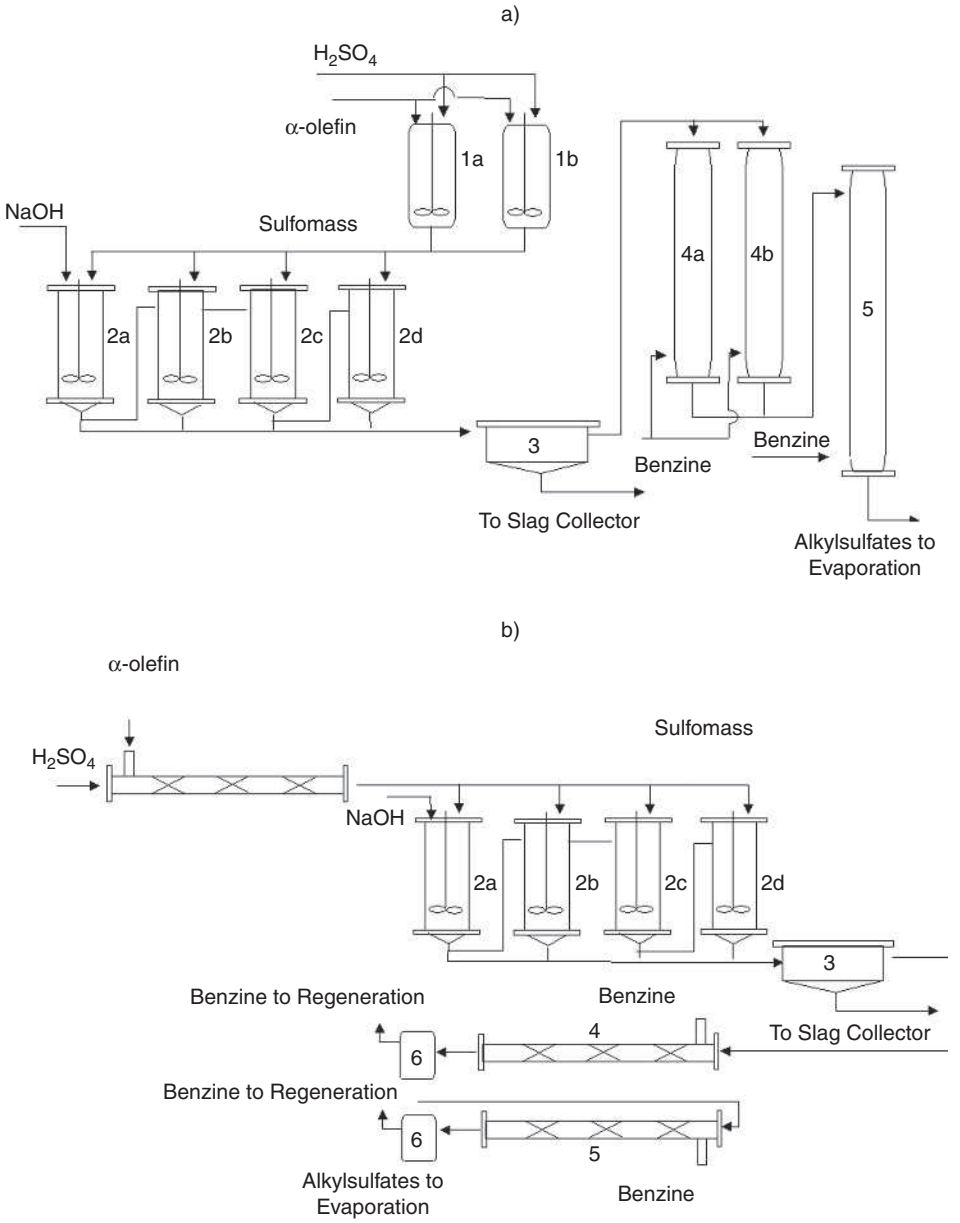


**Figure 5.15** Flow sheet of alkylsulfate production: 1a, 1b – large-scale sulfators with blade agitators ($v_r$ = 0.157–0.44 m$^3$); 4a, 4b – extracting column of the first stage ($v_r$ = 3.4 m$^3$); 5 – extracting column of the second stage ($v_r$ = 4.7 m$^3$); (scheme a), 1 – tubular turbulent sulfator ($v_r$ = 0.0086 m$^3$); 4 – first stage tubular turbulent extractor ($v_r$ = 0.003 m$^3$); 5 – second stage tubular turbulent extractor ($v_r$ = 0.005 m$^3$); 6 – settler; (scheme b), 2a–d – reactor-neutraliser with propeller agitators ($v_r$ = 3 m$^3$); and 3 – separator

Heat removal from the sulfomass may occur through the wall of the tubular reactor. Generally, the heat transfer coefficient is defined by the geometric parameters of the equipment, the thermal physical properties of the sulfomass, and its flow conditions over the cooled wall. To ensure the turbulent flow conditions of the sulfomass intensify significantly, heat is removed from the flow volume, as the turbulent flow velocity profile of the microlayers is different from that of laminar flow.

Taking into account that sulfation is a rapid chemical process and the released heat does not transfer completely through the device wall, secondary reactions occur in the heated sulfomass with the formation of by-products. To avoid this process, a cooled solvent or mixture of solvents is introduced into the organic product. Some heat from the heated sulfomass is transferred to the solvent, which is heated up to boiling point and passes into a gaseous state. As evaporation is an endothermic process, a large amount of heat is removed from the sulfomass. The most effective way of controlling the temperature increase of the sulfomass, moving in turbulent mode, is simultaneous internal and external heat removal.

Effective reactant mixing, using novel technology without ideal mixing reactors, increases the end-product yield, process productivity, product quality (decreases the amount of by-products which are insoluble in water), and decreases the equipment cost significantly.

A novel energy- and resource-saving flow sheet for commercial alkylsulfate production [13] based on small-sized tubular turbulent devices, at the stages of $\alpha$-olefin sulfation with sulfuric acid and alkylsulfate washing, has been proposed (**Figure 5.15b**).

More effective reactant mixing, using novel technology, will result in an increase of end-product yield in milder reaction conditions, compared with the conventional flow sheet.

### *5.4.8 Ethyl Chloride*

Ethyl chloride is commercially produced by the liquid-phase hydrochlorination of ethylene in large-scale reactors (2 $m^3$), in the presence of $AlCl_3$. Reactors are equipped with mechanical mixing devices and an external heat removal system; the temperature in the mixing zone may locally increase up to 100 °C or more.

There is no information on the specific reaction rate of the hydrochlorination of ethylene to chloroethane in the relevant literature or reference books. However, this reaction relates to rapid processes according to the technical rules, $\tau_{chem} = 5$ s at more than 93 mass% of the ethylene change ratio, which results in $k \geq 190$ l/mol·s (238 °C). Therefore, turbulent reactors are the most appropriate devices for this

process. Exothermic process simulation of the interaction between ethylene and HCl shows that, due to the intensive heat emission, it is practically impossible to maintain the reactor temperature ($R$ = 0.17 m) at the level of 273–283 °C, using external heat removal ($T_{cool}$ = 238 °C). However, using a tubular turbulent reactor of shell-and-tube design allows the maintenance of the optimal temperature in the device beginning from $N \geq 60$ ($R$ = 0.0216 m), even at $T_{cool}$ = 258 °C. Furthermore, the process may occur under quasi-isothermal conditions.

Novel technology of chloric ether synthesis, based on a typical shell-and-tube heat exchanger ($L$ = 7 m, $d$ = 0.8 m, 319 tubes with $d$ = 0.0019 m) has been proposed. The heat exchanger is used as a turbulent reactor mounted at an angle of 7°, with a combined gas separator [6, 29]. A brine solution is introduced into the tube side of the exchanger (255 °C). Heat transfer occurs due to external and partial internal heat removal (boiling of some chloroethane, $T_{boil}$ = 185.5 °C), which enables the reactor to work in a stable manner. Off-gases enter the upper part of the fractionation column leading to:

- Elimination of chloroethane emission from the reactor and colour defect products.
- Simplification of the technology and process equipment, keeping the main principles of the current flow sheet.
- Reduction of the reaction mixture residence time in the reaction zone (by more than a factor of 100 ± 20).
- Reduction of the amount of by-products, particularly the products of more than 50 mass%.
- 1.5–2.0 times reduction of power consumption, primarily saved due to the use of a different cooling agent (replacement of freon for ammonia cooling), as well as the removal of mechanical mixing devices.
- Reduction of the specific amount of expensive foreign equipment, particularly the replacement of carboxylic heat exchangers for Russian graphite ones.
- Use of off-test raw materials, particularly ethylene of any quality including one obtained as an absorbed gas from other processes.
- Reduction of product discharge containing up to 0.5% HCl.
- Increasing the process sustainability.

Some comparative data are given in **Table 5.8**.

| Table 5.8 Comparative data of current novel technologies based on a turbulent reactor of a shell-and-tube design for chloric ether production | | |
|---|---|---|
| **Characteristics** | **Current technology ($v_p$ = 2 m$^3$)** | **Novel technology based on shell–and-tube reactor ($v_p$ = 0.7 m$^3$)** |
| Relative productivity, ton/m$^3$ | 0.38 | 1.9 ± 0.2 |
| Ethylene change rate, mass% | 83.0 | Up to 99.8 |
| Process selectivity to chloric etheryield, mass% | 92.6 | Up to 99.8 |
| Residence time of reactive system in a device, $\tau_{pass}$, h | 0.5–1 | 0.0014 |

### *5.4.9 Gas-liquid Processes with a Large Volume of the Gas Phase*

Technological processes are characterised by various forms and methods. In some cases, chemical reactions occur in conditions of a large volume of gaseous products, which significantly exceeds the amount of liquid reactants. In commercial production, extremely large-scale devices are used where the interaction between the liquid and gaseous substances occur as a result of upflowing gas bubbles, during the mixing of the reaction mixture. In some cases, this technological arrangement is not optimal.

This is confirmed by the technology employed in the production of ethyl benzene, which enables the reaction of benzene and ethylene, or other olefins, in the presence of a catalytic complex at an elevated temperature and pressure, and is markedly defined by the mixing intensity of the interacting media. According to the conventional scheme, benzene, by-products, gaseous hydrocarbon (ethylene), and the catalytic complex enter the bottom part of the tubular column. Component mixing occurs under the influence of the motion of a large amount of ethylene bubbles. The chemical reaction rate is high, but the mixing is not efficient and therefore, the process selectivity is low. The heat released during the process is removed by the partial evaporation of unreacted benzene and the process is characterised by a low change ratio.

Hence, ethyl benzene synthesis may be realised in such a way where the component mixing consequently occurs in a turbulent mode. In this case, the tubular turbulent divergent-convergent device may be used (**Figure 5.16**) [30]. There are three stages of the process: during the first stage, mixing of the liquid hydrocarbons occurs (dry benzene, polyalkylbenzenes, recycled benzene), during the second stage, a fixed amount of ethylene is introduced into the mixture of liquid hydrocarbons, and during the third stage, the catalytic complex is introduced to the mixture.

The introduction of the catalytic complex to the mixture of liquid hydrocarbons and ethylene leads to a rapid and complete chemical interaction – benzene alkylation. The product yield may reach 50% or more during one passage of the reaction mixture. Excess heat is removed from the reaction mixture by internal heat removal, due to partial benzene evaporation, as well as by external thermostating of the tubular device walls.

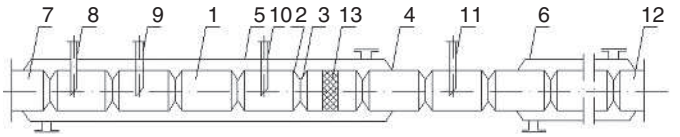


**Figure 5.16** A tubular turbulent divergent-convergent device for alkylbenzene synthesis. 1 – reactor vessel; 2 – convergent element; 3 – divergent element; 4 – cylindrical element; 5 – jacket for heating of the initial reaction mixture; 6 – jacket for reaction heat removal; 7, 8, 9, 10, 11 – tubes for the introduction of dry benzene, polyalkylbenzenes, recycled benzene, ethylene, and catalytic complex, respectively; 12 – tube for reaction mixture extraction; and 13 – packing for turbulisation

A similar process is the hydrogenation of acetylene hydrocarbons for isoprene production [31]. The main problem of this process is ensuring the homogeneous distribution of gaseous hydrogen, contained in the liquid phase, when the reaction mixture enters the catalyst zone. Turbulisation of the liquid reactant flows with the simultaneous introduction of the gas phase is one of the most effective ways of solving this problem (**Figure 5.17**). In tubular turbulent divergent-convergent devices, the gas is homogeneously distributed throughout the volume of the liquid, which contains isoprene and an impurity within isoprene i.e., acetylene hydrocarbons. The process occurs with the formation of a gas-liquid mixture with a developed surface of phase contact. The gas-liquid mixture enters the hydrogenation bed, where the selective hydrogenation of acetylene hydrocarbons takes place in the presence of a catalyst (**Figure 5.18**). Acetylene hydrocarbons are present in isoprene; the homogeneous distribution of hydrogen-containing gas in isoprene provides the conditions for the complete hydrogenation reaction of the acetylene hydrocarbons. Moreover, the quantity of process gas decreases, which results in a reduced possibility of isoprene hydrogenation to isoamylenes and isopenthane (**Table 5.9**); proposed technology may increase the isoprene quality and end-product yield.

### *5.4.10 Unleaded Gasoline*

As mentioned in the previous chapter, liquid component flows which are different in density and viscosity by at least by 20%, particularly glycerin and water, mix poorly. The formation of a homogeneous phase is a problem.

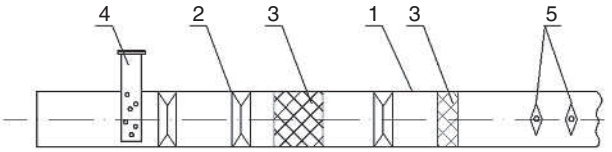


**Figure 5.17** Design of a tubular turbulent prereactor for monomer hydrogenation. 1 – tubular device; 2 – turbulisation section of convergent-divergent design; 3 – cellular body; 4 – tube for hydrogen introduction; and 5 – turbulisation section of dynamic design

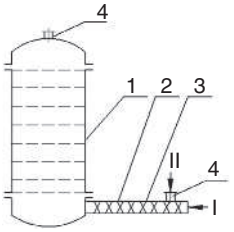


**Figure 5.18** Scheme of isoprene purification from acetylene hydrocarbons using a tubular prereactor. 1 – flow reactor of hydrogenation; 2 – tubular turbulent prereactor; 3– convergent-divergent turbulisers; and 4 – connection pipes. Flows: I – liquid monomer, and II – hydrogen

**Table 5.9 Comparative analysis of technological processes of isoprene purification from acetylene hydrocarbons**

| Conditions* | Volume flow rate, $m^3/h$ | | Content, mass% | | | |
|---|---|---|---|---|---|---|
| | | | Before hydrogenation | | After hydrogenation | |
| | Hydrogen-containing gas | Isoprene | Acetylene | Isoprene | Acetylene | Isoprene |
| 1 | 78.5 | 5.4 | 0.040 | 82 | 0.001 | 80.1 |
| 2 | 25.2 | 5.5 | 0.045 | 82 | 0.00005 | 81.8 |

*1: Hydrogenation in a large-scale flow reactor.
2: Hydrogenation in a large-scale flow reactor with preliminary formation of a gas-liquid mixture in a tubular turbulent prereactor of convergent-divergent design.

In order to produce automobile gasoline of the correct composition, the effective mixing of the high boiling point components of fuel (alkylates, hydrogenated and nonhydrogenated fractions of $C_9$-pyrocondensate, oligomers of olefins, high boiling point wastes from petrochemical production, and so on) with small volumes of high-octane additives (diisopropyl ether, methyl tert-butyl ether), and low boiling point components (*n*-butane, *n*-pentane, isopenthane or their mixture) is necessary. Subsequently, this component mixture is added to the rest of the component flows, which have a larger volume (the basis of unleaded gasoline, e.g., straight run gasoline, gasoline of catalytic cracking or reforming, and so on).

The commercial-scale process is complicated due to the gasoline components having various boiling points, densities, viscosities, and volume flow rates. Therefore, there are some problems with the choice of equipment for the process. Large-scale reactors with intensive mixing devices are used for an effective level of mixing at high process productivity. When a large number of components with various physical parameters (density, viscosity, surface tension, and so on) are introduced into the mixing device, there is the possibility of partial separation of the liquid phases, due to the low and nonuniform turbulence in the mixing zone. The process differs in the specific amount of metal and energy consumption. High-performance hydrodynamic mixing devices, used for these purposes, are of complicated design and are inefficient for the compounding of fractions with high boiling point temperatures, and for working with the large volume of technological flows.

To solve this problem, a scheme for the continuous production of unleaded gasoline, based on highly efficient small-sized tubular turbulent mixing devices of original design, has been proposed.

For commercial production, the following flows are required for effective mixing: 1) 1.4–0.6 ton/h (2–0.9 $m^3$/h) *n*-butane fraction; 2) 1.9–3.8 ton/h (1.9–3.8 $m^3$/h) methyl *tert*-butyl ether; 3) 14–27 ton/h (20–38.6 $m^3$/h) hydrogenised fraction of hydrocarbons $C_5$; 4) 3–1.5 ton/h (4.3– 2.15 $m^3$/h) polymer tetramers; 5) 1.5–3 ton/h (1.9–3.75 $m^3$/h) hydrogenised fraction of hydrocarbons $C_9$; 6) 1.5–3 ton/h (1.5–3 $m^3$/h) octane additives; and 7) 9.4–4.7 ton/h (13.4–6.7 $m^3$/h) straight run gasoline. Therefore, the total amount of mixed components is 45–60 $m^3$/h.

For the complete mixing of gasoline components, two tubular turbulent devices of convergent-divergent design connected in series are typically used. Here, the mixing occurs in a highly turbulent vortex. The mixing of initial gasoline components occurs in the first device (**Figure 5.19**); then, this mixture goes to the second device (**Figure 5.20**), where some gasoline returns from the recycling stage.

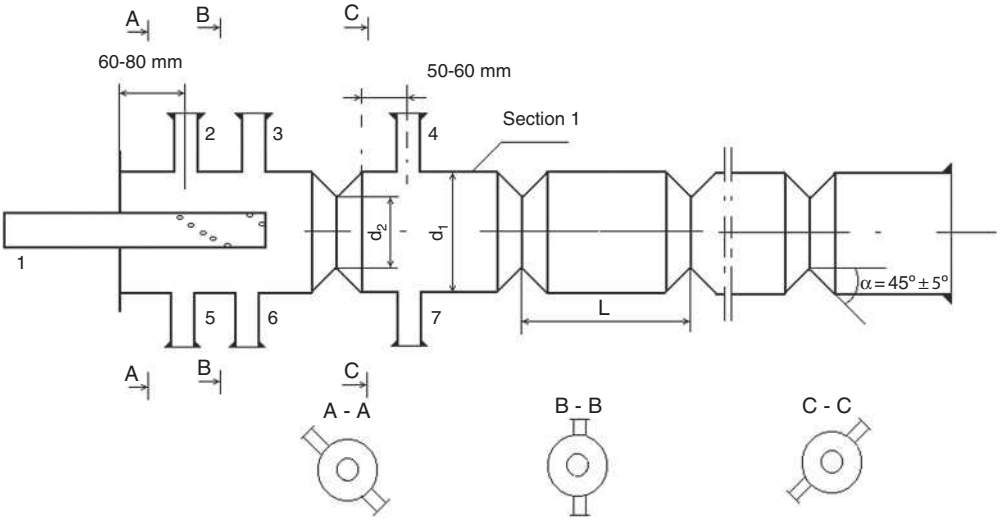


**Figure 5.19** General view of a tubular turbulent device for gasoline component mixing

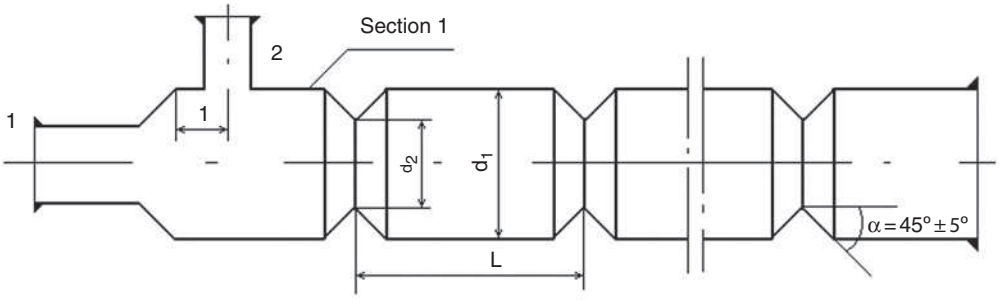


**Figure 5.20** General view of a tubular turbulent device for gasoline component mixing with recycling

The tubular turbulent device, at the stage of multicomponent mixture preparation (**Figure 5.19**), has the following operational principle. Tube 1, has a diameter of 25 mm and a length of 200 mm, is provided for the introduction of the octane additive, which is injected into the device volume through a hole system of 3 mm diameter (hole numbers 30–35), installed helically in the zone of tube 1, with a length of 100 mm. Tube 2, has a diameter of 50–60 mm – $C_5$ fraction. Tube 3, has a diameter of 30 mm – propylene tetramers. Tube 4, has a diameter of 30 mm – methyl *tert*-butyl

ether. Tube 5 has a diameter of 50 mm – straight run gasoline. Tube 6, has a diameter of 25–30 mm – $C_9$ hydrocarbon fractions. Tube 7 has a diameter of 20–25 mm – *n*-butane fraction. The mixing zone of the tubular turbulent device consists of seven convergent-divergent sections; its total length is approximately 3 m.

If mixed flow (gasoline) recirculation is necessary, up to 20 $m^3$/h (15 ton/h), a second mixing device of convergent-divergent design with six sections may be installed in series (**Figure 5.19**) (total length is up to 3 m) (**Figure 5.20**). The introduction of gasoline fraction recycling to the mixing device occurs perpendicularly to the main flow axis through tube 2, which is 50–60 mm in diameter, and is installed in the device at a length of 50 mm. The component mixture goes through tube 1, which is 100 mm in length, from the first tubular turbulent mixing device.

Novel mixing devices do not require the installation of additional mechanical agitators, which decrease the energy consumption of the process. The mixing mode provided by the construction features of the proposed device allows the compounding of any number of fractions with various boiling temperatures, densities, viscosities, and volume rates. Therefore, unleaded gasoline of stable composition is produced. Automobile gasoline of various grades may be produced using only one unit, consisting of two tubular turbulent mixing devices installed in series.

In conclusion, we may say that these novel devices have a very high specific output, enabling an essential decrease in the specific amount of metal per unit construction, and at the same time increasing the serviceability and ecological safety of the technology [32–35]. As a result, the economic production parameters are significantly improved, as the raw material and energy cost decrease, enabling the possibility of producing new types of materials.

## References

1. D.A. Bajzenberger and D.H. Sebastian in *Engineering Problems of Polymer Synthesis*, Khimiya, Moscow, Russia, 1988. [In Russian]

2. K. Denbig in *Theory of Chemical Reactors*, Nauka, Moscow, Russia, 1968. [In Russian]

3. H. Kramers and K. Vesterterp in *Chemical Reactors*, Nauka, Moscow, Russia, 1967. [In Russian]

4. A.A. Berlin, S.A. Volfson and N.S. Enikolopyan in *Polymerization Processes Kinetics*, Khimiya, Moscow, Russia, 1978. [In Russian]

5. A.G. Kasatkin in *Basic Processes and Machinery of Chemical Tehnology*, Khimiya, Moscow, Russia, 1983. [In Russian]

6. A.A. Berlin, K.S. Minsker and K.M. Djumaev in *Novel Unified Energy and Resource Efficient High Performance Technologies of Increased Ecological Safety Based on Tubular Turbulent Reactors*, Niitjehim, Moscow, Russia, 1996. [In Russian]

7. K.S. Minsker, V.P. Zakharov, I.R. Mullagaliev, J.B. Monakov and A.A. Berlin, *Zhurnal Prikladnoy Khimii*, 200, **73**, 11, 1895. [In Russian]

8. V.M. Busygin, G.S. Dyakonov, K.S. Minsker and A.A. Berlin, *Summa Tehnologiy*, 2000, **3**, 4, 48. [In Russian]

9. V.M. Busygin, L.M. Kurochkin, T.G. Burganov, N.R. Gilmutdinov, K.S. Minsker, G.S. Dyakonov, R.Y. Deberdeev and A.A. Berlin, *Himicheskaya Promyshlennost*, 2001, **2**, 3. [In Russian]

10. V.M. Busygin, R.T. Shiyapov, N.I. Uhov, A.S. Ziyatdinov, K.S. Minsker, V.P. Zaharov, A.A. Berlin, G.S. Dyakonov and R.Ya. Deberdeev, *Khimiya v Interesah Ustojchivogo Razvitiya*, 2003, **11**, 843. [In Russian]

11. V.P. Zaharov, *Zhurnal Prikladnoy Khimii*, 2006, **79**, 11, 1865. [In Russian]

12. K.S. Minsker, A.A. Berlin, V.P. Zakharov and G.E. Zaikov in *Fast Liquid-phase Processes in Turbulent Flows*, Brill Academic Publishers, Amsterdam, Netherlands, 2004.

13. K.S. Minsker, V.P. Zakharov, A.A. Berlin and R.Y. Deberdeev, *Himicheskaya Tehnologiya*, 2003, **3**, 30. [In Russian]

14. K.S. Minsker, A.A. Berlin, R.Y. Deberdeev and S.R. Ivanova, *Khimicheskaya Promyshlennost*, 2000, **11**, 26. [In Russian]

15. A.A. Berlin, K.S. Minsker and R.Y. Deberdeev, *Doklady Akademii Nauk*, 2000, **375**, 2, 218. [In Russian]

16. K.S. Minsker, R.Y. Deberdeev, G.S. Dyakonov, R.T. Shiyapov, O.V. Sofronova, A.D. Ishteryakov, A.S. Ziyatdinov, V.P. Zaharov, S.R. Ivanova, H.V. Mustafin, N.I. Uhov and V.N. Kalinin, inventors; Nizhnekamskneftekhim, assignee; RU2170237, 2001. [In Russian]

17. K.S. Minsker, A.A. Berlin, V.P. Zaharov, N.R. Gilmutdinov and R.Y. Deberdeev, *Vestnik Bashkirskogo Universiteta*, 2004, **2**, 20. [In Russian]

18. K.S.Minsker, R.Ya. Deberdeev, G.S. Dyakonov, A.A. Berlin, L.M. Kurochkin, R.G. Galiev, H.V. Mustafin, N.R. Gilmutdinov, Yu.I. Ryazanov, Z.A. Abzalin,

S.A. Axmetchin, T.G. Burganov, V.N. Paramonov, V.R. Latfullin, A.Sh. Ziyatdinov and V.A. Mixeeva, inventors; Nizhnekamskneftekhim, assignee; RU 2144843, 2000. [In Russian]

19. K.S. Minsker, A.A. Berlin, R.Ya. Deberdeev, G.S. Dyakonov, L.M. Kurochkin, R.G. Galiev, H.V. Mustafin, N.R. Gilmutdinov, V.A. Shamanskij, A.Sh. Ziyatdinov, T.G. Burganov, Z.A. Abzalin, R.G. Salaxutdinov and S.A. Axmetchin, inventors; Nizhnekamskneftekhim, assignee; RU 2141873, 1999. [In Russian]

20. A.A. Berlin, K.S. Minsker, R.Ya. Deberdeev, R.G. Galiev, Yu.I.Ryazanov, A.Sh. Ziyatdinov, V.P. Pogrebcov, Z.A. Abzalin, T.G. Burganov, A.I. Vorobiev, A.A. Blinov and G.V Baev, inventors; Nizhnekamskneftekhim, assignee; RU 2141872, 1999. [In Russian]

21. I.D. Afanasiev, O.I. Afanasieva, Z.A. Abzalin, L.M. Kurochkin, R.Ya. Deberdeev, K.S. Minsker, G.S. Dyakonov, R.G. Tahavutdinov, A.I. Syatkovskij, H.V. Mustafin, Yu.I. Ryazanov, V.A. Mixeeva, T.G. Burganov, G.V. Baev, V.N. Silantiev, A.Ya. Bashirov and Sh.Sh. Galyaviev, inventors; Nizhnekamskneftekhim, assignee; RU 2177957, 2000. [In Russian]

22. J.B. Monakov, A.G. Tolstikov in *Catalytic Polymerization of 1.3-Dienes*, Nauka, Moscow, Russia, 1990.

23. K.S. Minsker, A.A. Berlin, R.H. Rakhimov, P.I. Kutuzov and V.P. Zakharov, *Zhurnal Prikladnoy Khimii*, 1999, **72**, 6, 996. [In Russian]

24. R.H. Rahimov, K.S. Minsker, P.I. Kutuzov, A.A. Berlin and V.P. Zaharov, *Kauchuk i Rezina*, 1999, **4**, 2. [In Russian]

25. P.A. Kirpichnikov, V.V. Beresnev and L.M. Popova in *Flowcharts of Major Industrial Technologies of Synthetic Rubber Production*, Khimiya Leningrad, Russia, 1986. [In Russian]

26. P.A. Kirpichnikov, L.A. Averko-Antonovich and Y.O. Averko-Antonovich in *Chemistry and Technology of Synthetic Rubber*, Khimiya, Moscow, Russia, 1975. [In Russian]

27. V.F. Evganov, R.V. Evganov, T.R. Deberdeev, and R.Y. Deberdeev, inventors; R.V. Evganov and R.Y. Deberdeev, assignees; RU 2275391, 2006. [In Russian]

28. B.R. Serebryakov, T.K. Plaskunov, V.R. Nizheles and M.A. Dalin in *Higher Olefins*, Khimya, Leningrad, Russia, 1984. [In Russian]

29. K.S. Minsker, A.A. Berlin, Y.M. Abdrashitov, J.K. Dmitriev, V.D. Shapovalov, V.P. Malinskaya and N.V. Alekseeva, *Himicheskaya Promyshlennost*, 1999, **76**, 6, 41. [In Russian]

30. R.Ya. Deberdeev, H.E. Harlampidi, A.A. Berlin, T.R. Deberdeev, V.P. Zaharov and R.M. Garipov, inventors; R.Ya. Deberdeev and H.E. Harlampidi, assignees; RU 2294320, 2007. [In Russian]

31. V.M. Busygin, H.V. Mustafin, N.R. Gilmutdinov, Yu.I. Ryazanov, Sh.Sh. Galyaviev, N.I. Uhov, A.Sh. Ziyatdinov, N.P. Borejko, T.G. Burganov, V.N. Silantiev, Z.A. Abzalin, R.G. Gusamov, I.A. Belanogov, R.Ya. Deberdeev, H.E. Harlampidi, K.S. Minsker and T.R. Deberdeev, inventors; Nizhnekamskneftekhim, assignee; RU 2237051, 2004. [In Russian]

32. V.P. Zaharov, A.A. Berlin and J.B. Monakov, *Zhurnal Prikladnoy Khimii*, 2005, **78**, 5, 779. [In Russian]

33. V.P. Zakharov, A.A. Berlin, Y.B. Monakov and G.E. Zaikov in *Focus on Organic and Inorganic Chemistry*, Nova Science Publishers, Inc., Hauppauge, New York, NY, USA, 2006.

34. V.P. Zaharov, K.S. Minsker, A.A. Berlin, I.V. Sadykov and J.B. Monakov, *Vysokomolekulyarnye Soedineniya*, 2003, **45A**, 5, 709. [In Russian]

35. J.B. Monakov, I.R. Mullagaliev, V.P. Zaharov, A.A. Berlin and K.S. Minsker, *Neftehimiya*, 2001, **41**, 2, 135. [In Russian]

# 6 Conclusion

This book provides the results of research into the development of scientific fundamentals, the technical design and industrial application of brand new technologies and devices for fast liquid-phase turbulent processes in the chemical, petrochemical, and petroleum industries. The macrokinetic approach, considering processes of diffusion, hydrodynamics, and heat transfer, has been developed and used for the advancement of fundamental knowledge and technologically important equations to enable the calculation of mass and heat transfer processes, which accompany fast chemical reactions and well-developed turbulence. This new family of chemical devices has been proposed for the intensification of fast liquid-phase processes through the creation of optimal hydrodynamic conditions for reacting media flows in a reaction zone.

There are a large number of liquid-phase diffusion mode processes where the rate of a process is mostly determined by 'nonchemical' factors, such as diffusion and heat transfer. A high reaction rate can result in the process ending before reaching the required mixing degree, leading to the formation of complex feedstock and product concentration gradients. Exothermicity of the majority of fast chemical reactions is accompanied by the local emission of a substantial amount of heat, while the temperature field in a reaction zone is difficult to control using traditional methods of chemical technology. Traditional approaches to the instrumentation of fast chemical reactions, on the basis of mixing and plug flow reactors, always assumes processess of a nonisothermal mode, which are hard to control and often result in the unsatisfactory quality of consumer products. A single parameter, allowing optimisation of fast liquid-phase reactions, is an increase of the turbulent mixing level directly in the process area. A small-sized reaction zone makes tubular reactors a reasonable alternative as they are capable of creating intensive turbulent mixing of a reaction mixture, solely by means of the hydrodynamic energy of the rapidly moving flow of reactants (formation of a quasi-plug flow mode in turbulent flows at a ratio of $\tau_{mix} \leq \tau_{chem}$, at a characteristic mixing and chemical reaction time). Control of the time taken for reactants to pass through a reaction zone is necessary in order to achieve the conditions of a similar reaction and reactant time passing through a device ($\tau_{pass} \approx \tau_{chem}$); in addition, to provide efficient external heat removal, a substantial increase of the heat exchange surface and the creation of quasi-isothermic mode conditions are required.

As fast liquid-phase chemical processes obey the laws of mass and heat transfer, a macrokinetic approach is required for their calculation. The calculation of a fast liquid-phase chemical reaction, on the basis of hydrodynamic and diffusion models, revealed fundamental aspects of carrying out fast processes in turbulent flows:

1. Several macroscopic modes exist in turbulent flows, such as a 'torch' mode with a gradient of reactant concentrations, reaction rates, and temperatures in a reaction zone, and a 'planar' reaction front mode. The latter mode is suitable for carrying out fast processes in the plug flow mode at a low rate of longitudinal mixing.

2. There is a correlation between the reactor design, reactor geometry and process kinetics, and hydrodynamics as well as the final product yield. There is a critical device radius $R_{cr}$, indicating transition from a torch to a planar reaction mode and conditions, for carrying out fast reactions in the quasi-isothermal mode.

3. There are severe limitations on the reactor radius ($R_{min} < R < R_{cr}$) for the guaranteed creation of highly turbulent conditions and the formation of a planar reaction front. It results in a substantial increase of device efficiency compared with standard mixing machinery.

4. The increase of product yield and polymer quality in the case of a polymerisation process (molecular weight grows and molecular weight distribution shrinks). In the case of a faster reaction mixture passing through a reactor, 'compaction' of the reaction zone is observed.

Increasing the mixing intensity of the reaction mixture in tubular devices, by the formation of circulation zones, is an effective instrument for process control. Radial input of reactants and conical widening at the device input, as well as diffuser-confusor channel profiling, increase the turbulent mixing intensity of the reaction mixture by one order of magnitude, compared with standard mixing devices, and provides high efficiency along the full device length. It is possible to achieve uniform reactant concentration profiles in a single-phase reaction mixture and increase the interface boundary area in multiphase systems, as well as increase the convective heat exchange efficiency under conditions of external thermostating of fast exothermic reactions.

It is practically important to consider the known criterion of large-scale turbulent vortex formation, when viscosity does not influence the mixing efficiency of the reaction mixture (automodel flow mode in relation to viscosity). The solution for achieving high turbulisation in a diffuser-confusor reactor, with local hydrodynamic resistances, is feeding the reaction mixture at lower linear flow rates; enabling a substantial increase in the efficient application of tubular turbulent diffuser-confusor devices with lower reaction rate areas.

A decrease of device size, to the size of a 'torch' zone, provided opportunities for the efficient control of temperature profiles in a fast reaction zone under conditions of external heat removal. Original methods for efficient thermal mode control have been developed for fast chemical reactions, which result in intensive local heat generation, the change of reaction flow radius and mixture flow rate, and the input of reactants along the full length of the reactor. The necessity of external removal of a large local amount of heat explains the similar designs of reactors for fast liquid-phase processes and heat exchange equipment, both having a high specific heat transfer surface.

The analysis of a hydrodynamic mode of reactive system motion in tubular turbulent devices has revealed distinct differences between cylindrical and diffuser-confusor designs, and therefore differences in their industrial application. The hydrodynamic operation mode of tubular turbulent devices, with conical widening, is characterised solely by reactor geometry. A mode similar to plug flow mode is formed in a reactor with a low rate of longitudinal mixing and therefore, a narrow distribution of reactant pass time. Thus, such reactors are suitable for fast chemical reactions mostly occurring at reactant feed points in the quasi-plug flow mode. The presence of diffuser-confusor units creates the plug flow mode in a reactor. As the longitudinal mixing rate is high, in this case, and the distribution of the reactant pass time is wide, quasi-isothermic conditions can be created for fast exothermic reactions in tubular turbulent diffuser-confusor devices. Both ideal models of perfect mixing and plug flow can be achieved with a certain degree of approximation, depending on the ratio of axial and radial input rates; however, they cannot be achieved in standard reactors for chemical technology processes. It has been demonstrated for fast chemical reactions, with an interphase boundary, that the longitudinal mixing coefficient in a liquid phase decreases with an increase of the dispersed particle size in a two-phase flow, within tubular turbulent devices. This effect is proportional to the number of particles.

From the viewpoint of heat exchange efficiency, it is reasonable to provide deeply profiled channels in a tubular turbulent reactor, in the form of a diffuser-confusor design, for both fast exothermic reactions and heat exchange physical processes. A diffuser-confusor design of tubular devices provides an increase of 1.3–1.4 times their specific output and upto a twofold decrease of heat carrier (reaction mixture) pass time. The heat transfer coefficient of liquid flows is shown to depend on the hydrodynamic structure of the flow. The lower efficiency of heat exchange processes in a cylindrical device, compared with diffuser-confusor channels, is the effect of a high degree of flow structure to an undesirable plug flow mode, both in the internal and ring channels.

Analysing the sum total of all aspects of fast chemical reactions, we can conclude that tubular turbulent reactors belong to the new type of chemical technology reactors. Four main design modifications have been developed to date: cylindrical design

(ultrafast chemical reactions occurring solely in reactant input areas), diffuser-confusor design (fast heterophase reactions, heat exchange), shell-and-tube design (provides an opportunity to vary the ratio of the heat exchange surface to reaction mixture volume over a broad range), and zone design (decrease of adiabatic temperature growth in the reaction zone).

The main regularities observed in mass transfer limited liquid-phase chemical processes are applicable both to polymerisation reactions and to the synthesis of monomer products. In addition, variation of process conditions, which determine the rate (such as application of catalytic systems with different activities), set the basis for energy- and resource-efficient technologies with the tubular turbulent reactor design. An opportunity to develop the automodel mode in a highly viscous reaction mixture is the basis for efficient polymer-analogous transformations in polymer modification processes. An interesting and practically important approach is the subdivision of integral 'gross' processes into fast and slow stages, and the creation of optimal conditions (mostly hydrodynamic conditions) for each stage according to its specifics. It is achieved by the addition of a tubular turbulent prereactor which reduces the diffusion limitations during fast stages. This device is installed before the reaction mixture input to a high volume device, with a high pass time providing optimal conditions for lower rate processes; implementation of this design for the copolymerisation of olefins in the presence of Ziegler–Natta catalysts, results in a substantial increase of process rate and better quality of polymer products. Application limits have been revealed for tubular turbulent devices. The following fast chemical processes have been taken as model processes for: a single-phase reaction mixture (acid and alkali media neutralisation), 'liquid-liquid' system (sulfation of olefins by concentrated sulfuric acid), 'liquid-gas' system (liquid-phase oxidation of sodium sulfite by aerial oxygen), and 'liquid-solid' system (synthesis of barium sulfate and an antiagglomerator for synthetic rubbers based on calcium stearate). The results obtained from the study of these systems contribute to the broadening of their efficient industrial application range.

The general conclusion is that the tubular design device, with high turbulent mixing intensity, is a good solution for the implementation of fast chemical processes. It provides a substantial growth of product quality and methods to develop energy- and resource-efficient technologies for enhanced environmental safety.

# Glossary

| | |
|---|---|
| $\alpha$ | Heat transfer coefficient |
| $\beta$ | Product yield |
| $\varepsilon$ | Specific kinetic energy of turbulence dissipation rate |
| $\gamma$ | Diffuser opening angle |
| $\lambda$ | Wall thermal conductivity coefficient |
| $\mu$ | Dynamic viscosity coefficient |
| $\nu$ | Kinematic viscosity |
| $\Theta$ | The dimensionless duration of reactants pass through a reactor |
| $\rho$ | Reactive mixture density |
| $\sigma$ | Surface tension |
| $\delta$ | Characteristic dimension of the reaction zone |
| $\xi$ | The portion of heat removed in the cooling zone from the total thermal energy accumulated by the system at the inlet of this zone |
| $\Psi$ | The current function |
| $\omega$ | The vortex tension |
| $\Delta\alpha_2$ | The maximum difference between the volume fraction of a dispersed phase in the device's central axis and at its periphery |
| $\alpha_{2av}$ | The average volume fraction of a dispersed phase in a reaction flow |
| $\lambda_c$ | The effective heat conduction coefficient |
| $\tau_{chem}$ | Chemical reaction duration |
| $\alpha_i$, $\rho_i$, $\mu_i$ | The volume fraction, density and viscosity of $i^{th}$ phase respectively |
| $\tau_{mezo}$ | Characteristic time of mesomixing |
| $\Delta M_i$ | The amount of reacted monomer in the $i^{th}$ zone |
| $\tau_{micro}$ | Characteristic time of micromixing |
| $\tau_{mix}$ | Reactants mixing duration |

| | |
|---|---|
| $\mu_{mol}$ | Dynamic coefficient of molecular viscosity |
| $\chi_{mon}$, $\chi_{solv}$ | Monomer and solvent heats of evaporation |
| $(n_{AC})$ | The number of polymer chains per active centre |
| $\Delta P$ | The amount of oligomer obtained per reaction volume unit |
| $\tau_{pass}$ | Duration of chemical reactants passing through a reactor |
| $\alpha_{prof}$ | The thermal emission coefficients of a reaction mixture flow in the profiled channel |
| $\Delta q_{ad}$ | Adiabatic reaction heat |
| $\alpha_{smooth}$ | The thermal emission coefficient of a reaction mixture flow in a smooth channel |
| $\lambda_t$ | Temperature conductivity coefficient |
| $\mu_{turb}$ | Dynamic coefficient of turbulent viscosity |
| $\nu_{turb}$ | Kinematic coefficient of turbulent viscosity |
| $\tau_{turb}$ | Characteristic time of turbulent mixing |
| $\Delta p$ | A pressure drop |
| $\Delta p = (p_{in}\text{-}p_{out})$ | Input-output pressure drop |
| $\Delta T_{ad}$ | Adiabatic temperature increase in a reaction zone |
| $\Delta T_{heat}$ | The temperature difference along the device axis caused by reaction thermal effect |
| $\Delta T_i$ | Characteristic temperature difference in a reaction $i^{th}$ zone |
| $\Delta M$, $\Delta M_i$, $P_w$, $P_w^i$, $P_n$, $P_n^i$, $P_z$, $P_z^i$ | The amount of polymer, weight-average, number-average, and z-average polymerisation degrees of the polymerisation product in the entire reactor and in the $i^{th}$ zone respectively |
| $[\eta]$ | Characteristic viscosity of a polymer solution |
| $[A^*]_i$ | The amount of catalyst fed to the $i^{th}$ zone |
| $\Sigma C_a$ | The concentration of active centres |
| $Ar_{mod}$ | Modified Archimedes Number |
| $C_M$ | The concentration of a monomer |
| $d$ | The diameter of dispersed phase particles |
| $D$ | Overall reactor diameter |
| $d_1$, $d_2$ | The diameter of central (coaxial) and side nipples in a tubular device with radial input of flows |
| $d_{32}$ | Volumetric-surface diameter of droplets (bubbles) of a dispersed phase |

| | |
|---|---|
| $d_c = 2R_c$ | The diameter of a narrow section (confusor) of a tubular turbulent reactor with diffuser-confusor design |
| $d_{cr}$ | The critical size of dispersed phase particles (liquid, gas) being deformed in a turbulent flow |
| $d_d = 2R_d$ | The diameter of a wide section (diffuser) of a tubular turbulent reactor with diffuser-confusor design |
| $d_{\text{disp}}$ | The mean diameter of dispersed particles |
| $d_L$ | The return of the active centres to a reaction zone length |
| $d_{\text{stir}}$ | The stirrer diameter |
| $D_{\text{turb}}$ | Turbulent diffusion coefficient |
| $F$ | Heat exchange surface |
| $f$ | Diffuser opening angle function |
| $f_c$, $f_E$ | Reactor geometry functions ($d_d/d_c$, $L_c/d_d$) |
| $G_2$ | The volume gas flow rate |
| $G_r$, $G_{\text{cool}}$ | The flow rates of a reactive mixture and a cooling agent respectively |
| $K$ | Specific kinetic energy of turbulence |
| $K_d$ | Coefficient of polydispersity of two-phase reactive systems |
| $k_{ef} = k_p Ca$ | The effective constant of polymerisation reaction |
| $k_{in}$, $k_p$, $k_m$, $k_t$ | Reaction rate constants for initiation, chain propagation, transfer to monomer and chain termination reactions in a polymerisation process |
| $k^{\text{o}}_{\text{Al}}$ | Chain-to-aluminium-organic compound transfer reaction rate constant |
| $k^{\text{o}}_M$ | Chain-to-monomer transfer reaction rate constant |
| $K_{bt}$ | Heat transfer coefficient |
| $L$ | Device length |
| $L_c$ | The length of diffuser-confusor module of a tubular device |
| $L_{\text{chem}}$ | Chemical reaction zone length |
| $L_{\text{cool}}$ | Cooling zone length (reactor length in external heat removal conditions) |
| $L_i$ | The length of the heat removal zone |
| $L_{\text{mix}}$ | Reactor length required to achieve required level of reactive mixture homogenisation |

| | |
|---|---|
| $M_0$ | The monomer concentration in the starting mixture |
| $M_N$ | Number-average molecular weight |
| MW | Molecular weight |
| $M_W$ | Weight-average molecular weight |
| MWD | Molecular weight distribution |
| $M_Z$ | z-Average molecular weight |
| $N$ | The number of tubes in a shell-and-tube turbulent reactor |
| $n$ | The rotary speed of a stirrer. |
| $N_c$ | The number of diffuser-confusor modules in a tubular device |
| $N_g$ | The stirrer capacity consumed for stirring of the liquid-gas mixture. |
| $N_{pol}$ | The number of polymer chains in a reaction mixture |
| $N_{rpm}$ | Mechanical agitator rotation rate |
| $N_{stir}$ | The stirrer capacity consumed for stirring of a liquid |
| $Nu$ | Nusselt Number |
| $n_{wi}$, $n_{ni}$ | The weight and numeric share of particles with radius $r_i$ respectively |
| $P_n$, $P_w$, $P_z$ | Number-average, weight-average and z-average degrees of polymerisation respectively |
| Pr | Prandtl Number |
| $P_w/P_n$ | Polydispersity coefficient |
| $Q$ | The amount of heat, transferred through a heat exchange surface |
| $q$ | Reaction thermal effect |
| $r$ | The radius of dispersed phase particles |
| $R$ | Universal gas constant |
| $r_0$ | The total chain termination rate |
| $r_1$ | The copolymerisation constant |
| $R_c$ | The radius of a narrow part of a reactor (confusor) |
| $R_{cr}$ | The critical radius of a reactor, determining transfer from torch and intermediate modes to quasi-plug flow mode in turbulent flows |
| $R_d$ | The radius of a wide part of a reactor (diffuser) |
| Re | Reynolds Number |
| $Re_c$ | The centrifugal Reynolds Number |

| | |
|---|---|
| $\mathrm{Re}_{cr}$ | The Reynolds Number corresponding to automodel reaction reaction mixture behaviour in the above area in relation to viscosity |
| $R_{\max}$ | The maximum permissible radius of a reactor |
| $R_{\min}$ | The minimum permissible radius of a reactor |
| $r_n$ | The average numeric radii of particles in a polymer dispersion |
| $r_w$ | The average weight radii of particles in a polymer dispersion |
| $r_p$ | Polymer growth rate |
| $S$ | The factor depending on the kinetic activity distribution of polymerisation AC |
| $T$ | General temperature |
| $U$ | Polymer yield |
| $u$ | Polymer polydispersity |
| $V$ | Linear flow rate of a reaction mixture |
| $V'$ | The reduced gas velocity |
| $V_1$, $V_2$ | Linear input rates of central and side flows of a tubular turbulent reactor |
| $V_c$ | Linear flow rate in the narrow reactor section (confusor) |
| $V_{\text{flot}}$ | The gas bubble flotation rate |
| $V_p = k_{ef}C_m$ | The rate of the second-order polymerisation process |
| $V_r$ | Reactor volume |
| $v_r$ | Reaction zone volume |
| $w$ | Reaction mixture volume flow rate |
| $w$ | The volume of the liquid-gas mixture in a reactor. |
| $w_1$, $w_2$ | The volume flow rate of central and radial flows |
| $w_c$, $w_{int}$ | The volume flow rate of liquid in circular and internal channels of double pipe heat exchanger |
| $We$ | Weber Number |
| $We_c$ | The centrifugal Weber Number |
| $w_g$, $w_l$ | Volume flow rates of liquid and gas phases |
| $w_{\text{in. pol}}$ | Initial polymerisation rate |
| $X$ | The parameter of the size distribution of polymer globules. |
| $z$ | The length of mixing zone from dispersed phase (liquid, gas) input to the start of two-phase flow layering (the area of homogeneous flow formation with the uniform distribution of dispersed phase particles along device cross section) |

| | |
|---|---|
| Bo | Bodenstein Number (Péclet Number for longitudinal mixing) |
| $E$ | Longitudinal mixing coefficient |
| $E_M$ | Activation energy of chain transfer to monomer reaction |
| $E_m$ | The activation energy of the chain transfer reaction |
| $E_p$, $E_t$ | Activation energy of chain propagation and chain termination reactions |
| $E_p$ | The activation energy of chain growth reaction |
| $K_{ht}$ | Coefficient of heat transfer through a wall |
| $P$ | The ratio between the polymerisation reaction and diffusion limitations. |
| $P$ | General pressure |
| $P_{\text{in}}$ | Input hydraulic pressure |
| $P_{\text{out}}$ | Output hydraulic pressure |
| $C$ and $\Theta$ | The combination of dimensionless coordinates used for plotting the differential curves of the pass duration time distribution of reactants in a reaction zone |
| $C_0$ | The concentration of added indicator used for getting the information about pass duration time distribution of reactants |
| $C_a$ | Concentration of active centres |
| $C_i$ | Concentration of reactants with the duration $\tau_i$ of their flow through a reactor |
| $C_{m0}$, $C_m$, $C_c$ | Input and output concentration of reactants and catalyst concentration respectively |
| $C_r$ | Reactive mixture heat capacity |
| $C_p$ | Constant pressure heat capacity |
| $T_0$ | The initial temperature of an unreacted mixture |
| $T_{\text{ad}} = T_0 + DT_{\text{ad}}$ | Reaction mixture temperature in adiabatic conditions |
| $T_{\text{boil}}$ | Boiling temperature |
| $T_{\text{cool}}$ | Cooling agent temperature |
| $T_i$ | Average temperature in the $i^{\text{th}}$ zone |
| $T_{k\text{-}1}$ | The temperature in the previous reaction zone or at the inlet of the corresponding cooling zone |
| $T_p$ | Reactor temperature |

# Abbreviations

| | |
|---|---|
| AC | Active centres |
| BR | Butyl rubber |
| DCPD | Dicyclopentadiene |
| ENB | Ethylidene norbornene |
| EPDM | Ethylene propylene diene monomer |
| EPR | Ethylene propylene rubber(s) |
| MW | Molecular weight |
| MWD | Molecular weight distribution |
| Nd-Al | A neodymium-aluminium Ziegler–Natta catalytic system |
| SSEPT | Styrene-ethylene-propylene |
| THF | Tetrahydrofuran |
| Ti-Al | A titanium-aluminium Ziegler–Natta catalytic system |
| V-Al | A vanadium-aluminium Ziegler–Natta catalytic system |

# Index

2D, 132, 273-274
3D, 66

## A

Absorption, 226-230
Acceleration, 1, 69, 154, 227, 230, 272
Acid, 34, 83-84, 125, 207, 212, 216-225, 232, 237, 251-252, 273, 275, 290
  Acidic, 39, 84, 124, 218-219
  Acidity, 124-125
Activation, 6, 20, 73, 117, 151-152, 180
  energy, 180
Active centres, 5-6, 13-15, 39, 128-129, 145-147, 151-155, 157, 160, 164, 166-180, 182, 184-191, 193-199
Additives, 148-151, 162, 165, 280
Adhesion, 29, 137, 236-237, 252, 255-257, 268, 270
Adsorption, 62, 100-101, 165, 174-175
Agent, 2, 72, 76-77, 80, 82, 85, 92, 104, 136, 139, 144, 169, 216, 219, 248, 259, 268, 276
Agglomeration, 45, 240
Agitation, 2, 25, 50, 105, 202
Algorithm, 10, 179
Alkali, 207, 216, 218-219, 256, 268, 290
Aluminium, 124-125, 139, 145, 148, 153, 160, 169, 171, 193, 250, 261
  chloride, 124
Analysis, 2, 8, 12, 31, 46, 48, 51, 55, 69-70, 73-74, 78, 93, 100, 116, 118, 128, 148, 151, 154, 162, 165, 168, 170, 195, 197, 199, 212, 232-233, 247, 272, 279, 289
Anionic, 175, 220
Antioxidant, 137, 255-257
Application, 21, 31, 39, 43, 45-46, 48, 68, 70, 82, 86, 94, 105, 109, 124, 139, 160, 200, 214-215, 218, 231, 235, 272, 287-290
Aqueous, 144, 207, 218-219, 229, 232, 236-239, 242, 254-255, 270
  phase, 144, 239
  solution, 218-219, 229, 237-238, 254

Atmospheric pressure, 144, 223
Axial, 1, 9-10, 30, 50, 57-58, 74, 76, 96, 146, 208, 213-215, 217, 232, 258-259, 289

## B

Barium sulfate, 231, 290
Bimodal, 128, 172, 179
Blend, 1, 3, 32, 39, 129
Boiling, 70, 72-74, 80, 97, 99, 116, 119, 122, 221-223, 225, 247, 275-276, 280, 282
  point, 72, 80, 221, 225, 275, 280
Bond, 127-128, 135, 173-174, 176-177, 180, 259
Branch, 208, 210, 212, 215, 219, 229
  Branched, 161-162
  Branching, 142-143
Breaking, 46, 263
Bridge, 176-177
Bromobutyl rubber, 136
Bubble, 55, 65, 100, 135, 141-142, 227
Bundle, 224, 248-249
Butadiene, 1, 138, 144-145, 149, 154-155, 158, 160, 171-173, 188, 194, 196, 198-199, 236, 250-251, 259
Butyl rubber, 39, 134-137, 227, 251, 254-256, 258
By-product, 124

## C

Calorimetry, 172
Capacity, 70, 76-77, 105, 125, 136, 141, 217, 219, 221, 228, 230, 240, 242, 246, 248, 251, 270
Carrier, 77, 88, 103-104, 289
Catalysis, 204-205
  Catalyst, 2-5, 10-12, 15, 17, 19, 25, 39, 74-76, 115-116, 119-120, 123-126, 128-129, 131-132, 138, 145-155, 157-170, 172-173, 176, 179-180, 189, 191-192, 194-195, 198-199, 236, 254-255, 261-271, 278
  Catalytic activity, 191, 198
Cationic, 1-2, 4, 8, 10, 12, 83-84, 115, 119, 124-125, 127-129, 161, 165, 169, 172, 198-201, 250-251
  polymerisation, 1-2, 4, 8, 10, 12, 83-84, 124, 128, 172, 198
Cellular, 94, 279
Chain, 2-6, 20, 39, 73, 116-118, 124, 137-138, 145, 153-154, 157, 160-161, 165, 167-169, 172-174, 176, 178-180, 182, 190, 193, 196, 267-268
  transfer agent, 169, 268

Channel, 29-30, 34, 36, 38, 40, 44, 48, 60, 63-65, 68, 74, 86-89, 91, 95-96, 100, 102-104, 229-230, 234, 258, 288
Chemical, 1-26, 28-32, 34, 36, 38-40, 42-46, 48-52, 54, 56, 58, 60, 62-70, 72, 74, 76-78, 80-84, 86, 88, 90, 92-102, 104-110, 112-114, 116, 118, 120, 122, 124-126, 128, 130, 132-138, 140, 142, 144, 146, 148, 150, 152, 154, 156, 158, 160, 162, 164-166, 168, 170, 172, 174, 176, 178, 180, 182, 184, 186, 188, 190, 192, 194, 196, 198-202, 204, 206-216, 218-220, 222, 224-226, 228-232, 234-236, 238, 240, 242-250, 252, 254-256, 258, 260, 262, 264-266, 268, 270, 272-278, 280, 282, 284, 286-290
  industry, 105, 113, 250
  reaction, 2-4, 16-17, 25, 28-29, 31, 42-43, 48, 60, 70, 72, 76-77, 80, 95, 99, 102, 120, 130, 133, 135-136, 165, 196, 212-213, 215-216, 220, 225, 229, 235, 246-247, 249, 255, 258, 270, 272-273, 277, 287-288
  structure, 176
Chemistry, 1, 21, 30, 51, 107, 109-110, 112, 203-205, 243-244, 284-285
Chlorinated, 2, 134-137, 201, 255
Chlorobutyl rubber, 1, 134-136, 255-257, 259
Chromatography, 170, 188
Circular, 74, 77, 88-89, 92, 103-104
Classification, 1, 245, 248, 250
Clear, 2, 10, 120, 167
Coalescence, 60, 67, 142
Coefficient, 3, 6, 8, 10-11, 16, 26, 28, 31-37, 40-41, 43, 46, 52-53, 58, 65, 67, 69, 75-78, 80, 84-87, 89, 91-92, 94-95, 97-99, 101-105, 116-117, 121, 213, 226, 229-230, 233, 249, 267, 275, 289
Column, 136, 245, 256, 274, 276-277
Complex, 14, 53, 62, 72, 115, 125, 144-145, 147-148, 160, 167-169, 171-172, 183, 194, 197-198, 202, 255, 260-268, 277-278, 287
Component, 8, 10, 51, 55, 62, 99, 129, 147-149, 152, 155, 157, 168, 170, 175, 190-191, 199, 209, 241, 263, 272, 277-278, 280-282
Composite, 167, 202
Composition, 9, 25, 28, 59, 63, 72-73, 99, 136, 138, 143-145, 168, 170-173, 176, 198-199, 208, 237-240, 242, 245, 251, 260, 265, 280, 282
Compound, 145, 149, 153, 162, 168-169, 173-175, 177-178, 193, 232
  Compounding, 251, 280, 282
Compression, 18, 99, 273
Concentration, 2-3, 5-6, 10-12, 14, 17, 19, 25, 28, 31, 37-39, 43, 48, 52, 70, 73, 83, 86, 88, 93, 98-99, 102, 117, 119, 126, 128-129, 131, 139-140, 152-155, 157, 160-161, 163-164, 168-169, 171-172, 174, 189-191, 193, 196, 199, 212-213, 226-227, 231-232, 237-240, 246-247, 255, 262-263, 287-288
Condensation, 151, 231, 237-238
Condensor, 266, 271

Conduction, 117, 247
  Conductivity, 6, 77-78, 80, 86, 89
Construction, 25, 31, 210, 215, 223, 225-226, 229, 238-242, 246, 249, 251, 265, 282
Consumption, 61, 70, 124, 147, 154, 159-160, 199, 215, 222, 225, 227, 229, 237, 251, 254, 276, 280, 282
Conversion, 12-13, 15, 18-19, 39, 74, 85, 125-126, 129-130, 136, 147, 151, 155, 157-158, 160, 172-174, 185-187, 189-191, 193-196, 198, 219, 221, 236, 267
Cooling, 1-2, 72, 76-78, 80-85, 88-90, 92, 103-105, 122-123, 133, 217, 221, 223-225, 248, 271, 276
Copolymerisation, 1, 137-140, 144, 147, 169-171, 173, 179, 199, 236, 250, 260-265, 290
Core, 34, 86, 140, 161, 181-182
Correlation, 17, 30, 37, 43, 45, 81, 87-88, 92, 96, 98-100, 102, 105, 152, 163-164, 168, 170-172, 182, 188, 197, 199, 213, 231, 233, 268, 288
Corrosion resistance, 254
Cross-section, 85
Crosslinked, 125, 160-162, 165
  Crosslinking, 72, 128, 161, 164
Crystal, 164, 167, 175-178, 231-232, 234, 239, 242, 263-264
  Crystalline, 151, 175-176
  Crystalline structure, 151
  Crystallisation, 231, 239
Current, 9-10, 251, 270, 276-277
Cylinder, 142, 215, 217-219, 223, 225, 229, 238-241
  Cylindrical, 25-26, 29-31, 34, 36-37, 40-41, 46, 57, 60, 62-63, 65, 67, 71, 76, 78-79, 86-92, 95-96, 98-99, 103-104, 212, 248-249, 252, 278, 289

## D

Data, 10, 18, 29-31, 41, 56, 78, 93, 98, 100, 124, 129, 140, 142, 146, 148, 155, 162, 164-165, 170, 173-174, 181-182, 188-189, 198, 217, 232, 240, 276-277
Deactivation, 14-15, 162, 171, 173, 270-271
Decomposition, 39, 236, 250-252, 265
Defect, 276
Deform, 56
  Deformation, 47, 55-56, 60, 64, 97, 269
Degassing, 236-237, 240, 242, 255
Degradation, 135
Degree of conversion, 19
Degree of polymerisation, 5, 12, 164
Dehydrogenation, 124

Density, 8-9, 29, 34, 40, 46-47, 50-52, 55, 67-70, 77, 101, 118, 121, 125, 136, 144-145, 161, 179, 213-215, 217, 220, 257, 269, 273, 278, 280
Deposition, 170-171, 264, 270
Depth, 63, 68, 95, 100, 229-230, 272
Derivative(s), 57, 76-77, 93
Deterioration, 128, 138
Diameter, 1, 6, 29, 36, 38, 40, 45-49, 53, 55-57, 59-66, 68, 77, 82, 85-86, 88, 95, 98-100, 140-142, 146, 208, 211-212, 214-215, 219, 224, 227, 229, 232-233, 237-241, 248, 281-282
Dichloromethane, 172
Dicyclopentadiene, 139, 142-144, 250, 260, 264
Dielectric, 168
Dienes, 137-138, 144-145, 147, 150-152, 159, 161, 166, 168, 170-172, 174, 176-178, 188, 199-200, 231, 236, 284
Diethylene glycol, 173
Differentiation, 9, 148, 232
Diffusion, 2-4, 6, 8, 10, 12-17, 19, 21, 24, 26, 28, 31-37, 39-44, 46, 48-50, 52, 59, 62, 67, 70, 94-95, 102, 116, 119, 130, 138-140, 152, 155, 173, 180, 199, 207-208, 213, 215-216, 226, 228-229, 231-232, 239, 246-247, 249, 267, 287-288, 290
Dilution, 221-223
Dimension, 93, 117, 226
Dimensionless, 93
Dispersing, 50, 57, 60, 62, 68, 99, 150, 168, 249, 272
  Dispersion, 50-52, 55, 57-60, 62-63, 67-69, 100, 120, 135, 140, 150-151, 161, 176, 216, 226-230, 232, 272
Displacement, 1-2, 18, 20
Dissipation, 9-10, 20, 26-28, 37-38, 40-41, 43, 46-47, 50, 53, 55, 57, 234, 269
Dissolution, 83, 170, 226, 228, 230, 249
Dissolving, 62, 263
Distribution, 1, 3, 5, 7, 27, 32, 34, 37, 53, 56, 59, 63-64, 67-69, 73, 88, 93-95, 97, 115, 118-119, 128, 132, 136, 138, 143-144, 147, 149-152, 158, 166-167, 170-172, 174-176, 179-180, 182-185, 187-190, 194-199, 223, 233, 245, 247, 251, 255, 261, 265-267, 269, 273, 278, 288-289
Double bond, 127-128, 259
Drive, 225, 261
Droplet, 45, 55-56, 58
Drying, 124-125, 128-129, 237, 255-256
  oil, 124-125, 128-129
Dynamic(s), 8-9, 26, 29, 38, 43-46, 49, 51, 55, 135, 162, 270, 273, 279
  viscosity, 9, 29, 38, 44-45, 135, 270

## E

Efficiency, 12, 16-17, 20-21, 25, 34, 36, 43-44, 46, 50, 56, 60, 91-92, 94-95, 98, 102-104, 120, 133, 136, 140, 144, 150, 226-229, 231, 245, 249, 266, 288-289
Elastomer, 136, 257-259
Electric, 225, 265
Electron, 125, 168-169
Electrophilic, 1-2, 12, 105, 115, 124-125, 127-129, 252
Elevated temperature, 277
Emission, 77-78, 80, 84-86, 92, 103-104, 222, 246, 273, 276, 287
Emulsifier, 144
Emulsion, 50, 59, 62, 138, 144, 250, 272
Energy, 9-10, 22, 26-28, 30-32, 37-38, 40-41, 43-44, 46-47, 50, 52-57, 61, 63, 67, 86, 88, 100, 105, 111, 122, 129, 131, 133, 137, 147, 174-176, 180, 200, 219, 225, 228-229, 234, 236, 239, 242, 250-251, 254-255, 259, 269, 275, 280, 282-283, 287, 290
  consumption, 61, 147, 225, 229, 254, 280, 282
  dissipation, 50, 234
Engineering, 22, 24, 42, 82, 104-106, 108-110, 112-114, 202, 244, 248, 255, 282
Enthalpy, 10, 52
Equilibrium, 19, 139, 168-169
Equipment, 3, 82, 138, 182, 199, 236, 239, 245, 259, 270, 275-276, 280, 289
Ethylene, 1-2, 72, 80, 82, 84-85, 136, 138-139, 142, 144-145, 168, 170, 199, 207, 216, 236, 245, 250, 252, 259-260, 262-265, 268, 275-278
  propylene diene monomer, 136, 138, 142-144, 250, 266
  propylene rubber(s), 138-140, 142, 144, 260, 265
  propylene copolymers, 170
Ethylidene norbornene, 139, 143-144, 266
Evaporation, 73, 116, 222, 274-275, 277-278
Exothermic, 70-71, 216, 220, 273, 276, 288-289
Expansion, 29, 256, 263
Exposure, 109, 145, 198, 240, 265
  time, 145
Expression, 9, 118, 130, 233
Extraction, 39, 43, 137, 147, 216, 252, 255, 278

## F

Flask, 148, 232, 234
Flexible, 154, 272-273
Flow, 1-3, 6, 8-10, 13-20, 24-31, 33-34, 36, 38-40, 43-53, 55-57, 59-62, 64-70, 74-83, 86-101, 103-105, 109-110, 116-117, 120-123, 129-131, 133,

135-137, 140-142, 146-147, 149, 207-219, 221-222, 224-230, 232, 234, 237, 240-241, 245-251, 254-265, 268-276, 279-280, 282, 287-289
rate, 2, 17-20, 29-31, 34, 39-40, 44-51, 55, 60-62, 64-68, 76-77, 80, 86-93, 95-98, 103-105, 117, 120, 129, 136, 141, 146-147, 210, 213-215, 217-219, 222, 228, 237, 245-247, 249, 255, 269, 279, 289
Fluid, 51, 99, 110, 245, 247, 260
Foam, 65, 135, 227, 272-273
Fold, 132, 142, 150, 251, 259
Force, 52, 239
Formation, 1-2, 6, 11, 13-16, 18, 25, 31, 34, 40-43, 49-50, 53, 60, 62, 64-67, 70, 74-75, 80, 86-87, 92, 97-99, 102, 115-116, 123-124, 128-129, 131, 133, 137-138, 140, 142, 144-153, 155, 157-166, 168-169, 172-178, 180, 190, 192-199, 207-208, 210-217, 221, 231-232, 234-239, 241-242, 247, 250, 252, 255-258, 260-269, 272-273, 275, 278-279, 287-288
Forming, 2, 15, 18, 20, 56, 117, 147, 157, 161, 168, 170-172, 189, 199
Formula, 42, 69, 94, 222
Fraction, 52, 57, 68-69, 124, 143-144, 160-165, 170, 182, 188-191, 193-195, 197, 199, 225, 233, 252, 268, 271, 280-282
Fractionation, 170, 188-189, 276
Frequency, 56, 208
Friction, 52-53

## G

Gas(es), 2, 23, 49, 51, 64-68, 73-74, 77, 86, 97-102, 107, 118, 135, 139-144, 173, 180, 221, 223, 226-230, 245, 249-250, 254-255, 257-258, 260-263, 265-266, 276-279, 290
Gaseous, 135-136, 138-140, 144, 257-258, 260, 263-264, 275, 277-278
Gel, 160-165, 170, 188
Gelation, 128
Geometry, 3, 15, 18, 30-31, 34, 37-38, 40, 48-49, 55, 62-63, 67, 70, 77, 94-96, 98, 102, 130, 132, 135, 174, 177-178, 226, 229, 234, 249, 255, 288-289
Glass, 56, 77, 88
Grade, 62, 145, 160, 251
Gradient, 19-20, 53, 68, 70, 74, 174, 288
Grinding, 149, 152, 168, 191, 228, 240-241, 249
Growth, 1-2, 4, 6, 11, 18-20, 25, 37, 39, 59, 62, 65-68, 70, 72, 75, 77, 83-84, 99, 103-105, 120, 137, 145-147, 149, 151, 153-155, 157-158, 160, 162-164, 166-169, 172-174, 176, 178-180, 188, 190-199, 227, 229-232, 234, 238-239, 242, 250, 252, 254, 261, 263, 265, 267, 290

## H

Heat, 1-4, 6, 10-12, 19-21, 24-25, 27, 29, 31, 33, 35, 37, 39, 41, 43-45, 47, 49, 51-53, 55, 57, 59, 61, 63, 65, 67, 69-89, 91-93, 95, 97, 99, 101-107, 109, 111-113, 116-123, 125, 132-133, 136-137, 202, 217-224, 246-247, 249, 255, 272-273, 275-278, 287-290
  generation, 70, 83, 289
Heating, 70, 72-73, 80, 88-91, 115, 118, 217, 222-223, 247, 278
Height, 40, 139
Heterogeneous, 50, 146, 149, 154, 161, 165-167, 170-172, 179, 191, 231
High-density polyethylene, 145
High molecular weight, 171, 193
High-pressure, 245
High-speed, 99, 227
High temperature, 134
High viscosity, 139, 249, 256, 266
Hindered, 62, 175
Homogeneity, 15, 45, 208, 235, 265
  Homogeneous, 25, 49, 67-68, 97, 144, 150, 158, 162, 167, 170, 172-173, 175, 215, 231, 235-236, 245, 249-250, 252, 260, 263, 265, 272-273, 278
Horizontal, 102, 246
Hydraulic, 31, 40, 56, 88
Hydrocarbon, 62, 139, 220, 222, 227, 255, 260, 273, 277, 282
Hydrochloric acid, 219
Hydrogenated, 280
  Hydrogenation, 252, 278-279

## I

Impact, 56, 65, 147-158, 162-164, 190-191, 193, 196-197, 240-242
Impurity, 175, 278
*In situ*, 145, 147, 150-151, 194, 198-199, 235, 241
*In vitro*, 234
Indicator, 88-89, 93-96, 242
Industrial application, 39, 43, 94, 287, 289-290
Industry, 3, 30, 105, 112-113, 134, 145, 152, 200, 243, 250
Inhomogeneous, 50, 170, 182
Initiation, 4-5, 73, 137-138, 145, 147, 152, 174, 179, 199, 261, 265-266
  Initiator, 138, 144, 168-169, 250
Inorganic, 273, 285
Insoluble, 124, 160-165, 275
Institute, 107, 109-110, 113
Instrument, 20, 288

Instrumentation, 245, 247, 249, 251, 255, 257, 259, 261, 263, 265, 267, 269, 271, 273, 275, 277, 279, 281, 283, 285, 287
Integration, 50, 76
Intensity, 31-32, 36, 47, 50, 52, 59-60, 62, 65, 75, 86, 94-96, 101, 103, 141, 150, 154-155, 226, 230-231, 234-236, 238, 241, 267, 277, 288, 290
Interaction, 50-52, 83-84, 137, 145, 150, 161-162, 169-170, 174-178, 196, 199, 207, 212, 217, 220, 226, 232, 236-237, 251-252, 257, 263-264, 269-270, 272-273, 276-278
Interface, 49-50, 53, 55, 142, 258, 288
Interfacial tension, 52, 62-63
Intermediate, 13, 15-16, 95, 171, 208
Interphase, 55, 60, 62-63, 65, 67, 97, 100-102, 239, 257-258, 289
Ion, 231, 237
exchange, 231, 237
Ionic, 1, 124, 128, 166-170, 172, 196
Isomerisation, 171-172
Isoprene, 1, 39, 62, 124, 134, 138, 145-149, 151-158, 160-161, 164, 166-168, 174, 182-188, 190-192, 199, 236, 250, 252, 259, 265-269, 278-279
Isotactic, 145, 171, 176, 179
polypropylene, 145
Isothermal, 11-12, 16, 20, 72, 121, 129, 137, 214, 217, 224, 246-247, 249, 276, 288

## J

Jet, 3, 39, 80, 82-83, 133, 136-137, 140, 199, 210, 219, 221, 224, 269

## K

Kinetic, 2, 11, 15-19, 26-28, 30-32, 37-38, 40-41, 43-44, 46-47, 49-55, 57, 70, 73, 80, 104, 119, 123, 129-130, 132-133, 154-155, 157, 166-167, 169-171, 173-174, 179-180, 182-197, 199-200, 206, 213-215, 234, 269-270
energy, 26-28, 30-32, 37-38, 40-41, 43-44, 46-47, 50, 52-55, 57, 234, 269

## L

Lattice, 164, 167, 175
Layer, 86, 140, 165, 264
LED, 56, 68, 168, 170, 172, 211
Length, 1, 6-7, 12-13, 17, 20, 29-30, 36-40, 48, 67-68, 70, 74, 77-78, 80-86, 88, 95, 105, 116, 120-122, 133, 165, 187, 193, 216, 219, 221-225, 229, 232-233, 245-246, 248, 259, 268, 281-282, 288-289
Ligand, 169-170

Linear, 2, 15-16, 18, 28-29, 40, 43-49, 56, 60, 80, 117, 120, 134, 136, 146-147, 171, 208, 212-214, 217, 219, 221, 229, 232, 288
Liquid, 1-9, 11-13, 15, 17, 19-21, 23-27, 29, 31-41, 43-47, 49, 51, 53, 55, 57, 59, 61-75, 77, 79, 81, 83, 85, 87-103, 105, 107-109, 111, 113, 115, 117, 120, 124, 129, 135-136, 138-144, 173, 201-202, 207, 209-211, 213-217, 219-221, 226-231, 236-237, 242, 245, 248-251, 255, 257-258, 260-262, 265-266, 270-272, 275, 277-280, 283, 287-290
  phase, 26, 65, 70, 102, 115, 117, 139, 226, 228-230, 237, 261, 278, 289
Load, 89, 134, 268, 273
  Loading, 116, 119-120, 139
Loss, 40, 86, 88, 138
Low molecular weight, 12, 43, 48-49, 115, 184-185, 198, 207, 209, 211, 213, 215, 217, 219, 221, 223, 225, 227, 229, 231, 233, 235, 237, 239, 241, 243

## M

Macromolecular, 1, 21, 166, 188, 204-205
  Macromolecule, 4, 116, 140, 142-143, 147, 151, 160-161, 163, 165, 179, 188, 190-195, 197, 199, 252, 261, 263, 265
Macroscopic, 3, 12-15, 50-51, 207-208, 211-212, 215-216, 288
Magnetic, 148, 170
Maintenance, 217, 225, 242, 276
Material(s), 1-2, 130, 134, 137, 147, 202, 216, 251, 254, 276, 282
Measurement, 15, 93, 264
Mechanism, 28, 37, 39, 100, 115, 119, 123, 145, 167, 173, 199
Melt, 135, 142-143
Metallic, 75, 175, 263
Microstructure, 166-167, 171-172, 174, 188-189, 198-199
Mix, 44, 130, 217, 219-220, 273, 278
  Mixed, 10, 144, 147-148, 152, 188, 198, 209, 216, 247, 251, 261, 263, 280, 282
  Mixer, 28, 227, 231-232, 234, 236, 258, 266
  Mixing, 1-3, 8, 12-17, 19, 25-26, 28-32, 34, 36-40, 42-51, 55, 59, 65, 67, 70, 72, 74, 92, 94-103, 105, 130, 135, 137-138, 140, 144, 146-148, 150-151, 154-155, 157, 196-199, 207-213, 215-217, 220-221, 224-225, 227-228, 230-238, 240-242, 245-250, 252, 254-264, 266-273, 275-277, 280-282, 287-290
  Mixture, 3-4, 8-10, 15-20, 25-27, 30-32, 34, 36, 38-41, 44-49, 51, 53, 55, 59-63, 65-68, 70, 72-74, 76-77, 80, 83-84, 86-93, 96-97, 99, 101, 103, 105, 115-116, 118-119, 121-122, 125, 128-131, 135-144, 146-148, 150, 152-155, 157-160, 162-164, 169, 171, 191-196, 198, 209, 216-217, 219, 221-224, 226-230, 232, 234, 236-237, 239-240, 242, 245, 247, 249-250, 255, 258, 260-262, 265-268, 270-272, 275-282, 287-290

Model, 2, 6, 8-10, 12, 18, 26-28, 30-31, 40-41, 50, 53, 57, 62, 74-75, 82-83, 85-86, 94, 116, 121-122, 147, 173-174, 177-179, 182, 196, 209, 216, 218, 223-225, 231, 245, 267, 290
  reaction, 231
Modelling, 4, 12, 26, 29, 31, 50-51, 53, 88, 92, 173, 216
Modification, 134, 137, 147, 149-151, 162, 165, 191, 268, 290
  Modified, 1, 53, 69, 137, 149, 151, 158, 163-164, 174, 191, 250, 264
Molecular weight, 2-3, 5-6, 11-13, 15, 18, 20, 43, 48-49, 72-75, 115-121, 123-124, 127-129, 132, 135, 139-140, 144, 155-161, 163, 166-167, 171-174, 180, 182, 184-196, 198-199, 207-209, 211-213, 215-217, 219, 221, 223, 225, 227, 229, 231, 233, 235, 237, 239, 241, 243, 250-251, 253, 265, 267, 269, 288
  distribution, 3, 5-6, 11-13, 15, 20, 72-74, 76, 115-124, 128-129, 132, 139-140, 144, 157-158, 167-168, 170, 172-174, 179-180, 182, 184, 188, 193, 195-196, 251, 267, 269, 288
Monomer, 2-6, 10-15, 18-19, 25, 39, 72-74, 76, 115-119, 124-126, 129-130, 138-140, 144, 146, 148, 152-154, 157-158, 163, 167-169, 172-178, 180, 182, 184-187, 189-191, 193-194, 236, 242, 255, 259-261, 266-267, 269, 272, 279, 290
Mooney viscosity, 136, 144, 268
Motion, 39-41, 50-51, 62-63, 70, 77, 99-100, 116, 146-147, 210, 212, 214-216, 229-230, 233, 239, 245, 255-260, 270-272, 277, 289

## N

Neutralisation, 39, 81, 84, 137, 207, 212, 216-220, 252, 255, 259, 273, 290
Nitrogen, 135-136, 220, 245, 252, 255-256
Nozzle, 262-263
Nuclear magnetic resonance, 170
  spectroscopy, 170
Nucleation, 138, 199, 232

## O

Olefins, 1, 137-138, 144-145, 147, 167, 174, 176, 178-180, 199, 201, 207, 220-222, 224-225, 231, 236, 243, 245, 251, 277, 280, 284, 290
Oligomer, 125, 128, 200, 268-269
  Oligomeric, 129
Optimisation, 3, 36-38, 48, 105, 138, 167, 173-174, 183, 216, 242, 287
Organic, 135, 144-145, 153, 168-169, 173-175, 178, 193, 201-202, 204, 256, 273, 275, 285
  solvent, 135
Orientation, 175-176
Outlet, 129, 260, 270

Output, 7, 10-13, 29, 46, 65-67, 74, 80, 82-89, 93, 99, 221, 229, 252, 258, 270, 282, 289
Oxidation, 169, 226-230, 245, 252, 290
Oxygen, 226-230, 252, 290

## P

Particle(s), 45, 50-51, 53, 55-57, 59-61, 63-69, 93, 98-102, 140, 142, 145-154, 161-165, 167-169, 173, 199, 228, 231-242, 258, 264, 270, 272, 289
  size, 99, 102, 142, 149-150, 165, 231, 236, 238-239, 241-242, 289
Pattern, 12, 39, 61, 94-95, 195, 210
Performance, 22, 111, 128, 134, 142, 160-161, 200, 242, 249, 254, 280, 283
Petrochemical, 49, 280, 287
pH, 216, 242
Phase separation, 68-69, 146, 229, 237
Phosphate, 219, 251
Physical properties, 63, 275
Physics, 23, 51, 70, 108-109, 113, 203-204, 243
Pigments, 231, 236
Pipe(s), 88, 208, 210, 212, 215, 218-219, 229, 256, 260-263, 266, 279
  line, 237, 240
Planar, 75, 207, 288
Plant, 136-137, 219
Plasma, 23, 107
Polybutadiene, 145, 155, 159-160, 166, 171, 173-174, 176, 188-189, 193-195, 197-199, 252
  rubber, 252
Polycondensation, 1, 21, 150
Polydispersity index, 12, 159-160, 235-236
Polyester, 272
Polyethylene, 145, 172
Polyisobutylene, 4, 12, 17, 19, 116, 251, 255
Polyisoprene, 145, 152-153, 155, 157-158, 160-166, 168, 174, 176, 186, 190-191, 250, 268
Polymer, 3-6, 10-12, 15, 17-21, 23-24, 37-39, 43, 46, 48, 72-76, 105-106, 108, 115-125, 127, 129, 131-137, 139-145, 147, 149, 151-155, 157-173, 175, 177-183, 185, 187, 189-197, 199-201, 203-207, 236-237, 240, 242-243, 245, 249, 251-252, 255-256, 262, 264-265, 267-268, 270, 272, 280, 282, 288, 290
  Polymeric, 115, 119-120, 123-124, 128
  Polymerisation, 1-5, 7-8, 10-14, 17-20, 39, 43, 48, 72-75, 83-85, 105, 115-125, 128-130, 132, 134, 137-140, 142-164, 166-180, 182-199, 207, 231, 236, 245-246, 252, 260-261, 265-268, 272, 288, 290

conditions, 123, 154, 162, 169, 180, 182-183, 186-190, 261
rate, 39, 117, 124, 145, 153-154, 157, 159, 163, 168, 172, 176, 191, 266
Polyolefins, 170-171, 173, 176
Polypropylene, 145, 176
Polystyrene, 176
Polyurethane, 272-273
foam, 272-273
Potential, 62, 147, 174-176
Pouring, 146, 150
Powder, 137, 252, 255-257, 268, 270
Power, 69, 113, 232, 251, 265, 270, 276
Precipitate, 199
Precipitated, 152, 263-264
Prediction, 30, 174
Preparation, 129, 135-136, 140, 142-145, 147-148, 150-151, 169-170, 182, 198, 261, 265, 268, 272, 281
Pressure, 8-10, 31, 40, 46, 53, 57, 59, 61, 66, 68, 77, 87-88, 137, 142-144, 210, 223, 229, 245-246, 255, 260, 277
drop, 40, 46, 66, 87-88, 142
Probability, 89, 128, 130, 161, 164-165, 169-170, 174, 180, 182, 231-232
Procedure, 183-184, 223
Process, 1-6, 10-13, 15-18, 20, 25-27, 29, 31-32, 38-39, 43, 45-46, 48-49, 56-57, 60, 62, 68, 70-76, 80-86, 88, 92-93, 95, 98-102, 105, 116-117, 120, 122, 124, 129-130, 132-133, 135-140, 144, 146-155, 157, 161-164, 167-175, 180, 182, 184-185, 187-188, 190-196, 198-199, 207, 209, 211, 213-217, 219-221, 223-228, 230-231, 239-242, 245-251, 254-261, 263, 267-268, 270, 272, 275-278, 280, 282, 287-288, 290
Processability, 160, 272
Processing, 41, 56, 69, 93, 134
Product, 3-4, 7, 14-15, 17-20, 25, 28, 32, 43, 70, 72, 74, 76, 80, 83, 99, 120-125, 128, 137, 147, 152, 158, 160, 172, 192, 198, 207, 220, 237-238, 240, 242, 246-247, 253, 259-260, 265, 272, 275-276, 278, 287-288, 290
Production, 1, 3, 12, 25, 38-39, 43, 46-47, 75, 124-125, 137-138, 140, 142, 144-145, 147, 160, 201, 209, 216, 219-220, 225, 231, 236-237, 239, 242, 245, 247, 250-252, 254-257, 259-261, 265-266, 268-270, 272-275, 277-278, 280, 282, 284
Profile, 27, 30-31, 37, 74, 88, 104, 224-225, 229-230, 275
Propagation, 73, 115, 117, 137-138
Properties, 10, 25, 40, 63, 77, 143, 150, 161, 200, 245, 254, 261, 272, 275
Propylene, 1, 136, 138-139, 142-145, 170-171, 175, 179, 199, 236, 250, 259-260, 262-266, 268, 270, 281
Pump, 57, 135, 231-232, 255, 259, 270-272
Purification, 251, 279

## Q

Quality, 3-4, 12, 19-20, 32, 58, 120, 124, 135, 137-138, 140, 144, 148, 199, 216, 242, 249, 251, 255, 259-260, 265-266, 272, 275-276, 278, 287-288, 290

## R

Radial, 14, 19, 31-32, 34, 57-60, 94, 96-97, 208, 217, 288-289
Radius, 3, 12-13, 15-16, 18, 29, 69, 74-76, 80-83, 86, 105, 117, 121, 131-133, 148-152, 165, 175, 208, 217-218, 233-236, 249, 288-289
Rate constant, 48-49, 125, 127-130, 137, 139, 153-154, 157, 190, 193, 196, 211-213, 215-216, 267
Ratio, 1, 14-15, 17-18, 37-38, 40, 43, 53, 55, 59-66, 68-69, 86, 93, 95-96, 98-99, 123, 127-128, 130-131, 135, 143, 145, 164, 179-180, 193, 208, 210, 212-214, 217, 219-223, 226-227, 229-234, 238-239, 242, 249, 275, 277, 287, 289-290
Raw material, 134, 251, 254, 282
Reaction, 1-6, 8-20, 25-26, 28-32, 34, 36, 38-50, 53, 55, 59-63, 66-70, 72-84, 86-105, 115-125, 129-140, 144-148, 150, 152-155, 157-165, 169-174, 179-180, 183, 190-199, 207-209, 211-240, 242, 245-250, 252, 255, 257-258, 262-263, 266-268, 270-273, 275-278, 287-290
  conditions, 3, 213, 237, 270, 275
  mixture, 10, 18-19, 25-26, 30-32, 34, 36, 38-41, 44-49, 53, 59-63, 66-68, 70, 72-74, 76-77, 80, 83-84, 86-93, 96-97, 99, 101, 103, 105, 115-116, 118, 121-122, 125, 129-131, 135-139, 144, 146-148, 150, 152-155, 157-160, 162-164, 191-196, 198, 216-217, 219, 221-224, 226-230, 232, 234, 236-237, 239-240, 242, 245, 247, 249-250, 255, 262, 266-268, 270-271, 276-278, 287-290
  product, 70, 72, 80
  rate, 10, 17-18, 48, 60, 124-125, 131, 133, 153-155, 157, 169, 172, 190, 193, 196, 211-213, 215-216, 246-247, 258, 275, 277, 287-288
  temperature, 73-75, 135, 222
  time, 1-4, 12, 16-17, 120, 136, 207, 216, 220, 247, 255, 287
Reactivity, 169-172, 179, 190
  Reactor, 1-4, 6-7, 10-18, 20, 29-31, 34, 36-45, 48, 50-53, 56-57, 59-60, 63, 65-71, 74-76, 78-89, 92-94, 96, 99, 102-103, 105, 116-117, 120-123, 129-133, 135-144, 147, 199, 207-214, 216-230, 232-236, 238-242, 245-249, 251-252, 254-264, 266-279, 288-290
Reagent, 18, 131
Recycle, 271
  Recycled, 268, 277-278
Reduction, 11, 46, 72, 76, 83, 103, 120, 147, 149, 151, 160, 190-191, 224-225, 249, 251, 267, 270, 276
Regeneration, 116, 274
Reliability, 30, 38, 245
Replacement, 225, 276

Research, 3, 109, 174, 179, 216, 287
Rotation, 47, 69, 102, 175, 208, 227, 231, 234, 236
Rotor, 50, 107
Roughness, 40, 167
rpm, 148, 221, 227, 231, 234-236
Rubber, 1, 38-39, 62, 124, 129, 134-136, 138, 142-145, 160-161, 201, 203, 227, 244-245, 250-252, 254-260, 264-266, 268-271, 284

## S

Safety, 22, 38, 43, 111, 200, 242, 245, 251, 254, 282-283, 290
Saturated, 134, 221, 260
  Saturation, 138-140, 142, 230, 256, 260
Scale, 4, 18, 39-40, 44-45, 47, 51-52, 56, 129-130, 133-134, 136, 138, 142, 216, 236-237, 248, 251, 264, 266-267, 274-275, 277, 279-280, 288
Sectional, 33, 68, 72, 81, 265
Sedimentation, 57, 148, 165, 231-235
Selectivity, 124-125, 247, 277
Separation, 67-69, 76, 119, 138, 140, 144, 146, 182, 187, 229, 236-237, 242, 259, 261, 265, 280
Shape, 51, 56, 94, 151, 177, 179, 258
Shear, 59-60, 64, 142, 269
  rate, 142
Sheet, 245, 251, 256-257, 259-260, 265, 270, 273-276
Shell, 82-83, 85-86, 165, 218, 225, 276-277, 290
Simulation, 4, 8, 12, 179, 276
Simultaneous, 75, 161, 191, 275, 278
Size, 12, 14-15, 18, 20, 28, 30-32, 45, 51, 53, 55-56, 59-60, 63-65, 67, 99-102, 129-130, 141-142, 146, 148-150, 161, 165, 167-168, 180, 199, 224, 226-227, 229, 231, 233-234, 236, 238-242, 251, 270, 272, 289
Sodium hydroxide, 219
Solid, 18, 27-31, 68, 101-102, 149-150, 161, 165, 167, 174, 184, 218, 231, 233, 235-242, 264, 272, 290
Solubility, 34, 226, 229, 239
Soluble, 232, 237-238
Solution, 3, 6, 9-10, 15, 25-26, 36, 38-40, 44, 51, 55, 57, 70, 72, 83, 86, 94, 100-101, 116, 130, 134-137, 139-140, 144, 147, 161-162, 179, 181-182, 193-194, 206, 212, 218-219, 229, 232, 236-240, 242, 247, 252, 254-258, 260-262, 264-268, 276, 288, 290
  viscosity, 140
Solvent, 72-73, 116, 119, 124, 135, 137-138, 140, 144, 147, 152, 161, 163, 168-169, 213, 221-223, 227, 236, 242, 255-257, 260, 262-263, 266, 268, 271, 275
Sorption, 161
Specific heat, 289

Specific surface, 57, 59, 62-63, 98, 148, 151-152, 168, 199, 216, 221, 231
Specificity, 4, 20
Spectra, 142-143
Spectrometry, 180
Spectrophotometer, 89
Spectroscopy, 170, 172
Speed, 25, 47, 99, 141, 227
Sphere, 40
Spherical, 52, 56-57, 62, 148, 233
Split, 134, 183
Stabilisation, 34, 39, 116, 240, 242, 259
Stabiliser, 137, 252, 255-257, 259, 265-266
Stability, 34, 50, 53, 55, 60, 134, 171, 213, 239, 260, 265, 272
Standard, 26-28, 51, 53, 70, 82, 88, 131, 135, 142-143, 193, 232, 255, 288-289
Static, 95, 162, 258, 272-273
Steady state, 246-247
Stearic acid, 237
Stimulation, 234
Stirrer, 136, 141, 148
  Stirring, 122, 131, 133, 135, 137, 139, 141-144
Storage, 236, 240-241
Strain, 273
Strength, 124-125, 217
Structure, 88, 92-95, 97, 100, 103, 128, 134, 145, 149, 151, 155, 166, 175-179, 207-208, 212, 216, 251, 264, 270, 289
Styrene-ethylene-propylene, 265
Sulfur, 220, 223
Supply, 1, 208, 213, 217, 219-220, 223, 229, 231
Surface, 1, 34, 40, 49, 52, 56-57, 59-67, 76, 91, 97-103, 120, 140, 142, 145, 148-149, 151-152, 155, 161, 165-168, 174-180, 199, 203, 216, 220-221, 226-231, 239, 247, 258, 262-264, 273, 278, 280, 287, 289-290
  tension, 56, 62, 65, 100-101, 273, 280
Suspension, 231-242, 256-258, 260, 268-270, 272
Sustainable, 70, 78, 83, 86, 186, 193
Symposium, 204-205
Synthesis, 1, 3-4, 12, 15, 24, 37-39, 43, 48, 81, 105, 115, 117, 119, 121, 123-125, 127-131, 133, 135, 137-139, 141, 143-145, 147, 149-151, 153, 155, 157, 159, 161, 163, 165, 167, 169, 171, 173, 175, 177-179, 181, 183, 185, 187, 189, 191, 193-197, 199-201, 203-205, 207-209, 211, 213, 215-217, 219-221, 223, 225, 227, 229, 231, 233-239, 241-243, 245, 249, 259-260, 265, 269-272, 276-278, 282, 290
Synthetic rubber, 124, 138, 145, 201, 203, 244, 268, 284

## T

Tank, 57, 120, 130-132, 135-142, 256
Temperature, 1-2, 4-6, 8-15, 19-20, 25, 39, 52, 70, 72-81, 83-85, 89, 92, 102, 104-105, 115-123, 132-135, 137, 170-171, 180, 207, 216, 218-225, 245-247, 249, 255, 265, 275-277, 287, 289-290
  range, 2, 5, 72, 117, 135
Tension, 10, 27, 52, 56, 62-63, 65, 100-101, 273, 280
Termination, 4, 6, 116, 137, 169, 179-180, 182, 193
Terpolymer, 259
Test, 29, 276
Tetrahydrofuran, 169-170
Theory, 22, 53, 78, 106, 166, 206, 282
Thermal conductivity, 86, 89
Thermodynamic, 70, 161
Thermoplastics, 43
Thickness, 140, 165, 264
Three-component, 147-148, 152, 155, 191
Titanium-aluminium Ziegler-Natta catalytic system, 145-146, 148-151, 153-155, 157-158, 166, 190, 199, 236, 265-266, 269
Time, 1-4, 12, 14-17, 19-20, 25, 28-29, 31, 37, 39, 42-48, 50, 59, 61, 65, 67, 77, 81, 92-93, 95, 97-99, 120, 125, 129, 132-133, 135-136, 138, 142-143, 145-147, 152, 154, 156, 161, 173-174, 183, 195, 207, 211, 213, 216-218, 220-221, 225-226, 228, 232-234, 240-241, 245-247, 249, 252, 254-255, 264, 269-270, 272-273, 276-277, 282, 287, 289-290
Tool, 86, 92, 104-105
Transfer, 2-6, 10-11, 20, 24-27, 31-32, 34, 44-45, 51-52, 73, 76-77, 86, 88, 91-92, 103, 105-107, 112-113, 115-118, 120-121, 124, 139, 153-154, 157, 169, 173, 193, 202, 215, 226-227, 229-230, 234, 246-247, 249, 255, 266, 268, 275-276, 287-290
  agent, 169, 268
  reaction, 116, 153-154, 157, 193
Transformation, 8, 28-29, 177, 245
Transition, 15-16, 18, 44, 46, 62, 65, 73, 84, 86, 91, 98-99, 103, 145, 150, 167, 169, 174, 177-178, 210, 212, 217-218, 288
Tube, 40, 82-83, 85-86, 88, 218, 224-225, 248-249, 276-279, 281-282, 290
Two-component, 129, 147-149, 155, 157, 190
Tyres, 134, 160

## U

Ultraviolet, 26, 172
Uniformity, 25, 117, 136-137, 144

Unsaturated, 166-167, 177, 220, 260
  Unsaturation, 124, 128, 134
Unstable, 84, 210, 262

## V

Vanadium-aluminium Ziegler-Natta catalytic system, 149-150, 153, 199, 236, 261, 263-264
Vacuum, 148, 256
Vector, 52, 54, 210
Velocity, 10, 15-16, 18, 26-27, 35, 52, 141, 275
Vertical, 50, 101-102, 246
Vessel, 147-148, 240, 245, 247, 258, 262, 278
Vinyl group, 176
Viscometer, 142
Viscosity, 9, 26-29, 34, 38-40, 42, 44-47, 50, 52-53, 55, 62-63, 67, 77, 128, 135-137, 139-141, 144, 213-215, 220, 233, 236, 238, 249-250, 256, 264, 266, 268, 270, 272-273, 278, 280, 288
Viscous, 3, 24-25, 28, 37-39, 43-44, 62, 135, 147, 154, 247, 255, 290
Volume, 1-6, 8, 12, 25, 27, 32, 35, 37, 39, 42, 49-50, 52, 55, 57-70, 74-76, 78, 80, 83-84, 93, 96, 98-100, 108, 118, 125, 129, 131, 133, 135-136, 138, 140-142, 144, 146-148, 154, 161, 196, 199, 207, 215, 219, 221-222, 224, 226-228, 231-232, 234-241, 245-247, 249, 254, 258, 260-263, 266, 272-273, 275, 277-282, 290
  fraction, 52, 68-69

## W

Wall, 10-11, 20, 27, 40, 53, 66, 74-77, 80, 88-89, 116, 118, 120-122, 232, 234, 246, 249, 275
Washing, 137, 250-252, 255-257, 259, 265-266, 268, 273, 275
Water, 34, 56-57, 59, 62, 77, 83-85, 88, 90, 100, 135, 137, 144, 173, 212, 217, 226-230, 236-239, 250-252, 254-257, 259, 265-266, 268, 270, 275, 278
Weight, 2-3, 7, 10, 12, 43, 48-49, 51-52, 73, 115, 118, 122, 127, 155, 157-160, 171, 184-185, 189, 193, 198-199, 207, 209, 211, 213, 215, 217, 219, 221, 223, 225, 227, 229, 231, 233-235, 237, 239, 241, 243, 250-251, 255, 265, 267, 269-270, 288
Widening, 29, 31, 34, 50, 59, 95-97, 180, 182, 288-289
Width, 77, 120, 123, 157-158, 180, 183, 269

## Y

Yield, 14-20, 25, 70, 72, 80, 83, 99, 119, 124-126, 152-155, 157-160, 162-164, 168, 176, 188-192, 194-195, 246, 255, 264-265, 267, 272, 275, 278, 288

ISBN 978-1-90903-026-8
90000
9 781909 030268

Published by Smithers Rapra Technology Ltd, 2013

This book describes the fundamentals of fast liquid-phase chemical reactions and the principles of their scientific foundation, technical implementation and industrial application of new technologies. In addition, the equipment required to perform these reactions, in a turbulent mode in the chemical, petrochemical and petroleum industries, is also discussed. The macrokinetic approach has been developed with consideration of the diffusion, hydrodynamics, and heat transfer processes. Due to the advancement of fundamental knowledge, equations of practical engineering importance have been obtained for the calculations of mass and heat transfer processes carried out in conditions of high turbulence, and developed for the implementation in fast chemical reactions involving the synthesis of low molecular weight products and polymers. New methods for controlling the molecular characteristics of polymers have been developed based on the tailored regulation of the hydrodynamics of the reactive mixture flow. Typical processes have been used as model examples to reveal the influence of turbulence on the behaviour of fast chemical reactions used for the synthesis of low molecular weight products, in single-phase and two-phase reactive systems. Brand new tubular devices have been developed with the following characteristics: compact size, high productivity, and a quasi-perfect mixing operation mode in turbulent flows. These devices are subdivided into cylindrical, shell-and-tube, 'zone', and diffuser-confusor designs. Original solutions are proposed for the instrumental implementation of fast liquid-phase processes and development of continuous energy- and resource-efficient technologies for the synthesis of some large-scale compounds.

SMITHERS RAPRA

Shawbury, Shrewsbury, Shropshire, SY4 4NR, UK
Telephone: +44 (0)1939 250383
Fax: +44 (0)1939 251118
Web: www.polymer-books.com